HIGH INTERNAL PHASE EMULSION: SYNTHESIS OF NOVEL, HIGHLY POROUS, FUNCTIONAL POLYMERS, CHARACTERISATION AND APPLICATIONS

GANESH CHINDHU INGAVLE

POLYMER SCIENCE AND ENGINEERING GROUP

CHEMICAL ENGINEERING & PROCESS DEVELOPMENT DIVISION

NATIONAL CHEMICAL LABORATORY

PUNE 411 008

INDIA

February 2009

HIGH INTERNAL PHASE EMULSION: SYNTHESIS OF NOVEL, HIGHLY POROUS, FUNCTIONAL POLYMERS, CHARACTERISATION AND APPLICATIONS

A THESIS SUBMITTED TO THE

UNIVERSITY OF PUNE

FOR THE DEGREE OF

DOCTOR OF PHILOSOPHY

(IN CHEMISTRY)

BY

GANESH CHINDHU INGAVLE

RESEARCH GUIDE

Dr. S. PONRATHNAM

POLYMER SCIENCE AND ENGINEERING DIVISION

NATIONAL CHEMICAL LABORATORY

PUNE 411 008, INDIA

February 2009

CERTIFICATE

Certified that the work incorporated in this thesis entitled **"High Internal Phase Emulsion: Synthesis of Novel, Highly Porous, Functional Polymers, Characterisation and Applications "** submitted by **Ganesh C. Ingavle** was carried out under my supervision. Such material as obtained from other sources has been duly acknowledged in this thesis.

February 2009 **Dr. S. Ponrathnam**

Pune (Research Guide)

DECLARATION

I hereby declare that the thesis entitled **"High Internal Phase Emulsion: Synthesis of Novel, Highly Porous, Functional Polymers, Characterization and Applications"** submitted for Ph.D. degree to the University of Pune has been carried out under the supervision of **Dr. S. Ponrathnam** at the Polymer Science and Engineering Group, Chemical Engineering and Process Development Division, National Chemical Laboratory, Pune, India. The work is original and has not been submitted in part or full by me for any degree or diploma to this or any other University.

February 2009 (**Ganesh C. Ingavle)**

Pune

Dedicated to,

my mother, ...

ACKNOWLEDGEMENT

*By the grace of **Lord Ganesha**, my academic career so far has indeed been such a journey, full of exciting challenges. My research career in the last four and half years, in particular, have been filled with exhilarating intellectual experiences, to which many people have greatly contributed. I joyfully take this opportunity to express my gratitude to all of them.*

*First and foremost, I would like to thank my Ph.D. advisor, **Dr. S. Ponrathnam**, who is always a pleasant scientist and willing to discuss any topic reminiscent of science. He taught me many things about not only chemistry, but also life in general. He taught me to look at problems and challenges from multiple angles and to always look at the bright side of life. His hands off approach enabled me to grow as a researcher and as a person and he was always there to extend a helping hand. As a researcher, I have learned a lot from him about scientific knowledge, communication skills, and the most important one 'motivation', which has been the endless source for new ideas. I greatly appreciate him from the bottom of my heart.*

*Special thanks is extended to **Dr. C. R. Rajan**, my co-advisor, who guided me through scientific as well as managemental skills, and provided constant support that made this part of my journey completed a lot easier than it would have otherwise been. Despite his busy schedule, he would always find the time to discuss anything from intriguing experimental results to any issue related to survival in the scientific world.*

*As I look back at the past five years of research career, I feel so privileged to have had the opportunity to work with two advisors (**Dr. S. Ponrathnam** and **Dr. C. R. Rajan**), who are the best combination any student can ask for. I would like to thank them*

for their mentoring as well as for playing a strong role in my development as a researcher.

I am sincerely thankful to ***Mr. R. K. Tayal*** *and* ***Dr. Steve Merrigan*** *for their fruitful scientific discussions and encouragement at every stage of my work.*

I have been fortunate from my childhood as I met really nice people who helped and inspired me from time to time. During this research task, apart from my guide, there have been six mentors because of whom I feel I can stand and see the firmament. They are ***Mr. Dhananjay Mehta and Mrs. Arti Mehta****,* ***Mr. Ashok Phale*** *and* ***Mr. Ramesh Phale*** *(my cousins),* ***Mr. Pramod Deshpande*** *(Junior college teacher), and* ***Mr. Khire*** *(Sir). I could never have reached this goal without all the help from them. They fully understood my struggles with this endeavor, they were there for the minor victories and defeats, and they always helped me press forward. They instilled in me the value of education. Thank you for encouraging me to go all the way to the top, and for believing in me more than I believed in myself.*

Most importantly I would like to thank my family: my ***father, mother and brother, Sunil.*** *They instilled in me the qualities that have made me what I am today. Without them I could not have succeeded, I would have been no one and nowhere. Also, special thanks to my sister,* ***Sunanda*** *and brother-in-law for their strong support through these years to help me achieve what I set out to do. Moreover, I am grateful more than I can express for their constant help throughout from my academic life. They were essential to making the man I am today.*

Many of my past labmates have not only been helpful, but also made this experience more enjoyable. I would like to thank ***Dr. Ramesh Ghadge****,* ***Dr. Arika Kotha****,*

who helped me get started on my research project. I am also grateful to ***Dr. Tara Sankar Pathak, Dr. Rajkumar Patel****, and* ***Dr. Supriya Palimkar****, for all their advice, support, and encouragement. Special thanks to* ***Dr. Narhari Pujari, Avinash, Meghana*** *and* ***Timothy*** *for helping me out in the experimental work and making my journey memorable.*

I would like to thank ***Dr. Sarika, Mr. Wasif,*** *and* ***Mr. Sunil****, for not only being my labmates, but also for being my best friends that I will never forget. Thanks for providing an outlet for my frustrations, discussing work problems and keeping me always happy and fresh. I thank all my lab members* ***Dr. N. N. Chavan, Dr. D. R. Saini, Dr. Smita Mule****,* ***Harikrishna, Praveen, Abhijit, Sunny, Ravindra, Mohasin, Mulani, Kalpana, Sonali****,* ***Rajkiran*** *and* ***Archana****. All of them have not only been helpful, but also made this experience more enjoyable.*

How can I forget to mention my close friends, ***Shirish, Kailas, Amit****,* ***Manoj, Sham, Pramod, Mahesh and Vinod****. They helped me through hard times, and helped me celebrate the good times through Saturday night dinner parties at my home. Probably their timely help becomes the* ***turning point of my journey towards the research career****. I thank them all not only for help, but also for being with me in all bad as well as happy moments.*

Apart from laboratory, there are friends who are well-wishers, always encouraged and supported me. To mention a few are: ***Geetanjali, Dipti, Arti, Santosh, Harshada****,* ***Bhalchandra (Vinay), Anirudh, Shailesh, Trupti, Pallavi, Abhimanyu, Sudhir, Ranjit, Sachin1, Sachin2, Narendra****,* ***Sujesh, Mandar, Farukh, Anita, Praveen, Amol, Nitin, Sanjay, Anil, Somnath, Mukund and Suhas.*** *I am thankful to all of them.*

*I am greatly indebted to **Mr. Anil Gaikwad** for help in Scanning Electron Microscopy characterisation, without which this work would not have been possible. I thank my collaborators, **Dr. Nitin Fadnavis** (IICT, Hydrabad), **Dr. Rajendra Parshad** (RRL, Jammu) for immobilisation work, **Dr. Bains** (Geological Survey of India, Pune) for metal ion recovery work, **Dr. Sanjiv Choudary** (IIT, Mumbai), for arsenic determination.*

*I thank **Mr. S. Sathe** and **L. Giri** for their technical help.*

*I wish to thank **Dr. M. Badiger**, coordinator of Polymer Physics and Chemistry coursework for the help and teaching the subjects.*

*I am thankful to **Dr. B. D. Kulkarni**, Head, Chemical Engineering and Process Development Division, National Chemical Laboratory and **Dr. S. Sivaram**, Director, National Chemical Laboratory, Pune for the permission to submit this work in the form of thesis. Finally, I thank Council of Scientific and Industrial Research (CSIR) for the award of fellowship during the period of this work.*

Ganesh Chindhu Ingavle

TABLE OF CONTENTS

CHAPTER I

INTRODUCTION

CHAPTER II

AIMS AND OBJECTIVES

CHAPTER III

CO-POLYMERISATION: SYNTHESIS OF CO-POLYMERS BASED ON MULTIPLE EMULSION

CHAPTER IV

TER-POLYMERISATION: TER-POLYMERISATION BY MULTIPLE EMULSION

CHAPTER V

FUNCTIONALISED POLYHIPE MATERIALS FOR ARSENIC REMOVAL

CHAPTER VI

HYDROXY TERMINATED POROUS POLYMER

CHAPTER VIII

SUMMARY AND CONCLUSION

LIST OF FIGURES

Chapter I: INTRODUCTION

Chapter III: CO-POLYMERISATION: SYNTHESIS OF CO-POLYMERS BASED ON MULTIPLE EMULSION

Chapter IV: TER-POLYMERISATION: TER-POLYMERISATION BY MULTIPLE EMULSION

Chapter V: FUNCTIONALISED POLYHIPE MATERIALS FOR ARSENIC REMOVAL

Chapter VI: HYDROXY TERMINATED POROUS POLYMER

Chapter VII: MORPHOLOGICAL STUDY OF POROUS POLYMERIC MONOLITHS

LIST OF TABLES

Chapter I: INTRODUCTION

Chapter III: CO-POLYMERISATION: SYNTHESIS OF CO-POLYMERS BASED ON MULTIPLE EMULSION

Chapter V: FUNCTIONALISED POLYHIPE MATERIALS FOR ARSENIC REMOVAL

Chapter VI: HYDROXY TERMINATED POROUS POLYMERS

Chapter VII: MORPHOLOGICAL STUDY OF POROUS POLYMERIC MONOLITHS

LIST OF SCHEMES

Chapter III: CO-POLYMERISATION: SYNTHESIS OF CO-POLYMERS BASED ON MULTIPLE EMULSION

Chapter VI: HYDROXY TERMINATED POROUS POLYMER

Abstract

High Internal Phase Emulsion: Synthesis of Novel, Highly Porous, Functional Polymers, Characterization and Applications

High internal phase emulsions (HIPEs) are dispersions of water in a continuous oil phase with internal phase volumes up to 99%, that is the water, although the majority phase, is not continuous. They form readily on adding water slowly to a stirred solution of a surfactant of low hydrophilic–lipophilic balance (HLB) dissolved in the oil phase. The internal or discontinuous phase has to be at least 74% of the emulsion volume, as this is the theoretical volume of a cubic close packing of spheres. In case that the continuous phase consists of, or at least contains, polymerisable monomers, HIPEs can be used for polymerisations to produce isotropic, open celled, polymeric foams (PolyHIPE's). The aqueous internal, or discontinuous, phase constituted approximately 90 vol.% in each case and consisted of small droplets approximately 10 μm in diameter. Complete removal of the aqueous phase was achieved after polymerisation by exhaustive extraction with hot ethanol, leaving monolithic polyHIPE polymers with completely interconnected cellular structures and an overall very low bulk density. By adjustment of the amount of cross-linker and by use of either water to oil ratio, or surfactant concentration, a secondary pore structure can be generated within the cell `walls' of the polyHIPE polymers. Overall surface areas between 3 and 350 m^2/g have been achieved.

Porous materials are characterised by their size distribution, shape, pore size, extent of interconnectivity and amount of porosity (open or closed). The manufacturing techniques vary depending on the application for the porous material that is to be produced. High Internal Phase Emulsion method (HIPE) is a very good technique for preparing both beaded as well as monolithic porous materials. Applications of this

poly(HIPE) materials cover diverse markets from high technology biomedical and biotechnology applications to industrial processes, such as catalysts, carriers for drug delivery, enzyme immobilisation, scaffolds for tissue engineering. The most interesting applications exploit the unique aspects of micrometer-size, interconnected cavities that characterise these materials. Main application focus for poly(HIPE) porous polymers is so far still on chromatography and membrane technologies.

In the present investigation a thorough study was carried out on the synthesis of different types of porous poly(HIPE) materials (beaded and monoliths) by multiple emulsion methods followed by their characterisations.

Chapter I deal with the history and current state of knowledge in HIPE polymerisation and its importance in various applications. A review of fundamental and technical information as well as the different techniques of HIPE polymerisation and the porous properties obtained thereof are also presented. A thorough literature survey was carried out on types of polymerisation and methods of synthesis on both beaded as well as monoliths.

Chapter II deals with the study of HIPE polymerisation. Objectives and the rational of doing the same are presented.

Chapter III discusses HIPE W/O/W multiple emulsion copolymerisation of glycidyl methacrylate (GMA) - ethylene dimethacrylate (EGDM), allyl glycidyl ether (AGE) - ethylene dimethacrylate (EGDM) and 2-hydroxyethyl methacrylate (HEMA) - ethylene dimethacrylate (EGDM) monomer systems. All the above polymers were also synthesised using conventional suspension polymerisation using cyclohexanol as porogen. The polymerisations were carried out by changing the ratio of monomer and

internal water. The internal phase volumes were changed from 33.33% to the maximum of 90.9%. Effect of internal phase volume on the formation of porous structures has been studied extensively. Polymers of different CLDs (25, 50, 75, 100, 150 200 and 300) were synthesised. The effect of variation in reaction parameters on the morphology, porous properties and surface functionalities was studied. Finally, the properties were compared with the properties obtained by suspension technique.

Chapter IV divided into two parts. In first part, we deal with the terpolymerisation of styrene-GMA-DVB and styrene-GMA-EGDM via multiple W/O/W emulsion method. The terpolymers were prepared to improve the mechanical properties for the chromatography application or hydrophilic properties for evaluation as ion exchangers. As part of the investigation into reactive polymers having epoxy group as functional group, the present investigation was undertaken to see the porous properties of glycidyl methacrylate with styrene as a comonomer and divinyl benzene as crosslinker and to evaluate the influence. of various reaction parameter such as, crosslink density, type of initiator, position of initiator, type of surfactants, etc. The effect of these parameters on the particle size, particle size distribution, pore volume, surface area, surface epoxy groups, and morphology were investigated thoroughly.

In second half of the chapter, the above synthesised HIPE beads were functionalised with thiol and mercaptosulphonic acid groups. Their acid exchange values were calculated by standard titration method using phenolphthalein as indicator and tested in a manner akin to Amberlyst towards the synthesis of 4,4'-bisphenol A.

Chapter V deals with the synthesis of epoxy based GMA-EGDM and AGE-EGDM copolymers by W/O/W HIPE polymerisation. These polymers were modified

with polyethyleneimine and evaluated for the removal of arsenic from aqueous systems differing in pH. The aim of this work was also to evaluate the parameters affecting arsenic removal, especially those, which cannot be examined easily in pilot plant scale. The examined parameters were the monomer type, crosslink densities, PEI concentration, contact time and pH of the treated water. Systematic, comparative study of arsenic binding, covering both trivalent As (III) and pentavalent As (V) inorganic arsenic anions, with PEI a modified poly(HIPE) GMA-EGDM and AGE-EGDM bead is presented. Furthermore, this work was the first research attempt at evaluation of poly(HIPE) materials as sorbent materials. The polymers synthesised by HIPE showed maximum binding (up to 70 to 74%) with the arsenic (III) and As (V) as compared to polymers synthesised by conventional methods.

Chapter VI deals with the synthesis of porous 2-hydroxyethyl methacrylate (HEMA)-co-N,N'-methylene bisacrylamide (MBA) beaded polymer by inverse HIPE (O/W/O) polymerisation. The stable HIPE emulsion was formed using nonionic surfactant Brij 92 having HLB 4.9 and the polymerisation were carried out by sodium persulphate-ascorbic acid redox initiator system at room temperature. A detailed investigation on the effect of croslink densities, surfactant type and their concentration on particle size, porous properties such as surface area, pore volume and morphology is reported. Similarly, synthesis of hydroxy terminated HEMA-MBA in monolithic form using inverse O/W HIPE system and characterisation of pore characteristics and morphology is reported.

Chapter VII deals with the synthesis of porous acrylate polymers by W/O HIPE polymerisation. Here, investigation of influence of synthesis parameters on the porous

characteristics, morphology of the resultant polyHIPE materials is reported. The examined parameters were the initiator type and their placement in the oil and water phase, surfactant concentration, inhibitor concentration, and temperature and stirring speeds. The detailed study of effect of above mentioned parameters on the formation of cells and windows as well as on the surface area was investigated.

In chapter VIII deals with the overall conclusions of the work reported in this thesis.

Chapter I

INTRODUCTION

1 Introduction

1.1 Porous materials: General

Some chemists worry plenty about nothing . . .. Well, almost nothing. It's the holes inside solid materials that are on their minds.[1]

Porous materials are defined as solid containing pores (Figure 1.1). The porous materials, also called molecular sieves, cover microporous, mesoporous and macroporous domains, depending on their pore dimensions. The word comes from Latin *porus,* Greek *poros*, where it means *"passage."* A thing that is *porous* is having pores, and *porosity* is the condition or situation of being porous. Porosity and surface area are important characteristics of solid materials that highly determine the properties and performance of catalysts, sorbents, medicines, membranes, rocks, and so on. "How active is your catalyst" and "How efficient will medicines work" are questions related to these characteristics.

Pores are classified into two types: open pores, which connect to the outside of the material, and closed pores, which are isolated from the outside. Penetrating pores are a kind of open pores; these have at least two openings located on two sides of porous materials. In open pores, penetrating pores are necessary for industrial applications such as filters or in gas distribution. Closed porous materials are used mainly for sonic and thermal insulators. Introducing open pores changes the materials properties drastically. Two essential changes are the decreased density and the increased surface area. Large surface area is necessary for catalysis. In many applications of porous materials, high, open porosity is desirable to increase the specific surface area or fluid permeability. Different application of porous material requires different pore sizes.

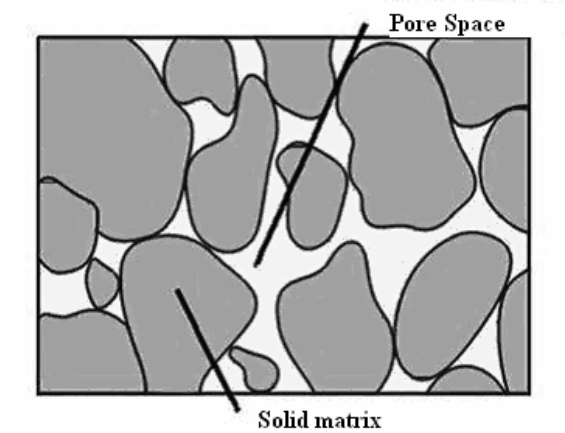

Figure 1.1. A solid matrix containing pores

In thinking about the micro-geometry of porous materials, a common approach is to consider them to be two-phase solid-pore composites, even though the solid phase can be heterogeneous. Properties like elastic moduli are essentially a function of the solid phase, but reduced and modified by the presence of the pores. If there is a fluid that fills the pore space, which can modify the dynamic elastic response, then both solid and pore characteristics must be dealt with an understanding of the elastic properties.[2] Elastic moduli decrease as the porosity increases.

Properties like diffusivity and permeability are functions of pore size, shape, and connectivity, and increase as the porosity increases. The topology of the pore space of a porous material is very important in determining its properties, and even in properly formulating ideas about the pore space in the first place. Topology defines how the pores are connected, if at all. If the pores are completely isolated from each other, then it is clear that one can discuss the shape and size of individual pores. The Figure1.2 (a) shows an example of this case, in 2-D, where the pores are random sized, non-overlapping

circular holes. In this case, it is quite easy to define the pore size distribution, a quantity that gives the number or volume of pores of a given size.

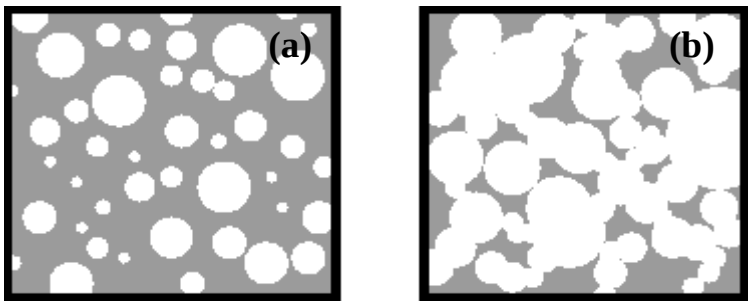

Figure 1.2. Two-dimensional picture of a) isolated circular pores, and b) connected pores.

When pores are fully connected to each other, as shown in the Figure 1.2 (b), there is really only one multiple-connected "pore" in the material. The number of pores is not a meaningful quantity anymore, and it is then difficult to talk about the shape and size of the "pores". However, in this case, the idea of "throats" can be important. If the pore space in many areas is shaped like the representation shown in Figure 1.3, then the idea of a throat shape and size may be loosely defined. The size of the "throat" limits the accessibility of the larger "pore," and is then the size of importance for many properties of the material.

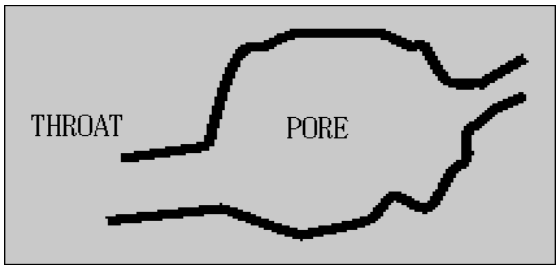

Figure 1.3. Schematic picture defining a throat and pore in the pore space of a porous material.

When there is such a 'throat' structure, then a pore throat size distribution, usually but erroneously called the pore size distribution can be defined. Techniques like nitrogen BET and mercury intrusion porosimetry (see Chapter 3) measure a pore throat size distribution that is convolved with the cross-sectional throat shape and the topology of the pore-throat network.[3,4] These techniques measure an equivalent circular cross-sectional throat diameter.[3,4] In practice, pore-throat combinations can only really be separated in terms of grossly simplified geometrical models of the pore microgeometry.

In most cases, porous materials are random materials, with random pore sizes, shapes, and topology. Because of this fact, most porous materials tend to be isotropic. This is not always the case, however. Many rocks have anisotropy built into them from how they were formed due to deposition of sediment.[5] When looking at a slice of a porous material, one must of course be aware whether the material is isotropic or not. We shall assume isotropy in the remainder of this chapter.

1.2 Classification of porous materials

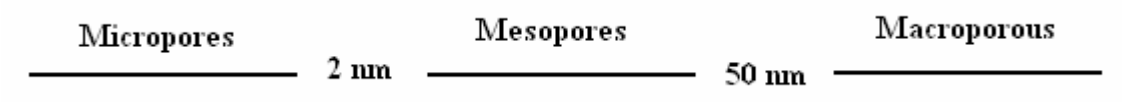

Figure 1.4. Pore size range

Porous materials have been used in many applications. The international Union of Pure and Applied Chemistry (IUPAC) has recommended specific nomenclature for porous materials: microporous (pore diameter < 2 nm), mesoporous (pore diameter between 2-50 nm), and macroporous (pore diameter >50 nm), as shown in Figure1.4. Classification may be based on different criteria such as pore size, pore shape, materials and synthesis methods. The porous matrix is used for particular application depending up

on the types of pore within it, as shown in Figure 1.5. Classification by pore size and by pore shape (Figure 1.6) is useful in considering application of porous materials (Table 1.1).

Table 1.1. Porous materials and their requirements for different applications

	Filter	**Catalyst**	**Bioreactor**	**Gas distributor**	**Sensor**	**Oil-Containing bearing**
Open porosity (%)	>30	>30	>30	>30	>30	20-40
Pore size	Appr. size depends on application	Appr. size depends on application	For bacteria: 5-30 μm For enzyme:10-100 nm	>μm	Depends on application	>μm
PSD*	Narrow	Narrow, bimodal depending on application	Narrow, bimodal depending on application	Narrow	Narrow	Insensitive
SSA*	Depending on application	1-2000 m^2/g	>1 m^2/g	Depends on pore size	>1 m^2/g	Insensitive
Permeability	High	Depends on application	Depends on application	High	Depends on application	Insensitive
Mechanical resistance	High	Depends on application	High, Depends on application	High, Depends on application	Depends on application	High
Others	Chemical resistance	Catalysis function	Appropriate surface potential	-	Sensing function Appropriate surface condition	Chemical & wear resistance

PSD* = Pore size distribution
SSA* = Specific surface area per unit volume

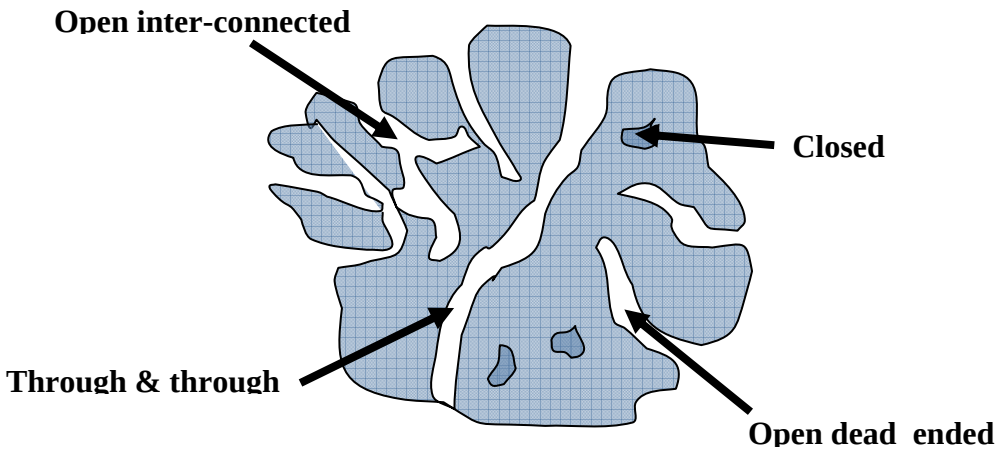

Figure 1.5. Types of pores in the solid matrix

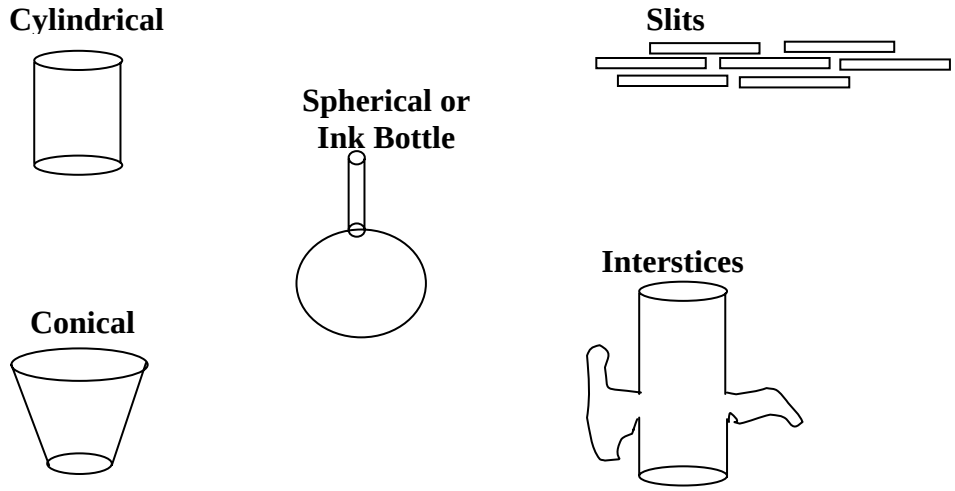

Figure 1.6. Shape of pores in the solid matrix

1.3 Types of porosities

There are several types of porosities, as presented below:

(i) Primary porosity: This is the original porosity system in a rock or unconfined alluvial deposit.

(ii) Secondary porosity: This is a subsequent or separate porosity system in a rock, which often enhances its overall porosity. This can be generated either due to chemical leaching of minerals or by fracturing. This can either replace the primary porosity or coexist with it [as indicated in (vi)].

(iii) Fracture porosity: This is a porosity associated with a fracture system or faulting. This can create secondary porosity in rocks that otherwise would not be reservoirs for hydrocarbons due to their primary porosity being destroyed (for example due to depth of burial) or of a rock type not normally considered a reservoir (for example igneous intrusions or meta-sediments).

(iv) Vuggy porosity: This is a secondary porosity generated by dissolution of large features (such as macrofossils) in carbonate rocks leaving large holes, vugs, or even caves.

(v) Effective porosity (also termed *open porosity*): This refers to the fraction of the total volume in which fluid flow effectively takes place and excludes dead-end pores or non-connected cavities. Effective porosity is important for groundwater and petroleum flow, as well as for solute transport.

(vi) Dual porosity: This refers to the concept of two interfacing and overlapping reservoirs. In fractured rock aquifers, the rock mass and fractures are often simulated as being two overlapping but distinct bodies. Delayed yield, and leaky aquifer flow solutions are both mathematically similar to that obtained for dual porosity; in all three cases water comes from two mathematically different reservoirs (even if these they are not physically different).

(vii) Macro-porosity: This refers to a case when the pores exceed 50 nm in diameter. Flow through macropores is described by bulk diffusion.

(viii) Meso-porosity: This refers to a case when the pore diameter is in the range 2 - 50 nm. Flow through mesopores is described by Knudsen diffusion.

(ix) Micro-porosity: This is due to pores smaller than 2 nm in diameter. Movement in micropores is by activated diffusion.

1.4 Measuring porosity

There are several methods to estimate the porosity of a given material or mixture of materials (material matrix), such as : (i) volume/density method, (ii) water saturation method, (iii) water evaporation method, (iv) mercury intrusion porosimetry, and (v) nitrogen gas adsorption.

1.4.1 Volume/density method

This method is fast and resonably accurate (normally within 2 % of the actual porosity). In this method, material is taken in a weighed graduated beaker, cylinder of known volume. The sides of the container is tapped till the material completely settles down and the volume occupied by the material is read off. The container is reweighed. The volume and the weight of the material are thus known. The weight divided by the density gives the volume that the material takes up, minus the pore volume. (The density of most rocks, sand, glass, etc. is approximated to be 2.65 g/cm^3. If a different material is being evaluated, its density needs to be known. The pore volume is simply the difference between actual and expected volumes.

1.4.2 Water saturation method

This method is a bit more difficult, but is more accurate and direct. Known volumes of material and water are used. Water is taken in beaker. Material under evaluation is added gradually, avoiding air bubbles. The beaker is then covered with a vinyl film such as parafilm to prevent evaporation of water and allowed to sit for few hours. The water above the material (unsaturated) is decanted carefully and measured to determine the volume of water that had entered the pores (saturated).

1.4.3 Water evaporation method

This method is perhaps the most difficult to perform, but is also the most accurate. Porous material is fully saturated, as indicated in Section 1.4.2, devoid of excess water. This is weighed accurately and gradually allowed to evaporate over several days till "bone-dry". This is weighed repeatedly till constant weight. The calculation is quite obvious if the density of porous material is known.

1.4.4 Mercury intrusion porosimetry

This method requires the sample to be placed in special filling device that allows the sample to be evacuated followed by the introduction of liquid mercury. The size of the mercury envelope is then measured as a function of increased applied pressure. The greater the applied pressure, the smaller the pore entered by mercury. Typically this method is used to evaluate pores in the range 300 to 0.0035 μm in materials as varied as from coal to fabrics. Because of increased concern over use of mercury, several non-mercury intrusion techniques have been developed.

1.4.5 Nitrogen gas adsorption

This method is used to determine fine porosity in materials such as charcoal. Nitrogen gas condenses on the walls of pores less than 0.090 μm. This condensation is measured either by volume or weight.

1.5 Choice of matrix /Support

A "matrix" is any material to which a biospecific ligand may be covalently attached.[6] The material to be used as an affinity matrix needs to be insoluble in the system carrying /containing the target molecule. The matrix is the most important component of an affinity chromatographic medium as it composes, for the most part, the largest volume of the adsorbent.

At present a wide range of high quality, high performance and economical matrices are commercially available. However, a carrier that fulfils the requirements of every application is not yet available. This presents the opportunity to design and synthesise.

1.5.1 General properties of solid matrix /support

Matrix should possess the following properties to be an ideal support:

1. Hydrophilic character: Hydrophilic character of matrix is essential for minimising nonspecific interactions and inactivation of bound enzyme. Hydrophobic character of matrix can decrease the stability of enzyme due to denaturation analogous to that generated by an organic solvent.

2. Chemically stable but easily chemically modifiable: The matrix should be chemically stable over a wide range of pH (2-12) and ionic strengths. It should be stable at elevated temperature and in organic solvents, conditions critical to modification of

matrix. On the other hand, support should possess a sufficient number of chemical groups amenable to facile modification to link affinity ligands or enzyme on it.

3. Resistance to microbial and enzymatic degradation: The matrix should not be attacked by microorganisms and enzymes.

4. Large surface area and free of nonspecific adsorption: Support should have the greatest possible surface area and at the same time be completely inert, have no nonspecific interactions with that might not differentiate the substance to be purified from the contaminants.

5. High rigidity and suitable form of particles: The flow characteristics of a matrix depend largely on rigidity, particle size and particle shape. Good flow properties are important to the success of affinity chromatography. The eluent should penetrate the support column at a sufficient rate even when the affinate is bound onto it. Matrix must be highly rigid to withstand the pressure of packing and solvent flow during elution and washing. Irregularly shaped particles lead to unequal path lengths for the substances to be separated, which ultimately leads to band broadening. Generally, the suitable shape is spherical. However, spherical beads may not be essential if a very rigid matrix is available. Excellent results have been obtained with irregular particles.[7] Increasing particle size reduces flow resistance and separation power whereas very small particles have too high a flow resistance and soon become clogged.[8] A narrow particle size distribution is not a critical parameter for affinity chromatography as in case of ion-exchange or reverse phase techniques. However, narrow particle size range will result in better and more efficient column capacity because of less frequent column channeling and greater concentration of final and eluted product. This is due to reduced void volume.

6. Porosity: Controlled porosity is attainable in the matrix by varying the reaction parameters.

Table 1.2. Features of different porous materials

	Paper	**Polymer**	**Metal**	**Glass**	**Ceramics**
Density	Low	Low	High	Medium	Medium
Permeability	Low	Low	High	High	High
Strength	Weak	Medium	Strong	Strong	Strong
Pore size	Large	Controllable	Controllable	Controllable	Controllable
Thermal resistance	Low	Low	High	High	Very High
Chemical resistance	Low	Medium	High	High	Very High
Life time	Short	Short	Long	Long	Long
Machinability	Very good	Very good	Good	Poor	Poor
Cost	Low	Low	Medium	High	Medium

A major challenge in chemistry and materials science is the development of new synthetic pathways to advanced materials with unique properties. Much of this research is increasingly focused on materials with intricate three-dimensional structures, which may involve complex stiochiometries, highly regular architecture or nanoscale control over the properties. New opportunities exist in optimising the construction of well defined, ordered, porous solids materials using monodispersed building blocks with tuned properties.[9] An understanding of material properties and effects of reaction variables on the porosity allows for better design choices and optimal material selection for specific applications.

1.6 Porous polymers

Synthetic polymers have attractive characteristics such as lower processing cost and a variety of thermal, physical and mechanical properties compared with other materials (Table 1.2). The polymeric materials can be easily subjected to various physical and chemical modifications.[10,11] Porous synthetic polymers have generated considerable interest in many industrial, medical and environmental applications that involve transport phenomena.

1.6.1 Historical remark

Porous cross-linked polymers are effective and efficient materials for many separation processes, and therefore they are widely used as ion-exchange resins and as specific sorbents. Hermann Staudinger and Huseman were the first to copolymerise styrene with divinylbenzene to yield a product that only swelled in good solvents.[12] The polymers were soft, gel-like at low DVB contents, and had a three-dimensional network structure, with solvent-filled pores in the range 3 to 50 nm. Applications were found, after sulphonation, as cation-exchange resins. These gels suffered from mechanical flexibility and the insufficient access to the inner parts of the gel due to very small sizes of the pores. New processes were found to generate macroporous poly(styrene-co-divinylbenzene) gels by the addition of porogens, the so-called macroreticular polymers. These polymers have high cross-linking densities (up to pure cross-linker alone), are mechanically more stable, and provide larger pore superstructures, which are also accessible in non-solvents. Porogens, which are removed after polymerisation, include structuring solvents, non-solvents or linear polymers.[13]

By late 1950s, suspension polymerisation was established to yield cross-linked polystyrene having a porous structure in the dry state.[14-24] A modern approach towards

porous polymers is the use of templates. Template synthesis concepts became increasingly important for supramolecular chemistry in the 1980s.[25] In the ensuing years synthesis of macroporous copolymer networks based on the various chemical compositions has been extensively studied. To distinguish these new materials from the conventional ones the terms 'macroporous' and `macroreticular' were introduced. Functional resins are produced in two basic morphological types:

1. Gel-type (microporous) resins without any inherent porosity in dry state, but generated on swelling in solvent.

2. Macroreticular (macroporous) resins with macropores even in the dry state, in addition to the micropores generated by the swelling of the polymer skeleton.

Macroporous networks usually have a broad pore size distribution ranging from 0.1 to 1000 nm.[26] A phase separation during network formation is responsible for the formation of porous structures.[27] In order to obtain macroporous structures, the phase separation must occur during the cross-linking process so that the two-phase structure is fixed by the formation of additional cross-links. This phase separation occurs at an early stage of polymerisation, leading to the formation of microscopic globular entities that keep growing but do not coalesce because of cross-linking. Eventually, these come into contact with each other and associate to form clusters consisting of both interconnected globules and voids or pores (Figure 1.7).[28]

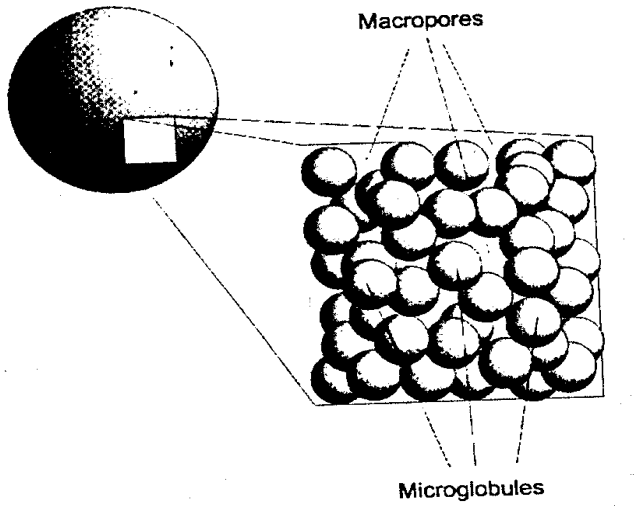

Figure 1.7. Schematic view of the morphology of macroporous polymer beads

1.6.2 Macroporous copolymer networks

The action of porogen in forming porous morphology in a macroporous resin is presented in Figure 1.8. Suspension polymerisation technique is generally used to prepare macroporous copolymer networks in bead form of diameter ranging from 0.1 to 1 mm, with majority in the range 200-600 micron. First, a monovinyl–divinyl monomer mixture containing a free-radical initiator is mixed with an inert diluent. The inert diluent must usually be soluble in the monomer mixture but insoluble in the continuous phase of the suspension polymerisation. The reaction mixture is then added into the continuous phase under agitation, so that it distributes in the form of droplets inside the continuous phase. The copolymerisation and cross-linking reactions take place in the monomer–diluent droplets to form beads haing a glassy, opaque, or milky appearance.

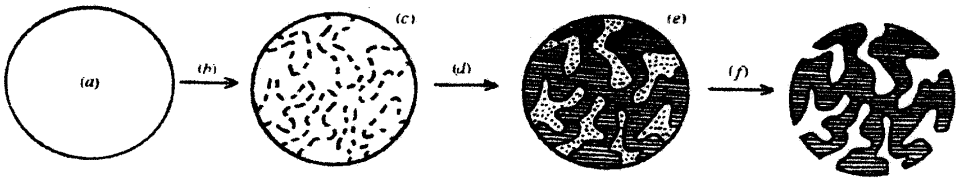

Figure 1.8. Action of porogen in forming porous morphology in a macroporous resin (a) monomer, cross-linker and porogen in isotropic solution; (b) polymerisation; (c) polymer network formation; (d) porogen and network start to phase separate; (e) porogen phase acts as a pore template; (f) porogen phase is removed to yield pores

Macroporous materials have a wide range of applications in chemistry.[29] Macroporous polymers, in particular, can be used as catalytic surfaces and supports,[30,31] separation and adsorbent media,[32-34] biomaterials,[35-39] chromatographic materials[40-42] and thermal acoustic and electrical insulator.[42-45]

The suspension polymerisation technique yields polymer particles with a relatively broad particle size distribution that are not used directly suitable for fine chromatographic separations. Alternate procedures, such as high internal phase emulsified suspension can afford monodisperse macroporous beads. Porous structures within the particles may be obtained up on the removal of the diluent after polymerisation.[46,47] Hydrophilic cross-linked macroporous particles have also received much interest in recent years. They can be prepared by the classical suspension polymerisation technique, in which water-insoluble derivatives of the monomers are used for the polymerisation.

Horak *et al*. used an aqueous solution of poly(vinyl pyrrolidone) as the water phase and a mixture of higher boiling alcohols as the diluent of the monomer phase to obtain cross-linked poly(2-hydroxyethyl methacrylate) beads.[48] They pointed out that the diluent in the monomer phase reduces the solubility of 2-hydroxyethyl methacrylate

(HEMA) in water. A number of researchers have studied various techniques for the synthesis of poly(HEMA) beads in an aqueous phase.[49-55] The presence of sodium chloride in the aqueous phase reduces the monomer solubility and thus allows formation of spherical, hydrophilic beads. Several diluents soluble in the monomer mixture have been tested for their suitability as inert diluents in the production of hydrophilic macroporous copolymer networks.[56-58]

Coupek *et al.* first described the synthesis of macroporous polymers from HEMA and ethylene dimethacrylate (EGDM).[59] Svec *et al.* prepared a series of macroporous glycidyl methacrylate (GMA)/EGDM copolymer beads by classical suspension polymerisation technique using lauryl alcohol/cyclohexanol diluent mixture.[60,61] The copolymers exhibited a high specific surface area, which increased markedly with increasing content of the cross-linker, EGDM. On increasing the relative volume of lauryl alcohol in the diluent mixture led to the formation of large pores and small surface areas. Synthesis of uniform sized porous GMA/EGDM beads was described by Smigol *et al.*[62,63] The distribution of pore size in a macroporous polymer is measured by mercury intrusion porosimetry.[64] The specific surface area is analysed by measuring nitrogen adsorption isotherm and using Brunauer-Emmet-Teller equation.[65]

1.6.3 Methodologies to obtain porous beaded polymers

Among the various techniques for the preparation of macroporous polymers, one can distinguish, three different routes: The first involves the use of gases as the void forming medium. The second approach is based on the intermediate of emulsion, formed tailor made block copolymers and the subsequent removal of dispersed phase. The third

category is clssified by the use of a phase separation process to generate a two-phase morphology, finally resulting in a porous morphology.

1.6.4 Synthetic strategies to porous polymer networks

Chemically the porous, beaded polymers can be obtained by suspension, emulsion and dispersion polymerisation; suspension being the most frequently used in both beaded as well as in monolithic form, as shown in Figure 1.9. Emulsion and dispersion polymerisation products are useful for coatings and adhesives while the particles prepared by suspension polymerisation are often used in molding plastics, as matrices for ion-exchange resins and as flocculating agents.[66] Permeability, mechanical strength, transparency, size exclusion or adsorption capacity of porous polymers depend on the connectivity of the pores. The range of obtainable porous polymer morphologies has become important, and each application is optimally served by a special architecture (Table 1.3).

The second concept of porogenesis relies on polymer-solvent phase separation processes. The phase separation can be induced throughout polymerisation and cross-linking in different ways: (a) by addition of a non-solvent to a polymer/solvent mixture (e.g. immersion techniques), chemically induced (e.g. the polymerisation is performed in a monomer/non-solvent mixture, the polymerisation itself depletes the monomer, and insolubility is induced), and (c) thermally induced phase separation (TIPS).

Foaming techniques use gaseous porogens. These are generated by evaporation of solvents during temperature increase or pressure drop (e.g. polystyrene foam), or are produced by chemical reactions during polymerisation (e.g. polyaddition of urethanes).

Formation of finer pore systems relies on the addition of surfactants, e.g. silicone surfactants.

Table 1.3. Techniques of porous polymer synthesis

Method	Porogen	Pore sizes[a]	Morphologies	Matrix polymers
Foaming	Gases Solvents Supercritical CO_2	10nm-1mm	Isotropic Open/closed pores	Polystyrene, polylactide, polymethacrylate, poly(2-hydroxyethyl methacrylate, polyurethane, polycarbonate,etc.
Phase separation Thermally induced Chemically induced Immersion techniques	Solvents	1μm- 1nm	Typically isotropic and open porous	Polystyrene, polylactide, poly(ether ether ketone), polyamide, poly(epoxide), Poly(dicyclopentadiene), etc.
HIPE [b]-polymerisation	Emulsion	10 μm-100 μm	Isotropic and open porous	Poly(styrene-DVB), poly(vinyl benzyl chloride - co-divinyl benzene), poly(aryl ether sulphone), etc.
Template synthesis Molecular imprinting Micellar imprinting	Molecules	1 nm- 10 nm	Isotropic Open/closed pores	Poly(methacrylic acid), poly(ethylene dimethacrylate), polyurethane, polystyrene.
Colloid crystal imprinting	Micelles	10 nm- 50 nm		
	Colloid crystals	50 nm- 1μm		
Polymerisation of biocontinuous microemulsion	Bio. microemulsion	5 nm- 10 μm	-	-
Polymerisation of liquid crystalline mesophases	Lytropic mesophases PETs[c]	5 nm- 10 μm	Isotropic-anisotropic Open/closed pores	Poly(hydroxyethyl methcrylate), poly(acrylic acid), poly(acrylamide), poly(methyl methacrylate)

[a]Typical pore diameters. [b]HIPE, high internal phase emulsion. [c]PET, polyelectrolyte–surfactant complexes.

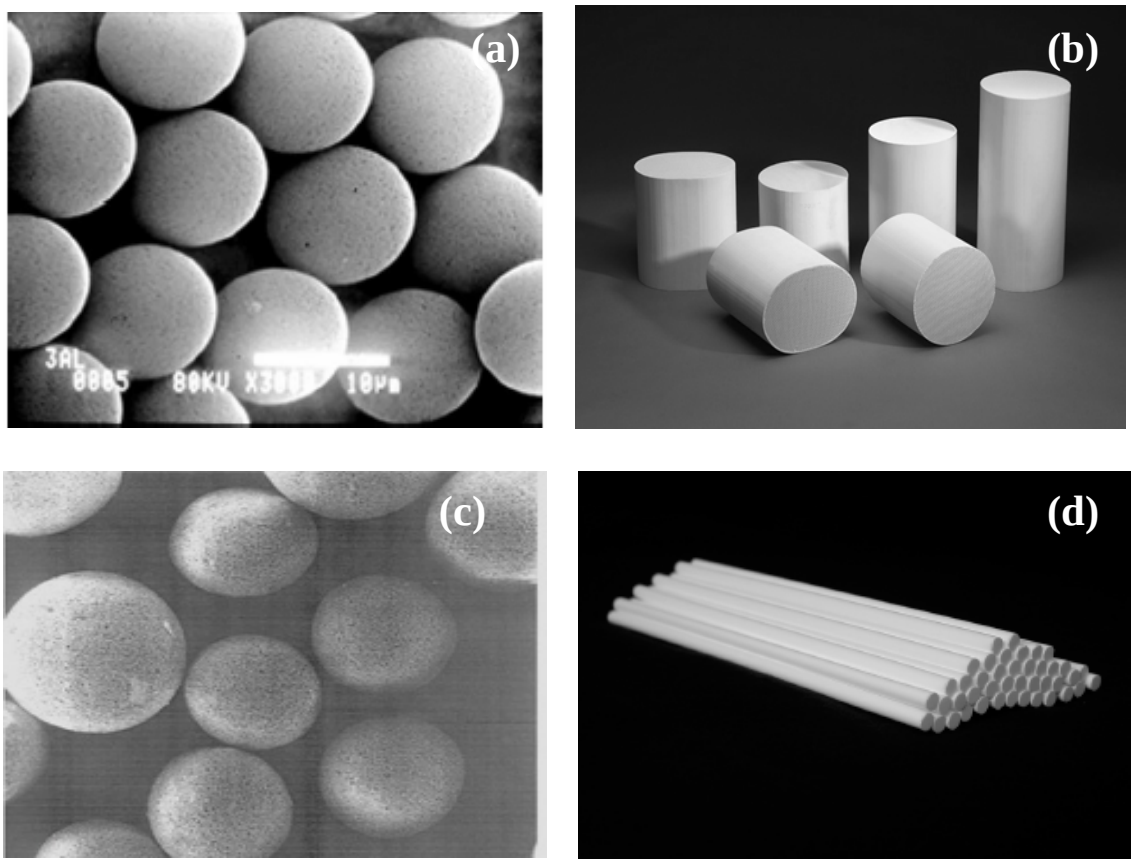

Figure 1.9. Different shapes of porous polymeric materials a) Nonporous beaded polystyrene-DVB, b) porous monoliths having diameter between 25-76 mm, c) porous spherical polystyrene-DVB. d) porous monolithic materials for chromatographic column

Pores can also be implemented by the concepts of supramolecular and colloid chemistry, which aim to generate new functional materials by arranging matter on the nanometer to micrometer length scale. Syntheses within self-organised media are convenient one-step template reactions and open manifold opportunities to control the pore architecture in a much broader range than possible by other techniques. The highest goal of a template synthesis, namely the direct replication of a self-organised structure into a permanent (polymeric) material, is, however, complicated by changes of the mixing thermodynamics throughout polymerisation.

A majority of porous polymers are, however, made by in-reaction precipitation from solvent–non-solvent mixtures, to obtain liquid filled porous polymers. Hydrocarbon phases are generally employed to precipitate the polymer and to form the pores. The porous polymer gels desired are essentially spherical gel particles or beads in the size range between 2 and 20 micron. Such particles are then slurry-packed into stainless steel columns for size exclusion chromatography, HPLC, and other variations of chromatography. To optimise separation power at optimal flow, monodispersity of the particles is highly advantageous. The size of the particles seriously influences the pressure at which these columns have to be operated: the smaller the particles are, the higher the separation power, but higher will be the pressure.

Polymer beads prepared by a suspension polymerisation process do not show large flow-through channels, and only the macroporous system within the spheres is preserved due to the lack of interfacial tension between aqueous and organic phases. Control of the kinetics of the overall process through changes in reaction time, temperature, and overall composition allows the fine-tuning of the macroporous structure and provides an understanding of the mechanism of large pore formation within the porous gels. A lower reaction temperature slows down the polymerisation rate and, coupled with low conversion at shorter reaction times, leads to porous polymers with larger flow-through channels.[67]

Suspension polymerisation is used for the preparation of spheres. The monomer/porogen mixture is dispersed in an inert solvent using stabilisers (protective colloids). For hydrophobic monomers water is used as the dispersion medium, and high boiling hydrocarbons are used for polar monomers. Porogens should not dissolve in or

interfere with the continuous phase and they should have the same polarity as the monomer mixture.

A staged, templated suspension polymerisation method was used to prepare 5-50 micron beads from mixtures of styrene and several substituted styrene monomers, with divinylbenzene in the presence of various amounts of linear polystyrene and dibutyl phthalate as porogens.[68] The nature of the monomer and percentage of porogen in the polymerisation mixture had a large effect on the porous properties and surface morphology of monodisperse beads. Beads with large pores could only be obtained if the percentage of porogen in the mixture exceeded a threshold value to induce phase separation within droplets sufficiently early in the network formation process. This threshold varies with the type of monomers involved in the polymerisation. The incompatibility of the functional polymer gel strands formed by polymerisation with the linear polystyrene present as structure controlling porogen is an important variable that affects both the pore properties and the outer morphology of the beads.

The precipitation polymerisation of divinylbenzene (55 wt.%) in acetonitrile containing up to 40 vol.% toluene or other cosolvents resulted in monodisperse porous poly(divinylbenzene) microspheres with diameters between 4 and 7 microns, total pore volumes of up to 0.52 $cm^3\ g^{-1}$, and surface areas of up to 800 $m^2\ g^{-1}$. The generated particles were free of residues and could be used without further purification.[69]

Other methods of preparing porous polymers are by (i) thermally induced phase separation (TIPS); (ii) immersion precipitation and chemically induced phase separation (CIPS); (iii) template syntheses such as molecular imprinting, colloid crystal templating

and polymerisation from microemulsions/lyotropic liquid crystals and (v) Polymerisation of high internal phase emulsions (HIPE).

1.7 Suspension polymerisation

Hoffman and Delbruck first developed suspension polymerisation in 1909.[70] Suspension polymerisation, a heterogeneous polymerisation, is a system in which a solution of initiator and monomers, which are relatively insoluble in water, are suspended as liquid droplets, and the resultant polymer is obtained as a dispersed solid phase. When water insoluble monomers are dispersed in water as continuous phase it is termed as oil-in-water (O/W) suspension. For water-soluble monomers like acrylamide, 2-hydroxyethyl methacrylate etc. the dispersant phase can be oil, which makes them water-in-oil (W/O) suspension. This process is also known as inverse suspension polymerisation. Terms synonymous with suspension polymerisation are pearl and bead polymerisation, especially when porosity is not of critical importance. Several detailed and complete literature reviews on suspension polymerisation have already been published.[71-79]

The interfacial tension, the degree of agitation, and the design of the stirrer/reactor system govern the dispersion of monomer droplets, typically with diameters in the range of 10 μm to 5 mm. The presence of suspending agents (stabilisers) hinder the coalescence of monomer droplets and the adhesion of partially polymerised particles during the course of polymerisation, so that the solid beads may be produced in the same spherical form in which the monomer was dispersed in the aqueous phase. The monomer phase is subjected to either turbulent pressure fluctuations or viscous shear forces, which break it into small droplets that assume a spherical shape under the

influence of interfacial tension. These droplets undergo constant collisions, with some of the collisions resulting in coalescence. Eventually a dynamic equilibrium is established, leading to a stationary mean particle size. Individual drops do not retain their unique identity but instead undergo continuous break up and coalescence.

The most important issue in the practical operation of suspension polymerisation is the control of the particle size distribution. The size of the particles will depend on the monomer type, the viscosity change of the dispersed phase with time, the type and concentration of stabiliser and the agitation conditions in the reactor. In the case of large monomer droplet in the continuous phase, nucleation predominantly occurs in the droplets and each polymerising droplet behaves as an isolated batch polymerisation reactor.

The notation 'suspension polymerisation' is reserved for systems where nucleation occurs in the monomer droplet and the average number of radicals per particle is very high (10^2 to 10^6), especially if the droplets are larger than 1 μm. In principle, large particles are obtained but it also results in a small fraction of polymer particles below 1 micron.[80] The small particles are thought to be the result of nucleation in the aqueous phase and subsequent latex polymerisation. According to the Laplace pressure, smaller droplets are thermodynamically less stable than larger ones and undergo Ostwald ripening. The addition of hydrophobe lowers the chemical potential and prevents the diffusion of the monomer to large droplets. This leads to bimodal particle distribution with one fraction below 1 micron and the other one can be adjusted between 20 and 500 μm.[81-84] Agitation system design is critical to achieving the desired particle size distribution in the final product, to balance the phenomena of coalescence/dispersion,

droplet and particle suspension, and heat transfer. The initial particle size distribution achieved in the monomer/water would not necessarily be the same as that for the final polymer product even if particle coalescence can be completely prevented.

There have been a number of studies on the effect of agitation on droplet size.[85-89] The combination of continued agitation and the addition of a suitable stabiliser (often a surface active polymer) have a stabilising effect, hindering both the coalescence and further break-up of monomer droplets. The size of the initial emulsion droplets formed is dependent upon the balance between droplet break-up and droplet coalescence. This is, in turn, controlled by type and speed of agitator used, volume fraction of monomer phase and type and concentration of stabiliser.

The stabilised monomer droplets may be considered as "microreactors", with the polymerisation proceeding therein.[90-93] Type and concentration of suspending agent plays an important role in the tendency of droplets to coalesce. As the suspension polymerisation proceeds, the viscosity of a monomer–polymer droplet increases with conversion. Hence, the physical behavior of the droplets is not the same during the process. When dispersible material is added to the existing stabilised drops, the new material and existing drops can remain segregated for significant amounts of time.[94] The increasing viscosity of the suspended droplets with polymerisation makes a quantitative analysis of suspension polymerisation a complex problem.[95] It is possible to establish a number of special factors, apart from the free-radical polymerisation-that exert an important influence on particle size and particle size distribution.[96-98]

1. Geometric factors of the reactor: Profile, type of stirrer, stirrer diameter relative to the reactor dimensions, bottom clearance of the stirrer, and internal fittings.

2. Operating parameters: Stirrer velocity, stirring and polymerisation time, phase volume ratio, fill level of reactor and reaction temperature.
3. Substance parameters: Dynamic viscosities (η_c) and (η_d), and densities (p_c) and (p_d), of the continuous and discontinuous phases, and the interfacial tension (σ).

A typical water insoluble organic monomer has lower surface tension than water. When such a monomer is mixed in a continuous phase of water with no surfactants present, an unstable dispersion is formed due to the continuous break up and coalescence of monomer droplets. Agitation must be sufficient to prevent separation of dispersion because of the difference of specific gravity between the two phases. Agitation system design is critical to achieving the desired particle size distribution in the final product. The optimal agitation system design balances the phenomena of coalescence/dispersion, droplet and particle suspension, and heat transfer.

Advantages of suspension polymerisation process are: (i) Easy heat removal and temperature control; (ii) Low dispersion viscosity; (iii) Low levels of impurities in the polymer product; (iv) Particle size control over fairly narrow range; (v) High surface area to volume ratio for small drops or particles and good heat transfer and (vi) Low cost of conversion with flexibility to vary the particle properties.

The disadvantages of suspension polymerisation are: (a) Polymer build up on the reactor wall, baffles, agitators and surfaces; (b) Waste water problems; (c) Difficulty in producing homogeneous copolymer composition; (d) Lower productivity for the same reactor capacity as compared to bulk and (e) It only applies to free radical processes. Agitation is critical because as the viscosity within the bead rises, the reaction rate increases suddenly (Trommsdorff effect), generating a surge in heat, which is not usually

observed in solution or emulsion polymerisation. Problems associated with continuous suspension polymerisation are deposition of polymer on the wall of the reactor during polymerisation (which affects the heat transfer through the reactor jacket) and difficulty in achieving high conversion.

1.8 Emulsion polymerisation

1.8.1 Emulsions: Definition of emulsion

Emulsions have applications in many industries, such as: pharmaceutical, cosmetic, papermaking, food and agriculture. The variety of uses for emulsion system has resulted in a wide variation in the definition of the term "emulsion". The many definitions possess conceptual advantages for the respective industrial practices; however, from a surface or colloid chemistry viewpoint, the definition may be meaningless. A comprehensive definition was provided by Becher.[99]

> "An emulsion is a heterogeneous system, consisting of at least one immiscible liquid intimately dispersed in another in the form of droplets, whose diameters, in general, exceed 0.1 microns. Such systems possess a minimal stability, which may be accentuated by such additives as surface-active agents, and finely divided soils."

The minimal stability of emulsion system is attributed to an increased surface free energy, which accompanies the emulsification process. The surface-active agents, which are added to an emulsion to increase its stability by action at the interface, are known as emulsifiers or emulsifying agents. There is also a distinction between the types of

emulsions based on rheological (physical) properties. Emulsions, which are transparent, thermodynamically stable, and have small particle size (5-100 nm) are termed micro-emulsion, whereas opaque, kinetically stable emulsion with a larger particle size (200-10000 nm) are termed macro-emulsions, or simply emulsions. Micro-emulsion has a much longer shelf life than macro-emulsion because of their stability. The basic properties of emulsions therefore, render them of particular interest in the efficient nebulisation of oil samples and their subsequent instrumental analysis.

1.8.2 Types of emulsions

1.8.2.1 Micro-emulsion

Micro-emulsion have been defined as dispersions of either 'water-in-oil' (W/O) or 'oil-in-water' (O/W) that are stabilised by pure or mixed amphiphiles.[100] More recently Garcia-Rio et al. described micro-emulsions as pseudo-homogeneous mixture of water-insoluble organic compounds, water and a surfactant/ cosurfactant mixture.[101] The amphiphiles (surfactant/ cosurfactant mixtures) are involved in lowering the oil-water interfacial tension by means of their interfacial adsorption thereby minimising the positive free energy of dispersion associated with surface formation. The micro-emulsion formed are isotropic, have a low viscosity and are thermodynamically stable. They have prolonged shelf life and average particle size of 5-100 nm.

Other characteristic includes optical transparency (the droplets are too small to scatter visible light) and polydispersity, which decreases with decreasing particle size. There are different types of micro-emulsions including polar oil, polymer oil, biological etc. The spontaneous formation of micro-emulsions infers that the free energy change

must become negative in order to fulfill the thermodynamic requirement as seen in following Equation 1.1

$$-\Delta G = \gamma_{o/w} \Delta A \qquad \textbf{1.1}$$

where, $\gamma_{o/w}$ is the interfacial tension between oil and water and ΔA is the change in the surface area due to emulsification. Since ΔA is always positive, $\gamma_{o/w}$ must be negative. A minimal $\gamma_{o/w}$ is sufficient to form a stable dispersion with the slightest agitation where the kinetic energy of the molecules is sufficient to achieve dispersion.[102]

Micelles are microscopically organised chemical assemblies formed by self-aggregation of individual surfactant molecules. Micelle exist as monomers in very dilute solutions but when the concentration exceeds the critical micellar concentration (cmc) of the surfactant, the monomers associate spontaneously, forming aggregates of colloidal dimensions called micelles. As the surfactant concentration increases above the cmc, the addition of fresh monomer results in the formation of new micelles in such a way that the monomer concentration in solution remains essentially constant and approximately equal to the cmc. Thus, the micelles are in dynamic equilibrium with the dissolved monomers of the surfactants, which remain at an approximately equal concentration after the cmc has been reached. Micro-emulsions can evolve from the addition of oil to a micellar (aqueous solution of surfactant) and the resulting swollen micelles gradually change into micro-emulsion droplets with further addition of the oil (Figure 1.10).

Water-in-oil micro-emulsions are topologically similar to reverse micelles in that polar heads of the amphiphile are oriented inward and the nonpolar tails are oriented towards the oil continuum. Compositions having mobile or free water satisfying the

hydration requirements of the amphiphile head groups and counter ions are then called micro-emulsions. Mixtures of water, oil and non-ionic amphiphiles separate within a well-defined temperature interval into 3 liquids phases: an aqueous phase, oil-rich and amphiphile-rich phases. In the amphiphile-rich phase the maximum mutual solubility between water and oil can be found combined with a minimum interfacial tension. The temperature range in which micro-emulsion are formed is shifted systematically depending on the length of the alkyl or ethylene oxide chain of the amphiphile and the polarity of the organic medium.[103]

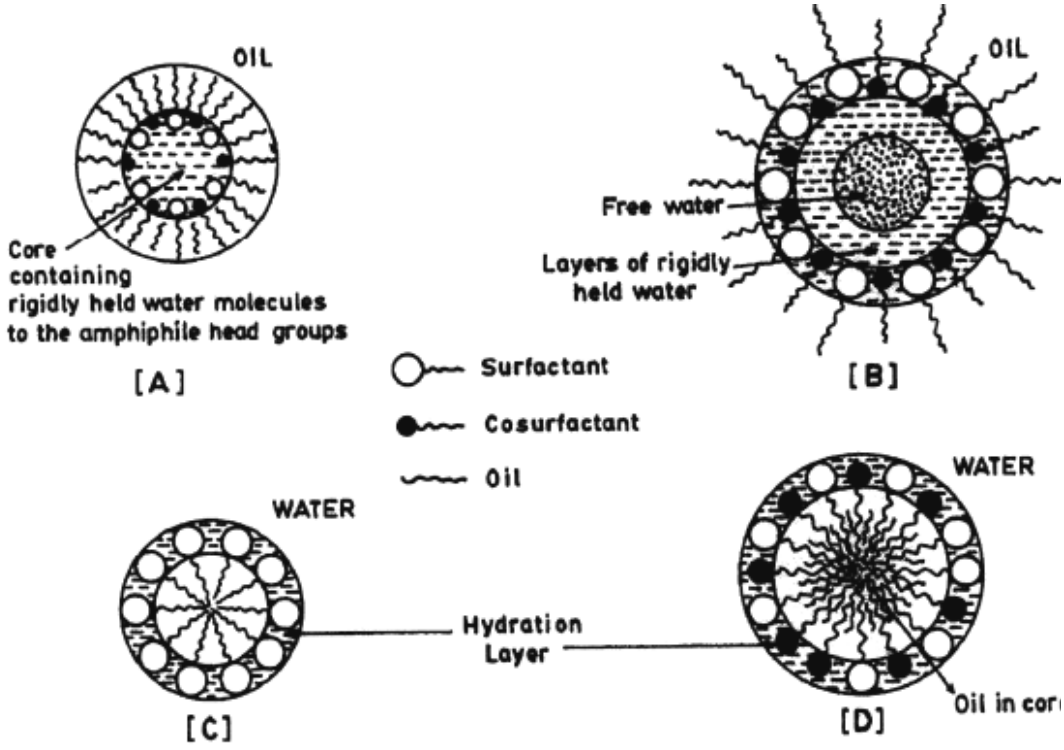

Figure 1.10. Pictorial representation of micelles and micro-emulsion: A) reverse micelle, B) water-in-oil micro-emulsion, C) normal micelle, and D) oil-in-water micro-emulsion

1.8.2.2 Macro-emulsion

Macro-emulsion (normally termed emulsions), on the other hand, have larger particle size (200-10000 nm in diameter), are not transparent, have short stability and limited handling. They are, therefore, kinetically stable in comparison to the thermodynamically stable micro-emulsion, which can be formed spontaneously using the thermal energy of the system. In emulsion the dispersed phase and the dispersion medium are both fluids. The most common fluids are oil and aqueous media. These may be of two types: oil-water-emulsions (fine oil droplets dispersed in the aqueous phase) or water-in-oil emulsions (aqueous droplets dispersed in oil). A discontinuous emulsion is formed when one phase forms a continuous network in the other. Dispersions of fine gas bubbles in liquid have been found to exist in solutions of gas at high pressure in liquids (e.g. carbonated drinks). An aerosol can also be considered as a dilute liquid-in-gas emulsion.[104]

In order to tell the difference between the types of emulsions, the effect of dilution of one of the phases can be studied such as adding water to an oil-in-water emulsion to dilute it. Adding oil, however, causes the oil phase to form a separate layer. Oil-in-water emulsion has electrical conductivities similar to those of the water phase, whereas water-in-oil emulsions are not significantly electrically conductive. Water-in-oil emulsions can be coloured by oil soluble dyes but oil-in-water emulsions are only faintly dyed. The converse is true when water-soluble dyes are used. If the two phases have different refractive indices, microscopic examination of the droplets will reveal their type. A droplet will appear brighter if its refractive index is greater than the continuous phase- this is used to identify the component if the refractive indices are known. In filter

paper tests, a drop of an oil-in-water emulsion produces an immediate wide and moist area while a water-in-oil emulsion does not.[105]

As previously mentioned, emulsions are formed by the dispersion of droplets of the liquids into the other. This causes a large increase in the interfacial area and the accompanying free energy make the system thermodynamically unstable. The presence of the emulsifying agent helps to stabilise the interfacial regions. It does this by reducing the interfacial tension between the two liquids so that the increase in energy associated with increase in area is reduced. It also reduces the rate of coalescence of the dispersed liquid droplets by forming mechanical, steric and/or electrical barriers around them. The steric and electrical barriers prevent droplets from getting too close enough to coalesce. The mechanical barrier increases the resistance to coalescence up on shock or shear.[104]

The stability of emulsions is affected by:

- The physical nature of the interfacial film: A condensed film with very strong lateral forces and good elasticity will be an excellent barrier to collision coalescence. Preparing a system where the interfacial components push the surfactant film into the liquid crystal phase creates a highly viscous phase. This phase resists coalescence and sterically prevents molecules from getting close enough for van der Waals forces to cause attraction.
- Electrical or steric barriers: The presence of charge on the dispersed droplets will cause electrostatic repulsion.
- Viscosity: If the continuous phase has a high viscosity, the motion of the dispersed phase and their diffusion will be slowed and the rate of coalescence will be minimised.

- The size distribution of the droplets: This affects stability where a more uniform distribution causes a more stable emulsion. Ostwald ripening causes the larger droplets in a broad range of droplets to grow at the expense of the small droplets.
- The volume of the dispersed phase: As the volume of the dispersed phase increases, the continuous phase must spread out further to cover all the droplets. This increases the probability of collision and decreases the emulsion stability.
- Temperature: Emulsions are very sensitive to temperature changes and are more stable when the temperature is near the point of minimum solubility of the emulsifying agents.

Inversion between emulsion types can be carried out by changing the: (i) order of mixing of components; (ii) nature of the emulsifier; (iii) volume ratio of water to oil; (iv) phase in which the emulsifier was originally dissolved; (v) temperature of the system and (vi) amount of electrolyte.

1.8.3 Preparation of emulsion

1.8.3.1 Emulsifier and HLB values

Amphiphilic surfactants are characterised by the hydrophile-lypophile (HLB), which is a relative ratio of polar and no-polar groups in the surfactant.[106] This is based on the theory proposed by Griffin that emulsifying agents contain oil-soluble and water-soluble groups. It is the balance of the size and the strength of these groups that is referred to as HLB.[107] A surfactant that is lipophilic in character is assigned a low HLB value (below 9) and one that is hydrophilic is assigned a high HLB value (above 11). Those in the range of 9-11 are intermediate. The HLB of a surfactant or blend of surfactants is an excellent indication of what the surfactant system will do whether it will

make an oil-in-water emulsion or a water-in-oil emulsiom, or even act as a solubiliser for some oil (Table 1.4). The HLB of a surfactant class or blend is also an indication of the efficiency of chemically related surfactants, or of a blended pair of surfactants, for performing any given emulsification task. The HLB is not an indication of the relative efficiency of one class to another. The "class" efficiency is more related to chemical structure and the relationship to the chemical structure of the material to be emulsified.

Table 1.4. Classification of surfactants by HLB values

HLB range	Use
4-6	W/O emulsifier
7-9	Wetting agent
8-18	O/W emulsifier
13-15	Detergent
10-18	Solubiliser

Knowing the HLB value, the chemical type of surfactant can be matched to the oil. As previously mentioned, the HLB allows for the blending of two surfactants in order to achieve the exact HLB needed instead of using only one surfactant. The blend can be adjusted to suit the oil or other active ingredients instead of adjusting the active ingredient to suit the surfactant. The most stable emulsion system usually consists of blends of two or more surfactants where one has lipophilic tendencies and the other hydrophilic. The right chemical type is related to the chemical family of the surfactant whether it is stearate, laurate, palmitate or oleate, each blended to have the correct HLB. For example, a polyethoxy sorbitan oleate ester type of blend (Tween 80) with its unsaturated lipophilic oleate "tail" in the oil is compatible with oils having unsaturated bonds. Tween 60 (stearate), Tween 20 (laurate) and Tween 40 (palmitate) are all more

compatible with oils having saturated bonds. Thus, although both oils might require the same HLB, which these types of surfactants have, the emulsifier, which attracts the oil, will be more effective.

This classification system completely disregards the interaction of the surfactant with the oil and only considers water solubility.[108] Surfactants with low HLB are more oil soluble and are thus suitable for preparing water-in-oil emulsions whereas those surfactants with high HLB values have good water solubility thereby rendering them suitable for oil-in-water emulsions. Among non-ionic surfactants comprised of ethylene oxide segments, the larger the portion of ethylene oxide units (hydrophilic part of the surfactant molecule), and the more water-soluble will be the surfactant. The hydrophobic part of the surfactant embeds itself in the oil droplet and the hydrophilic ethylene oxide part interacts with the water to surround the oil droplet and form an emulsion. Surfactant must remain in solution to perform their function. In contrast to salts, which dissolve more readily in hot water, the solubility of non-ionic surfactant has a temperature limit termed as cloud point. At this temperature the surfactant drops out of solution and causes the solution to become turbid. Surfactant activity and performance are usually at an optimum below the cloud point.

The deficiency in the HLB scheme prompted the development of the PIT (Phase inversion Temperature) system by Shinoda,[109] which provides information about the types of oils, phase volume relationships and concentration emulsifier. It was established on the idea that the HLB of a non-ionic surfactant changes with temperature and that the inversion of emulsion type occurs when the hydrophile and lipophile tendencies of the emulsifier are just balanced. No emulsion would form at this temperature. Emulsions

stabilised with non-ionic surfactants are oil-in-water types at low temperatures and invert to water-in-oil types with temperature.

1.8.4 Multiple emulsion systems

Water-in-oil-in-water (W/O/W) multiple emulsions are emulsion systems where in small emulsion droplets are in turn dispersed in a continuous water phase. The presence of a reservoir phase inside droplets of another phase can be used to prolong release of active ingredients. Thus multiple emulsions find applications in pharmaceuticals and cosmetics.[110]

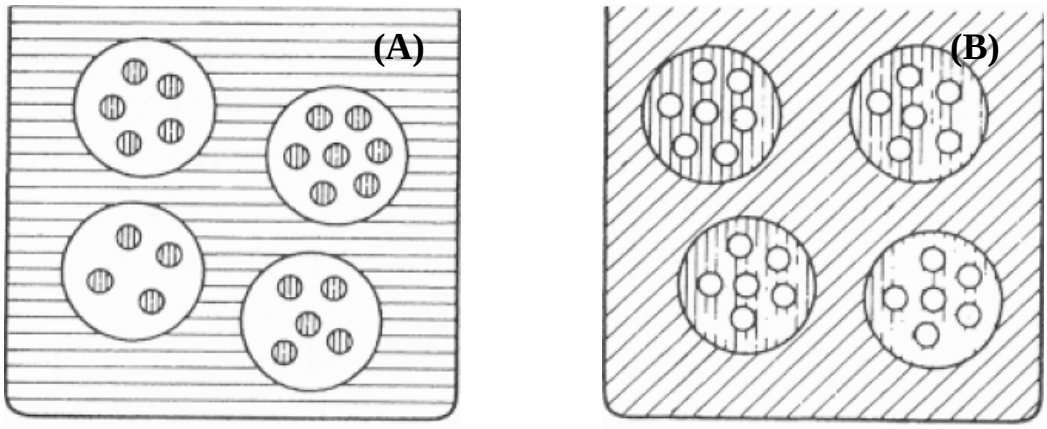

Figure 1.11. (A) W/O/W double emulsion, (B) O/W/O double emulsion

As shown in Figure 1.11 two types of multiple emulsions known are (A) W/O/W double emulsion and (B) O/W/O double emulsion. Consider for either diagram: each interface needs a different HLB value. The curvature of each interface is different. Multiple emulsion W/O/W emulsions contain both W/O and O/W simple emulsions and require at least two surfactants in the system.[111] One that has low Hydrophile-Lipophile Balance (HLB) value stabilises the primary W/O emulsion and one that has a high HLB value stabilises the secondary O/W emulsion,[112] The low HLB surfactant is dominantly

hydrophobic and is added to the oil phase. The high-HLB surfactant is dominantly hydrophilic and is added to the outer aqueous phase.

The concentration ratio of these two surfactants is important to obtain stable and high yields of W/O/W emulsion.[111] There are two interfaces in a W/O/W emulsion. The primary interface, lying between the inner aqueous phase and the oil phase, contains the low-HLB surfactant. In contrast, both the high and low HLB surfactants are present at the secondary interface (between the multiple droplets and the outer continuous aqueous phase).[113]

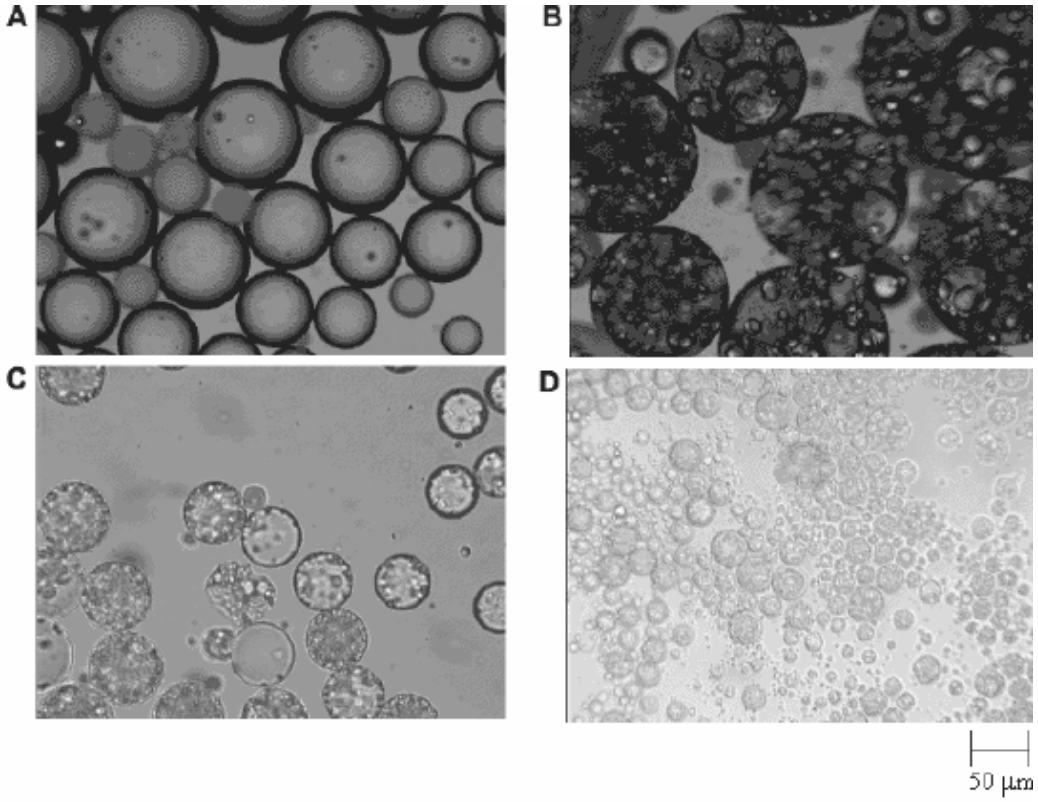

Figure 1.12. Photomicrograph of freshly prepaid W/O/W emulsions Vs surfactant concentration in oil phase. A) 0.1 %; B) 1.0 %; C) 5 % and D) 20%
***AAPS PharmSci* 2003; 5(1) Article 7 (http:// www.pharmsci.org)**

When the hydrophilic surfactant in the continuous aqueous phase exceeds its critical micelle concentration, the resultant micelles may solubilise the hydrophobic surfactant that was originally present in the oil phase and carry it into the outer continuous aqueous phase, resulting in a decrease in the concentration of hydrophobic surfactant in the oil phase. This can eventually lead to rupture of the oil layer and loss of the internal aqueous droplets.[114] A high concentration of hydrophobic surfactant will be needed to prevent the oil layer from rupturing. On the other hand, to avoid any potential toxicity associated with surfactants, pharmaceutical preparation would require a minimal concentration of the hydrophobic surfactant. Therefore, the optimal concentration of hydrophobic surfactant needed is determined during formulation development. Figure 1.12 shows the influence of surfactant concentration on the formation of dispersed doplets in the continuous oil phase.

1.8.5 Concentrated emulsion: High internal phase emulsions (HIPE)

High internal phase emulsions (HIPEs) are dispersions of water in a continuous oil phase with internal phase volumes up to 99 %, that is the water, although the majority phase, is not continuous. They form readily on adding water slowly to a stirred solution of a surfactant of low hydrophilic–lipophilic balance (HLB) dissolved in the oil phase. The internal or discontinuous phase has to be at least 74 % of the emulsion volume, as this is the theoretical volume of a cubic close packing of spheres. Lissant classed high internal phase emulsions, or HIPEs, as emulsions containing grater than 70 % phase volume. A more precise definition is that HIPE have an internal phase or discontinuous phase volume above 74.05 %.[115] This figure represents the maximum volume occupiable

by a number of uniform spheres packed into a given volume in the most efficient manner.[116]

These concentrated emulsions have been referred to by a number of different names in the literature, including high internal phase ratio emulsions (HIPREs),[115,117-121] gel-emulsions[122-128] and hydrocarbon gels.[129, 130]

1.8.5.1 HIPE formation

The first criteria for the formation of a HIPE are, of course, the presence of two immiscible liquids, one of which is water (or aqueous solution), almost without exception. The nature of organic, or oil, phase can vary to a considerable extent, although the most stable HIPEs are generally produced with more hydrophobic liquids. However, it is the nature of the surfactant employed to stabilise the HIPE, which will ultimately facilitate its formation. Above a certain critical limit of internal phase volume, an emulsion will tend to invert to the opposite type, i.e. oil-in-water (O/W) emulsion will become the water-in-oil (W/O) variety, and *vice-a-versa* (Figure 1.13). This can be prevented from occurring by careful choice of surfactant, such that it is completely insoluble in the dispersed phase of the emulsion. The HIPE is formed generally by careful addition of the internal phase to solution of surfactant in the external phase, under constant agitation. HIPEs may form under other circumstances, however.[131] When a centrifugal field is applied to an emulsion, the droplets can be forced into contact with each other and deformation into polyhedra occurs. The excess continuous phase is forced out of the emulsion, forming a separate phase. This process is known as “creaming”.

Additionally, emulsion may creamed over a period of time under the influence of gravity, forming a layer of HIPE either on the top of the dilute emulsion, in the case of oil-in-water emulsions, or below the bullk emulsion for W/O system.

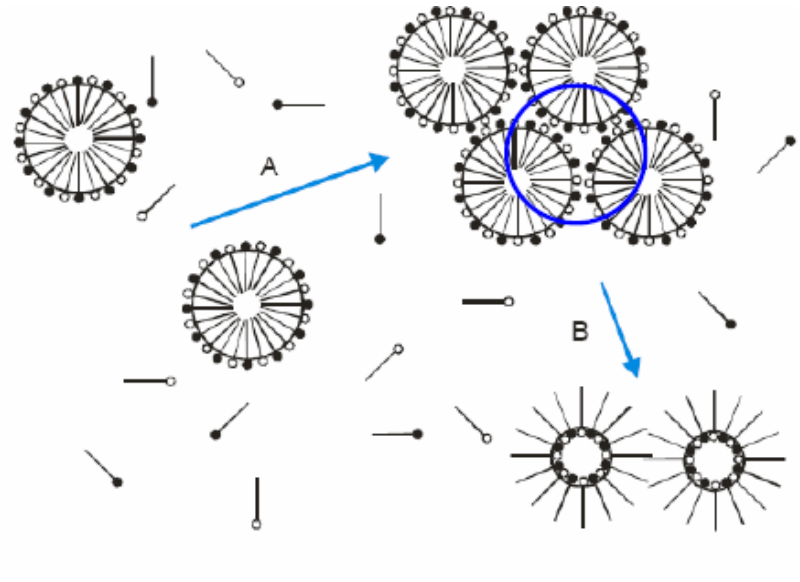

Figure 1.13. Phase inversion

1.8.5.2 Geometry of droplets in high internal phase emulsion

It has been known that if a monodisperse system of rigid spheres is packed in the most advantageous manner, the spheres will occupy a little over 74% of the total volume of the system. However, a higher density can be achieved by carefully arranging the spheres as follows. Start with a layer of spheres in a hexagonal lattice, then put the next layer of spheres in the lowest points you can find above the first layer, and so on as shown in Figure 1.14. This natural method of stacking the spheres creates one of two similar patterns called cubic closed packing and hexagonal close packing. Each of these two arrangement has an average density of ~ 74%. The Kepler conjecture says that this is the best that can be done-no other arrangement of spheres has a higher average density than this.

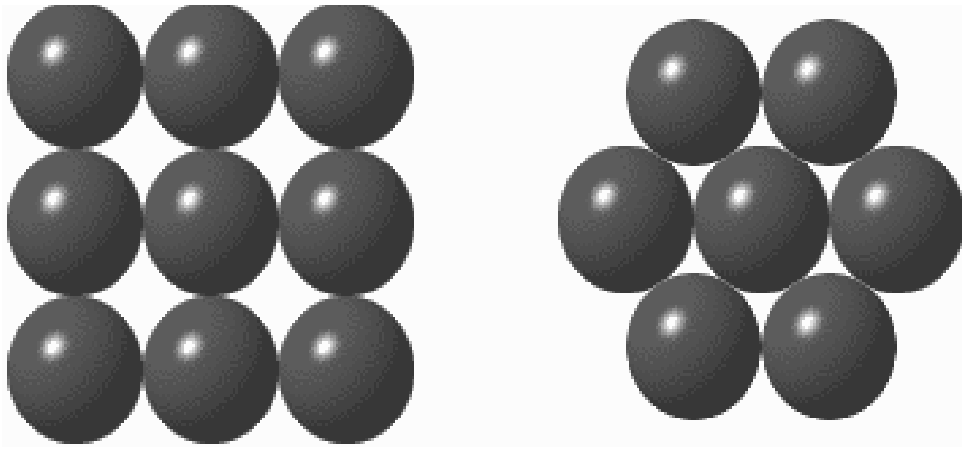

Figure 1.14. Highest possible volume occupied by solid spheres

According to the definition, HIPE contain an internal phase volume fraction greater than 0.74. Since this is the maximum volume which can be occupied by uniform, unreformed spherical particles, the dispersed phase droplets must either be non-uniform, i.e. polydisperse, or deformed into non-spherical, polyhedral cells.

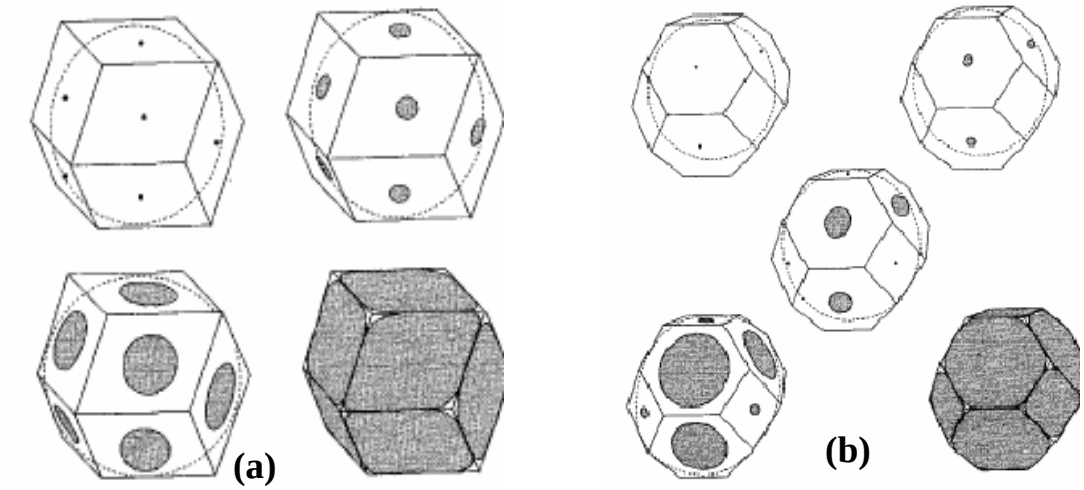

Figure 1.15. Transition from sphere to polyhedra: (a) rhomboidal dodecahedron and (b) tetrakaidecahedron [117]

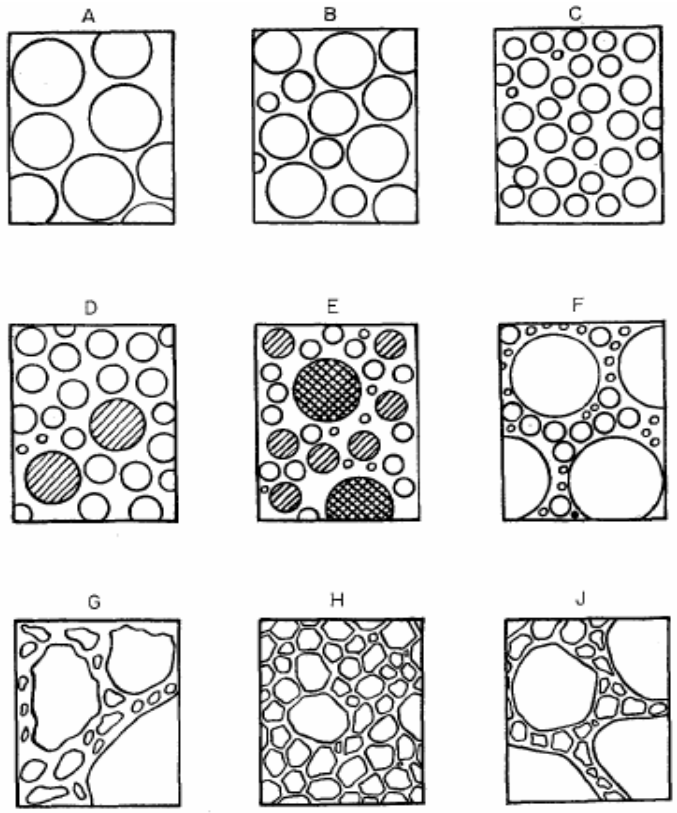

Figure 1.16. Different geometry of dispersed droplets in concentrated emulsion [119]

The first production of true high-internal-phase- ratio emulsions (greater than 74 % by volume internal phase) was in the late 1950's. In 1965 Becher cited examples of high-internal-phase-ratio emulsions.[132] In theoretical treatment of the geometry of HIPEs Lissant showed that, for a monodispersed system, the dispersed phase droplets would assume a rhomboidal dodecahedral (RDH) packing from 74 % to 94 % internal phase volume, with increasing deformation into polyhedra.[119] Above 94 %, the packing changes to tetrakaidecahedral (TKDH) (truncated octahedral) as shown in Figures 1.15 (a) and (b). Figure 1.16 shows the different geometries of dispersed droplets formed during the high internal phase preparation influenced by different parameter such as water to oil ratio, stirring speed, surfactant types and concentration, etc.

1.8.5.3 Polymerisation of continuous phase

When polymerisation is triggered in a high internal phase emulsion (HIPE) in which the continuous phase contains one or more monomeric species, a novel type of highly porous material is produced. Polymers of this type are referred to as PolyHIPE, using the nomenclature devised by Unilever scientists.[133]

In case the continuous phase consists of, or at least contains, polymerisable monomers, HIPEs can be used for polymerisations to produce isotropic, open celled, polymeric foams (PolyHIPEs).[134] In 1996, Li Benson of Biopore Corporation advanced this technology and succeeded in producing HIPE polymers as distinct, spherical particles, Unilever's approach yielded polymers in blocks.[135] The spheres exhibit the same physical characteristics of the original Unilever material in that these are composed of large, micrometer-size cavities that are interconnected by smaller pores. The polymers are further characterised by especially high porosity with void volumes in the range 70% to 90%. This results in a highly permeable structure that gives a low-density product. A photograph of this unique morphology is shown in Figure 1.17.

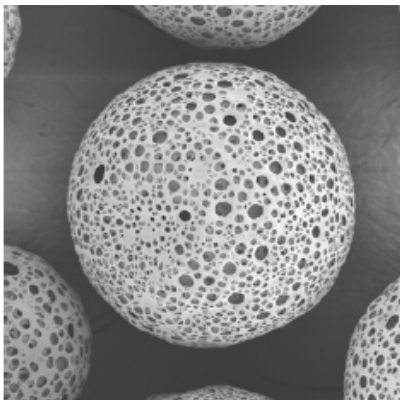

Figure 1.17. Porous morphology of spherical polyHIPE material[136, 137]

A range of polyHIPEs have been prepared by polymerisation of the styrene-divinylbenzene continuous oil phase of a number of high internal phase emulsions (HIPE).[138] The aqueous internal, or discontinuous, phase constituted approximately 90 vol.% in each case and consisted of small droplets approximately 10 μm in diameter. Complete removal of the aqueous phase was achieved after polymerisation by exhaustive extraction with hot ethanol, leaving monolithic polyHIPEs with completely interconnected cellular structures and an overall very low bulk density. By adjustment of the amount of cross-linker (divinylbenzene) and by use of either a precipitating porogen, petroleum ether, or a solvating porogen, toluene, in the comonomer oil phase, a secondary pore structure could be generated within the cell `walls' of the polyHIPEs. Overall surface areas between 3 and 350 m^2/g were achieved. Scanning and transmission electron micrographs confirmed the cellular structure of the polyHIPEs, and the porous structure of their walls.

The formation of the interconnected morphology of open-cell styrene/ divinylbenzene (DVB) co-polyHIPEs has been studied by scanning electron microscope (SEM) on frozen HIPE samples at different stages of polymerisation by cryo-SEM.[139] The transition from discrete emulsion droplets to interconnected cells occurred around the gel-point of the polymerising system. This suggests that the formation of holes between neighbouring cells is due to the contraction of thin monomeric films on conversion of monomer to polymer, as a result of the entropic forces and conformational restrictions of the latter (Figure 1.18). Their defining characteristic is an internal (droplet) phase volume ratio of greater than 96%, this number representing the maximum volume

that can be occupied by uniform spheres when packed into a given space in the most efficient packing arrangement as shown in Figure 1.19.

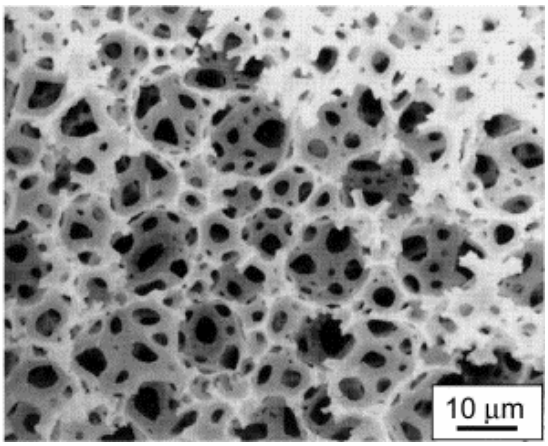

Figure 1.18. SEM micrograph of a poly(styrene-co-DVB) foam[139]

In HIPEs, therefore, the droplets are either spherical and polydisperse, or are deformed into polyhedrons. The materials themselves are highly porous and, usually, extremely permeable, due to a very high degree of interconnection between cavities throughout the matrix. The morphology shown in Figure 1.19 is quite striking and is rather different from that of foams prepared by other techniques, such as gas blowing. The large spherical cavities are termed 'voids', whereas the circular holes connecting adjacent voids to one another are known as 'interconnects'.

The type of porogen added to the continuous phase of HIPEs containing divinylbenzene can strongly influence the morphology of the resulting foams. The cell size was reduced, as the solvent became a better co-surfactant. This caused the windows connecting adjacent cells to increase, to such an extent that the cellular morphology was lost and the porous gels were mechanically very weak. This could be compensated by

appropriate mixtures of solvents to optimally produce materials with good mechanical properties, having a cellular morphology and surface areas up to 554 m^2 g^{-1}.

Microporous polymer synthesised by suspension polymerisation | **Macroporous polymer synthesised by suspension polymerisation** | **Microporous polymer synthesised by HIPE polymerisation**

Figure 1.19. Schematic diagram showing the comparative pore architecture in porous polymers

Elastomeric and highly porous PolyHIPE had been prepared by polymerisation of the continuous phase of high internal phase emulsions (HIPEs) containing styrene, divinylbenzene and varying amounts of either 2-ethylhexyl acrylate or the corresponding methacrylate.[140]

Thermally stable polyHIPEs were prepared from the engineering plastic material poly(aryl ether sulphone) (PES).[141] For that, a maleimide-terminated aryl ether sulphone macromonomer was copolymerised with styrene, divinylbenzene (DVB), or a bis(vinyl ether) species in the continuous phase of a HIPE. Furthermore, a novel, non-aqueous HIPE methodology was employed, since only dipolar aprotic solvents were able to cosolubilise the polymeric precursor and surfactant. HIPEs of petroleum ether, dispersed in a dipolar aprotic solution of maleimide-terminated PES, poly(ethylene oxide)-*b*-poly(propylene oxide)-*b*-poly(ethylene oxide) (PEO-PPO-PEO) block copolymer surfactants, co-monomer, and 2,2'-azobisisobutyronitrile (AIBN), were used for

polymerisation. The cellular structures and porosities of the resulting materials were characterised by SEM, solvent imbibition, mercury porosimetry, and a BET evaluation of nitrogen adsorption results. All synthesised systems possessed an open-cellular morphology and a secondary pore structure within the polymer walls.

An alternative method for the preparation of highly porous monolithic polymer material is polymerisation of the continuous phase of a high internal phase emulsion (HIPE). Typically, the yielding polymer has an open cellular structure with interconnects, which is the result of the internal phase being trapped inside the continuous phase during the polymerisation. After the extraction of internal phase, the porous structure remains. Such monolithic polymers, termed PolyHIPE[133] were initially prepared as styrene/divinylbenzene copolymers and applied as precursors for reactive species,[142] as biocatalysts supports[143] and as supports for filtration.[144] With the addition of 4-vinylbenzyl chloride as a monomer, a reactive PolyHIPE monolith was produced, functionalised and utilised as a scavenger in a flow through mode.[145] The porosity of such a material can be further enhanced by adding a porogenic solvent to the continuous phase and monoliths with surface area up to 700 m^2/g were prepared in such manner.[146]

1.8.5.4 Porous structures

As indicated earlier, resins can be classified under three categories: (a) microporous (b) macroporous and (c) macroreticular. Microporous resins are prepared from a vinyl monomer and a difunctional vinyl comonomer in the absence of any solvating media (porogen). In the dry state they are microporous, with polymer chains being separated by intermolecular distances. The preparation of macroporous resin is the

same as microporous resin but with the inclusion of an inert solvent (porogen). When the solvent solvates both monomer and polymer a fully expanded network is formed with a considerable degree of porosity. Removal of solvent causes a reversible collapse of the matrix and in the dry state such matrix are called microporous resin. Figure 1.20 clearly shows that irregular pores are formed in the suspension polymer while more uniform pores are formed in HIPE, in which cells and windows are present due to stable emulsion with appropriate choice of surfactant.

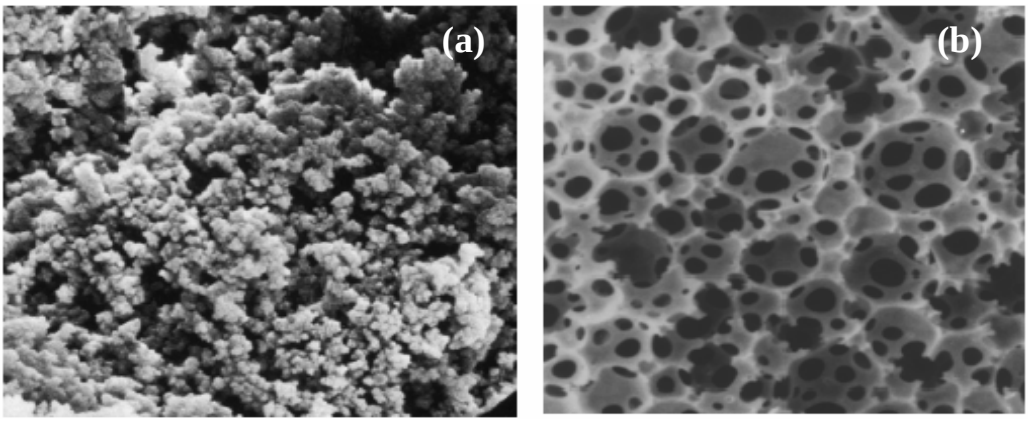

Figure 1.20. SEM microstructure showing the internal phase morphology, (a) microporous polymers by suspension and (b) microporous polymers by HIPE

Macroreticular resins are formed when solvent used is freely miscible with monomer but is a precipitant for polymer. These resins are highly porous and rigid which retain the overall shape and volume once the precipitant is removed. The structure of these resins are quite different from those of microporous and macroporous resins. They have large and permanent pores and reaction sites may be regarded as being located on a permanent interior surface of the resin.

1.8.5.5 Formation of porous structure

The free-radical cross-linking copolymerisation system for the production of

macroporous copolymers includes a monovinyl monomer, a divinyl monomer (cross-linker), an initiator and inert diluent. The decomposition of the initiator produces free-radicals which initiate the polymerisation and cross-linking reactions. After a certain reaction time, a three-dimensional network of infinitely large size may start to form. The term `infinitely large size', according to Flory, refers to a molecule having dimensions of an order of magnitude approaching that of the containing vessel.[147] At this point (the gel point) the system (monomer–diluent mixture) changes from liquid to solid-like state. Continuing polymerisation and cross-linking reactions decrease the amount of soluble reaction components by increasing both the amount and the cross-linking density of the network. After complete conversion of monomers to polymer, only the network and the diluent remain in the reaction system.

Cross-linked copolymers prepared by free-radical cross-linking copolymerisation exhibit different structures and properties depending on the amounts of the cross-linker and the diluent present during the reactions as well as on the solvating power of the diluent. In free radical cross-linking copolymerisation, inhomogeneous gel formation always occur due to the fact that the cross-linker has at least two vinyl groups and therefore, if one assumes equal vinyl group reactivity, the reactivity of cross-linker is twice that of the monomer. As a consequence, the cross-linker molecules are incorporated into the growing copolymer chains much more rapidly than the monomer molecules so that final network exhibits a cross-link density distribution.[148]

Dusek proposed that a phase separation occurred during gel formation, proceeding either in the form of macrosynersis or microsynersis.[149] The sensitive dependence of the properties of the porous structure on the synthesis parameters allows

one to design a tailor-made macroporous material for a specific application. The main experimental parameters are the type and the amount of the diluent, the cross-linker concentration, the polymerisation temperature and the type of initiator. Extensive study of macroporous morphology and formation of porous structure have been conducted for beaded, cross-linked styrene-divinyl benzene resins.[150,151] The internal structure of the resin beads can be controlled by different parameters in the polymerisation process, such as the amount of cross-linking monomer used, type and volume of diluent/porogen/pore generating solvent (an inert organic solvent) added to the monomer phase.

1.8.5.6 Effect of the porogen on the formation of porous structure

Porous structures start to form when the amount of the diluent (porogen) and the amount of the cross-linker pass a critical value. The solvating power of the diluent has a critical effect on the porous structure of macroporous copolymers. The net solvating power of the medium (unreacted monomer mixture + diluent) changes during the course of the reaction as the monomers get consumed and this change is particularly severe where the diluent is a non-solvent for the copolymer.

The preparation of macroporous copolymer beads is generally achieved as a result of the phase separation, which occurs during the copolymerisation of a monomer mixture containing appropriate amounts of monomer, a cross-linking comonomer and a porogenic solvent. Surface morphology generated by porogen is seen in Figure 1.21 for (a) suspension polymerisation and (b) HIPE polymerisation where through and through openings are seen at the surface.

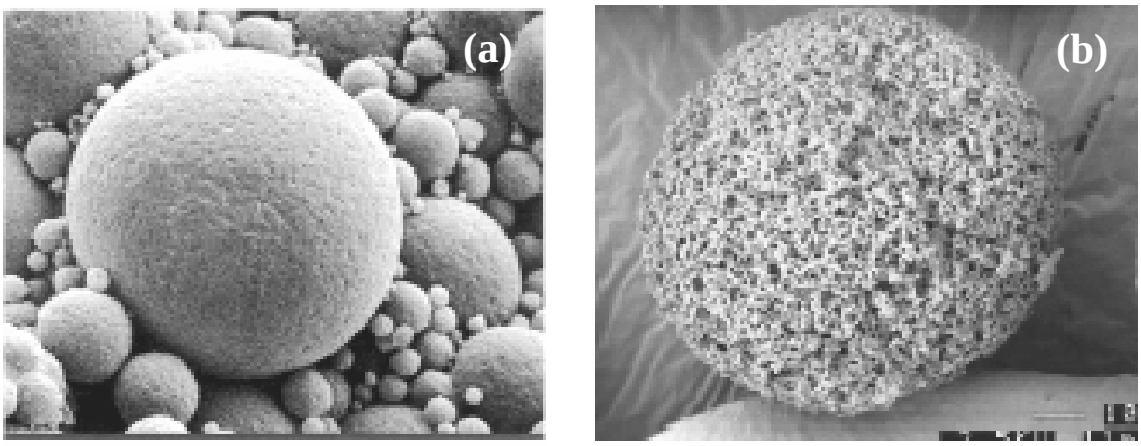

Figure 1.21. SEM micrograph of surface morphology of polymers prepared by (a) suspension polymerisation and (b) HIPE polymerisation

The porogen is a low molar mass or polymeric substance that is miscible with the monomers but does not react during the copolymerisation and at the end of the reaction can be easily removed from the formed copolymer product.[152] The porogen may remain in the network (gel) phase throughout the copolymerisation, resulting in the formation of expanded (swollen) particles or may separate out of the network phase resulting in the formation of porous particle. The distribution of the diluent between network and diluent phases (diluent in the pores) at the end of the copolymerisation determines the total porosity of the resulting copolymer and their swelling ratio in solvent. Control of porosity by porogen, therefore the effective surface area, has been extensively investigated for polystyrene, polyacrylamide, polymethacrylates etc.[153-177] Three main classes of porogens known are: (i) solvents for the polymer (ii) non-solvents and (iii) polymers soluble in the monomer(s).[178,179]

Polymeric porogens produce only large pores. The molecular weight is then an important parameter. The pore volume is large when the molecular weight of the porogen is high.[180] The most complex and frequently investigated systems are those incorporating

a non-solvating diluent.[181] Here, as initially proposed by Kun and Kunin[182] and later observed experimentally by Jacobelli *et al*, the bead contains large agglomerates of microspheres (100-200 nm).

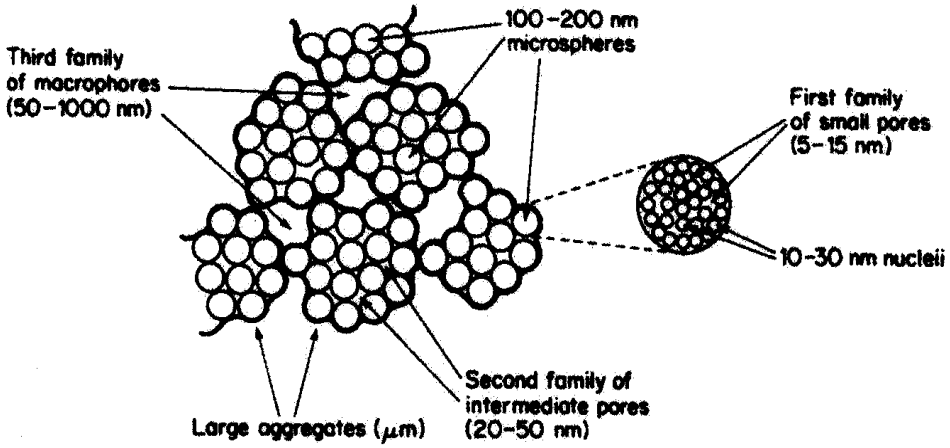

Figure 1.22. Schematic representation of the structure of macroporous domain

Each microsphere consists of smaller nuclei (10-20 nm), which are more or less fused together. In between the nuclei, there is a first family of very small pores (5-15 nm), which are mainly responsible for high surface areas of these materials. In between the microspheres a second family of intermediate pores (mesopores) is observed (20-50 nm) which account for moderate surface areas (up to 100 m^2/g). A third family of pores is responsible for higher pore volumes, which can be seen when very high relative volume of diluent is used. Figure 1.22 represents the macroporous resin structure. The choice of porogen has a great influence on the shape and size of pores. The task of this porogen is to create cavities in the polymeric structure by dissolution of the monomer, while acting as a precipitant towards the growing polymer. Naturally, the total amount of porogenic solvent in the polymerisation mixture has to be sufficiently large to ensure a porous

structure and a pore volume that allows operation at reasonably low pressures in a flow through system.

The polymer phase separates from the solution during polymerisation because of its limited solubility in the polymerisation mixture that results from either (or both), a molecular weight that exceeds the solubility limit of the polymer in the given solvent system or insolubility derived from cross-linking. The presence of porogen in the monomer phase is necessary if porous beads are to be obtained. In its absence, only non-porous, transparent beads are formed. However, some non-porous beads also appeared among the opaque porous beads. This was related to the phase separation occurring before the gel point when the thermodynamically poor diluent partly separates from the polymerisation mixture. Polymerisation then results in non-porous beads.

1.9 Functionalisation of porous polymers

For all physical applications, implementation of a distinct pore structure into the polymer gel is sufficient to obtain the desired properties, e.g. lightweight design or low dielectric constant. For chemical applications, another (practically orthogonal) parameter is key, namely the polarity and the chemical functionality of the very large surface of the pore system. This surface structure determines wettability or hydrophilicity/ hydrophobicity, which are important for solvent uptake and interaction with the environment. Distinct chemical groups are important for selective binding or the catalytic properties. The demand for functional polymers has been increasing. A functional polymer has chemically bound specific functional groups that can be used as a reagent, catalyst, protecting group etc. or performs a specific function (imbibing). It is one of the very big advantages of porous polymers (as compared with the porous inorganics) that

this functionalisation is comparably easy and is sometimes just performed by copolymerisation with an appropriate functional co-monomer.

The polymer can be modified by active functional group introduced into the polymer chain using following processes by:

(i) direct polymerisation/copolymerisation of monomers containing the desired functional group;

(ii) chemical modification of preformed polymer or

(iii) a combination of both of above.

A difficulty may arise in the process (i) due to considerable manipulation of co-polymerisation procedure which is necessary to ensure a good yield of the required polymer. The second process is reliable because the functional group can be easily introduced by using standard organic synthetic procedure. The chemical modification of a resin can depend substantially on the physical properties of the resin. Functionalised polymeric support must possess a structure which permits adequate diffusion of reagent into the reactive sites, a phenomenon which depends on the extent of swelling, the effective pore size, pore volume and the chemical and mechanical properties of the resin under conditions of particular chemical reaction. Figure 1.23 shows the post-modification of polyHIPE materials with different chemical moieties.

Functionalisation of highly cross-linked porous poly(styene-co-divinylbenzene) beads with tert-butyl groups resulted in a material suitable for very fast separation of pollutants.[183] By functionalisation of porous resin particles resin-loaded membranes were produced which can be used for solid-phase extraction (SPE).[184] Using such efficient particles for separation could replace liquid extraction procedures, which require large

amounts of organic solvents.

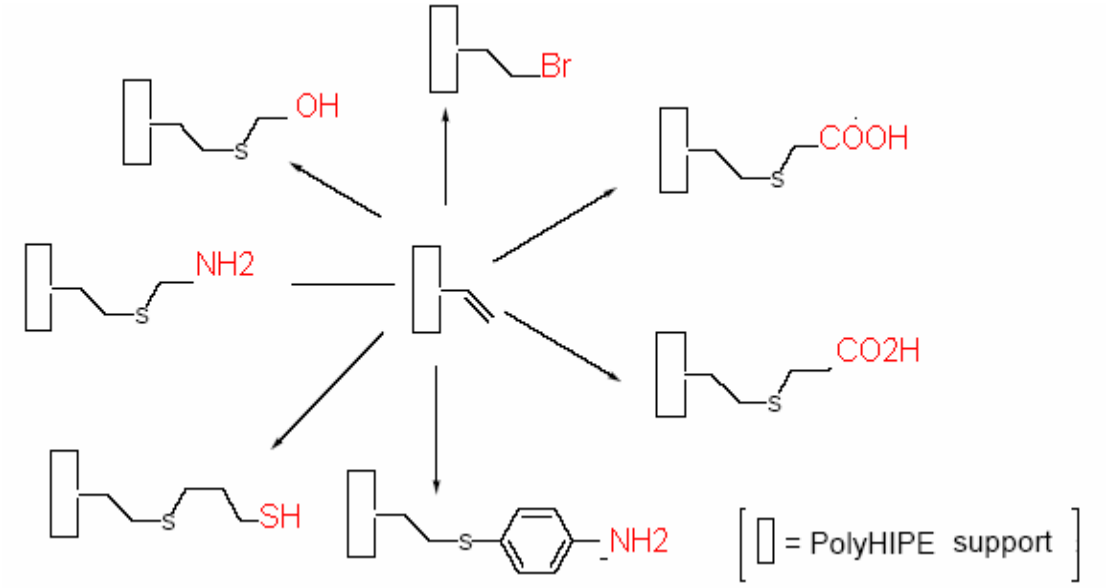

Figure 1.23. Different chemical post-modification of polyHIPE materials

A continuous monolith of porous poly(glycidyl methacrylate-co-ethylene dimethacrylate) has been prepared by a free radical polymerisation within the confinement of a 16 mm glass column.[185] The epoxide groups of the polymer have been modified *in situ* by their reaction with diethylamine to afford the ionisable weak base 1-N,N-diethylamino-2-hydroxypropyl functionalities that are required for the ion-exchange chromatographic mode. A copolymer comprised of glycidyl methcrylate and N,N-methylene bis(acrylamide) has been described that can used to coat solvent-impregnated resin (SIRs). Vinyl groups on the surface of a cross-linked macroporous support were used to anchor the polar copolymer to the surface of the bead. The coated SIR containing di(2-ethylhexyl) phosphoric acid maintained a high level of metal ion complexation [96 % Cu (II)] over five cycles while the uncoated SIR dropped from 93% to 11 % Cu(II) complexed in three cycles.[186]

PolyHIPES bearing pendant vinyl functionality were prepared by chemical

postfuctionalisation.[187] The large pores and large channels of polyHIPEs allow liquids and solvents to be driven through the molded monolith at very low pressure. A number of electrophilic substitution reactions, namely sulphonation, nitration and bromination were performed for the functionalisation of highly porous poly(styrene/DVB) polyHIPE monoliths.[188] Mild hydrophobic reagents and homogeneous reaction conditions were sought in an effort to achieve uniform chemical modification at a reasonable degree of substitution throughout the large porous polymer gel. Disks obtained by polymerisation of high internal phase emulsions had completely open pore structures and were used as a carrier material for the immobilisation of 10-ethyl-*iso*alloxazine (flavin).[189] Three methods for immobilisation are described: (1) chemical modification of chloromethylated polyHIPE with flavin and triethylamine; (2) deposition of a polyelectrolyte complex of flavin-containing polycations and poly(sodium styrene sulphonate) onto the (internal) surface of a polyHIPE; and (3) complexation of flavin-cntaining polycations on the (internal) surface of a polyHIPE. The catalytic activity per flavin moiety in the continuous aerobic oxidation of 1-benzyl-1,4-dihydronicotinamide depends on the method of immobilisation and on the loading with the catalytic moieties, factors influencing the accessibility and the distribution of catalytic sites over the pore surface and the matrix of the polyHIPE.

An effective strategy for immobilisation enzymes covalently onto a sold polyHIPE support was developed by Cameron et al., where in large fraction of the enzyme can be trapped.[190] N-Hydroxy succinimide esters were introduced into highly porous monolithic support for covalent coupling with the lysine residues present in proteins. When the activity of the well-known lipase *Candida antartica* lipase B (Cal-B)

immobilised on polyHIPE was compared with the commercially available standard, Novozyme 435, a remarkable increase in both activity and stability was observed.

1.10 Applications

Porous polymer gels or materials can possess outstanding and unusual properties in nature as well as in technology. Application for polyHIPE materials cover diverse markets from high technology biomedical and biotechnology applications to industrial processes and consumer goods. The most interesting applications exploit the unique aspects of micrometer-size, interconnected cavities that characterise these materials.

1.10.1 Catalysis

There are many opportunities for commercial product involving polyHIPE and catalysis. Any catalytic materials attached to poly(HIPE) material surfaces would have more efficient interaction with reactants due to large cavities and interconnected pores. This unique structure permits reactants to flow into spheres, interact with the catalyst, form products, and still allows room for products to flow out and away from newly arriving reactants. Such accessibility of the catalyst to reactants is important for rapid and efficient reactions. This approach was successfully used to catalyse spherical particulates of polyolefins.[191]

1.10.2 Chromatography and bioprocessing

Large interconnected cavities contained within chemically stable polymer matrices are ideally suited for liquid chromatography applications, including bioprocessing. Because cavities of PolyHIPEs materials are relatively uniform and are individually connected through a network of smaller pores, samples molecules find clear ingress and egress through the matrix, and diffusion limitations characteristic of

conventional porous polymers are absent. Thus, mass transfer characteristics are extremely attractive. Separation of proteins and other biopolymers on conventional macroporous polymers occurs only in the outside few angstroms of the spheres. In contrast, because of the interconnections, separation on polyHIPE materials occurs throughout the entire volume of beads. Furthermore, since there are no irregular, terminating pores with the HIPE polymers, pressure drop through columns of these particles is extremely low. Linear flow velocities of several hundred cm/min are readily accomplished. These properties, and the suitability of such structures for containment and separation of biopolymers, make them ideal candidates for bioprocess applications.

1.10.3 Cell culture application

In 1992, Lee et al. described successful utilisation of HIPE materials as a cell culture media.[192] The work showed that micrometer-size cavities could be used in development of vaccines for both human and animal use. Cell may be bound internally in cavities, fed nutrients through interconnecting pores, and allowed to produce virus particles that would migrate outward. In general, vaccine production utilises cells that require microcarriers for growth in cell culture tanks. Microcarriers have the advantage of protecting cells from shear stresses of bioreators and enabling higher concentrations of cells, with concomitant economic benefits.

1.10.4 Drug delivery

Landgraf et al. discovered that certain HIPE polymers exhibit surprising release characteristic.[193] When used as carriers for active pharmaceuticals, these polymers release their contents over a 24-hour period, following near zero-order kinetics. Thus,

these polymers are ideally suited for providing constant blood levels of many drugs. It appears the zero order release is independent of drug composition or form, and entirely dependent up on morphology of particular HIPE polymers.

1.10.5 Immobilised Enzymes

The large cavities characteristic of this technology seem ideally suited as solid support for enzyme immobilisation applications. Steric hindrance impairs conventional porous materials, but micrometer-size cavities of HIPE polymers allow substrates full access to active regions of enzymes and interconnecting pores provide clear egress to enzyme-substrate products. Hsuanyu, who reported surprising stability and lifetime of such products compared with conventional porous polymers,[194] described this approach to enzyme immobilisation.

1.11 Conclusion

Synthesis of high internal phase emulsion (HIPE) polymers represents development of the first significant porous polymer morphology in more than forty years. Conventional "macroporous" polymers, developed in the late 1950s, have led to a variety of products and applications that enjoy widespread use. However, irregular pores that terminate in the matrix limit the performance and applications of these materials. HIPE polymers are expected to lead to development of higher performing products both in the particulate and monolithic forms and altogether new applications, not heretofore possible. With increasing complexity and material performance, porous polymers and resins became also more important, not only for fundamental research, but also for technical applications. Classical synthesis routes towards porous polymers and resins, such as induced phase separation or the use of gaseous and liquid porogens, were continually

optimised to obtain high performance polymers for certain applications, for instance electrophoresis gels or supports for solid-phase chemistry. In the last 10 years also supercritical media, such as supercritical carbon dioxide ($scCO_2$) were added to the list of porogens, providing a number of advantages. Application of porous polymers is as diverse as molecular recognition, high throughput analysis and separation media, or solid support for high throughput synthesisers. New tools for porogenesis will inspire researchers and engineers to develop new techniques which will influence science as well as daily life, for instance for biotechnological and pharmaceutical applications. Finally, tissue engineering or design of bio-convertible implants and transplants relies on biodegradable chemically functionalised porous polymer scaffolds which bridge between the worlds of synthetic polymers and the biological world.

Significant advances in porous polymer synthesis techniques have opened the way to the development of polymers with tailored morphological architectures and physical properties. By carefully controlling polymerisation reactions, synthetically well-known polymers and cross-linked networks can be produced with novel microstructures and morphologies. Synthetic schemes are partly aimed at the development of new approaches and methods for the preparation of large molecules with defined architecture and shape. High internal phase emulsion (HIPE) polymerisation provides a versatile and facile methodology for the preparation of polymers with control of the major variables that affect polymer properties. For diverse monomer and initiator systems, well-defined polymers can be prepared with low degrees of compositional or morphological heterogeneity. Selective technologically advanced examples of various porous highly polymers are presented to authorise the adaptability of HIPE polymerisation.

References

[1] Gorman, J. *Science News*. June 23, **2001**, Vol. 159, 25, 398.

[2] (a) Biot, M. A. *J. Appl. Phys*. 33, **1962**, 1482-1498 (b) Biot, M. A. *J. Acoust. Soc. Am*. 34, **1962**, 1254-1264.

[3] Dullien, F.A.L. *Porous Media: Fluid Transport and Pore Structure 2nd Edition* (Academic Press, San Diego, 1992).

[4] Garboczi, E. J. *Powder Tech*. **1991**, 67, 121-130.

[5] Hornby, B. E.; Schwartz, L. M.; Hudson, J. A. *Geophysics* 1994, 59, 1570-1583.

[6] Hermanson, G. T.; Mallia A. K.; Smith, P. K. *"Immobilized Affinity Ligand Techniques*," Academic Press Inc., San Diego (**1992**), 1.

[7] Adenson, P. A.; Jervis, L. *Biochem. Soc.* Trans. **1978**, 6, 263.

[8] Adenson, P. A.; Jervis, L. *Biochem. Soc.* Trans. **1978**, 6, 263.

[9] Harfenist, S. A.; Wang, Z. L.; Whetten, R. L.; Vezmar, I.; Alvarez, M. M. *Adv. Mater*. **1997**, 9, 817.

[10] Hienmenz, P. C. *Polymer Chemistry*, Marcel Dekker, new York (**1984**).

[11] Hay, A. S. *High Performance Polymers: Their origin and Development* (Seymaur, R. B. and Kirshenbaum, S. eds), Elsevier, New York (**1986**).

[12] Staudinger, H.; Huseman, E. *Berichte*, **1935**, *68,* 1618.

[13] Seidl, J.; Malinsky, J.; Dusek, K.; Heitz, W. *Adv. Polymer Sci*. 1967, **5**, 113-213.

[14] Dusek, K. *J. Polym. Sci*., B **1965**, *3*, 209.

[15] Abrams, I. M. *Ind. Eng. Chem*. **1956**, *48*, 1469.

[16] Meitzner, E. F.; Oline, J. A. US Patent, 4, 224, 415, (**1980)**.

[17] Abrams, I. M. US Patent, 2,844,546 (**1958**).

[18] Lloyd, W. G.; Alfrey, T. *J. Polym. Sci*. **1962**, *62*, 301.

[19] Kunin, R.; Meitzner, E. F.; Bortnick, N. *J. Am. Chem. Soc*. **1962**, *84*, 305.

[20] Kunin, R.; Meitzner, E. F.; Oline, J. A.; Fisher, S.; Frish, N. *Ind. Eng. Chem. Prod. Res. Develop*. **1962**, *1*, 140.

[21] Kun, K. A. *J. Polym. Sci*. A, **1965**, *3*, 1833.

[22] Millar, J. R.; Smith, D. G.; Marr W. E.; Kressman, T. R. E. *J. Chem. Soc*. **1963**, 218.

[23] Millar, J. R. Smith, D. G. Marr and T. R. E. Kressman, J. Chem. Soc., **1963**, 2779.

[24] Millar, J. R.; Smith, D. G.; Marr W. E.; Kressman, T. R. E. *J. Chem. Soc*., **1964**, 2740.

[25] Lehn, *Supramolecular Chemistry*, Wiley-VCH, Weinheim (**1995)**.

[26] Sing, K. S. W.; Everett, D. H.; Haul, R. A. W.; Moscou, R.; Pierotti, A.; Rouquerol, J.; Siemieniewska, T. *Pure Appl. Chem*. **1985**, *57,* 603.

[27] Kuroda, H.; Osawa, Z. *Eur. Polym. J*. **1995**, *31*, 1, 57.

[28] Svec, F.; Frechet, J. M. J. *Science*, **1996**, *273*, 205.

[29] Wijnhoven, J. E. G. J.; Vos, W. L. Science, **1998**, *281*, 802.

[30] Tanev, P. T.; Chibwe, M.; Pinnavaia, T. J. *Nature*, **1994**, *368*, 321.

[31] Deleuze, H.; Schultze X.; Sherrington, D. C. *Polymer*, **1998**, *39*, 6109.

[32] Bhave, R. R. *Inorganic Membranes, Synthesis, Characteristic and Applications*, Van Nostrand Reinhold, New York, **1991**.

[33] Lewandowski, K.; Murer, P.; Svec F.; Frechet, J. M. J. *Anal. Chem*. **1998**, *70*, 1629.

[34] Akolekar, D. B.; Hind A. R.; Bhargava, S. K. *J. Colloid. Interface Sci*. **1998**, *199*, 92.

[35] Maquet, V.; Jerome, R. *Mater. Sci. Forum* **1997**, *250,* 15.

[36] Peters, M. C.; Mooney, D. J. *Mater. Sci. Forum* **1997**, *250*, 43.

[37] Bancel, S.; Hu, W. S. *Biotechnology Prog*. **1996**, *12,* 398.

[38] Schugens, C.; Maquet, V.; Grandfils, C.; Jerome, R.; Teyssie, P. *Polymer*,

1996, *37*, 1027.

[39] Tennikov, M. B.; Gazdina, N. V.; Tennikova T. B.; Svec, F.; J. Chromatography A **1998**, *798*, 55.

[40] Palm, A.; Novotny, M. V. *Anal. Chem*. **1997**, *69*, 4499.

[41] Xie, S.; Svec F.; Frechet, J. M. J. *J. Chromatography A* **1997**, *775*, 65.

[42] Litovsky, E.; Shapiro, M.; Shavit, A. *J. Am. Ceram. Soc*. **1996**, *79*, 1366.

[43] Seino, H.; Haba, O.; Mochizuki, A.; Yoshioka M.; Ueda, M. *High Perform. Polym.* **1997**, *9*, 33.

[44] Senkevich, J. J.; Desu, S. B. *Appl. Phys. Lett*. **1998**, *72*, 258.

[45] Sedev, R.; Ivanova, R.; Kolarov T.; Exerowa, D. *J. Dispersion Sci. Technol*. **1997**, *18*, 751.

[46] Cheng, C. M.; Micale, F. J.; Vanderhoff J. W.; El-Aasser, M. S. *J. Polym. Sci., Polym. Chem. Ed*. **1992**, *30*, 235.

[47] Cheng, C. M.; Vanderhoff J. W.; El-Aasser, M. S. *J. Polym. Sci., Polym. Chem. Ed*. **1992**, *30*, 245.

[48] Horak, D.; Svec, F.; Kalal, J.; Gumargalieva, K.; Adamyan, A.; Skuba, N.; Titova, M.; Trostenyuk, N. *Biomaterials* **1986**, *7*, 188.

[49] Mueller, K. F.; Heiber, S. J.; Plankl, W. L. US Patent, 4,224,427 (**1977**).

[50] Robert, C. C. R.; Buri, P. A.; Peppas, N. A. *J. Appl. Polym. Sci.* **1985**, *30*, 301.

[51] Barr-Howell B. D.; Peppas, N. A. *Eur. Polym. J.* **1987**, *23*, 591.

[52] Scranton, A. B.; Mikos, A. G.; Scranton L. C.; Peppas, N. A. *J. Appl. Polym. Sci.* **1990**, *40*, 1, 997.

[53] Jayakrishnan, A.; Sunny M. C.; Thanoo, B. C. *Polymer* **1990**, *31*, 1339.

[54] Okay, O.; Gurun, C. *J. Appl. Polym. Sci*. **1992**, *46*, 401.

[55] Horak, D.; Lednicky, F.; Bleha, M. *Polymer* **1996**, *37*, 4243.

[56] Chirila, T. V.; Chen, Y. C.; Griffin B. J.; Constable, I. J. *Polym. Int.* **1993**, *32*, 221.

[57] Shea, K. J.; Stoddard, G. J.; Shavelle, D. M.; Wakui, F.; Choate, R. M. *Macromolecules* **1990**, *23*, 4497.

[58] Xie, S.; Svec, F.; Frechet, J. M. J. *J. Polym. Sci. A, Polym. Chem*. **1997**, *35*, 1013.

[59] Coupek, J.; Krivakova, M.; Pokorny, S. *J. Polym. Sci. C* **1973**, *42*, 185.

[60] Svec, F.; Hradil, J.; Coupek J.; Kalal, J. *Angew. Makromol. Chem*. **1975**, *48*, 135.

[61] Svec, F. *Angew. Makromol. Chem.* **1986**, *144*, 39.

[62] Smigol, V.; Svec, F. *J. Appl. Polym. Sci*. **1992**, *46*, 1439.

[63] Smigol, V.; Svec, F.; Frechet, J. M. J. *Macromolecules* **1993**, *26*, 5615.

[64] Gregg, S. J.; Sing, K. S. W. *Adsorption, Surface Area and Porosity* (2nd ed), Academic Press, New York, **1982**, p-173.

[65] Brunauer, S.; Emmett P. H.; Teller, E. *J. Am. Chem. Soc*. **1938**, *60*, 309.

[66] Munzer, M.; Trommsdroff E. in "*Polymerisation Processes*", (Schildknecht, C. E.; skeist, I. ed.) *High Polymers*, Vol. 29, Wiley Interscience, London, **1977**, p-106.

[67] Svec, F.; Frechet, J.M.J. *Chem. Mater*. **1995**, 7, 707-715.

[68] Lewandowski, K.; Svec, F.; Frechet, J.M.J. *J. Appl. Polym. Sci*. **1998**, 67, 597-607.

[69] Li, W. H.; Stover, H. D. H. *J. Polym. Sci. Part A: Polym. Chem*. **1998**, 36, 1543-1551.

[70] Hoffman, F.; Delbruck, K. *Ger Pat*. 150. 690, **1909**.

[71] Peter, D. J.; Brian, V. *Colloids and Surfaces A*, **2000**, *161*, 259.

[72] Hofman, F.; Delbruk, K.; *German Patent*, 250,690 (**1909**); 254,672 (**1912**); 255,129 (**1912**).

[73] Gottlob, K. *US Patent*, 1,149,577 (**1913**).

[74] Bauer, W.; Lauth, H.; *German Patent* 656,134 (**1931**).

[75] Vivaldo-Lima, E.; Wood, P. E.; Hamielec, A. E.; Penlidis, A. *Ind. Eng. Chem*.

Res. **1997**, *36*, 939.

[76] Arshady, R. *Colloid Polym. Sci*. **1992**, *270*, 717.
[77] Brooks, B. W. *Makromol. Chem., Macromol. Symp*. **1990**, *35/36*, 121.

[78] Geoffrey, A.; Bevington, J. C. Eds, *Comprehensive Polymer Science*, Pergamon Press, Oxford, Great Britian, **1989**, Vol. *4*, Chapter 14.

[79] Yuan, H. G.; Kalfas G.; Ray, W. H. *J. Macromol. Sci., Rev. Macromol. Chem. Phys. C* **1991**, *31,* 215.

[80] Landfester, K. *Macromol. Rapid. Commun*. **2001**, *22,* 896.

[81] Azad, A. R. M.; Fitch, R. M. in: *Polymer Colloids II*, Fitch, R. M. Ed, Plenum Press, New York, **1980**, p-95.

[82] Hodge, P.; Sherrington D. C. (Eds), *Synthesis and Separations using Functional Polymers,* Wiley, Chichester, **1998**, p-43.

[83] Maugh, T. M. *Science* **1984**, *223*, 155.

[84] Kotha, A.; Rajan, C. R.; Ponrathnam, S.; Shewale, J. G. *React. Funct. Polym*. **1996**, *28*, 227.

[85] Winslow, F. H.; Matreyer, W. *Ind. Eng. Chem*. **1951**, *53*, 1108.

[86] Hohenstein, W. P. *Polymer Bull*. **1945**, *1*, 13.

[87] Church, J. M.; Shinnar, R. *Ind. Eng. Chem*. **1961**, *53*, 479.

[88] Sulvian, D. M.; Lindsey, E .F. *Ind. Eng. Chem. Fundam*. **1962**, *1*, 87.

[89] Hopff, H.; Lussi H.; Gerspocher, *Makromol. Chem*. **1964**, *24*, 37, 78.

[90] Hohenstein, W. P.; Mark, H. *J. Polym. Sci*. **1946**, *1*, 127.

[91] Hopff, H.; Lussi, H.; Hammer, E. *Makromol. Chem*. **1965**, *82*, 175.

[92] Hopff, H.; Lussi, H.; Hammer, E. *Makromol. Chem*. **1965**, *82*, 184.

[93] Trommsdorff, E.; Kohle, H.; Legally, P. *Makromol. Chem*. **1948**, 1, 169.

[94] Zerfa, M.; Brooks, B. W. *Chem. Eng. Sci*. **1996**, 51, 3591.

[95] Hashim, S.; Brooks, B. W. *Chem. Eng. Sci*. **2002**, 57, 3703.

[96] Wenning, H. *Makromol. Chem*. **1956**, 20, 196.

[97] Wenning, H. *Kunstst. Plast*. **1958**, 5, 328.
[98] Trommsdorff, E. *Makromol. Chem*. **1954**, 13, 76.

[99] Becher, P. *Emulsions, Theory and Practice,* Reinhold Publishing Co., New York, **1965**, p-2.

[100] Moulik, S. P.; Paul, B. K. *Adv. Colloid Interface Sci*. **1998**, 78, 99-195.

[101] Garcia-Rio, L.; Leis J. R.; Moreira J. A. *J. Am. Soc*. **2000**, 122, 10325-10334.

[102] Paul, B. K.; Moulik, S. P. *J. Disp. Sci. Tech*. **1997**, 18, 301.

[103] Schwuger, M. J.; Stickdorn, K. *Chem. Rev*. **1995**, 95, 849-864.

[104] Everett, D. H. *Basic Principles of Colloid Science*. **1989**, pp 182-184. London: Royal Society of Chemistry.

[105] Chapter 8 Rosen. Retrieved August 21, **2001**, from http://www.olemiss.edu/courses/che545/notes/R_Chapter_8.html.

[106] *The HLB System –a time saving guide to emulsifier selection*. May **1992**, Delaware: ICI Surfactants.

[107] Griffin. W.; *Encyclopedia of Chemical technology*, Vol. 18, Second Edition, john Wiley and Sons, Inc., new York, **1965**, pp. 135-137.

[108] Prince. L. M. (Ed.). *Formation in Microemulsions Theory and practice*. **1997.** pp 33-56. New York : Academic press Inc.

[109] Shinoda, K.; Saito, H. *J. Colloid Interface Sci.* **1968**, 26, 70.

[110] Matsumoto, S.; Kita, Y.; Yonezawa, D.; *J. Collid Interface Sci*. **1976**, 57, 353-361.

[111] Opawale, F. O.; Burgess, D. J. *J. Pharm Pharmocol*. **1998**, 50, 965-973.

[112] Florence, A. T.; Whitehill, D. *Stability and stabilization of water-in-oil-in-water multiple emulsions. In: Shah, ed. Macro-and Microemulsions; Theory and Applications.* ACS Symposium Series 272. Washington, DC: American Chemical Society, **1985**, 359-380.

[113] Shinoda, K.; Yoneyama, T.; Tsutsumi, H. *J. Disper. Sci Technol*. **1980**, 1, 1-12.

[114] Hou, W.; Papado poulos. K. D. *Colloids Surf A: Physico-chemical and engineering Aspects*. **1997**, 125, 181-187.

[115] Lissant K. J. (ed) **1974** Emulsion and Emulsion Technology, Part I Marcel Dekker, New York. Chap. I.

[116] Ostwald, W. *Z. Kolloid* **1910,** 6, 103, ibid, 7,64.

[117] Lissant, K. J. *J. Coll. Interf. Sci.* **1966,** 22, 462.

[118] Lissant, K. J. *J. Soc. Cosmetic Chem.* **1970**, 21, 141.

[119] Lissant, K. J.; Mayhan, K. G. *J. Coll. Interf. Sci.* **1973**, 42, 201.

[120] Lissant, K. J.; Pearce, B. W.; Wu, S. H.; Mayhan, K. G. *J. Coll. Interf. Sci* **1974**, 47, 416.

[121] Princen, H. M. *Langmuir* **1988**, 4, 486.

[122] Ravey, J. C.; Stebe, M. J. *Progr. Coll. Poly. Sci*. **1990**, 82, 218.

[123] Solans, C.; Dominguez, J. C.; Parra, J. I.; Heuser, J.; Friberg, S. E., *Coll. Poly. Sci*. **1992**, 266, 570.

[124] Pons, R.; Solans, C.; Stebe, M. J.; Erra, P.; Ravey, J. C. *Progr. Coll. Poly. Sci*. **1992**, 89, 110.

[125] Kunieda, H.; Yano, N.; Solans, C. *Coll. Surf.* **1987**, 24, 225.

[126] Solans, C.; Pons, R.; Zhu, S.; Davis, H. T.; Evans, D. F.; Nakamura, K.; Kunieda, H. *Langmuir* **1993**, 9, 1479.

[127] Kunieda, H.; Yano, N.; Solans, C. *Coll. Surf.* **1989,** 36, 313.

[128] Kunieda, H.; Evans, D.; Solans, F. C.; Yoshida, M. **1990**, ibid 47, 35.

[129] Ebert, G.; Platz, G.; Rehage, H. *Ber. Bunsenges Phys. Chem*. **1988**, 92, 1158.

[130] Hoffmann, H. *Adv. Coll. Interf. Sci.* **1990**, 32, 123.

[131] Princen, H. M. *J. Coll. Interf. Sci*. **1979**, 71, 55.

[132] Becher, P. *Emulsions, Theory and Practice*, Reinhold Publishing Co., New York, 1965, pp. 61-67.

[133] Barby, D.; Haq, Z. *Eur Pat*, 0060138 (**1982**).

[134] Barby, D.; Haq, Z. *European Patent* 60,138 (**1982**).

[135] Li, Nai-Hong, Benson, J. R. "*Polymeric Microbeads and Method of preparation*" US patent No. 5, 583,162 (**1996**).

136] Kitagawa, Naotaka. "*Hydrophillic Polymeric Microbeads*" US Patent No. 6,048,908 (**2000**).

[137] Kitagawa, Naotaka, "Hydrophillic Polymeric Microbeads and Method of preparation" US Patent No. 6,218,440 (**2000**).

[138] Hainey, P.; Huxham, I. M.; Rowatt, B.; Sherrington, D. C.; Tetley, L. *Macromolecules* **1991**, 24, 117-121.

[139] Cameron, N. R.; Sherrington, D. C.; Albiston, L.; Gregory, D. P. *Colloid. Polym. Sci.**1996,*** 274, 592-595.

[140] Cameron, N. R.; Barbetta, A. *J. Mater. Chem*. **2000**, 10, 2466-2472.

[141] Cameron, N. R.; Sherrington, D. C. *Macromolecules* **1997**, 30, 5860-5869.

[142] Cameron, N. R.; Sherrington, D. C.; Ando, I.; Kurosu, H. J. *Mater. Chem.* **1996**, 6, 719.

[143] Schoo, H. F. M.; Challa, G.; Rowatt, B.; Sherrington, D. C. *React. Polym.* **1992**, **16**, p-125.

[144] Walsh, D. C.; Stenhouse, J. I. T.; Kingsbury, L. P.; Webster, E. J. J. *Aerosol. Sci.* **1996**, 27 (Suppl. 1), p-S629.

[145] Krajnc, P.; Brown J. F.; Cameron, N. R. *Org. Lett.* **2002**, 4, 2497.

[146] Cameron N.R. Barbetta, A. *Macromolecules* **2004**, 37, 3188.

[147] Flory, P. J. *J. Am. Chem. Soc*. **1941**, *63*, 3083.

[148] Funke, W.; Okay O.; Muller, B. J. *Adv. Polym. Sci*. **1998**, *136*, 139.

[149] Dusek, K. in: Chompff, A. J.; Newman, S. Editors, *Polymer Networks*: Structure *and Mechanical Properties*, Plenum Press, New York, **1971**, p-245.

[150] Hodge, P.; Sherrington, D. C. *Polymer Supported Reactions in Organic Synthesis*, Wiley, New York-London, **1980**.

[151] Jacobelli, H.; Bartoline, M.; Guyot, A. *J. Appl. Poly. Sci*. **1979**, *23*, 927.

[152] Horak, D.; Lednicky, F.; Bleha, M. *Polymer*, **1996**, *37*, 4245.

[153] Muller, K. F.; Heiber, S.; Flank, W. *US Patent* 4,224,472 (**1978**).

[154] Seidel, J.; Malinsky, J.; Dusek, K.; Heitz, W. *Adv. Polym. Sci*. **1967**, *5*, 113.

[155] Moore, J. C. *J. Polym. Sci., Part A*, **1969**, *2*, 835.

[156] Coupek, J.; Krivakova, M.; Pokorny, S. *J. Polym. Sci., Polym. Symp*. **1973**, *42*, 185.

[157] Heitz, W. *Adv. Polym. Sci*. **1977**, *23*, 1.

[158] Kalal, J. *J. Polym. Sci., Polym. Symp*. Ed. **1978**, *62*, 251.

[159] Horak, D.; Pelzbauer, Z.; Bleha, M.; Havsky, M.; Svec, F.; Kalal, J. *J. Appl. Polym. Sci.* **1980**, *26*, 411.

[160] Horak, D.; Svec, F.; Bleha, M.; Kalal, J. *Angew. Makromol. Chem*. **1981**, *95*, 109.

[161] Wieczorek, P. P.; Ilavsky, M.; Kolarz B. N.; Dusek, K. *J. Appl. Polym. Sci*. **1982**, *27*, 277.

[162] Guyot, A.; Bartholin, M. *Prog. Polym. Sci*. **1982**, *81*, 277.

[163] Ohtsuka, Y.; Kawaguchi, H.; Yamamoto, Y.; *J. Appl. Polym. Sci*. **1982**, *27*, 3279.

[164] Galina, H.; Colaz, N. B.; Wiezorek P. P.; Woiszynska, M. *Br. Polym. J*. **1985**, *17*, 215.

[165] Dimonie, M.; Dschell, H.; Hubca, G.; Mateescu, M. A.; Oprescu, C. G.; Todireanu, S.; Maior, O.; Languri, J.; Iosif, M.; *J. Macromol. Sci. Chem. A* **1985**, *22*, 729.

[166] Robert, C. C. R.; Buri P. A.; Peppas, N. A. *J. Appl. Polym. Sci*. **1985**, *30*, 301.

[167] Horak, D.; Svec, F.; Kalal, J.; Gumaragalieve, K.; Adamyan, A.; Skuba, N.; Titova M.; Trostenyuk, N. *Biomaterials* **1986**, *7*, 188.

[168] Okay, O. *J. Appl. Polym. Sci*. **1986**, *32*, 5533.

[169] Okay, O. *Angew. Macromol. Chem*. **1986**, *143*, 209.

[170] Okay, O. *Angew. Macromol. Chem*. **1987**, *153*, 125.

[171] Barr-HoWell B. D.; Peppas, N. A. *Eur. Polym. J*. **1987**, *8*, 591.

[172] Okay, O. *Angew. Macromol. Chem*. 1**988**, *157*, 1.

[173] Park, T. G.; Hoffman, A. S. *J. Biomed. Mater. Res*. **1990**, *24*, 21.

[174] Park, T. G.; Hoffman, A. S. *Biotech. Bioeng*. **1990**, *35*, 152.

[175] Loraz, B. N.; Wojaczyriska, M.; Trochimczuk, A. W. *Macromol. Chem*. **1990**, *194*, 1299.

[176] Okay, O.; Funke, W. *Makromol. Chem. Commun*. **1990**, *11*, 583.

[177] Park, T. G.; Hoffman, A. S. *J. Polym. Sci. Polym. Chem*. *Ed*. **1992**, *30*, 505.

[178] Seidl, J.; Malinsky, J.; Dusek K.; Heitz, W. *Adv. Poly. Sci*. **1967**, *5*, 113.

[179] Millar, J. R.; Smith, D. G.; Marr W. E.; Kressman, T. R. E. *J. Chem. Soc*. **1963**, 218.

[180] Sederel, W. L.; DeJong, G. J. *J. Appl. Polym. Sci*. **1973**, *17*, 2835.

[181] Hilgen, H.; DeJong, G. J.; Sederel, W. L. *J. Appl. Polym. Sci*. **1975**, *19*, 2647.

[182] Kun, K. A.; Kunin, R. *J. Poly. Sci. A-1* **1968**, *6*, 2689.

[183] Klampfl, C. W.; Spanos, E. *J. Chromatography A* **1995**, 715, 212-218.

[184] Fritz, J. S.; Dumont, P. J.; Scmidt, L. W. *J. Chromatogr. A* **1995**, 691, 133-140.

[185] Svec, F.; Frechet, J. M. J. *Biotechol. Bioeng*. **1995a**, 48, 476-480.

[186] Alexandratos, S. D.; Ripperger, K. P. *Ind. Eng. Chem. Res*. **1998**, 37, 4756-4760.

[187] Mercie, A.; Deleuze, H.; Mondain-Monval, O. *React. Funct. Polym*. **2000**, 46, 67-79.

[188] Cameron, N. R.; Sherrington, D. C.; Ando, I.; Kurosu, H. *J. Mater. Chem*. **1996**, 6, 719-726.

[189] Schoo, H. F. M.; Challa, G.; Rowatt, B.; Sherrington, D. C. *React. Polym*. **1992**, 16, 125-136.

[190] Pierre, S J.; Thies, J. C.; Dureault, A.; Cameron, N. R.; van Hest, J. C. M.; Carette, N.; Michon, T.; Weberskirch, R. *Adv. Mater*. **2006**, 18, 1822-1826.

[191] Sunstorm research Corporation, unpublished results.

[192] Lee, D. W.; Piret, J. M.; Gregory, D.; Haddow, D. J.; Kilburn, D. G.*"Polystyrene Macroporous Bead Suppport for Mammalian Cell Culture"* in Biochemical Engineering VII, (Dibiasion, D.; Mutharason, R. eds.) Ann. N. Y. Acad. of Sci. **1992**, 665, 137-145.

[193] Landgraf, W.; Li, N-H.; Benson, J. "*Polymer microcarrier exhibiting zero order release*" Drug Delivery Technology, Jan-Feb **2003**.

[194] Hsuanyu, Y. "*Functionalised polystyrene Cavilink TM beads for Enzyme Immobilisation"*, **2002**, http/www.sunstorm-research.com.

Chapter II

AIMS AND OBJECTIVES

2 Aims and Objectives

2.1 Origin and importance of task

Porous materials play a significant role in the international market and account for many billions of dollars revenue each year. The applications of porous materials are varied: thermal insulation, ion-exchangers, filters and purifying systems, bone implants, catalytic substrates, porous battery electrodes, fuel cells, aerators, sorbents, silencers, kiln furniture, fiber optics, etc. Porous materials are characterised usually by their size distribution, shape, pore size, extent of interconnectivity and total amount of porosity [open or closed] of the pores. Depending on the application for the porous structural material that is to be produced, the dimensions and characteristics of the porous phase required do vary. For industrial applications it is essential that the method chosen to produce the porous material is cost effective. This creates need for developing novel techniques for the manufacturing of porous materials, especially porous polymers. Porous polymers have a wide range of applications as solid supports in catalysis and chromatography. Polymers based on styrene-divinylbenzene have attracted significant attention. Glycidyl methacrylate and hydroxyethyl methacrylate polymers also have attracted researchers owing to the wide scope of modifications possible due to the presence of modifiable functional groups.

Chapter I outlined that multiple emulsion or high internal phase emulsion (HIPE) polymerisation method allows synthesis of novel porous materials both in beaded as well as in monolithic forms. It also outlined some conventional methods of preparation of porous materials such as suspension and emulsions.

In this work, newer methodology, high internal phase emulsified suspension, was investigated and optimised for preparation of beaded porous polymer particles in the range suitable for chromatographic applications. The reactions were conducted in a scaled-down cylindrical reactor. Information on the effect of stirrer design, as well as synthesis variables on the particle size and its distribution was collected. Syntheses were carried out using water-in-oil-in-water polymerisation system to prepare the following copolymers: (i) styrene-divinyl benzene; (ii) glycidyl methacrylate-ethylene dimethacrylate; (iii) allyl glycidyl ether-ethylene dimethacrylate and (iv) hydroxyethyl methacrylate-ethylene dimethacrylate. Within each series, the copolymer composition, the internal surfactant type and its volume, inner water volume, the effect of porogen, initiator types and their placements (water and/or organic phase) as well as protective colloid type and amount (in the bulk aqueous phase) on surface area, particle size, its distribution, pore volume, pore size and its distribution as well as internal morphology were investigated. The copolymers were tested for chelation of heavy metal ions. The ter-polymers were suitably modified and tested in a manner akin to Amberlyst. Newer method for the development of HEMA-EGDM porous polymers both in beaded as well as in monoliths form has been developed by redox system at room temperature, which is very helpful for biological applications.

Series of highly porous acrylic monoliths has been synthesised using W/O HIPE emulsion methodology. Exhaustive study was carried out to see the effect of various synthesis parameters on the porous morphology of acrylic monoliths.

2.2 Objectives

The goals of this research was to synthesise and evaluate co-and terpolymers both by beaded and monolithic via multiple emulsion (HIPE) technique and understand the effect of various parameters on the porous properties. The goals were:

1. To establish synthesis strategies to prepare styrene-divinyl benzene copolymers in a beaded macroreticular form, in the 3-20 micron size range, suitable for chromatographic applications by a high internal phase emulsified suspension in a batch reactor at constant speed.

2. Synthesis of functional copolymers such as 2-hydroxyethyl methacrylate-ethylene dimethacrylate (HEMA-EGDM), allyl glycidyl ether-ethylene dimethacrylate (AGE-EGDM), glycidyl methacrylate-ethylene dimethacrylate (GMA-EGDM) under optimised conditions.

3. Control of porosity, pore volume, and inner pore morphology of the beads by an interplay of the type, volume of water-in-oil surfactant and optional porogen (solvent, non-solvent, polymeric) in the polymerising phase, while controlling particle size and its distribution.

4. Modification of styrene-divinyl benzene polymer beads (sulphonation) and testing in parallel to the performance of traditional macroreticular polymers such as Amberlyst-15 for catalytic applications.

5. Modification of (AGE-EGDM) and (GMA-EGDM) through amine functionalities for chelation of toxic metal ions.

6. Characterisation of polymer morphology and polymer properties by techniques like FTIR, BET, mercury porosimetry, particle size analyser, optical microscopy, scanning electron microscopy etc.
7. Synthesis of porous acrylic monoliths by novel methods and characterisation of formation of porous network by optical microscopy and scanning electron microscopy.

2.2.1 Copolymerisation

Chapter III discusses HIPE W/O/W multiple emulsion co-polymerisation of glycidyl methacrylate (GMA)- ethylene dimethacrylate (EGDM), allyl glycidyl ether (AGE)- ethylene dimethacrylate (EGDM) and 2-hydroxyethyl methacrylate (HEMA)-ethylene dimethacrylate (EGDM) systems. All the above polymers were also synthesised using (O/W) conventional suspension polymerisation using cyclohexanol as porogen. The polymerisations were conducted changing the ratio of monomer to internal water. The internal phase volumes were changed from 33.3 to a maximum of 90.9%. Effect of internal phase volume on the formation of porous structures has been extensively studied. The polymers of different cross-link densities (mole percent of multivinyl to monovinyl monomer; CLDs) such as 25, 50, 75, 100, 150 200, 300, etc were synthesised. One objective was also to compare the characteristic of an O/W emulsion and a W/O/W emulsion formulated with similar ingradients. The effect of variation in reaction parameters on the morphology, porous properties and surface functionalities were investigated. Finally, the properties were compared with the properties of identical polymers obtained by suspension technique.

2.2.2 Terpolymerisation

This is the fourth chapter, I report the first synthesis of a functional porous terpolymer poly(styrene-GMA-DVB) via multiple emulsion method. The terpolymers were prepared to improve the mechanical properties, for the chromatography or hydrophilic properties of the ion-exchangers. As part of the investigation of the reactive polymers having epoxy group as functional group, the present investigation was undertaken to see the porous properties of glycidyl methacrylate with styrene as a comonomer and divinyl benzene as cross-linker influenced by various reaction parameter such as, cross-link density, type of initiator, position of initiator, type of surfactants, etc. The effect of these parameters on the particle size, particle size distribution, pore volume, surface area, surface epoxy groups, and morphology investigated thoroughly.

In second half, the HIPE beads were functionalised into thiol and mercaptosulphonic acid groups, their acid exchange values estimated and tested as catalysts in a manner akin to Amberlyst-15 to synthesise 4,4'-bisphenol A.

2.2.3 Funtionalised polyHIPE materials for arsenic removal

Chapter 5 consists of synthesis of epoxy based GMA-EGDM and AGE-EGDM copolymers by W/O/W HIPE polymerisation with different cross-link densities. These polymers were modified with polyethyleneimine and tested for removal of arsenic from contaminated water.

The modified polyHIPE materials were evaluated to bind arsenic from water and to investigate the parameters affecting arsenic removal, especially those which cannot be examined easily in pilot plant scale. The examined parameters were the monomer type,

cross-link densities, PEI concentration, contact time and pH of the treated water. Systematic, comparative research for arsenic removal; covering both trivalent As (III) and pentavalent As (V) inorganic arsenic anions using PEI a modified poly(HIPE) GMA-EGDM and AGE-EGDM bead are presented. Furthermore, this work is the first research at applying poly(HIPE) materials as sorbents for the removal of arsenic from water.

2.2.4 Hydroxy terminated porous polymers

Until now, the preparation of poly(HIPE) has been achieved predominantly by thermal curing. In order to introduce biological species, polymerisation would need to be conducted at the ambient temperature using redox initiation. Our main emphasis was not only on the preparation of tuned porous architecture of the polymer matrix but also in the exploration of poly(HIPE) as useful biomaterials. This investigation aimed to synthesise, design and characterise a porous hydroxy terminated polymers at room temperature with tuned morphology that would provide increased surface area within beaded as well as in monolithic form for use in different applications.

In the sixth chapter, inverse HIPE emulsion polymerisation was used to synthesise hydroxy terminated polymers such as 2-hydroxyethyl methacrylate (HEMA)-co-N,N'-methylene bisacrylmide (MBA). Inverse HIPE methodology using redox system for the preparation of beaded HEMA-MBA polymers, a novel methodology, is being examined for the first time.

2.2.5 Morphological study of porous polymeric monoliths

Porous materials are characterised by their size distribution, shape, pore size, extent of interconnectivity and amount of porosity (open or closed). Chapter 7 consists of

synthesis of porous polyacrylates by W/O HIPE polymerisation. In this chapter, thorough investigation of influence of synthesis parameter on the porous characteristics, morphological studies of the resultant polyHIPE materials prepared from acrylate monomers were carried out. The examined parameters were the initiator type and their placement in the oil and water phase, surfactant concentration, inhibitor concentrations, and temperature and stirring speeds. The detailed study of effect of above mentioned parameters on the formation of cells and windows as well as on the surface area is reported in this chapter.

Chapter III

Copolymerisation: Synthesis of copolymers based on multiple emulsion

3 Copolymerisation: Synthesis of copolymers based on multiple emulsion

3.1 Introduction

Multiple emulsions, or emulsions having ternary, quaternary, or even more complex structures, have been studied since their first description in 1925.[1] The simplest multiple emulsions, sometimes called "double emulsions" are in fact ternary systems, having either a water-in-oil-in-water ($W_1/O/W_2$) or an oil-in-water-in-oil ($O_1/W/O_2$) structure, in which the dispersed droplets themselves contain even smaller droplets of a different phase. In the case of water-in-oil-in-water multiple emulsions, the oil droplets have smaller water droplets dispersed within them, and the oil droplets themselves are dispersed in a continuous water phase. Oil-in-water-in-oil multiple emulsions, on the other hand, consist of tiny oil droplets entrapped within large water droplets, which in turn, are dispersed in a continuous oil phase. They, thus, differ from the familiar water-in-oil-or oil-in-water simple two-phase emulsions in that they have three distinct phases.[2] Water-in-oil-in-water multiple emulsions are abbreviated as O/W/O. In order to avoid confusion footnotes1 and 2 are sometimes used to differentiate the phases in a multiple emulsion system, e.g. $W_1/O/W_2$ and $O_1/W/O_2$, where 1 represents the inner dispersed phase and 2 represents the outer continuous phase, respectively.

Multiple emulsions have shown promise, particularly in cosmetic, pharmaceutical and separation science. Their potential pharmaceutical applications,[3] which take advantage of the presence of reservoir phase inside droplets of another phase, include use as (i) adjuvant vaccines;[4] (ii) prolonged drug delivery systems;[5-7] (iii) sorbent reservoirs in drug overdose treatment[8] and (iv) in immobilisation of enzymes.[9] Multiple emulsions

have been used as the basis of liposome-like lipid vesicles[10] and as a mean for the preparation of Lupron Depot and other microsphere injectables.[11]

Beaded porous polymer particles are widely used as ion-exchange resins or packing materials for chromatography. At present a wide range of high quality, high performance and economical matrices are available. Still, no perfect matrix material has been established for every application. Therefore, great concern has been taken for the production of single-size (monodisperse) porous polymer particles. The general properties include adequate particle size, particle size distribution, particle shape, porosity, sufficient stability (both mechanical and chemical) etc. Good flow properties are paramount for large-scale operations, which are highly dependent on particle size, particle size distribution and rigidity. A narrow particle size distribution offers better column capacity. Similarly, spherical particles with high compression resistance impart good flow properties. Uniformity of particle size is an important factor in performance in terms of reproducible separation. Generally, polymer particles are made by the process of suspension polymerisation, in which fine droplets of monomers are suspended in a dispersion medium with a stabiliser. The most important issue in the practical operation of suspension polymerisation is the control of the average diameter and preferably the size distribution of the product particle. Therefore, it is very difficult to obtain uniform particle size and expected pore size distribution by normal suspension methodology.

Two different polymerisation procedures were investigated in order to synthesise polymers having desired properties viz; suspension and high internal phase emulsion (HIPE) polymerisation or multiple emulsion method. The monomers were chosen are epoxies such as glycidyl methcrylate (GMA), allyl glycidyl ether (AGE) and hydroxy

based 2-hydroxyethyl methacrylate (HEMA). GMA and AGE polymers are another class of reactive resins that have received much attention. These polymers were discovered in mid-1970's by Svec et al.[12] Due to presence of epoxy groups, a wide range of modifications are possible. A number of modifications of the cross-linked GMA polymers have been carried out. The derivatised polymers have been used in a variety of analytical applications including chromatographic separation media,[13] ion-exchange resins,[14-15] catalysts supports[16,17] and for enzyme immobilisation.[18-20] The hydroxyl group in poly(2-hydroxyethyl methacrylate) (PHEMA) can be derivatised to produce a wide range of polymeric reagents suited to pharmaceutical, chromatographic applications as well as to immobilise biopolymers (enzymes, antibodies, cells), encapsulate mammalian cells and other sensitive compounds.[21-29] In the form of beads, in the size of hundreds of micrometers, these are utilised as reactive supports and carriers, fillings of chromatographic columns, and in diagnostics.[21-23] Spherical particles are typically produced, in addition to suspension polymerisation (a major disadvantage of which is the formation of broad size distribution) or by multi-step seeded polymerisation.[30]

Here, GMA-EGDM copolymers of differing mole ratio of GMA:EGDM, cross-link densities (CLD) were synthesised by suspension polymerisation. The typical CLDs were in the range 25, 50, 75, 100, 150 200 and 300. The copolymers were synthesised in the presence of pore generating solvents such as cyclohexanol. The effect of CLDs and the porogen on porous properties of copolymers were studied. AGE-EGDM and HEMA-EGDM copolymers of varying cross-link densities were also synthesised using the same technique.

All the above copolymers were also synthesised using multiple emulsion HIPE methodology. The polymerisations were conducted changing the ratio of monomer and internal water. The internal phase volumes were changed from 33.3 to maximum of 90.9 %. It is known that the emulsion containing internal phase volume more than 74% are called HIPEs. Emulsions containing internal phase volumes from 20 to 70% are known as medium internal phase emulsions (MIPEs).[31] We have studied the effect of internal phase volume on the formation of porous structures. The polymers of different CLDs (25, 50, 75, 100, 150 200 and 300) were synthesised. The effect of variation in reaction parameters on the morphology, porous properties and surface functionalities was studied. AGE-EGDM and HEMA-EGDM copolymers of varying cross-link densities were also synthesised using the same HIPE methodology and finally the properties were compared with the properties of polymers obtained by suspension technique.

3.2 Experimental

3.2.1 Materials

Analytical grade glycidyl methacrylate (GMA), allyl glycidyl ether (AGE), 2-hydroxyethyl methacrylate (HEMA) and ethylene dimethacrylate (EGDM) were obtained from Sigma-Aldrich, USA. Sorbitan monooleate (Span 80) was from LOBA CHEMIE, Mumbai, India. Potassium peroxydisulphate was from Merck, India. Azobisisobutyronitrile (AIBN) obtained from SISCO, India was crystallised from methanol before use. Poly(vinyl pyrrolidone) (PVP) from Fluka (Germany) was used as protective colloid.

3.2.2 Preparation of microporous beads

3.2.2.1 By suspension

The synthesis was conducted in a double walled cylindrical polymerisation reactor of 11 cm diameter and 15 cm height. The continuous phase comprised of a one-percent aqueous solution of PVP. The discontinuous phase consisted of GMA/AGE/ HEMA, EGDM, pore generating solvent (cyclohexanol) and initiator, azobisisobutyronitrile (AIBN). Stirring was started under a nitrogen overlay and the temperature was raised to 70 ºC. Polymerisation was allowed to proceed for 3 hours. The copolymer beads obtained were then thoroughly washed with water and methanol and acetone. The beads were dried overnight at 50 ºC under vacuum.

The copolymers of differing CLDs synthesised are presented in Table 3.1 for GMA-EGDM system, Table 3.2 for AGE-EGDM system and Table 3.3 for HEMA-EGDM system.

3.2.2.2 By HIPE: multiple emulsion method

The synthesis was conducted in double walled cylindrical reactor. The outer continuous aqueous phase (W_2) comprised of 0.5 wt. % aqueous solution of poly(N-vinyl pyrrolidone) (PVP) in 200 mL distilled water. The continuous organic phase (Oil phase) consisted of glycidyl monomers (GMA/AGE), cross-linking divinyl monomer (EGDM). The compositions are shown in Tables 3.4 and 3.5 for GMA-EGDM and AGE-EGDM systems, respectively. Polymerisation initiator azobisisobutyronitrile (AIBN) (0.108 mol) and nonionic surfactant span 80 (17 wt.%) having hydrophile-lipophile balance (HLB) 4.9 was added to this monomer phase. The inner discontinuous aqueous phase (W_1) comprised of water and water-soluble potassium peroxydisulphate initiator (0.118 mol).

HIPE (primary W_1/O) emulsion was formed by introducing inner aqueous phase into the discontinuous oil phase gradually (20 mL per minute) at 1400 rpm with six bladed Ruston turbine stirrer outside the reactor at room temperature. This stable HIPE emulsion was added to outer aqueous (W_2) suspension medium at a flow rate of 4-5 mL/minute in a 300 mL reactor fitted with Ruston turbine until the suspension reached about 20% HIPE**.** This makes the ternary water-in-oil-in-water ($W_1/O/W_2$) emulsified suspension. Temperature was maintained at 70^oC by circulating thermostated water. To form the microbeads, polymerisation was continued for 3 hours at 250 rpm.

The copolymer obtained in beaded form was separated by decantation, washed sequentially with water and methanol and dried at room temperature under reduced pressure after soxhlet extraction for a day. The dried polymers stored in the sealed plastic bags in the desicator in order to avoid contamination from acid vapors which may cause the opening of epoxy ring of GMA-EGDM and AGE-EGDM copolymers

Similarly, a series of HEMA-EGDM copolymers were prepared, as shown in Table 3.6. The copolymerisation reactions (GMA-EGDM, AGE-EGDM and HEMA-EGDM) are shown in Schemes 3.1, 3.2 and 3.3, respectively. In suspension polymerization the cyclohexanol plays important role in the formation of pore architecture, while in HIPE water act as pore generating solvent. Different types of morphologies can be achevied by differening the ratio of internal water to oil phase, which ultimately influence porous properties of copolymers.

3.2.3 Reaction Schemes

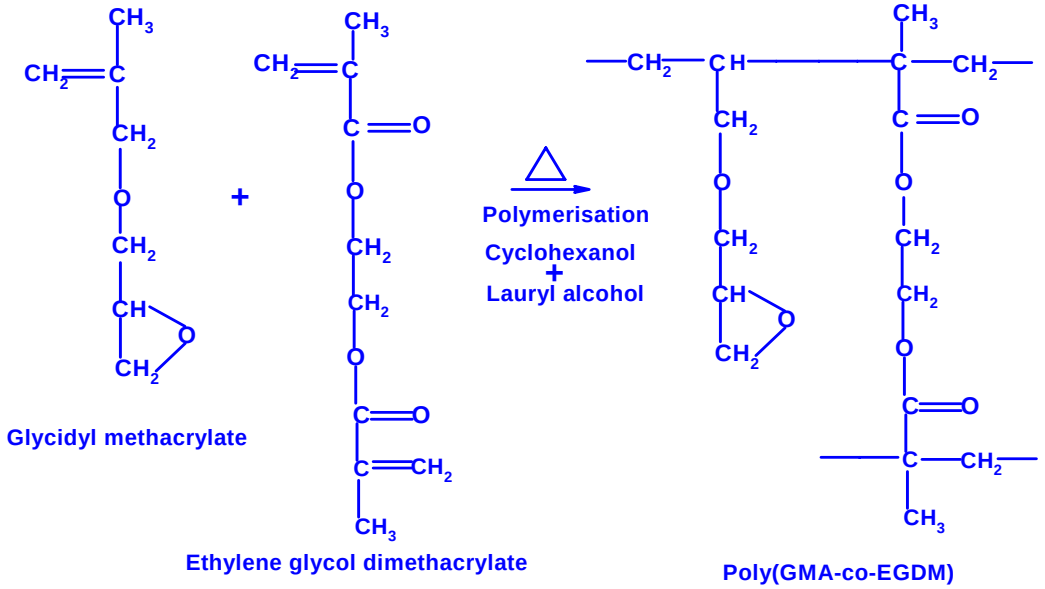

Scheme 3.1. Synthesis of glycidyl methcrylate (GMA) - ethylene dimethacrylate (EGDM) co copolymer

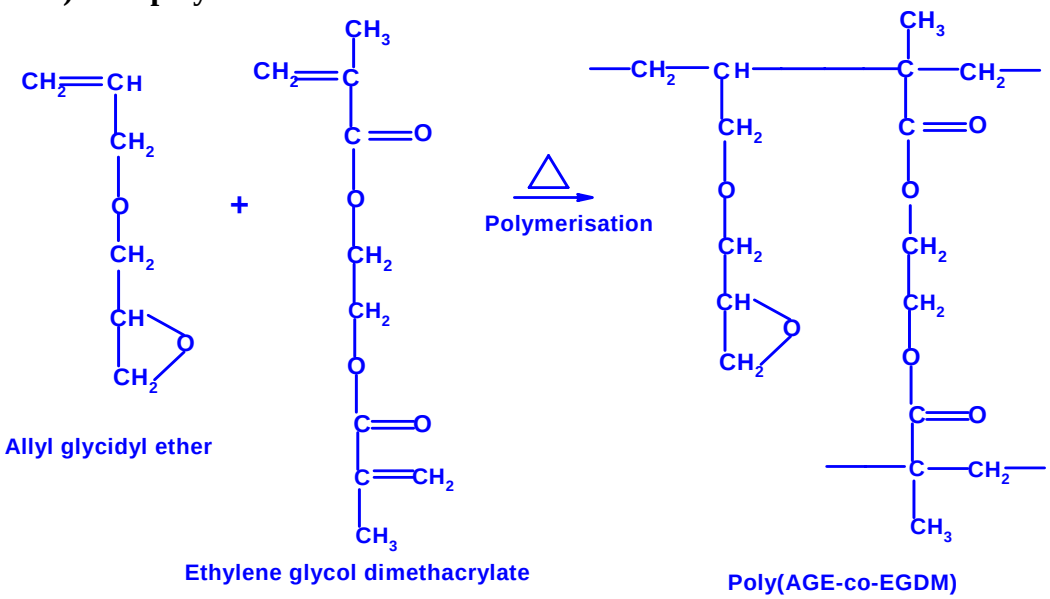

Scheme 3.2. Synthesis of allyl glycidyl ether (AGE) -ethylene dimethacrylate (EGDM) co-polymers

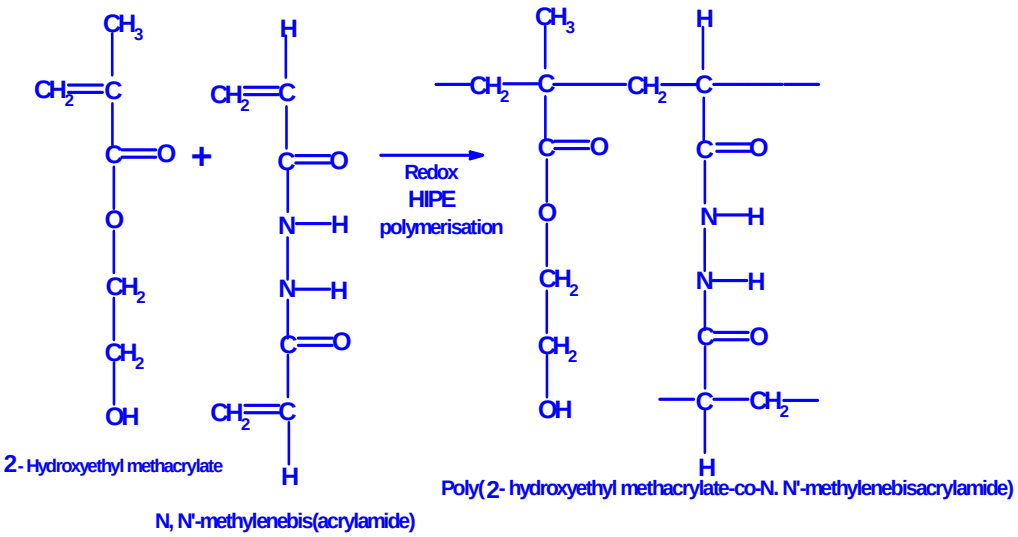

Scheme 3.3. Synthesis of 2-hydroxyethyl methacrylate (HEMA - ethylene dimethacrylate (EGDM) copolymer

Table 3.1. Glycidyl methacrylate-ethylene dimethacrylate copolymer beads by conventional suspension polymerisation using cyclohexanol as porogen

Expt. Code	GMA mol	EGDM mol	CLD %	Mass g	(Epoxy) mmol/g
GES11 and GES21	0.04904	0.01225	25	9.3988	5.2177
GES12 and GES22	0.03899	0.01951	50	9.4111	4.1434
GES13 and GES23	0.03240	0.02428	75	9.4192	3.4395
GES14 and GES24	0.02771	0.02768	100	9.4250	2.9397
GES15 and GES25	0.02148	0.03218	150	9.4326	2.2768
GES16 and GES26	0.01752	0.03505	200	9.4375	1.8562

CLD is the mole percent of cross-linking monomer relative to the moles of reactive functional comonomer. AIBN: 0.2 g; Water: 100 mL; PVP: 1 g. GMA: fw = 142.16; d = 1.042; molar volume = 136.4299; EGDM: fw = 198.22; d = 1.051; molar volume = 188.6013; Total volume of monomers = 9.00 mL; Expts GES11, GES 12, GES 13, GES14, GES 15 and GES 16 had monomer to porogen ratio of 1:1.6. Expts GES21, GES 22, GES 23, GES24, GES 25 and GES 26 had monomer to porogen ratio of 1:2.

Calculations for 25% CLD : 9.00 = (142.16/1.042)a + [(0.25x198.22)/1.051]a; solve for a; GMA volume = (142.16/1.042)a; EGDM volume = [(0.25x198.22)/1.051]a; Moles of GMA (mol) is calculated as [(6.69 x 1.042)/142.16]; Mass (g) is calculated as = [6.69 x 1.042 + 2.31 x 1.051]; (Epoxy) [mmol/g] is calculated as = (GMA)/Mass, which isi[0.05495/8.8787].

Table 3.2. Allyl glycidyl ether-ethylene dimethacrylate copolymer beads by conventional suspension polymerisation using cyclohexanol as porogen

Expt. Code	AGE mol	EGDM mol	CLD %	Mass g	(Epoxy) mmole/g
AES11 and AES21	0.05495	0.01315	25	8.8787	6.1890
AES12 and AES22	0.04222	0.02116	50	9.0131	4.6843
AES13 and AES13	0.03464	0.02593	75	9.0932	3.8094
AES14 and AES24	0.02933	0.02927	100	9.1493	3.2057
AES15 and AES25	0.02242	0.03362	150	9.2223	2.4311
AES16 and AES26	0.01812	0.03632	200	9.2677	1.9552

Cross-link density (CLD) is defined as the mole percent of cross-linking monomer relative to the moles of reactive functional comonomer. AIBN: 0.2 g; Water: 100 mL; PVP: 1 g. AGE: fw = 114.14; d = 0.962; molar volume = 118.6486; EGDM: fw = 198.22; d = 1.051; molar volume = 188.6013; Total volume of monomers = 9.00 mL. Expts AES11, AES 12, AES 13, AES14, AES 15 and AES 16 had monomer to porogen ratio of 1:1.6. Experiments AES21, AES 22, AES 23, AES24, AES 25 and AES 26 had monomer to porogen ratio of 1:2.

Table 3.3. 2-Hydroxyethyl methacrylate-ethylene dimethacrylate copolymer beads by conventional suspension polymerisation using cyclohexanol as porogen

Expt. Code	HEMA mol	EGDM mol	CLD %	Mass g	Hydroxyl Mmol/g
HES11 and HES21	0.05343	0.01336	25	9.6016	5.5647
HES12 and HES22	0.04172	0.02089	50	9.5703	4.3593
HES13 and HES23	0.03422	0.02572	75	9.5516	3.5826
HES14 and HES24	0.02902	0.02906	100	9.5369	3.0429
HES15 and HES25	0.02226	0.03340	150	9.5175	2.3389
HES16 and HES26	0.01806	0.03611	200	9.5081	1.8994

Cross-link density (CLD) is defined as the mole percent of cross-linking monomer relative to the moles of reactive functional comonomer. AIBN: 0.2 g; Water: 100 mL; PVP: 1 g. HEMA: fw = 130.14; d = 1.073; molar voulme = 121.2861; EGDM: fw = 198.22; d = 1.051; molar volume = 188.6013; Total volume of monomers = 9.00 mL; Expts HES11, HES 12, HES 13, HES14, HES 15 and HES 16 had monomer to porogen ratio of 1:1.6. Experiments HES21, HES 22, HES 23, HES24, HES 25 and HES 26 had monomer to porogen ratio of 1:2.

Table 3.4. Glycidyl methacrylate-ethylene dimethacrylate copolymer beads by high internal phase emulsified suspension (HIPE's) polymerisation

Expt code	GMA mol	EGDM mol	CLD %	Mass g	(Epoxy) mmol/g
GEH11, GEH21, GEH31	0.04904	0.01225	25	9.3988	5.2177
GEH12, GEH22, GEH32	0.03899	0.01951	50	9.4111	4.1434
GEH13, GEH23, GEH33	0.03240	0.02428	75	9.4192	3.4395
GEH14, GEH24, GEH34	0.02771	0.02768	100	9.4250	2.9397
GEH15, GEH25, GEH35	0.02148	0.03218	150	9.4326	2.2768
GEH16, GEH26, GEH36	0.01752	0.03505	200	9.4375	1.8562

Monomer (O) phase: Monomer (GMA) + cross-linker (EGDM) + Span 80=1.6 g, AIBN= 0.2 g, Total volume of monomers = 9.00 mL; Inner water (W_1) phase: inner water = 9 mL/18 mL/45 mL+ $CaCl_2$=4 wt.%, Outer aqueous (W_2) phase: Water = 200 mL+ PVP= 2 g, Stirring speed during primary (W_1/O) HIPE formation = 1400 rpm, stirring speed during polymerisation= 300 rpm, polymerisation temperature = 70ºC, Time = 3 h. Total volume of monomers = 9.00 mL. GEH 11, GEH 12, GEH 13, GEH 14, GEH15 and GEH 16 had monomer to inner water ratio of 1:1. GEH 21, GEH 22, GEH 23, GEH 24, GEH 25 and GEH 26 had monomer to inner water ratio of 1:2 and GEH 31, GEH 32, GEH 33, GEH 34, GEH 35 and GEH 36 had monomer to inner water ratio of 1:5.

Table 3.5. Allyl glycidyl ether-ethylene dimethacrylate beads by high internal phase emulsified suspension (HIPE's) polymerisation.

Expt. Code	AGE mol	EGDM mol	CLD %	Mass g	(Epoxy) mmol/g
AEH11, AEH21, AEH31	0.05495	0.01315	25	8.8787	6.1890
AEH12, AEH22, AEH32	0.04222	0.02116	50	9.0131	4.6843
AEH13, AEH23, AEH33	0.03464	0.02593	75	9.0932	3.8094
AEH14, AEH24, AEH34	0.02933	0.02927	100	9.1493	3.2057
AEH15, AEH25, AEH35	0.02242	0.03362	150	9.2223	2.4311
AEH16, AEH26, AEH36	0.01812	0.03632	200	9.2677	1.9552

Monomer (O) phase: Monomer (AGE) + cross-linker (EGDM) + Span 80=1.6 g, AIBN= 0.2 g, Total volume of monomers = 9.00 mL; Inner water (W_1) phase: inner water = 9 mL/18 mL/45 mL+ $CaCl_2$=4 wt.%, Outer aqueous (W_2) phase: Water = 200 mL+ PVP= 2 g, Stirring speed during primary (W_1/O) HIPE formation = 1400 rpm, stirring speed during polymerisation= 300 rpm, polymerisation temperature = 70ºC, Time = 3 h. AEH 11, AEH 12, AEH 13, AEH 14, AEH15 and AEH 16 had monomer to inner water ratio of 1:1. AEH 21, AEH 22, AEH 23, AEH 24, AEH 25 and AEH 26 had monomer to inner water ratio of 1:2 and AEH 31, AEH 32, AEH 33, AEH 34, AEH 35 and AEH 36 had monomer to inner water ratio of 1:5.

Table 3.6. 2-Hydroxyethyl methacrylate-ethylene dimethacrylate copolymer beads by high internal phase emulsified suspension (HIPE's) polymerisation.

Expt. Code	HEMA mol	EGDM mol	CLD %	Mass g	Hydroxyl Mmol/g
AEH11, AEH21, AEH31	0.05343	0.01336	25	9.6016	5.5647
AEH12, AEH22, AEH32	0.04172	0.02089	50	9.5703	4.3593
AEH13, AEH23, AEH33	0.03422	0.02572	75	9.5516	3.5826
AEH14, AEH24, AEH34	0.02902	0.02906	100	9.5369	3.0429
AEH15, AEH25, AEH35	0.02226	0.03340	150	9.5175	2.3389
AEH16, AEH26, AEH36	0.01806	0.03611	200	9.5081	1.8994

Monomer (O) phase: Monomer (HEMA) + cross-linker (EGDM) + Span 80=1.6 g, AIBN= 0.2 g, Total volume of monomers = 9.00 mL; Inner water (W_1) phase: inner water = 9 mL/18 mL/45 mL+ $CaCl_2$=4 wt.%, Outer aqueous (W_2) phase: Water = 200 mL+ PVP= 2 g, Stirring speed during primary (W_1/O) HIPE formation = 1400 rpm, stirring speed during polymerisation= 300 rpm, polymerisation temperature = 70ºC, Time = 3 h. HEH 11, HEH 12, HEH 13, HEH 14, HEH15 and HEH 16 had monomer to inner water ratio of 1:1. HEH 21, HEH 22, HEH 23, HEH 24, HEH 25 and HEH 26 had monomer to inner water ratio of 1:2 and HEH 31, HEH 32, HEH 33, HEH 34, HEH 35 and HEH 36 had monomer to inner water ratio of 1:5.

3.3 Characterisation

The porous properties of the resins are shown below to be dependent on the methodology used.

3.3.1 Particle size analysis

Single particle optical sensing (SPOS) AccuSizer 780 automatic particle sizer with light sensors LE 2500-15 and LE 500-0.5 was used to obtain the particle size of synthesised copolymer beads. Accusizer 780, comprised of auto dilution followed by light scattering system, quickly covers the particle range from 0.02 to 2000 μm, thus constructing a true particle size distribution (PSD).

There are two physical methods that traditionally have been used to implement the SPOS technique: Light extinction (LE) and Light Scattering (LS). The LE method is

based on a measurement of the decrease in the intensity of light transmitted across a flow channel carrying particles suspended in a fluid, caused by the momentary passage of an individually particle through the light beam. The LS method measures the increase in the intensity of light caused by scattering from particles, which pass through the optical sensing zone. The Accusizer combines the advantage of LE method (large size and relative intensitivity to particle composition) with the advantage of the LS method (high sensitivity-lower diameter limit).

The Sample (0.05-0.10 g) was mixed with a 1% solution of surfactant Noigen120, in water (5 mL). This mixture was sonicated for 1 min using sonicator (Ultrasonic Processor, Model CV26, resonating frequency 20KHz ± 50Hz). The suspension was then analysed in the auto-dilution mode.

3.3.2 Morphology and internal structure

Surface morphology of poly(GMA-EGDM), poly(AGE-EGDM) and poly(HEMA-EGDM) beads were observed using scanning electron microscopy (SEM). Specimen preparation was as follows: dried poly(GMA-EGDM) beads were mounted on stubs and sputter-coated with gold. Micrographs were taken on a JEOL JSM-5200 SEM instrument.

3.3.3 Pore volume and surface area

The pore volume and surface area were determined using mercury intrusion porosimetry and nitrogen adsorption methods. Mercury intrusion porosimetry was carried out using Autoscan 60, Quantachrome, USA, in the pressure range 0-66000 psig. BET surface areas were determined using NOVA 2000e surface area analyser from

Quantachrome, using nitrogen as adsorbate. The samples were degassed for 3 h at 60ºC and then analysed.

Physical and chemical gas adsorption (so called BET) as well as mercury intrusion porosimeter are the most widely used techniques to characterise powders and solid materials. These techniques can provide reliable information about the pore size/volume distribution, the particle size distribution, the bulk density and the specific surface area for porous solids regardless of their nature and shape. However, the applicable pore size ranges of each technique are different. Figure 3.1 shows a limit of application of both techniques.

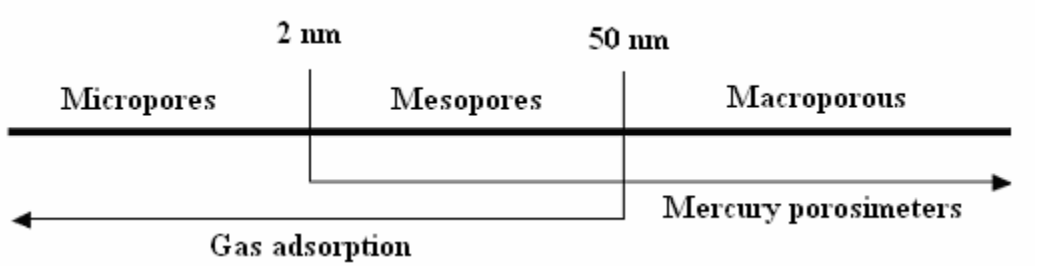

Figure 3.1. Pore size range applicable for mercury intrusion and nitrogen adsorption techniques

Although both methods are based on surface tension, capillary forces and pressure, two different physical interactions take place. It can be shown thermodynamically that vapour condensation-evaporation and mercury intrusion - extrusion into and out of the pore are similar processes operating in the two diametrically opposite extreme ends of pore size.[32] Pore size defines an ability of the analyte molecules to penetrate inside the particle and interact with its inner surface.[33]

3.3.4 Mercury intrusion porosimetry (MIP)

Mercury intrusion porosimetry (MIP) spans the measurement of pores ranging from a few nanometer, to several hundred micrometers. Mercury is a non-wetting liquid for almost all substances and consequently it has to be forced into the pores. Submerging the sample under a confined quantity of mercury and hydraulically increasing the pressure of mercury accomplish pore size and volume quantification. With increase in applied pressure the radius of the pores, which can be filled with mercury decreases and consequently the total amount of mercury intruded increases.

Mercury porosimetry is based on the Washburn equation, 3.1.[34]

$$\mathbf{p.r = -2.\gamma.\cos\theta} \qquad \mathbf{3.1}$$

Where, p is pressure, r is the radius of the pore that mercury intrudes, γ is surface tension of mercury and θ is contact angle of the mercury on the surface of the solid sample. The surface tension and contact angle of mercury are 480 mNm^{-1} and 140^{o}, respectively. The Washburn equation (3.1) can be derived from the equation of Yang and Dupre:

$$\mathbf{\gamma_{SV} = \gamma_{SL} + \gamma_{LV} .\cos\theta} \qquad \mathbf{3.2}$$

Where, γ_{SV} is the interfacial tension between solid and vapour, γ_{SL} is interfacial tension between solid and liquid, γ_{LV} is interfacial tension between liquid and vapour and θ is the contact angle of the liquid on pore wall. The work, W, is required to move liquid up the capillary. During capillary rise, when the solid-vapour interface disappears, solid-liquid interface appears as:

$$\mathbf{W = (\gamma_{SL}-\gamma_{SV}).\partial A} \qquad \mathbf{3.3}$$

Where, ∂A is the area of the capillary wall covered by liquid when their level rises. According to equations 3.2 and 3.3:

$$\mathbf{W = - (\gamma_{LV} .\cos \theta).\partial A} \qquad \mathbf{3.4}$$

The work required to raise a column of liquid through a height h in a capillary with radius r is identical to work required to force the liquid out of the capillary. When a volume V of liquid is forced out of the capillary with a gas at constant pressure above ambient ∂P_{gas}, the work is presented as:

$$\mathbf{W = V\partial P_{gas}} \qquad \mathbf{3.5}$$

Equations 3.4 and 3.5 are combined to yield:

$$\mathbf{\partial P_{gas}. V = -(\gamma. \cos \theta). \partial A} \qquad \mathbf{3.6}$$

When the capillary is circular in cross section, parameters V and ∂A are given by $\pi r^2 L$ and $2\pi rL$, where L is the length of the capillary.

$$\mathbf{p. r = -2.\gamma. \cos \theta} \qquad \mathbf{3.7}$$

This is known as Washburn equation, the operating equation in mercury porosimetry. The product pr is constant on keeping γ and θ constant. This implies that pressure is inversely proportional to radius. Thus, mercury will intrude progressively into narrower pores with increase in pressure. Using θ (140^o) and γ (0.480 N/m), the Washburn equation is $p = 0.736/r$.

The experimental method is dependent on the wetting or contact angle between mercury and surface of the solid. This contact angle exceeds 90^o for non-wetting liquids but is less than 90^o for wetting liquids (Figure 3.2). In the experiment, gas was evacuated from the sample cell and mercury was transferred into the sample cell under vacuum.

Pressure was applied to force mercury into the sample. During measurement, applied pressure p and intruded volume of mercury (V) were registered. As a result of analysis, an intrusion and extrusion curve was obtained.

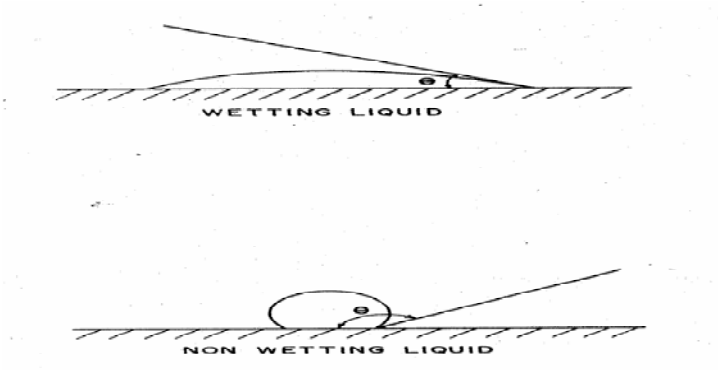

Figure 3.2. Contact angle of wetting and non-wetting liquid

3.3.5 Surface area measurement

Gas adsorption measurement is widely used for the characterisation of a variety of porous solids (e.g. oxides, carbons, zeolites and organic polymers). Of particular importance is the application of physisorption (physical adsorption) of the determination of the surface area and the pore size distribution of catalysts, industrial adsorbents, pigments, filters and the materials. Nitrogen (at 77ºK) is the recommended adsorptive determining the surface area and mesopore distribution, but it is necessary to employ a range of probe molecules to obtain a reliable assessment of the micropore size distribution. Although the role of modern techniques in characterising adsorbents and catalysis is ever increasing, classical methods based on adsorption on solid are still very popular and well utilised in surface chemistry. The classical measurement provides information about properties of a solid with respect to the adsorbing species. The classical and still most pertinent measurement in adsorption studies is the adsorption-

desorption isotherm, used in the calculation of the surface area of adsorbents.[35] The methods used to determine surface area, are most frequently based on the determination of the monolayer capacity of a given adsorbent by the BET method. BET theory is a well-known rule for the physical adsorption of gas molecules on a solid surface. In 1938, Stephen Brunauer, Pual Hugh Emmet, and Edward Teller[36] published the BET theory. "BET" consists of the first initials of their family names. The concept of the theory is an extension of the Langmuir theory, which is a theory foe monolayer molecular adsorption, to multiplayer adsorption with the following hypotheses: (a) gas molecules physically adsorb on a solid in layers infinitely; (b) there is no interaction between each adsorption layer; and (c) the Langmuir theory can be applied to each layer. The resulting BET equation is expressed by:

$$\mathbf{P/ V (P_0- P) = 1/ V_mC +(C-1/ V_mC). (P/P_0)} \qquad \mathbf{3.8}$$

Where, V is the volume adsorbed, V_m is volume of monolayer, P is sample pressure, P_0 is saturation pressure and c is constant related to the enthalpy of adsorption (BET constant). The specific surface area (S_{BET}) is then calculated from V_m by the following equation:

$$\mathbf{S_{BET} =V_m. n_a. a_m/ m.V_L} \qquad \mathbf{3.9}$$

Where, n_a is the Avogadro constant, a_m is the cross-sectional area occupied by each nitrogen molecule (0.162 nm^2), m is the weight of the sample and V_L is the molar volume of nitrogen gas (22414 cm^3).

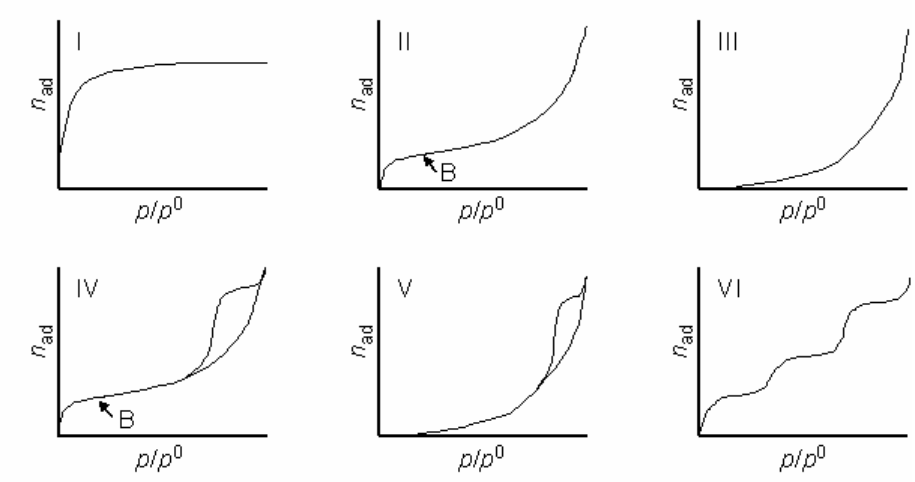

Figure 3.3. Types of adsorption isotherms

There are six classes of isotherms according to BDDT classification[37] as shown in Figure 3.3. Type I isotherms are given by microporous solids having relatively small external surfaces, the limiting uptake being governed by the accessible micropore volume rather than by the internal surface area. The reversible Type II isotherm is the normal form of isotherm obtained with non-porous or macroporous adsorbent. The Type II isotherm represents unrestricted monolayer multilayer adsorption. In reversible Type III isotherm adsorbate-adsorbent interaction plays an important role. Characteristic features of the Type IV isotherm is its hysterisis loop, which is associated with capillary condensation taking place in mesopores, and the limiting uptake over a range of high P/P^0. Type V isotherm is uncommon; it is related to the Type III isotherm in that the absorbate-adsorbent interaction is weak, but is obtained with certain porous adsorbent. Type VI isotherm, in which the sharpness of the steps depends on the system and the temperature, represents stepwise multilayer adsorption on uniform non-porous surface.

3.3.6 Mercury Vs nitrogen adsorption

Pore structure analysis by mercury porosimetry is faster than that by nitrogen adsorption. With mercury porosimetry, large pores are filled first and with increase in hydraulic pressure smaller pores get progressively filled. With nitrogen adsorption, the smallest pores are measured first at the adsorption phase and with increase in adsorbate pressure larger pores are filled.[38] The two processes occur in reverse since nitrogen and mercury are wetting and non-wetting liquid respectively on most of the surfaces. The determination range of high-pressure mercury porosimetry is wider (pore diameter 3 nm-14 μm) than that of nitrogen adsorption (0.3-300 nm), and mercury porosimetry determines larger pores that are out of the detection range of nitrogen adsorption (Figure 3.1). With nitrogen adsorption, the smallest pores that are out of range of mercury porosimetry can be determined. However, results of two methods can be compared. The complete parameters are total pore volume, volume pore size distribution and specific surface area/ total surface area. Although the pore size range that can be determined with adsorption is narrower than that obtained with mercury porosimetry, it is more widely used.[39]

Comparison has been made between surface areas measured by porosimetry and gas adsorption with the results ranging from poor to excellent. The difference between the two methods can be used to deduce the useful information not obtained by either method. For example, when surface area calculated from adsorption data is large compared to the area measured by porosimetry, it implies that pores smaller than those penetrated by mercury at maximum pressures contribute substantially to volume. Pore wall roughness is another factor that leads to slightly larger adsorption areas than those

from porosimetry. Slight surface roughness will not alter the porosimetry surface area since it is calculated from pore volume while the same roughness will be measured by gas adsorption. Ink-bottle shaped pores, with a narrow entrance into a wider inner body, generate larger surface areas in porosimetry than those from nitrogen adsorption. Intrusion into wider inner body will not occur until sufficient pressure is applied to force mercury into the narrow entrance. It will therefore appear as if a large volume intruded into narrow pores, generating excessively high surface areas.

3.4 Results and discussion

Multiple emulsions, either W/O/W or O/W/O emulsion, are generally prepared by a two step procedure.[40] For W/O/W emulsions, the primary emulsion (W/O) is first prepared using water and a low-HLB surfactant solution in oil. In the second step, the primary emulsion (W/O) is re-emulsified in an aqueous solution of a high-HLB surfactant to produce a W/O/W multiple emulsion. The first step- that is the preparation of the primary emulsion- is usually carried out in high-shear device to produce very fine droplets. The second emulsification step is carried out in a low shear device to avoid rupturing the multiple droplets. HIPE structures are formed when an oil, water and suitable emulsifier are mixed with agitation. The water becomes dispersed in the oil phase and as its concentration increases, the consistency of the mixture changes to a thick liquid. This viscous liquid is called high internal phase emulsion (HIPE) and is quite stable as shown in Figure 3.4 (a, c, e). These are suspended in a large amount of water containing appropriate protective colloid, and uniform spheres of HIPE are formed, as shown in Figure 3.4 (b, d, f).

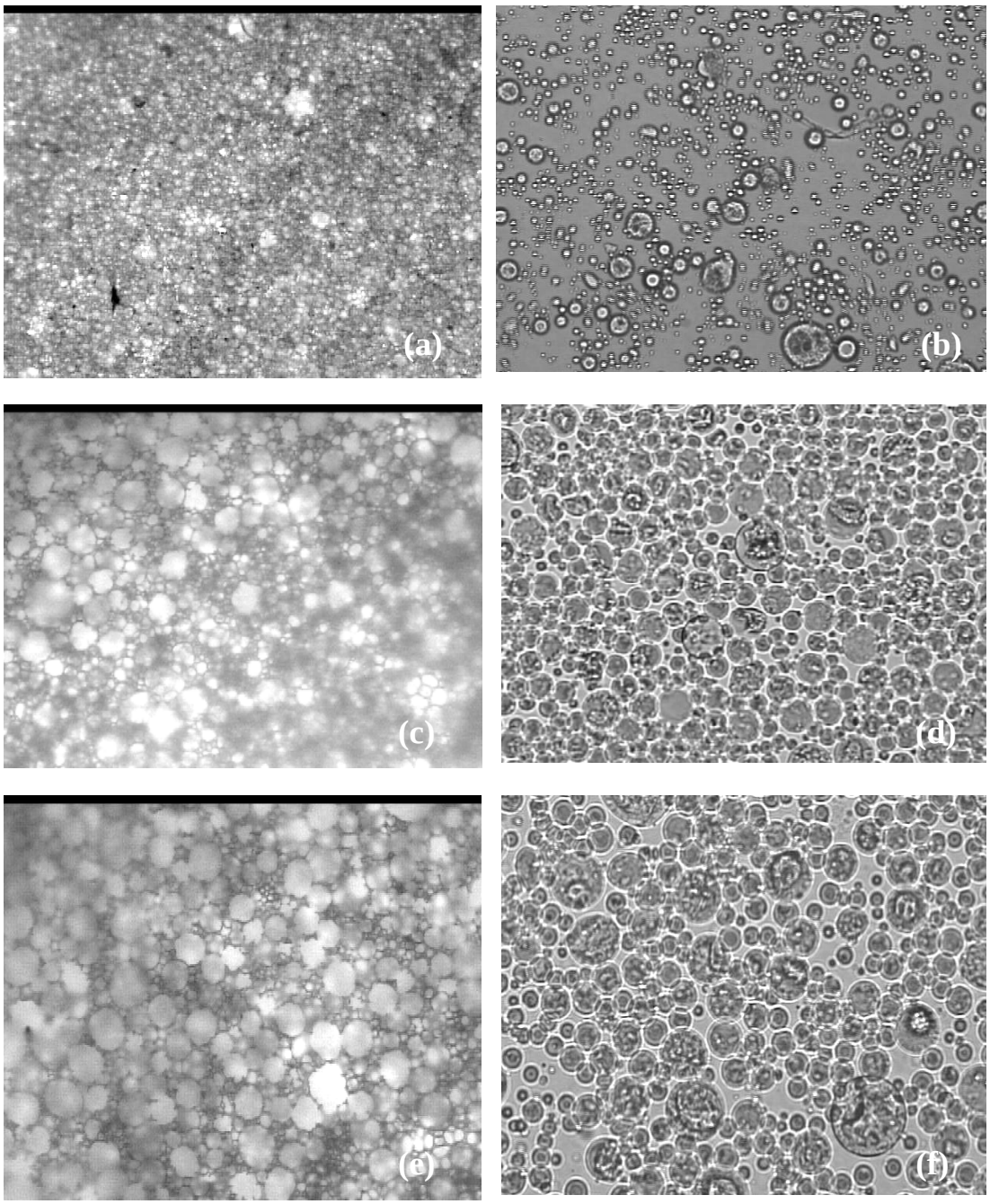

Figure 3.4. Optical microscopy: Primary W_1/O and secondary $W_1/O/W_2$ emulsion. (a) GMA-EGDM primary W_1/O, (b) GMA-EGDM secondary $W_1/O/W_2$ emulsion, (c) AGE-EGDM W_1/O primary emulsion, (d) AGE-EGDM secondary $W_1/O/W_2$ emulsion, (e) HEMA-EGDM primary W_1/O, and (f) HEMA-EGDM secondary $W_1/O/W_2$ emulsion

As shown in Figure 3.4 (a) GMA-EGDM primary emulsion (W_1/O) was formed using span 80 low-HLB surfactant that was poured into secondary water phase forming ($W_1/O/W_2$) multiple emulsion. Figure 3.4 (b) clearly indicates the entrapment of small water droplets into the primary W_1/O emulsion droplets, which was dispersed in secondary aqueous phase.

Similarly, the primary emulsions of AGE-EGDM and HEMA-EGDM are shown in the Figure 3.4 (c) and (e), respectively. The secondary emulsified droplets of AGE-EGDM and HEMA-EGDM formed are shown in Figure 3.4 (d) and (f). Here dispersion of primary emulsion is quite uniform and slightly bigger in droplet size as compared to GMA-EGDM secondary emulsion under identical shear field.

3.4.1 Particle size and distribution

Droplets of the primary HIPE emulsion, containing GMA/AGE/HEMA and EGDM, were subsequently suspended in a secondary water phase, comprising water, a stabiliser (PVP) and an initiator. This was done simply by a slow drop-wise addition of the primary water-in-oil (W_1/O) to the secondary aqueous phase while stirring at 300 rpm. Continuous stirring of the multiple emulsions at 70ºC yielded solid polymer particles. Optical microscopy revealed spherical nature of the polymers in Figure 3.5 wherein Figure 3.5 (a), (c) and (e) show uniform spherical nature of GMA-EGDM, AGE-EGDM and HEMA-EGDM copolymers, respectively at 40X magnification while Figures 3.5 (b), (d) and (f) show spherical nature of GMA-EGDM, AGE-EGDM and HEMA-EGDM copolymers at a magnification of 500X. The composition of the oil phase with regards to the monomers and the cross-linker was found to have a significant effect on

the particle-size distribution. Particles were photographed using an Olympus 300U optical microscope and the images analysed with Imagepro software.

The beads obtained by suspension polymerisation in the presence of pore generating solvent were opaque indicating the porous nature of copolymers. The beads obtained by both the methodologies (suspension and multiple HIPE emulsion) were opaque and mostly spherical. In case of multiple emulsion polymerisations the beads obtained were smaller than those by suspension polymerisation.

In suspension polymerisation, the monomer is initially dispersed in continuous aqueous phase by the combined action of surface-active agent and agitation. All reactants (monomers and initiators) reside in the monomer droplets that are progressively transformed into sticky, viscous monomer-polymer particles 50-500 μm in diameter. One of the most important issues in operation of a suspension polymerisation is control of final particle size distribution (PSD). The initial monomer droplet size distribution as well as the final polymer PSD in general depends on the type and concentration of the surface active agents, the quality of agitation, and the physical properties (eg. density, viscosity and interfacial tension) of the continuous and dispersed phases. The transient droplet/PSD is controlled by two dynamic processes, namely, the drop breakage and drop coalescence rates. The former mainly occurs in regions of high shear stresses (i.e., near the agitator blades) or as a result of turbulent velocity and pressure fluctuations along the surface of a drop. When drop breakage occurs by viscous shear forces the monomer droplets are first elongated into two fluid lumps separated by a liquid thread. Subsequently, the deformed droplet breaks into two almost different size droplets. Only in rare case does the deformed liquid droplets break up into two equal drops.

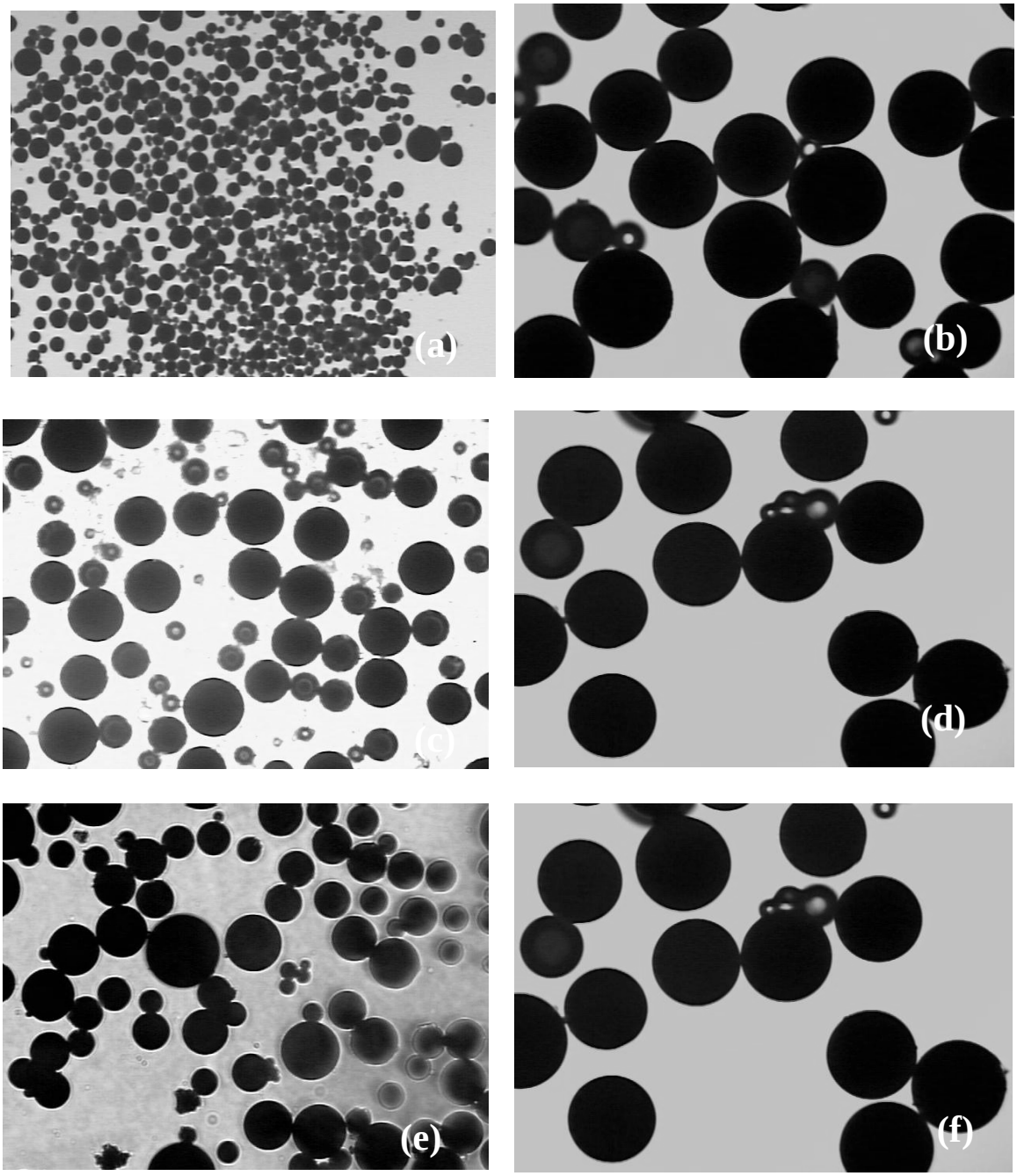

Figure 3.5. Optical microscopy of copolymers synthesised by HIPE, (a) GMA-EGDM at 40x, (b) GMA-EGDM at 500x, (c) AGE-EGDM at 40x, (d) AGE-EGDM at 500X, (e) HEMA-EGDM at 40X and (f) HEMA-EGDM at 500X magnification

On the other hand, a droplets suspended in a turbulent flow field is exposed to local pressure and relative velocity fluctuations. For nearly equal densities and viscosities

of thetwo liquid phases, the droplet surface can start oscillating. When the relative velocity is close to that required to make a drop marginally unstable, a number of small drops are stripped out from the initial one. The influence of all these parameters makes the beads polydispersed (bimodal in nature) as shown in Figures 3.5 (a), (c) and (e).

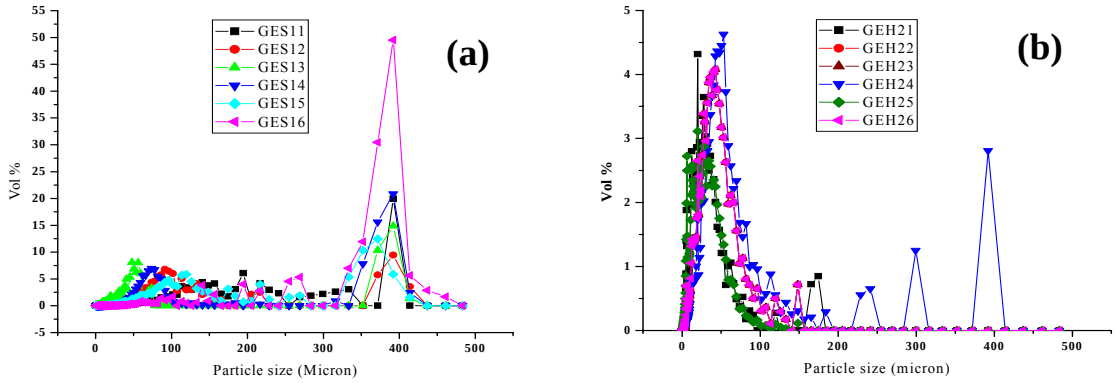

Figure 3.6. Particle size distribution of GMA-EGDM copolymers (a) by suspension using 1:2 monomer to porogen ratio, (b) by HIPE using 1:2 oil to water ratio

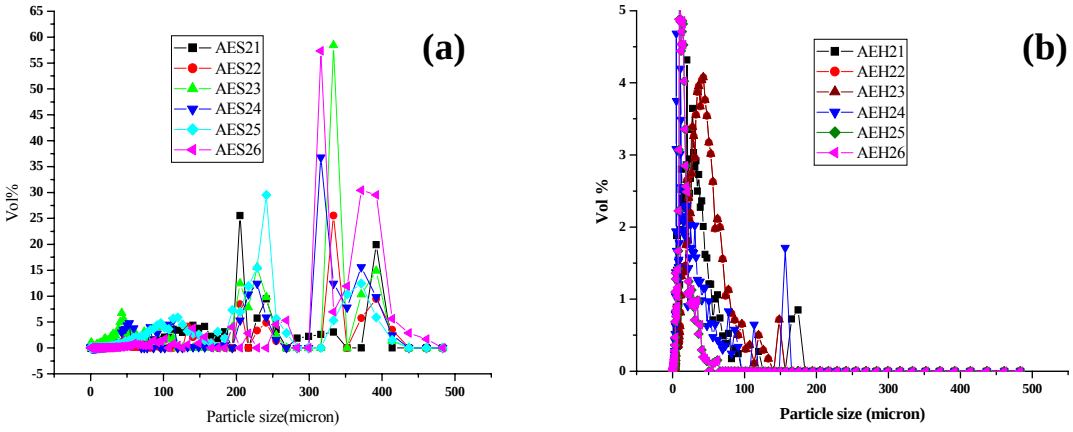

Figure 3.7. Particle size distribution of AGE-EGDM copolymers (a) by suspension using 1:2 monomer to porogen ratio, (b) by HIPE using 1:2 oil to water ratio

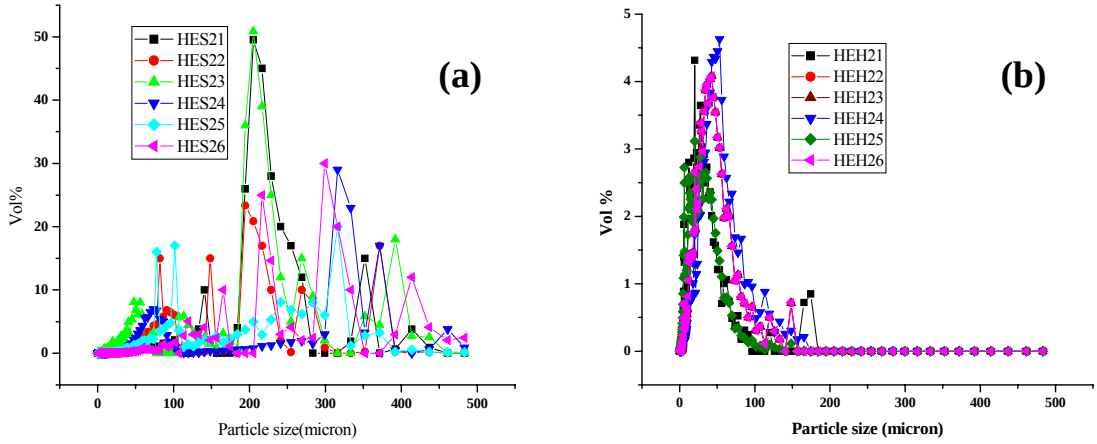

Figure 3.8. Particle size distribution of HEMA-EGDM copolymers (a) by suspension using 1:2 monomer to porogen ratio, (b) by HIPE using 1:2 oil to water ratio

The particle size distribution of suspension and multiple emulsion polymerised beads are shown in the Figures 3.6, 3.7, and 3.8. The beads obtained by suspension polymerisation were in the range of 100-500 μm while those obtained by multiple emulsions or HIPE polymerisation was in the range of 0.5-150 μm at similar stirring speeds. The narrow particle size distribution in HIPE as compared to the suspension polymerisation results because of the initial stirring speed during the primary HIPE (W_1/O) formation (1400 rpm).

Unlike suspension polymerisation, the particle size in high internal phase emulsion polymerisation is determined by the initial rate of stirring. Here, the polymerisation proceeds in confined droplets, which are already formed at the beginning. Stirring speed determines the particle size. It is established that increase in agitation speed causes a reduction of droplet size formed, which is primarily governed by its growth time prior to detachment. This is effectively reduced at higher shear stress as a result of higher agitation speed. Another factor, which affects the particle size distribution in HIPE, is ripening time between primary HIPE emulsion and

polymerisation. During this ripening time, the droplets will come to swelling equilibrium. Studies show that the ripening time is of the order of seconds to minutes. Secondly, the narrowness of the particle size distribution predicted on the ability to nucleate nearly all of the droplets over a short period of time. The properties of emulsion like structure depends on the stability of emulsion in the primary emulsion stage, on the composition thickness and the viscoelasticity of the adsorbed stabilising layer at the oil-water interface. The stability of the emulsion, with respect to creaming and coalescence, depends mainly on the droplet size distribution, the state of aggregation of the droplets and rheology of aqueous dispersion medium. The droplet size distribution is mainly dependent on the energy inputs during the emulsification and so the particle size distribution. Figures 3.6 (a), 3.7 (a) and 3.8 (a) show the broad particle size distribution in the GMA-EGDM, AGE-EGDM and HEMA-EGDM copolymers, synthesised by the suspension polymerisation using cyclohexanol as porogen, while Figures 3.6 (b), 3.7 (b) and 3.8 (b) show the relatively narrow particle size distribution of GMA-EGDM, AGE-EGDM and HEMA-EGDM copolymers synthesised by the multiple $W_1/O/W_2$ emulsion method, respectively.

3.4.2 Pore volume, surface area and pore size distribution

Both mercury intrusion porosimetry and nitrogen adsorption isotherm were used to evaluate morphology of beaded, cross-linked, porous GMA-EGDM, AGE-EGDM and HEMA-EGDM copolymers synthesised by suspension and high internal phase emulsion (HIPE) polymerisation.

In case of suspension polymerisation, the internal pore structure can be controlled by several parameters such as amount of cross-linker, type and volume of porogen (also

termed as diluent or pore generating solvent) added to the monomer phase. Porogen generates permanent pores in macroreticular polymers. The larger pores, which are responsible for higher pore volume, are located in between agglomerates and arise when larger amount of cross-linker and porogen are used. Macroporous and mesoporous morphology in beaded polymers arise due to formation of gel microspheres, agglomeration of these and binding together of the agglomerates to form the beads. The appearance of gel microsphere is dependent on the cross-linker and to a smaller extent on the porogen.

During polymerisation, the polymer phase separates from the solution due to its limited solubility in the polymerisation mixture either due to build of molecular weight beyond that is soluble in the solvent (fractionation) or due to cross-linking. Phase separation generates microspheres. The task of porogen is to create cavities in the polymeric structure by dissolution of the monomer, while acting as a precipitant towards the growing polymer.

Mercury porosimetry shows that copolymers prepared from monomer feed ratios low in the cross-linking comonomer (EGDM) and porogen (cyclohexanol) have low pore volume and surface area because a large number of nuclei are formed which tend to grow through each other. The data on pore volume and surface area of polymers synthesised by suspension methodology are presented in Tables 2.4, 2.5 and 2.6.

The copolymer formed in suspension possesses a very broad pore size distribution in the meso and macro range as shown in the Figures 3.9 (a), 3.10 (a) and 3.11 (a). These matrices are suitable to immobilise variety of enzymes and also to anchor chiral ligands, for use in stereoselective resolution. Pore structure of polymer network is fixed during

the gel formation process when the network is in the rubbery state. Figure 3.9 (a) presents the differential pore size distributions in poly(GMA-EGDM) beads of differing copolymer composition (cross-link density) at constant monomer:porogen volume ratio of 1:1.6. At higher cross-link density, the pore size distribution broadens over the entire range from 5-500 nm. Similar results are obtained with AGE-EGDM and HEMA-EGDM copolymer series as shown in Figures 3.10 (a) and 3.11 (a), respectively. Figures 3.9 (b), 3.10 (b) and 3.11 (b) show the pore size distribution in copolymers of similar composition but at higher porogen:monomer ratio of 2:1. In this case there is a marginal increase in the pore volume and surface area, as shown in Tables 3.6, 3.7, and 3.8. This increase is seen over the entire composition (CLD) range, relative to that at lower porogen volume.

While pores are present over the entire range of composition in AGE-EGDM copolymer series (Figures 3.10 (a) and (b)) a somewhat bimodal distribution is noted. In HEMA-EGDM copolymers only a marginal uniformity is noted in macroporous region at 1:1.6 monomer to porogen ratio (Figure 3.11 (a)) but not at the monomer to porogen ratio of 1:2. Here, pore size observed covers the entire range, from 5–500 nm, as seen in Figure 3.11 (b). The median pores are now in the mesoporous range (30-50 nm) and are independent of copolymer composition. A glance at the data (Table 3.7) generated for poly(GMA-EGDM), with cyclohexanol as porogen, shows that pore volume increases with increases in cross-link density and relative porogen concentration due to increase in the number of pores. Phase separation of copolymer from the porogen present in the monomer phase contributes to the generation of pores rather than phase separation from the monomers yet to be polymerised and about to be linked to the growing copolymer

chains. At lower cross-link density and lower volume of porogen, the inner pore volume is negligible because most porogen molecules are embedded in the network (gel) phase throughout the copolymerisation. At higher cross-link density and volume of porogen, separation of the porogen out of the network (gel) phase generates highly porous structure and results in high pore volume.

The data on surface area, presented in Tables 3.7, 3.8 and 3.9 were determined on copolymer particles whose diameter ranged between 100 and 450 nm. In all these Tables the polymers synthesised using 1.1.6 v/v monomer to porogen ratio are termed 11 series and the polymers formed using 1:2 v/v monomer to porogen ratio are termed as 21 series. During the polymerisation micropores are generated, which are identifiable in the surface area but not in mercury porosimetry measurements. Thus, surface area is very low at low cross-link density and lower amount of porogen (1:1.6), and increases with increasing cross-link density and volume of porogen, for copolymers of similar particle size distribution. At higher porogen:monomer ratio (1:2), the surface area increases with relative increase in porogen volume. This increase is enhanced at higher cross-link densities, as shown in Table 3.7. Since micropores contribute extensively to surface area and macropores contribute like-wise to pore volume, it can be said with some certainty that both micro- and macropores increase with cross-link density and that there is a polydispersity in pore size, especially at higher cross-link densities. These pore geometries are ideally suited to anchor macromolecules such as enzymes. GMA-EGDM copolymers have surface area in the range of 62 –110 m^2/g at monomer to porogen ratio of 1:1.6. This increased marginally to 65-112 m^2/g at monomer to porogen ratio of 1:2, as shown in Table 3.7. Similar trend was obtained for AGE-EGDM copolymer series as

shown in Table 3.8, wherein surface area for AGE-EGDM copolymer series were in the range 21-56 m^2/g at 1:1.6 monomer to porogen ratio and were 32-110 m^2/g at 1:2 monomer to porogen ratio. This indicates that cyclohexanol does not phase separate as effectively in presence of allyl glycidyl ether.

Table 3.7. Pore volume and surface area of GMA-EGDM copolymers (monomer:porogen: 1:1.6 and 1:2 v/v)

Polymer Code	CLD%	Pore volume (mL/g)	Specific surface area (m^2/g)
GES11, GES21	25	0.45, 0.54	62.57, 65.21
GES12, GES22	50	0.56, 0.48	68.35, 66.76
GES13, GES23	75	0.41, 0.68	42.52, 69.80
GES14, GES24	100	0.64, 0.65	71.25, 72.71
GES15, GES25	150	0.74. 0.78	87.43, 91.64
GES16, GES26	200	0.72, 0.93	108.36, 112.53

Thus, the effect is more pronounced at lower cross-link densities. In HEMA-EGDM copolymer series a regular trend could not be noted. However, with increase in porogen amount surface area showed an increase as shown in Table 3.9.

Table 3.8. Pore volume and surface area of AGE-EGDM copolymers (monomer:porogen: 1:1.6 and 1:2 v/v)

Polymer Code	CLD%	Pore volume (mL/g)	Specific surface area (m^2/g)
HES11, HES21	25	0.36, 0.23	44.02, 12.65
HES12, HES22	50	0.40, 0.56	40.65, 98.23
HES13, HES23	75	0.69, 0.45	56.74, 79.99
HES14, HES24	100	0.20, 0.66	36.54, 81.24
HES15, HES25	150	0.62, 0.91	88.61, 95.21
AES16, AES26	200	0.77,0.98	90.32, 96.52

Table 3.9. Pore volume and surface area of HEMA-EGDM copolymers (monomer:porogen: 1:1.6 and 1:2 v/v)

Polymer Code	CLD%	Pore volume (mL/g)	Specific surface area (m^2/g)
HES11, HES21	25	0.36, 0.23	44.02, 12.65
HES12, HES22	50	0.40, 0.56	40.65, 98.23
HES13, HES23	75	0.69, 0.45	56.74, 79.99
HES14, HES24	100	0.20, 0.66	36.54, 81.24
HES15, HES25	150	0.62, 0.91	88.61, 95.21
AES16, AES26	200	0.77,0.98	90.32, 96.52

The evaluated surface area by BET and pore volume by mercury porosimetry for GMA-EGDM, AGE-EGDM and HEMA-EGDM copolymer series synthesised by HIPE and varying oil:water ratios are presented in Tables 3.10, 3.11 and 3.12, respectively. There is drastic change in the surface area, pore volume and pore size distribution on increasing the relative volume of inner discontinuous (water) phase with respect to the continuous oil (monomer) phase. Unlike suspension polymerisation, in HIPE method the pore size and pore size distribution is dependent on the inner water phase, cross-linking, droplet formation, surfactant and their concentrations.

As shown in Figures 3.12, 3.13, and 3.14, polyHIPEs generally yield materials with narrow pore size distribution, in the micro and mesoporous range unlike the product of suspension polymerisation. The dimensions are dictated by the surfactant type and its concentration in the oil phase and by the relative volume of inner discontinuous phase. A series of experiments were conducted varying relative volume of the inner, discontinuous aqueous phase, as well as cross-link density (relative percent mole ratio of divinyl to monovinyl monomer). Three differing volume ratios of discontinuous to continuous

phase (1:1, 2:1 and 5:1) were studied. These were termed as 11, 21 and 31 series, respectively. The data is shown in Tables 3.10, 3.11 and 3.12. It is well known that with cross-linking density phase separation during polymerisation is enhanced and as a result the morphology of polymer, pore size distribution, specific surface area, and the mechanical strength of polymer, are altered.[41] Therefore, the effect of these factors were investigated using Span 80. The effect of its relative amount on the microporous structure was also investigated at different cross-link densities.

The results, shown in Tables 3.10, 3.11 and 3.12, depict the effect of cross-link density, from 25 to 200%, at a fixed concentration of surfactant i.e, 17% of the monomer phase. Micro and mesoporous structures were formed, as shown in Figures 3.12 (a, b, c) for GMA-EGDM, 3.13 (a, b, c) for AGE-EGDM and 3.14 (a, b, c) for HEMA-EGDM copolymers at 1:1, 1:2, and 1:5 oil to water ratios. At the relative concentration of Span 80 used (17% of monomer) reverse micellar aggregates will be formed.[42] Therefore, the surfactant phase, composed of a large amount of reverse micellar aggregates, would favor the formation of micro and mesopores. The mercury porosimtery data on pore volume of GMA-EGDM system at different oil to water ratios are presented in Table 3.10. The total pore volume of the system goes through either a maximum (CLD up to 75%) or minimum (CLD 100 to 200) when oil to inner water ratio was changed progressively from 1:1 to 1:5. Surface area was seen to go through a minimum at low CLD (up to 50%). Very narrow microporous pore size distribution was obtained, as seen in Figure 3.12 (a, b, c). The apparent increase in the porosity and microporous pore size distribution could be achieved not only by the increase in the cross-linking density but also by the increase in the inner water phase with respect to monomer phase.

In case of AGE-EGDM system (Table 3.11) there was no increasing trend in pore volume at lower cross-linking density at 1:1 and 1:2 oil to water ratios, but increasing trend was noted at higher cross-link densities. At 1:5 both pore volume and surface area increased from 0.5 to 1.06 cm^3/g and 72-158 m^2/g, respectively. When the amount of inner water level in primary HIPE emulsion is increased the water droplets break into smaller size and try to occupy as much as space is possible within the continuous oil phase. The low interfacial tension due to Span 80 (surfactant) prevents the merging of two dispersed droplets. They deform the polyhedra leaving behind small windows on the interface of oil to water phase. These small windows on the wall are responsible for higher surface area. So high surface areas (up to 158 m^2/g) at 1:5 oil to water ratio for the AGE-EGDM system was due to the combination of cell and interconnecting windows (Table 3.11). In this copolymer series pores were generated in the entire range of 5-100 nm, as shown in Figure 3.13 (a, b, c).

Table 3.10. Pore volume and surface area of GMA-EGDM copolymers (oil:water = 1:1, 1:2, 1:5 v/v) by BET isotherm

Polymer Code	**CLD %**	**Pore volume mL/g**	**Specific surface area m^2/g**
GEH11, GEH21, GEH31	25	0.58, 0.89, 0.65	21.77, 18.11, 78.12
GEH12, GEH22, GEH32	50	0.66, 0.97, 0.72	30.24, 27.28, 89.36
GEH13, GEH23, GEH33	75	0.82, 1.10, 0.89	18.98, 48.99, 75.87
GEH14, GEH24, GEH34	100	1.14, 0.86, 1.11	13.33, 45.02, 95.36
GEH15, GEH25, GEH35	150	1.25, 1.02, 1.56	22.34, 29.77, 115.78
GEH16, GEH26, GEH36	200	1.19, 0.88, 1.43	37.01, 51.73, 150.63

Table 3.11. Pore volume and surface area of AGE-EGDM copolymers (oil:water = 1:1, 1:2, 1:5 v/v) by BET isotherm

Polymer Code	CLD %	Pore volume mL/g	Specific surface area m^2/g
AEH11, AEH21, AEH31	25	0.64, 0.99, 0.55	24.89, 23.43, 74.56
AEH12, AEH22, AEH32	50	0.55, 0.60, 0.68	38.74, 31.12, 112.09
AEH13, AEH23, AEH33	75	0.53, 0.63, 1.27	35.74, 39.82, 90.78
AEH14, AEH24, AEH34	100	0.58, 0.52, 0.99	48.50, 40.10, 105.76
AEH15, AEH25, AEH35	150	0.48, 0.72, 1.06	32.78, 56.74, 116.78
AEH16, AEH26, AEH36	200	0.42, 0.80, 1.46	39.74, 78.15, 158.09

The pore size distribution, as shown in the Figures 3.13 (a, b, c), broadens at higher cross-link density while it is narrow at lower cross-link densities. The distribution is bimodal, in the range 5-50 nm at 1:1 oil to water ratio, 5-100 nm at 1:2 oil to water ratio and 5-300 nm at 1:5 oil to water ratio. We can see from the Figure 3.14 (a, b) that there is bimodality in pore size distribution only because of bigger cells and smaller windows. In the third system, HEMA-EGDM, HEMA is slightly water-soluble. During the polymerisation there will be transfer of some monomer molecules into the inner aqueous phase and as a result there is a broad pore size distribution, as seen in Figure 3.14 (c). The pore volume and surface area of HEMA-EGDM at three different oil to water ratios are presented in Table 3.12. There is increasing trend in the pore volume with increase in CLD from 0.56-0.66 cm^3/g for 1:1 ratio, 0.69-1.20 cm^3/g at 1:2, and 0.98-1.98 cm^3/g at 1:5. The surface area of HEMA-EGDM series lies in the range 85-165 m^2/g at the lowest oil to water ratio i.e. 1:5.

When the series of polymers of identical CLD range, prepared by HIPE and suspension methodologies are compared, pore size distributions in polymers obtained by HIPE are quite narrow while that by suspension are broader. Here, the larger pores and interconnected pore present on the wall of continuous phase contribute towards the narrow and bimodal distribution. In HIPE mainly long through and through channels are formed due to the formation of change in spherical micelle to rod shape micelles well above critical micelle concentration (CMC).

Table 3.12. Pore volume and surface area of HEMA-EGDM copolymers (oil:water = 1:1, 1:2, 1:5 v/v) by BET isotherm

Polymer Code	CLD %	Pore volume mL/g	Specific surface area m^2/g
HEH11, HEH21, HEH31	25	0.57, 0.69, 0.98	31.37, 22.60, 85.87
HEH12, HEH22, HEH32	50	0.66, 0.68, 0.99	104.00, 22.13, 88.51
HEH13, HEH23, HEH33	75	0.68, 0.72, 1.23	101.80, 70.10, 90.32
HEH14, HEH24, HEH34	100	0.70, 0.68, 1.56	20.43, 26.78, 111.10
HEH15, HEH25, HEH35	150	0.58, 0.95, 1.25	19.29, 57.67, 132.24
HEH16, HEH26, HEH36	200	0.66, 1.20, 1.98	11.81, 25.84, 165.47

As shown in the Table 3.12, at 50 and 75 % CLD surface areas of HEMA-EGDM copolymers with 1: 5 oil : water ratio are 88.51m^2/g and 90.32 m^2/g which are less than the HEMA-EGDM copolymers prepared at 1:1 ratio. This might due the formation of meso and maropores in the systems. At higher crosslink densities the surface areas drastically increased upto 165.47 m^2/g with 1:5 oil to water ratio and decreased upto 11.81 m^2/g in case of 1: 1 oil to water ratio.That means at higher oil to water ratio more and more micropores are generated which results in increase in surface area.

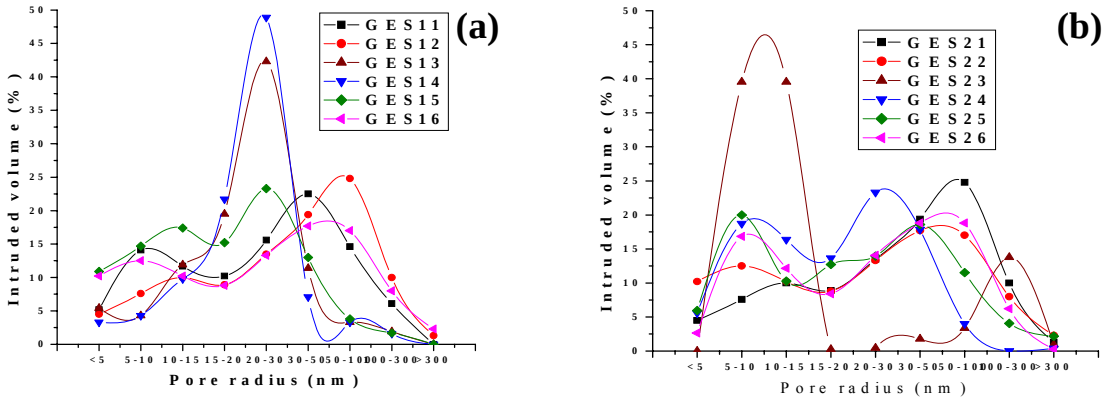

Figure 3.9. Pore size distribution of GMA-EGDM copolymers by suspension polymerisation (a) using 1:1.6, (b) 1:2 monomer:porogen ratio v/v

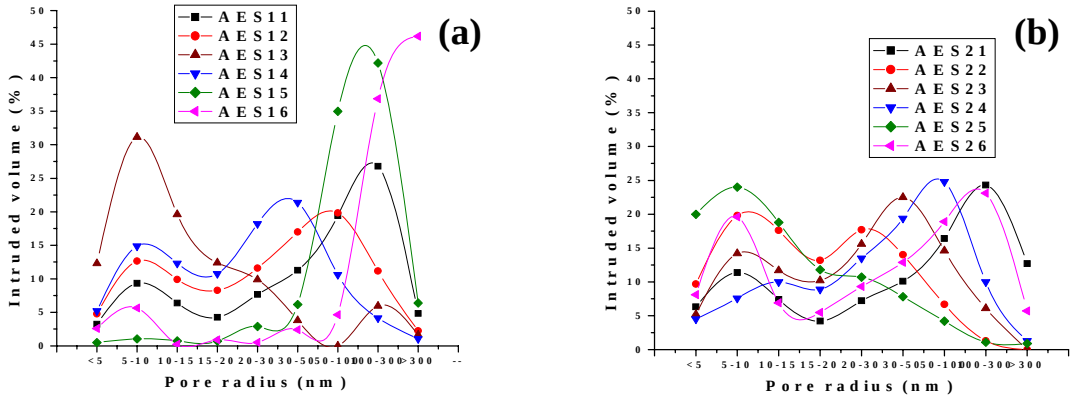

Figure 3.10. Pore size distribution of AGE-EGDM copolymers by suspension polymerisation (a) using 1:1.6, (b) 1:2 monomer:porogen ratio v/v

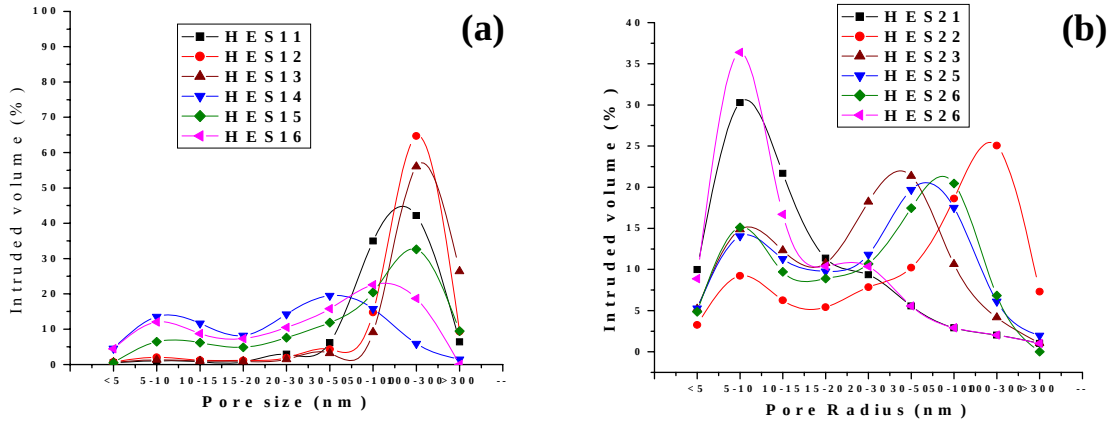

Figure 3.11. Pore size distribution of HEMA-EGDM copolymers by suspension polymerisation (a) using 1:1.6, (b) 1:2 monomer:porogen ratio v/v

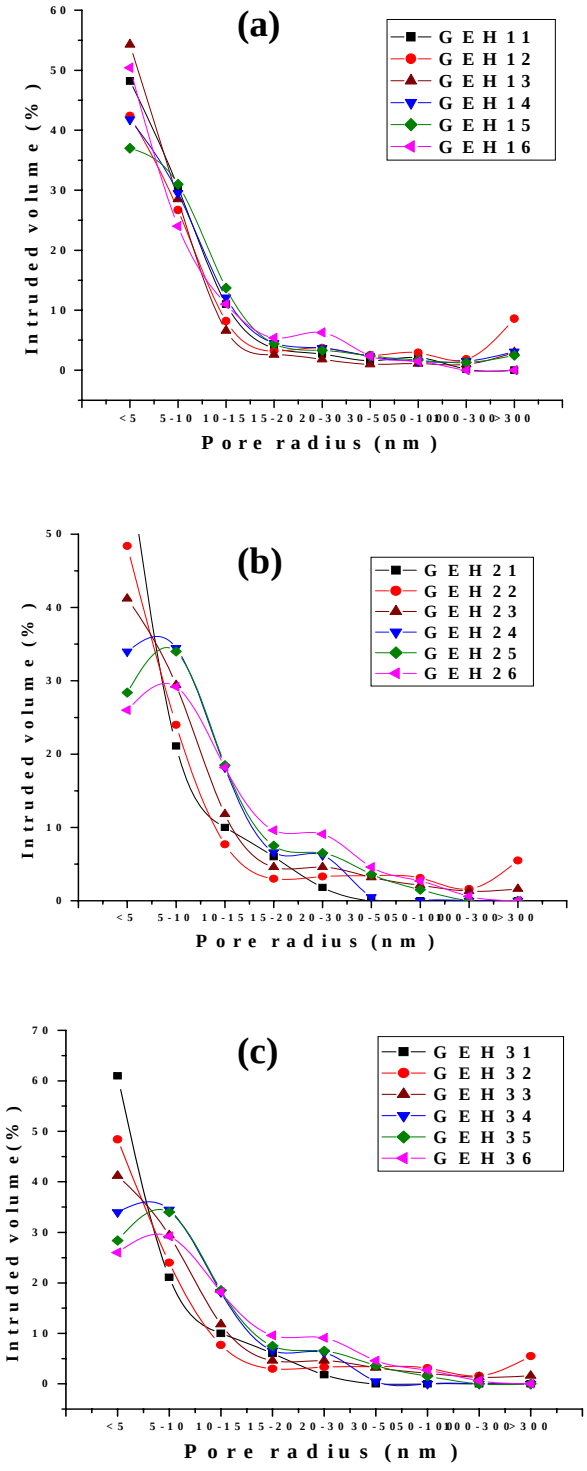

Figure 3.12. Pore size distribution of GMA-EGDM copolymers by multiple emulsion polymerisation (a) using 1:1 oil to water ratio, (b) 1:2 oil to water ratio, and (c) 1:5 oil to water ratio

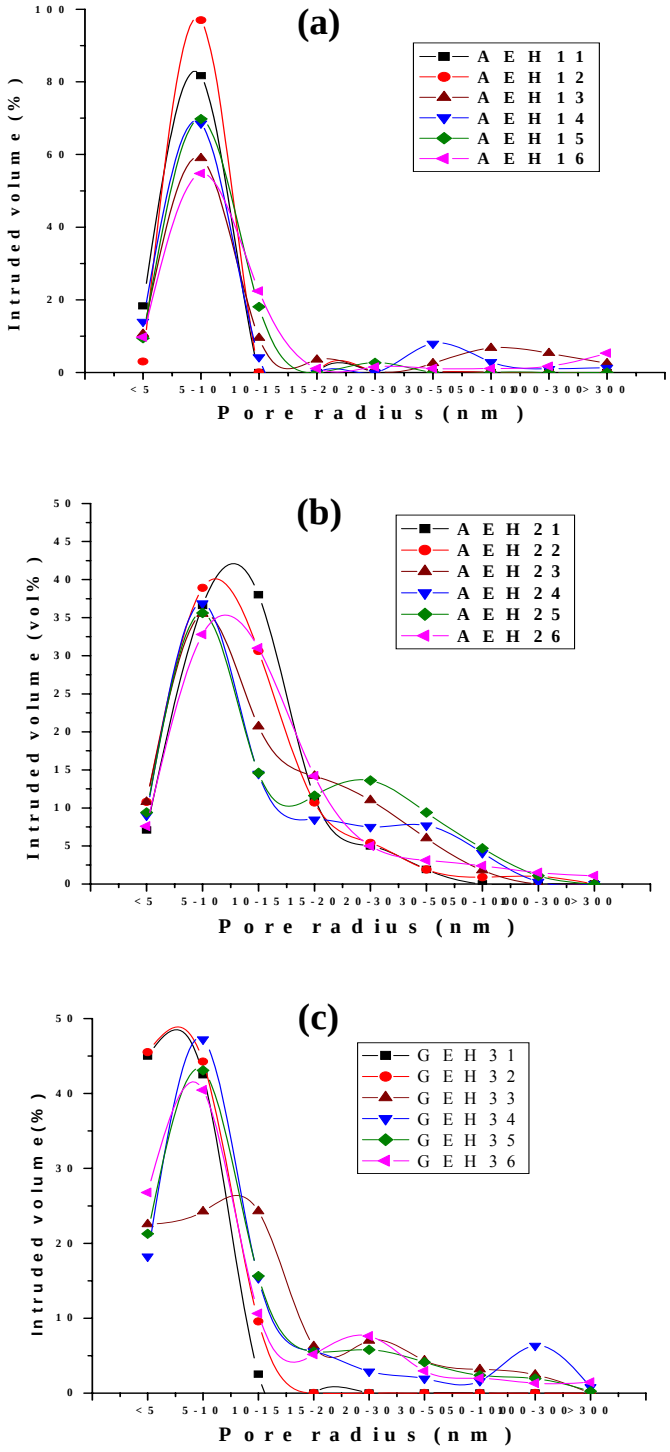

Figure 3.13. Pore size distribution of AGE-EGDM copolymers by multiple emulsion polymerisation (a) using 1:1 oil to water ratio, (b) 1:2 oil to water ratio, and (c) 1:5 oil to water ratio

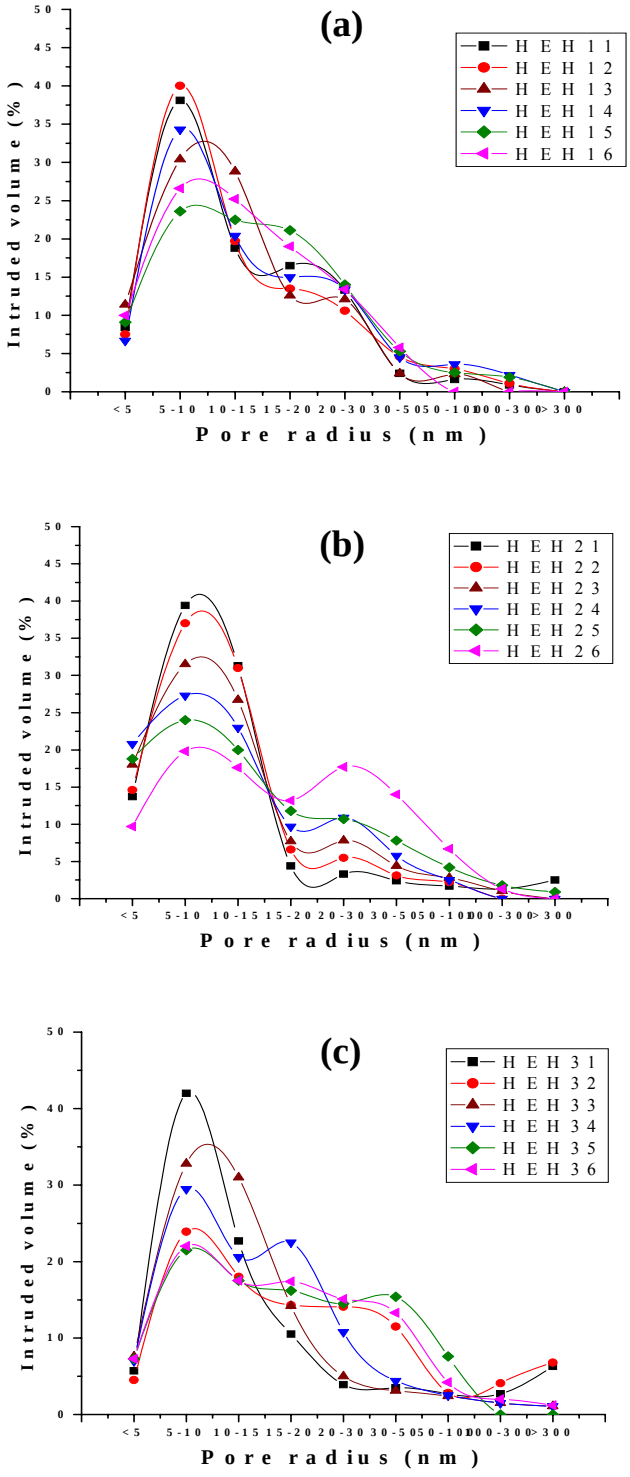

Figure 3.14. Pore size distribution of HEMA-EGDM copolymers by multiple emulsion polymerisation (a) using 1:1 oil to water ratio, (b) 1:2 oil to water ratio, and (c) 1:5 oil to water ratio

3.4.3 Surface as well as internal morphology

PolyHIPE materials have complex morphologies. They possess spherical cavities, known as voids, and windows that interconnect these voids.[43] Furthermore, a much finer porous texture within the walls of the base material can be created.

Both mesoporous and macroporous polymers are prepared by suspension polymerisation. In this process oil in water suspensions are achieved by rapidly stirring liquid monomers (the oil phase) along with a dispersing agent present in larger amount of water used as the continuous phase. Droplets of monomers are formed and are stabilised by the dispersing agent. If the monomer mixture also contains a polymerisation initiator, a porous polymer is formed as reaction temperature is increased above the activation temperature of initiator. HIPE spheres prepared in this study are also polymerised by suspension methodology but the starting material is not a simple combination of porogen, monomers and thermal initiator. Before the suspension polymerisation can occur, unique HIPE structures or HIPE primary emulsion must be prepared in a separate, preliminary step. HIPE structures are formed when an oil, water and suitable emulsifier are mixed with intense agitation. Water gets dispersed in the organised oil phase comprised of monomer, and surfactant and as its concentration increases, the consistency of the mixtures changes to a very viscous liquid. This viscous liquid is termed high internal phase emulsion and is quite stable, as shown in Figure 3.4 (a, c, e). When the HIPE is suspended in a large amount of water containing appropriate protective colloid, uniform spheres are formed, as shown in Figure 3.4 (b, d, f). The end result is a three-dimensional structure containing interconnected cavities having chemical properties of GMA-EGDM,

AGE-EGDM and HEMA-EGDM, but unique physical attributes not generated in beads prepared by suspension polymerisation.

Morphological investigations by SEM revealed that by increasing the phase volume we could modify the morphology. It is possible to influence density, surface area and cavity size. Polymerisation in this unique morphology does not alter chemical properties since chemical composition of the monomer is not affected in synthesis processes; however physical properties are changed. Resulting products exhibit a highly permeable structure that is easily dried to give a low-density material. HIPE polymers are clearly differentiated, characterised by the regularity of its cavities, much larger cavity diameters and clearly visible interconnecting pores. Conventional porous polymers exhibit an amorphous structure, clearly lacking the internal regularity of HIPE.

Figure 3.15 shows SEM photographs of GMA-EGDM copolymers prepared by multiple emulsion (HIPE) methodology at different magnifications. Figure 3.15 (a) shows the monodisperse nature of the particles, having diameter in the range 5-100 microns, and Figure 3.15 (b) shows the open surface pore morphology of the copolymer prepared using 1:1 v/v oil: water ratio. The morphologies and internal structure of the copolymers are distinctly different from those present in the beads made by suspension polymerisation. The morphology of the resulting materials is determined by the structure of the emulsion prior to gelation. The morphologies and the internal structure of the copolymers reflect the structure of the emulsion in case when the emulsions are stable and do not separate into individual components before gelation. During the polymerisation, phase separation occurs within the developing polymer structure between the internal phase droplets.[44] The properties of emulsion like structure, stability and

rheology depend on the composition, thickness and the viscoelasticity of the adsorbed stabilising layer at the oil-water interface.

The stability of the emulsion with respect to creaming and coalescence depends mainly on the droplet size distribution, the state of aggregation of droplets and the rheology of aqueous dispersion medium. The droplet size distribution is mainly dependent on the energy inputs during emulsification, as well as nature and amount of emulsifying agent. Figures 3.15 (c) and (d) show spherical nature and surface morphology of GMA-EGDM copolymer at 75% CLD, prepared by multiple emulsion method using 1:2 v/v oil:water ratio. In this case, the internal structure shows the presence of open pores at the surface. The pores are non-uniform and the cell size and windows size are not well defined. As already stated, these emulsions do not classify as HIPES, since they contain low discontinuous phase volumes, typically less than 74%. Figure 3.15 (e) represents the uniform particle size distributions of the beads prepared by 1:5 oil to water ratio. When, a HIPE is formed the shape of discontinous phase droplet changes from spherical to polyhedral. When the polymerisation occurs, the contact areas between the droplets give rise to pore throats that lead to highly interconnected pore structure, as seen in Figure 3.15 (f) at 5:1 water:oil ratio (83% inner phase volume).

When GMA was replaced with AGE in AGE-EGDM, the same trend in morphology was noted with respect to increase in internal water phase. Figures 3.16 (a), (c) and (e) show the monodispersed particle size distribution of AGE-EGDM copolymers for 1:1, 1:2, and 1:5 v/v oil-water ratios, respectively.

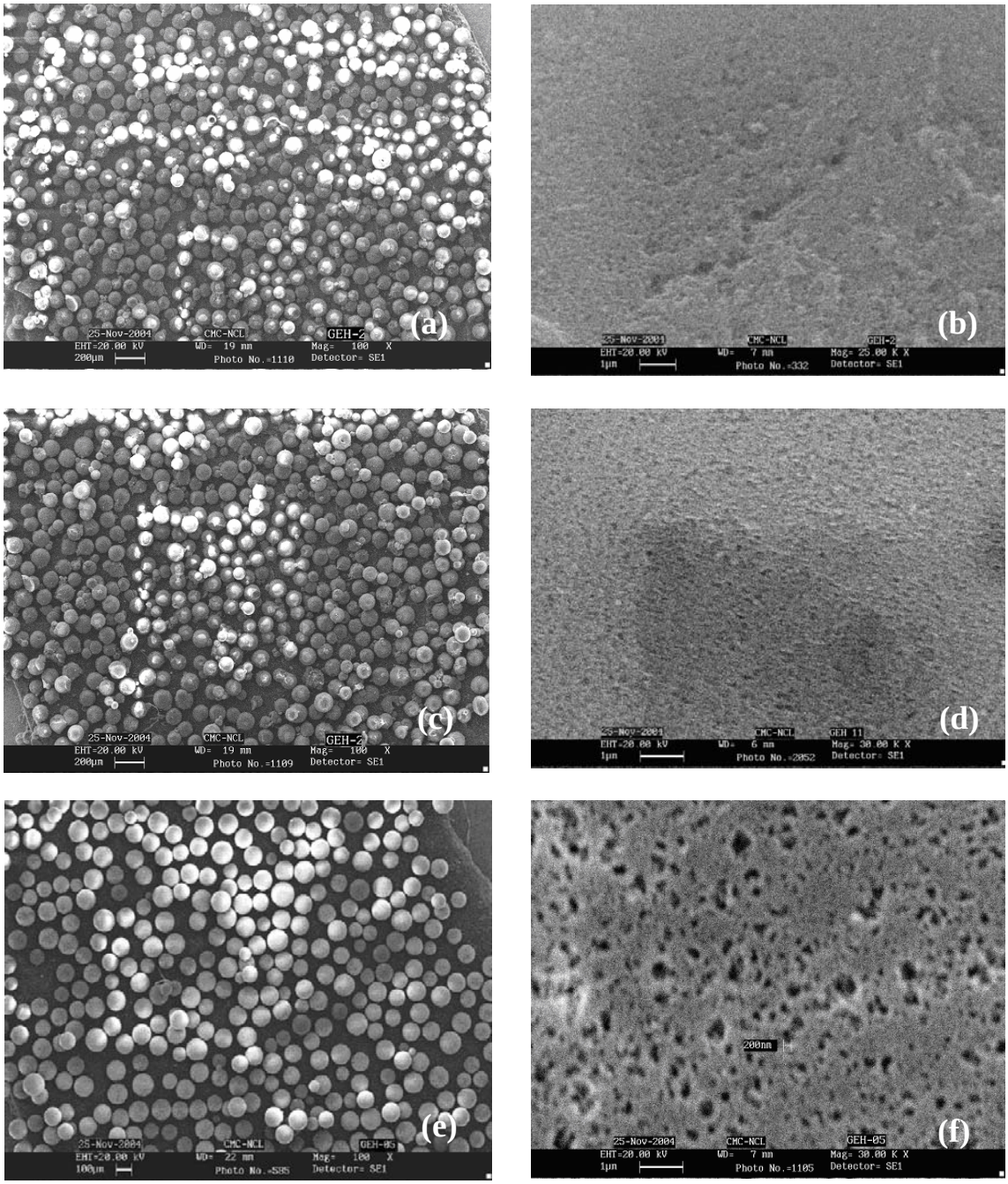

Figure 3.15. Scanning electron micrographs of GMA-EGDM copolymers synthesised using different inner water volumes; (a) particle morphology at 100x and (b) surface morphology at 30000 X magnification at 1:1 Water: oil v/v, (c) particle morphology at 100x and (d) surface morphology at 30000 X magnification at 2:1 Water: oil v/v, and (e) particle morphology at 100x and (f) surface morphology at 30000 X magnification at 5:1 Water : oil v/v.

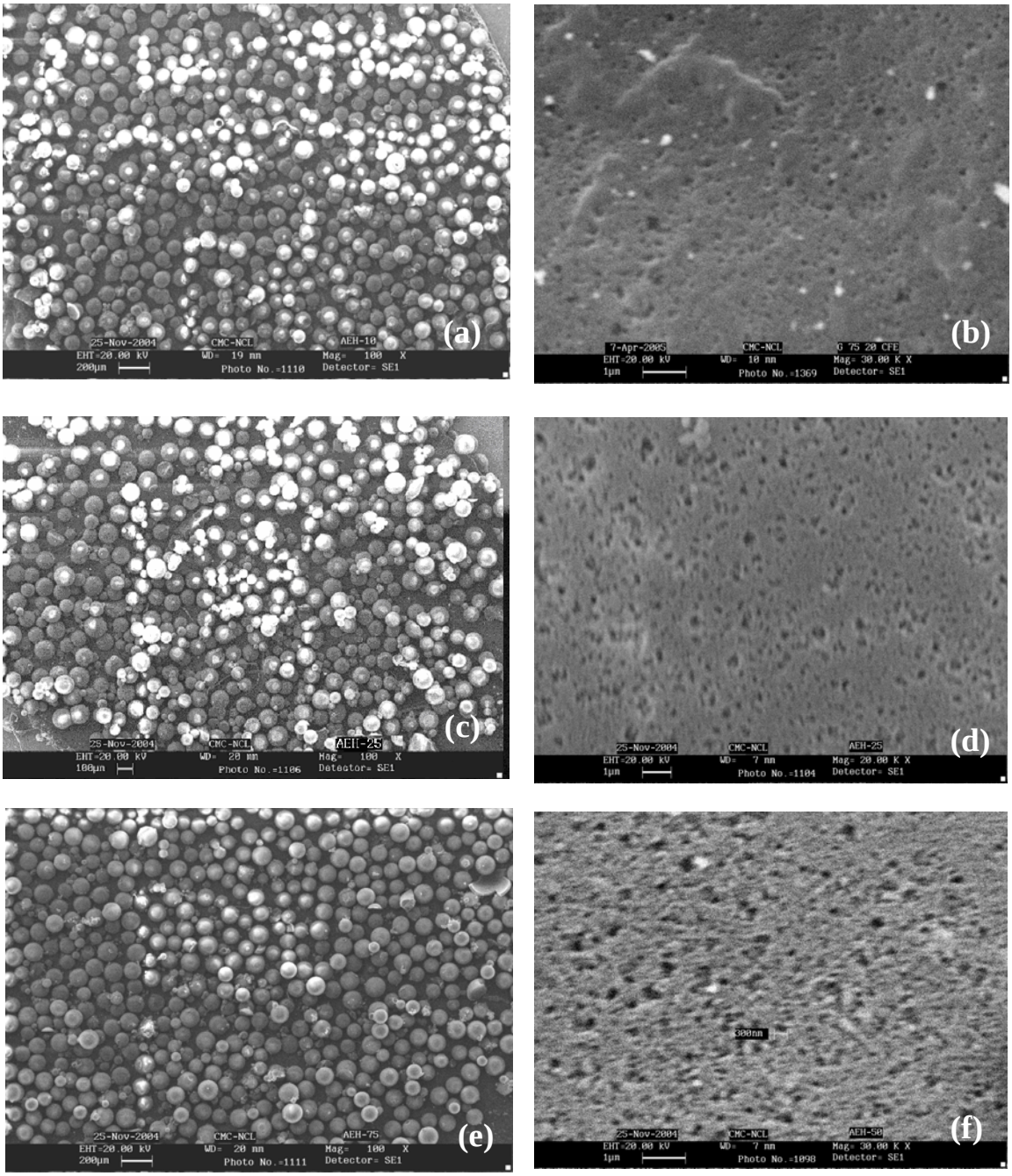

Figure 3.16. Scanning electron micrographs of AGE-EGDM copolymers synthesised using different inner water volumes; (a) particle morphology at 100x and (b) surface morphology at 30000 X magnification at 1:1 Water: oil v/v, (c) particle morphology at 100x and (d) surface morphology at 30000 X magnification at 2:1 Water: oil v/v, and (e) particle morphology at 100x and (f) surface morphology at 30000 X magnification at 5:1 Water : oil v/v.

The change in the porous structure with change in the discontinuous phase is shown in Figures 3.16 (b), (d), and (f) for 1:1, 1:2, and 1:5 oil-water ratios (i.e., 50, 66, and 83 % inner water phase) respectively. The skin formation is also observed at the highest amount of internal water phase. The bead surface shows the interconnected network of pores.

In HEMA-EGDM system, surface morphology is somewhat reduced, as the HEMA is slightly soluble in the aqueous phase. So the internal phase water could diffuse to the external phase water leading to a less porous material. As shown in Figures 3.17 (a), (c) and (e), particle size of HEMA-EGDM copolymers at 75% CLD is more pronuncedly bimodal at 1:1, 1:2, and 1:5 oil:water ratios, respectively. Figures 3.17 (b), (d), and (f) show the progressive openings of the pores on the surface of beads by increasing the inner aqueous phase by 50, 66, and 83 % (1:1, 1:2 and 1:5 oil:water v/v), respectively.

In the suspension polymerisation, the morphology and properties of the copolymers beads depend on the compositon of the monomeric mixture and on the polymerisation condition. The reaction mixture in suspension copolymerisation system for the production of macroporous copolymers includes a monovinyl monomer, a divinyl monomer (cross-linker), an initiator, and the inert diluent. The decomposition of the initiator produces free radicals, which initiate the polymerisation and cross-linking reactions. After a certain reaction time, a three-dimensional network of infinitely large size will start to form. This is known as gel point and at this stage the liquid reactants change to solid like state.[45]

As polymerisation proceed beyond the gel point the amount of soluble reaction components decrease and after complete conversion of monomers, a stage is reached where only the copolymer network and diluent remain in the system. The copolymer exhibits the different structure and properties depending on the amount of the cross-linker and the diluents present during the reaction as well as on the solvating power of the diluent. The bead is an aggregate of microspheres. Each microsphere consists of smaller nuclei, which are fused together.

The beads obtained by suspension polymerisation are shown in Figures 3.18 (a), (c) and (e) for GMA-EGDM, AGE-EGDM, and HEMA-EGDM, respectively, at 75% CLD using cyclohexanol as porogen and 1:1.6 monomer to porogen ratio. Here, particle size is polydispersed because it depends on the initial agitation during the gel point stage. Same observation can be made in Figures 3.19 (a), (c) and (e) at higher 1:2 monomer to porogen ratio for GMA-EGDM, AGE-EGDM, and HEMA-EGDM, respectively.

Figures 3.18 (b), (d) and (e) show the internal surface morphology of GMA-EGDM, AGE-EGDM, and HEMA-EGDM copolymer beads, respectively, prepared using 1:1.6 monomer to porogen ratio. All copolymer systems have less, irregular, and nonuniform pore openings on the surface. Porosity is barely visible in the SEM evaluation. However, when the amount of porogen increased to twice the monomer volume (1:2), cauliflower like morphology was observable as in Figures 3.19 (b), (d) and (f) for GMA-EGDM, AGE-EGDM, and HEMA-EGDM copolymer systems, respectively.

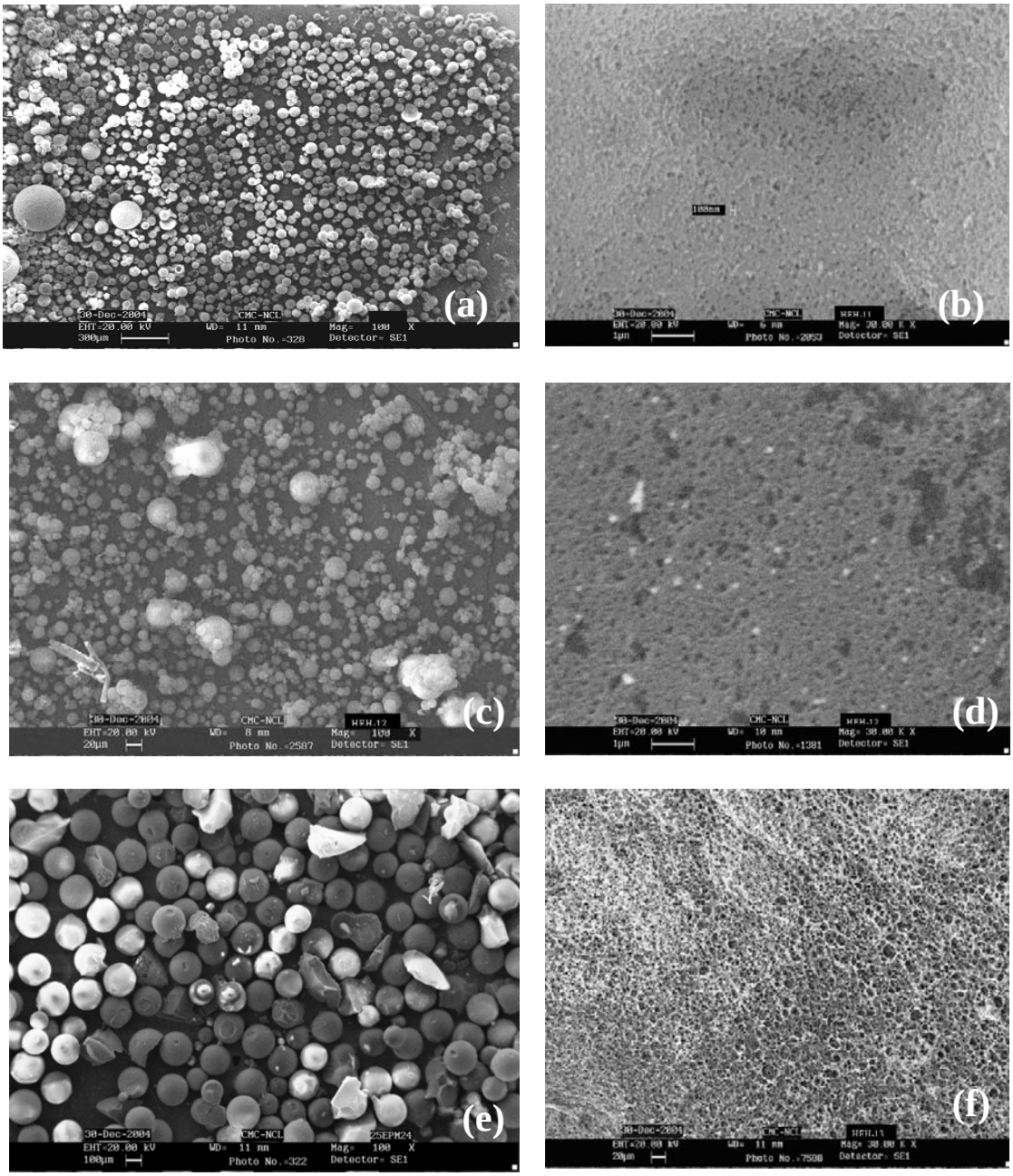

Figure 3.17. Scanning electron micrographs of HEMA-EGDM copolymers synthesised using different inner water volumes; (a) particle morphology at 100x and (b) surface morphology at 30000 X magnification at 1:1 Water: oil v/v, (c) particle morphology at 100x and (d) surface morphology at 30000 X magnification at 2:1 Water: oil v/v, and (e) particle morphology at 100x and (f) surface morphology at 30000 X magnification at 5:1 Water: oil v/v.

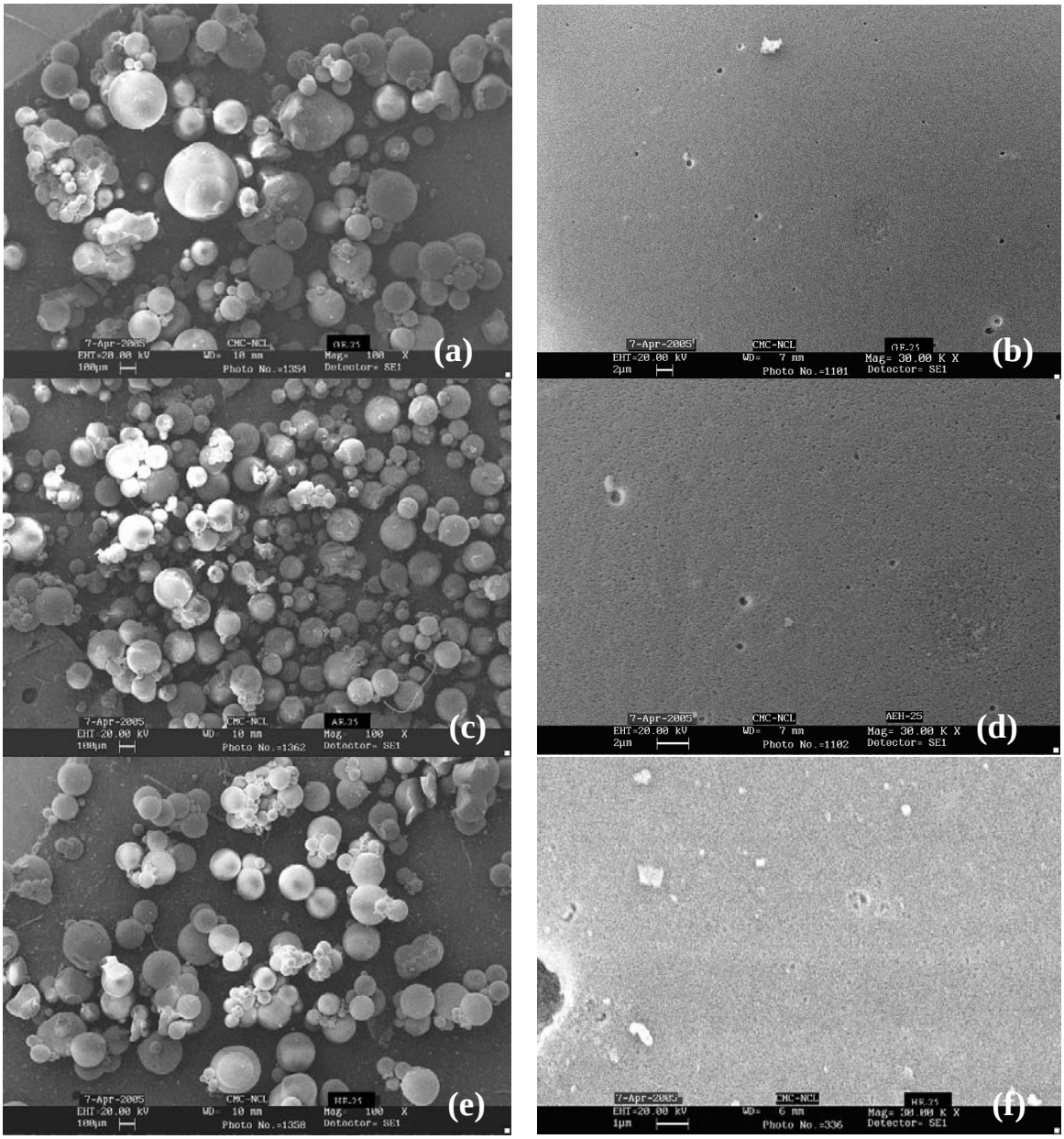

Figure 3.18. Scanning electron micrographs of copolymers synthesised by classical suspension methodology using 1:1.6 monomer to porogen ratio; (a) particle morphology at 100x and (b) surface morphology at 30000 X magnification for GMA-EGDM copolymers, (c) particle morphology at 100x and (d) surface morphology at 30000 X magnification for AGE-EGDM copolymers, and (e) particle morphology at 100x and (f) surface morphology at 30000 X magnification for HEMA-EGDM copolymers.

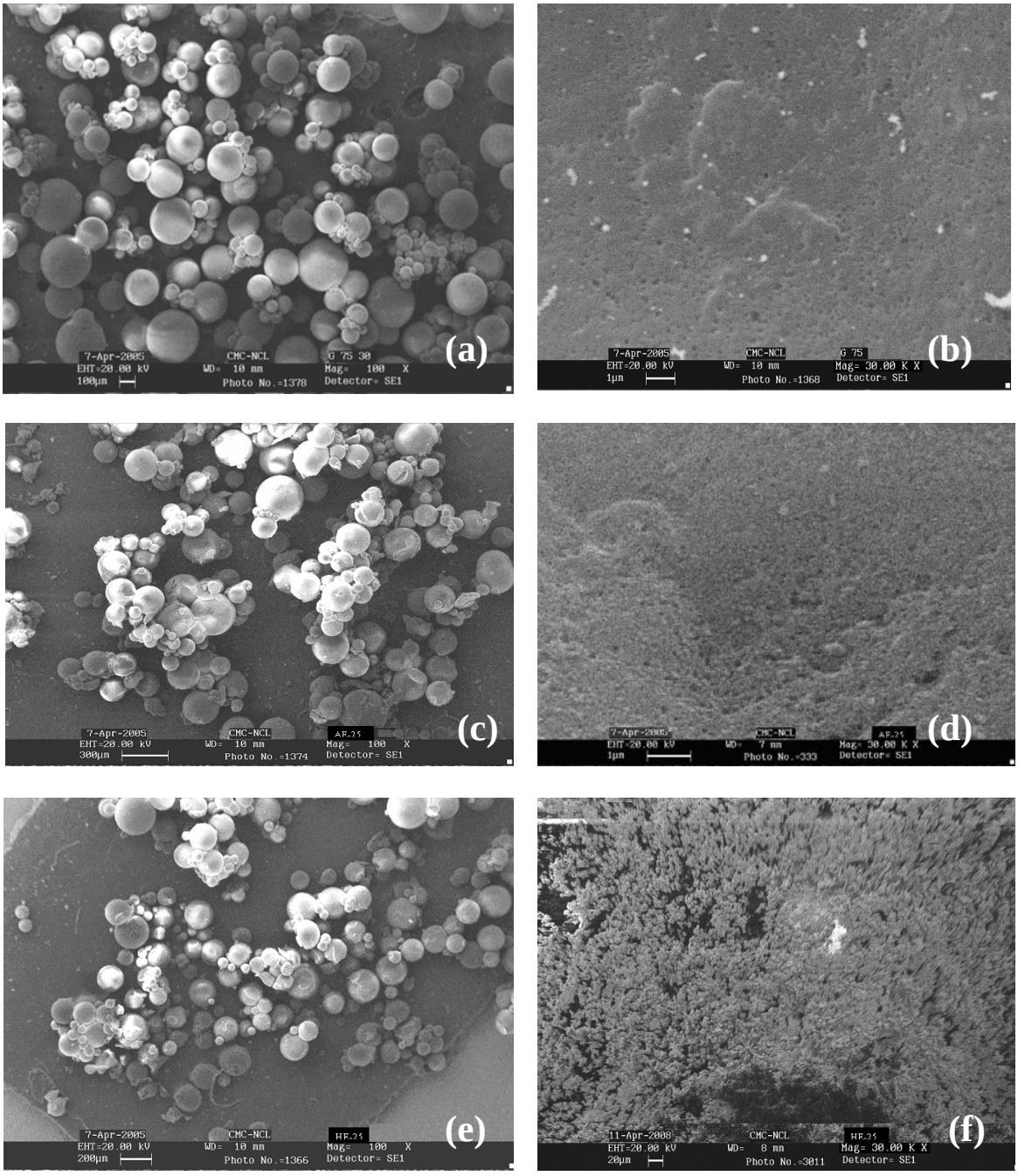

Figure 3.19. Scanning electron micrographs of copolymers synthesised by suspension using 1:2 monomer to porogen ratio; (a) particle morphology at 100x and (b) surface morphology at 30000 X magnification of GMA-EGDM copolymers, (c) particle morphology at 100x and (d) surface morphology at 30000 X magnification of AGE-EGDM copolymers, and (e) particle morphology at 100x and (f) surface morphology at 30000 X magnification of HEMA-EGDM copolymers

References

[1] Seifriz, W., Studies in emulsions. *J. Phys. Chem*. **1925**, 29, 738.

[2] Pal, R., Multiple O/W/O emulsion rheology. *Langmuir* **1996**, 12, 2220.

[3] Davis, S. S., The emulsion-obsolete dosage form or novel drug delivery system and therapeutic agent? *J. Clin. Pharm*. **1976**, 1, 11-27.

[4] Lanier, J. G.; Newman, M. J.; Lee, E. M.; Sette, A.; Ahmed, R. *Vaccine* **1999**, 18 (5-6), 549-557.

[5] Elson, L. A.; Mitchley, B. C. V.; Collings, A. J.; Schneider, R. *Rev. Europ. Etudes. Clin. Biol.* **1970**, 15, 87-90.

[6] Collings, A. J. British Patent 1235667, **1971**.

[7] Brodin, A. F.; Kavaliunas, D. R.;Frank, S. G. *Acta. Pharm. Suec*. **1978**, 15, 1-10.

[8] Frankenfield, J. W.; Fuller G. C.; Rhodes C. T. *Drug Dev. Commun*. **1976**. 2 (4-5), 405-419.

[9] Goldstein, L.; Freeman, A.; Sokolovsky, M. *Biochem. J*. **1974**, 143(3), 497-509.

[10] Matsumoto, S.; Kohda, M.; Murata, S. *J. Collioid Interface Sci*. **1977**, 62 (1), 149-57.

[11] Okada, H. *Adv. Drug Delivery Rev*. **1997**, 28 (1), 43-70.

[12] Svec, F.; Hradil, J.; Coupeck, J.; Kalal, *J. Angew. Mackromol. Chem*. **1975**, 48, 135.

[13] Svec, F.; Jelinkova, M.; Votavova, E. *Angew. Mackromol. Chem*. **1991**, 188, 167.

[14] Azanova, V.; Hradil, J.; Svec, F.; Pelzbauer, Z.; Panarin, E. F. *React. Polym*. **1990**, 12, 247.

[15] Jelinkova, M.; Shataeva, L. K.; Tishchenko, G. A.; Svec, F. *React. Polym*. **1989**, 11, 253.

[16] Setinek, K.; Blazek, V.; Hradil, J.; Svec, F.; Kalal, J. *J. Catal*.1983, 80,123.

[17] Rolland, A.; Herault, D.; Touchard, F.; Saluzza, C.; Duval, R.; lemaire, M. *Tet. Asymmetry* **2001**, 12, 811.

[18] Petro, M.; Svec, F.; Frechet, J. M. J. *Biotechnol. Bioeng*. **1996**, 49, 355.

[19] Kotha, A.; Raman, R. C.; Ponrathnam, S.; Kumar, K. K.; Shewale, J. *React. Funct. Polym*. **1996**, 28, 235.

[20] Radivoje, P., Slobodan, J.; Zoran, V. *Biotechnol. Lett*. **2001**, 23, 1171.

[21] Guyot, A.; Bartholin, M. *Prog. Polym. Sci.* **1982**, *8*, 277.

[22] Kahovec, J.; Jelinkova, M.; Coupek, J. *Polym. Bull.* **1987**, *18*, 495.

[23] Hodge, P.; Sherrington, D. C. In *Syntheses and Separations Using Functional Polymers*, Wiley: New York **1989**.

[24] Piskin, E. *Int. J. Artif. Organs* **1986**, *9*, 289.

[25] Horak, D.; Svec, F.; Kalal, J.; Adamyan, A.; Volynskii, O.; Voronkova, L. K.; Gumargalieva, K. *Biomaterials* **1986**, *7*, 467.

[26] Robert, C.; Buri, P. A.; Peppas, N. A. *J. Controlled Release* **1987**, *5*, 151.

[27] Kamei, S.; Okubu, M.; Matsumoto, T. *J. Appl. Polym. Sci.* **1987**, *34*, 1439.

[28] Stevenson, W. K. T.; Sefton, N. O. *Biomaterials* **1987**, *8*, 449.

[29] Okay, O. *Prog. Polym. Sci.* **2000**, *25*, 711.

[30] Naghash, H. J.; Okay, O.; Yildirim, H. *J. Appl. Polym. Sci.* **1995**, *56*, 477.

[31] Lissant K. J. *J. colloid. Int. Sci*. **1966**, 22, 462.

[32] Westermarck S., Academic dissertation, Use of mercury porosimetry and nitrogen adsorption in characterisation of the pore structure of mannitol and microcrystalline cellulose powders, granules and tablets, University of Helsinki, **2000**.

[33] Sing, K. S. W.; Everett, D. H.; Haul, R. F. V.; Moscou, L.; Pierotti, R. A.; Rouquerol, J.; Semieniewska, T. *Pure and Appl. Chem*. **1985**, 57, 603-919.

[34] Van Brakel, J.; Modry, S.; Svata, M. *Powder technol*. **1981**, 29, 1-12.

[35] Cortes, J. *Adv. Collod Int. Sci.***1985**, 22, 151.

[36] Brunauer, S.; Emmett, P.; Teller, E. *J. Am. Chem. Soc.* **1938**, 60, 309.

[37] Brunauar, S.; Deming, L. S.; Deming, W. S.; Teller, E. *J. Am. Chem. Soc*. **1940**,

61, 1723.

[38] Webb, P. A.; Orr, C. Analytical methods in fine particle technology, Micromeritics Instrument Corp., Atlanta, Georgia, p-301, **1997**.

[39] Allen T. "Particle size measurement", 5th Ed., Chapmann and Hall, New York, USA, p-251, **1997**.

[40] Matsumoto, S.; Kita, Y.; Yonezawa, D. *J. Colloid Interface Sci*. **1976**, 57, 353-361.

[41] Gomez, C. G.; Alvarez, L. C.; Strumia, M. C. *Polymer* **2004**, 45 (18), 6189-94.

[42] Wei-Qing, Zhou.; Ting-Yue, Gu.; Zhi-Guo, Su.;Guang-Hui, Ma. *Polymer* **2007,** 48**,** 1981.

[43] Cameron, N. *Polymer* **2005***,* 46, 1439.

[44] Sherrington D. C. *Chem. Commun*. **1998**, 2275.

[45] Okay O. *Prog. Polym. Sci*. **2000**, 25, 711-779.

Chapter IV

Terpolymerisation: Terpolymerisation by multiple emulsion

4 Terpolymerisation by multiple emulsion

4.1 Introduction

2,3-Epoxypropyl methacrylate (or glycidyl methacrylate) is an interesting monomer, exhibiting a polymerisable methacrylic unsaturation and an oxirane function of potential reactivity. This monomer has been homo- or copolymerised by means of free-radical initiators[1,2] (organic peroxides or azo-catalysts) known to selectively attack the methacrylic double bond. The repeat unit thus contains pendant epoxy substituents. Glycidyl methacrylate copolymerises with many conventional monomers and offers an economical means for introducing reactive functional groups into polymer molecules. Homo- and copolymers of glycidyl methacrylate exhibit a variety of reactions characteristics of epoxides.

Macroporous polymers,[3-9] known since 1950's, have an internal porosity that persists in both the swollen and dry state. These are typically synthesised as polymeric spherical beads by suspension polymerisation. The macroporous structure results from phase separation of an inert organic solvent (porogen).[10] Hydrophilic macroporous matrices find commercial use in catalysts, enzyme immobilisation, HPLC supports (ion-exchange resins), drug delivery, adsorbents, etc.[11-15] The polymerisation occurs in the discontinuous phase as droplets comprised of monomers, initiator and porogen. The nuclei size is dependent on the chosen reactive concentration of the cross-linking divinyl monomer (such as divinyl benzene) and porogen. The polymer formed phase separates, being cross-linked and insoluble in the mixed solvent composed of monomer and porogen. Porous properties are generally controlled by the type of porogen selected and the amounts of porogen and cross-linker used.[16-20] The porogen is a low molar mass

compound or polymer that is miscible with the monomers but does not react during the copolymerisation and at the end of reaction can be easily removed from product.[21-25] The nuclei develop to the size of globules during copolymerisation, and can attach themselves to generate microspheres, which associate to form particles. The development of microspheres and particles, which constitute clusters, depends on the porogen.

Alternative method to prepare the porous beads is through multiple emulsions i.e. $W_1/O/W_2$ or $O_1/W/O_2$ methods. In multiple emulsion method droplet of emulsion is dispersed in third medium, yielding a three-phase system with either a water-in-oil-in-water ($W_1/O/W_2$; water-in-oil emulsion droplets are dispersed in an aqueous medium) or an oil-in-water-in-oil ($O_1/W/O_2$; droplets of oil-in-water emulsion are dispersed in an oil medium). During the synthesis of copolymer particles by multiple emulsion, kinetic stability of the system is very important since it must withstand the polymerisation temperature and stirring speed. Therefore, surfactant with a near exact hydrophilic-lipophilic balance (HLB) is required for the emulsion stability at that temperature. To prepare an open cellular polymer a primary emulsion with high volume fraction of internal phase is first prepared. Such an emulsion, termed high internal phase emulsion (HIPE), is dispersed in secondary aqueous or oil phase to form a multiple emulsion. In HIPE system the inner phase volume occupies more than 74% of emulsion volume. In this manner, we prepared porous beaded poly(HIPE) polymers. In 1996, Le and Benson developed the poly(HIPE) method by dispersing HIPE in external aqueous phase and spherical poly(HIPE) beads were formed.[26-28]

Due to their porous nature, poly(HIPE)s can be used in various applications such as chromatography, drug delivery, catalysis etc. For these applications, the dimensional

accuracy (monodisperse spheres), mechanical strength, pore size and pore volumes are important. Monodispersity of spherical beads is very important in chromatographic packing because pressure drop will be minimised. However, in catalytic applications, the surface morphology is more important. No commercial catalyst using HIPE technology has been established as yet, due to lower mechanical strength of HIPE beads, even at high cross-link densities. The terpolymers were prepared in this study to improve the mechanical properties, as packing materials for chromatography or the hydrophilic properties of the ion-exchangers.[29]

We report the first synthesis of a functional porous terpolymer poly(styrene-GMA-DVB) via multiple emulsion method. As part of the investigation of the reactive polymers having epoxy group as functional group, the present investigation was undertaken to see the porous properties of glycidyl methacrylate with styrene as a comonomer and divinyl benzene and/or ethylene dimethacrylate (EGDM) as cross-linker. The influence of various reaction parameters such as cross-link density, type of initiator, position of initiator, type of surfactants on the particle size, particle size distribution, pore volume, surface area, surface epoxy groups, and morphology were investigated thoroughly. Post functionalisation yielded sulphonic as well as mercaptosulphonic acid group on the terpolymers. The catalytic evaluation of these polymers, for the synthesis of bisphenols, is discussed. The reaction considered was the synthesis of 4,4'-bisphenol-A (4,4'-isopropyl diphenol).

4.2 Experimental

4.2.1 Materials

Analytical grade glycidyl methacrylate (GMA), obtained from Aldrich, was used as received. Styrene (Aldrich) and DVB (85%, 15% ethyl styrene, Aldrich) were washed with 5% sodium hydroxide to remove the inhibitors. Poly(vinyl pyrrolidone) [PVP] (Polysciences, USA, M_w = 40,000) was used as protective colloid. Azobisisobutyronitrile [AIBN], (M/S SISCO India) was recrystallised from methanol before use as initiator. Sorbitan monooleate (Span 80) was purchased from Loba Chemie, Mumbai. Brij 52, poly(dioxyethylene cetyl ether), was obtained from Aldrich. Calcium chloride hexahydrate and cyclohexanol, both from Merck, were used as received.

4.2.2 Terpolymerisation

A series of networked, cross-linked, porous styrenated terpolymers with styrene, glycidyl methacrylate (GMA) and divinyl benzene (DVB) were synthesised by water-in-oil-in-water ($W_1/O/W_2$) high internal phase emulsion (HIPE) polymerisation using azobisisobutyronitrile as initiator.

To synthesise styrene-GMA-DVB terpolymer with 25% cross-link density (CLD), 3.21 mL styrene, 3.82 mL GMA were mixed with 1.99 mL DVB. To this 1.6 g (17 wt.%) Span 80 (HLB = 4.9) and 0.2 g AIBN were added and stirred to homogenise. This is the inner oil phase. To make primary water-in-oil (W_1/O) HIPE emulsion 27 mL (75.02% of total volume) of 4 wt.% aqueous calcium chloride phase was added to the monomer (oil) phase at 1400 rpm at room temperature.

To make water-in-oil-in-water ($W_1/O/W_2$) emulsion system the above water-in-oil primary emulsion was added drop-wise at 250 rpm to the second 200 mL aqueous system comprised of 0.5 wt.% PVP to act as protective colloid.

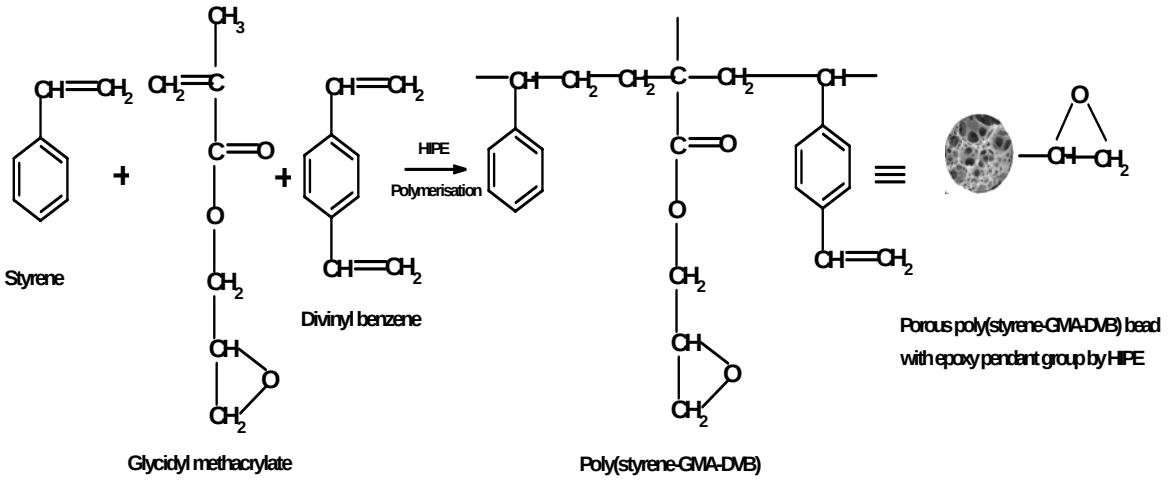

Figure 4.1. Terpolymerisation of styrene-GMA-DVB by HIPE

The polymerisation was allowed to proceed for six hours for complete conversion of monomer into the terpolymers. The uniform porous beads were filtered using Whatmann filter paper. The polymer beads were washed with water and methanol to remove the residual surfactants. The polymer was dried under vacuum at 60ºC for 18 h. Similarly, terpolymers of other CLD were synthesised, as shown in Table 4.1. The terpolymerisation scheme is presented in Figure 4.1.

Keeping all the other reaction parameters and comonomers constant DVB was replaced with an equivalent concentration of EGDM as cross-linker to alter the hydrophobicity of the terpolymer as well as to see the effect of cross-linker on pore size and pore size distribution. The composition of Styrene-GMA-EGDM is given in Table 4.2. The two sets of terpolymers were characterised for surface epoxy, IR, pore volume (mercury intrusion porosimetry), surface area (nitrogen adsorption) and morphology (scanning electron microscopy).

Table 4.1. Styrene-GMA-DVB terpolymerisation composition

Ex. No. (HIPE)	CLD %	Styrene		GMA		DVB		Epoxy mmol/g
		mL	mole	mL	mole	mL	mole	
SGDV-11/SGDV - 21	25	3.21	0.0288	3.82	0.0281	1.99	0.0139	3.1751
SGDV-12/SGDV-22	50	2.60	0.0220	3.12	0.0225	3.31	0.0230	2.6193
SGDV-13/SGDV-23	75	2.21	0.0192	2.63	0.0192	4.13	0.0289	2.2561
SGDV-14/SGDV-24	100	1.91	0.0166	2.28	0.0166	4.77	0.0334	1.9598

Experiment code **SGDV-11, 12, 13 and 14** series is indicative of terpolymer synthesised with 17 wt.% Brij 52 and series **SGDV-21, 22, 23 and 24** indicate the terpolymers synthesised with 17 wt.% Span 80

Table 4.2. Styrene-GMA-EGDM terpolymerisation composition

Ex. No. (HIPE)	CLD %	Styrene		GMA		EGDM		Epoxy mmole/g
		mL	mole	mL	mole	mL	mole	
SGEG-31	25	3.01	0.0260	3.50	0.0256	2.56	0.0135	3.1273
SGEG-32	50	2.34	0.0204	2.79	0.0204	3.85	0.0204	2.1831
SGEG-33	75	1.93	0.0168	2.30	0.0168	4.71	0.0249	1.9252
SGEG-34	100	1.60	0.0139	2.00	0.0146	5.41	0.0286	1.4659

4.2.3 Functionalisation

4.2.3.1 Sulphonation of HIPE beads

A mixture of distilled water : isopropanol : sodium sulphite (40 mL) in the ratio of 75:15:10 (wt./wt./wt.) was prepared and homogenised by stirring. This mixture was added to 4 g of Styrene-GMA-DVB terpolymer (SGDV-23) and refluxed for 5 hours at 80°C, cooled, filtered, washed sequentially with 100 mL of 0.5 M sulphuric acid,

deionised water until neutral, acetone and dried. Similarly, other terpolymer beads were sulphonated.

4.2.3.2 Thiolation of HIPE beads

To sodium thiol solution in methanol (4%; 55 mL) was added 4 g of styrene-GMA-DVB (SGDV-23) terpolymer beads, refluxed for one hour at 70 ^{o}C, cooled and filtered, washed with 0.5% ammonia solution, followed by distilled water, acetone and dried in vacuum.

4.2.3.3 Mercapto sulphonic acid substituted polyHIPE beads

Sulphonation of thiolated styrene-GMA-EDM terpolymer HIPE beads were carried out as per synthesis procedure in Section 4.3.1.

4.2.3.4 Sulphonation at aromatic pendant position of the sulphonic acid beads

Dried sulphonated styrene-GMA-DVB terpolymer beads were treated with 10 mL 1,2-dichloroethane, 3 mL chloro sulphonic acid at ambient temperature for 48 h. It was diluted with 1,2-dichloroethane (20 mL), filtered, washed with 20 mL 1,2–dichloroethane and 100 mL dry acetone, washed with deionised water until the washings were neutral and dried. Similarly, sulphonation of styrene in the mercaptosulphonic acid beads consisting of styrene-GMA-EGDM terpolymer beads were conducted.

4.2.4 Synthesis of bisphenol A using sulphonic acid / mercapto sulphonic acid

The catalyst (0.5 g) was taken in a 50 mL flask, neutral alumina (0.2 g) and 4A molecular sieves (2 g), phenol (19.8 mL; 0.225 mol), acetone (3.3 mL; 0.045 mol) were added and refluxed at 100 ^{o}C for 16 hours. The product was analysed by GC for percent

yield of phenolic products as well as the selectivity to 4,4'-bisphenol A. The performance of catalysts were evaluated relative to Amberlyst-15.

4.3 Terpolymer characterisation

4.3.1 Mercury porosimetry

The pore structure in the copolymers was investigated using mercury intrusion porosimetery in the pressure range 0 – 4000 kg/cm^2. (Autoscan, 60 mercury porosimeter, Quanta chrome, USA). The mercury contact angle was 140^o.

4.3.2 Specific surface area

The specific surface area measurements were made using single point nitrogen adsorption (BET) method using Quantachrome (USA) equipment.

4.3.3 Scanning electron microscopy

A more direct insight into the structure of poly(styrene-GMA-DVB) HIPE beads was made using scanning electron microscopy (SEM). Specimen preparation was as follows: dried poly(styrene-GMA-DVB) beads were mounted on stubs and sputter-coated with gold, in order to visualise the bead. Micrographs were taken on a JEOL JSM-5200 SEM instrument.

4.4 Results and discussion

As emulsion polymerisation is highly sensitive to even small changes in the numerous reaction parameters involved, its control can become complex, especially in terpolymerisations due to the different reactivity ratios of the reacting monomers. The type and concentration of the monomers, cross-linker, the type and concentration of

surfactants, the amount of internal water, stirrer type and stirring speed strongly affect the final particle size, and porous properties.

4.4.1 Preparation of high loading divinyl benzene (DVB) polyHIPE beads

Multiple emulsions are emulsion systems in which the disperse phase contains dispersed droplets of the external phase. Water-in-oil-in-water (W/O/W) type emulsions are oil-in-water emulsions in which the dispersed oil drops themselves contain smaller dispersed aqueous droplets. First, a stable W/O emulsion (the primary emulsion) must be prepared. Furthermore, HIPE can be suspended in an aqueous suspension phase to yield suspended droplets of emulsion, as shown in Figure 4.2. The aqueous suspension phase comprises a stabiliser that promotes the formation of a stable suspension of HIPE droplets.

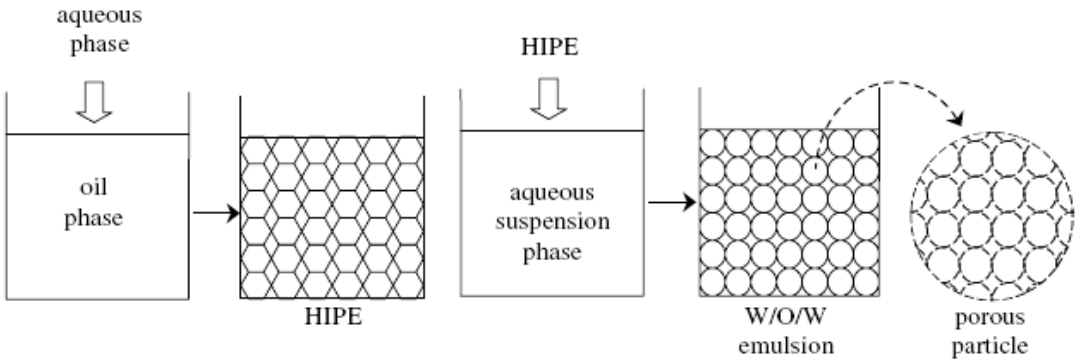

Figure 4.2. Preparation of porous terpolymeric beads by W/O/W multiple emulsion[31]

Terpolymerisation of styrene, GMA and divinyl benzene without a porogen yields glassy transparent beads. These materials are amorphous and cross-linked, having interpenetrating polymer chains without any fine structure. The polymer chains are in molecular contact with each other and resins have low surface area, in dry state, less than 10 m^2/g. These materials swell in good solvents, which creates temporary porosity in

polymers. Table 4.1 shows series SGDV-11, 12, 13, and 14 terpolymers synthesised using the surfactant Brij-52, with a HLB value of 5.3.

The required amount of surfactant, monomer and initiator were mixed and water was added with stirring at 1400 rpm for 5 minutes as described in para 4.2.2. The emulsions were transparent and unstable on standing. This mixture containing monomer, surfactant and water after stirring was immediately added to a stirred aqueous phase (200 mL) containing protective colloid (0.5 wt.% PVP) and to polymerise the dispersed droplets in a HIPE suspension polymerisation methodology.

In this technique surfactant is used to form reverse micelles. The relative amount of water solubilised in micelles determines the size of droplets inside St-GMA-DVB and this in turn controls the size of the pores that can be generated. Non-ionic surfactants and twin tail surfactant can individually generate micro emulsions.[32] These systems form a middle phase microemulsion where organic and aqueous phases consist of interconnecting domains and surfactant molecules are locked at the interface. After polymerisation the surfactant is removed by soxhlet extraction and on drying, terpolymers with permanent pores are obtained, characterised by pore volume and surface area.

4.4.2 Effect of cross-link type and density

Figure 4.3 illustrates how the pore size distribution of terpolymer varies with the DVB concentration and hence CLD at a fixed monomer concentration and fixed oil to internal water ratio. Increasing the relative concentration of DVB increases the number of micro- and mesopores in a terpolymer. The terpolymers have a narrow pore size distribution in the range 0.5 to 50 nm as shown in Figure 4.3 (a). The increase in cross-

linking (DVB content) increases the tendency for phase separation during terpolymerisation. Individual, localised gel structures are formed in free radical terpolymerisation. These gel particles phase separate yielding water-swollen micro-gel particles that contain reactive groups on their surfaces. The micro-gel particles agglomerate, react, and form a nano scale porous, heterogeneous polyHIPE wall.[33]

The specific surface area of porous terpolymer, shown in Table 4.3, is an indicator that the number of micropores increases with an increase in relative DVB content. The meso and micropores account for most of the surface area if the CLD due to DVB is in between 25 to 50%, but their contribution diminish as the CLD due to DVB concentration increases to 75% and 100%. When the amount of the DVB decreases, the size of the microspheres and the nuclei decreases. The pore volume remains nearly invariant but the pore radii shifts to lower values and its number increases appreciably to increase the surface area. As micropores contribute more to the overall surface area of the polymers, an increase in surface area is observed up to 168.40 m^2/g for terpolymers with 75 and 100% CLD. Only 2-5% pore radii are in the region 100-500 nm as seen in Figure 4.3 (a). Total pore volume in the terpolymer series increases with increasing average pore size.

Another interesting pore-forming system is the polymerisation of styrene and glycidyl methacrylate using ethylene dimethacrylate (EGDM) as the cross-linker. Since EGDM is less hydrophobic than DVB, the emulsion formed is less stable at the higher temperature, which consequently results in very rapid phase separation at low conversion during the terpolymerisation. In this case, very broad pore size distribution was observed over the range of 5 to 600 nm, as shown in Figure 4.3(b).

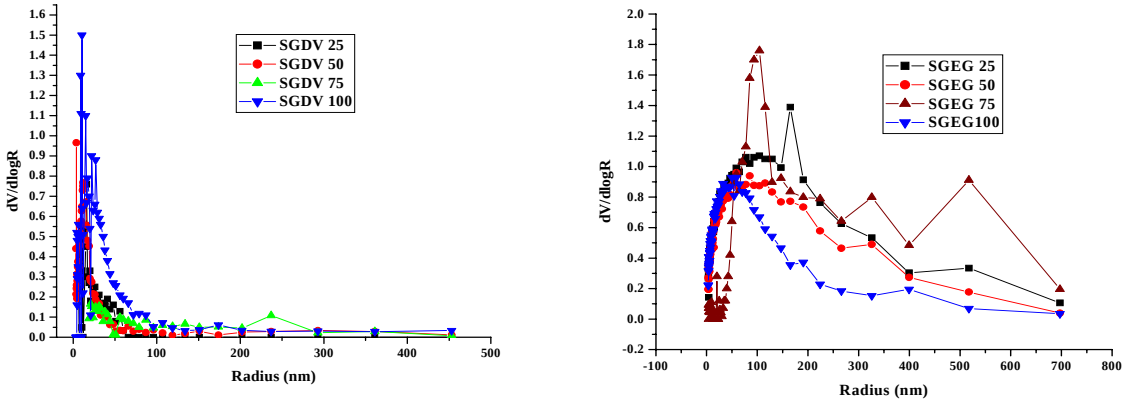

(a) **(b)**

Figure 4.3. Pore size distribution of (a) styrene-GMA-DVB and (b) styrene-GMA-EGDM terpolymers

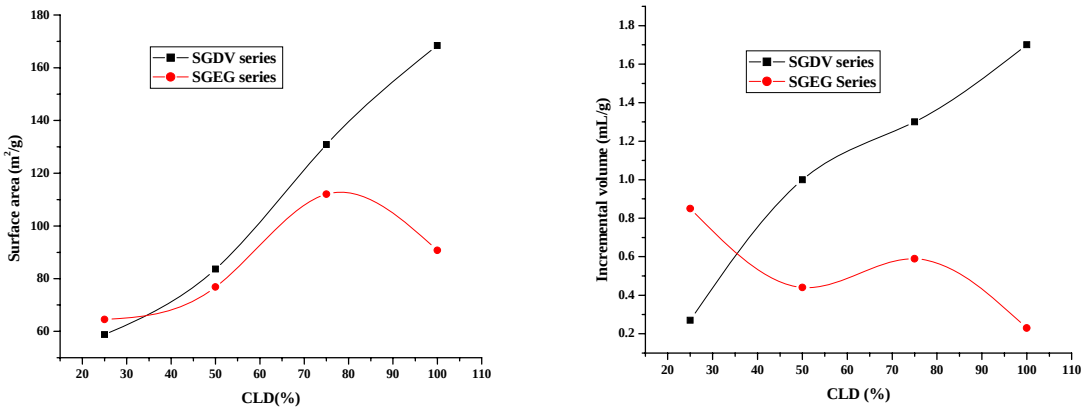

(a) **(b)**

Figure 4.4. Comparison of (a) specific surface area and (b) total pore volume of styrene-GMA-DVB and styrene-GMA-EGDM terpolymers

As the cross-link density increases the surface area in this terpolymer series increases from 64.59 to 112.07 m^2/g. However, at 100% CLD the surface area is reduced to 90.73 m^2/g (Table 4.3) due to large number of meso- and macrospores. Increasing the cross-linking comonomer content (EGDM) further, however, destabilises the HIPE and leads to Ostwald ripening, fusing small droplets into larger ones.

Figure 4.4 is the comparison of surface areas of the two terpolymer systems. Terpolymers with DVB as cross-linker yielded beads with higher surface area than the corresponding terpolymer of identical composition with EGDM as cross-linker. Interestingly, in styrene-GMA-EGDM terpolymers pore volume is found to decrease with increasing CLD, unlike that noted in polymers prepared by conventional suspension polymerisation. This indicates that choice of surfactant is critical to the design of pore structure and hence surface area and pore volume. The systems need to be studied with non-ionic surfactants of varying HLB before any quantitative inferences can be drawn.

Table 4.3. Pore volume and surface area relative to CLD in styrene-GMA-DVB and styrene-GMA-EGDM terpolymers

Polymer code	CLD (%)	Pore volume (cm^3/g)	Specific surface area (m^2/g)
SGDV-11, SGEG- 31	25	0.27, 0.85	58.81, 64.59
SGDV- 12, SGEG- 32	50	1.00, 0.44	83.63, 76.83
SGDV- 13, SGEG- 33	75	1.3, 0.59	130.84, 112.07
SGDV-14, SGEG- 34	100	1.7, 0.23	168.40, 90.73

4.4.3 Effect of surfactant type and its concentration

There is a significant difference in the surface area of terpolymers synthesised with the two surfactants (Table 4.4). With Span 80 a thick viscous emulsion was obtained while with Brij-52 emulsion was less viscous after addition of water to the oil phase.

It is well known that cross-linking density affects phase separation during co- and terpolymerisation. As a result the morphology of terpolymer, pore size distribution, specific surface area are all altered. We thought it necessary to establish the effects of

other parameters on pore morphological features at a fixed polymerisable composition. Therefore, the effect of Span 80 amount on the mesoporous and macroporous structure at a higher cross-linking degree was investigated. In Table 4.4 (SGDV 21, 22, 23 and 24) the synthesis of terpolymers, using Span 80 (sorbitan monooleate), with a HLB of 4.3, at 100% CLD, and fixed oil to internal water ratio (1:3 v/v), is presented. Span 80 is a saturated sorbitan monoester with 14 -CH_2- groups. The yield, pore volume and surface area of polymer microspheres are also listed in Table 4.4.

The percentage yield after polymerisation for a fixed time of 6 hours decreases from 87 to 47% with increase in Span 80 concentration. This is due to enhanced radical termination brought forth by increased number of -OH groups due to Span 80. The particle size obtained were mainly in the range of 102-120 μm, the average particle size is also listed in Table 4.4. Sorbitan fatty acid esters are effective reducers of interfacial tension. Molecules of sorbitan monostearate with smallest molecular area are able to pack more tightly at all the interface and lower the interfacial tension more than other surfactants. Nitrogen adsorption studies showed that surface area was in the range 23.24-103.36 m^2/g and pore volume was in the range 0.34-0.89 cm^3/g (Table 4.4).

The formation of meso- and macropores are closely related to the surfactant concentration in the oil phase (monomer phase). When the concentration of surfactant in solution is increased beyond the critical micelle concentration (*cmc*), numbers of surfactant molecules gather to form a micelle. Reverse micelles are formed in non-aqueous solution above *cmc* as is the case in this study. When the surfactant concentration increases further above *cmc*, the number of reverse micelles increases and different types of reverse micelles are formed, as shown in Figure 4.5. Spherical micelles

are formed when the surfactant concentration is close to *cmc* and the aggregation number (average number of surfactant molecules forming a micelle) is about 30–40. When the concentration of surfactant is 10 times higher than *cmc*, the aggregation number increases and a type of clubbed reverse micelles are formed.

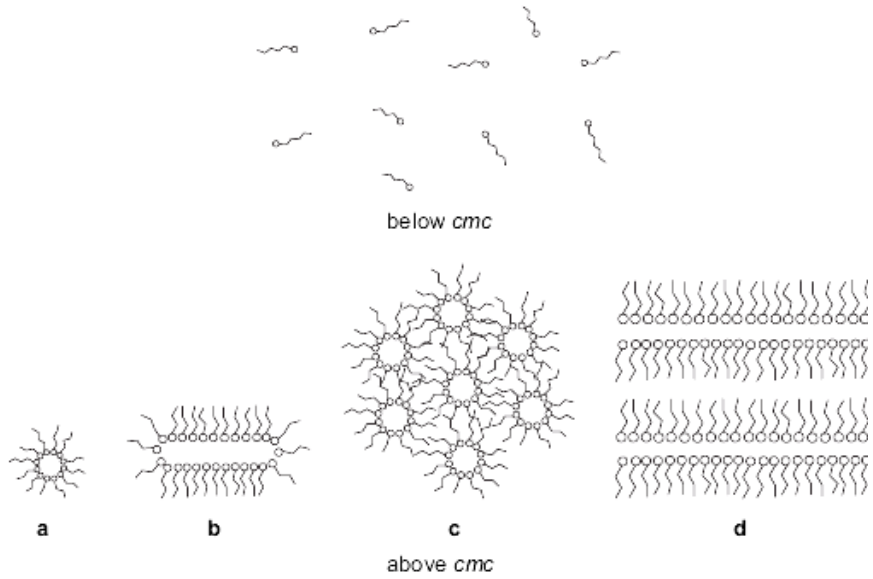

Figure 4.5. Different types of micelle formed with increase in surfactant concentration

The clubbed reverse micelles aggregate to a hexagonal cluster when the surfactant concentration increases further and the lamellar reverse micelles are obtained at a rather high concentration of surfactant.When the amount of Span 80 was 17 wt.% (based on the total amount of styrene, GMA and DVB), the pore size was not so large (around 50 nm). When it was increased to 34%, the pore size became very large, up to 500 nm, as shown in Figure 4.6(a). However, when the concentration of Span 80 exceeded 50%, the polymer beads did not have structural integrity and were easily broken. It is seen in Figure 4.6(a) that the mesoporous-macroporous structure was formed at 54% of Span 80 when the cross-linking degree was 100%. The pores formed had a bimodal distribution in

the range 2-50 nm and 150-250 nm. When Span 80 concentration attained 68%, shape of spherical droplets changed to polyhedral with thin wall.

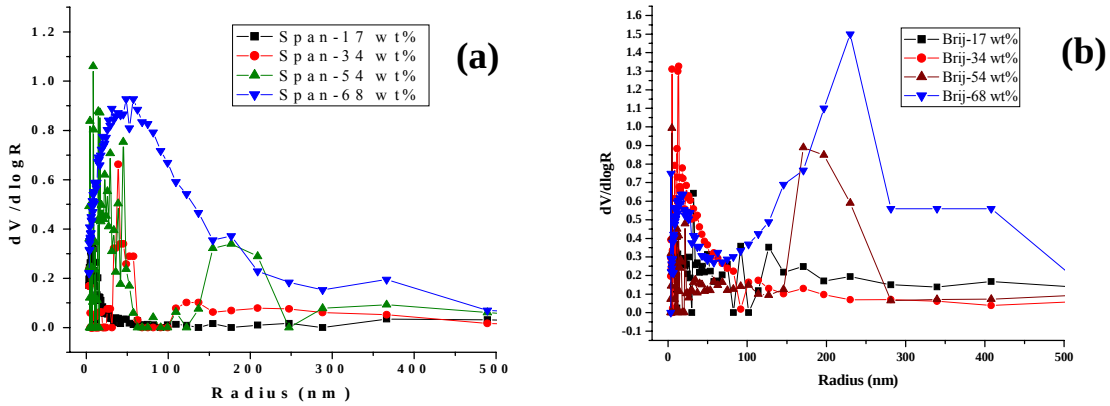

Figure 4.6. Pore size distribution of SGDV terpolymers of 100% CLD synthesised by HIPE with differing concentrations of (a) Span 80 and (b) Brij 52

At 54 and 68 wt.% of Span 80 (based on the total amount of styrene, GMA and DVB) at 100% as in this study, reverse micellar aggregates should be formed. A large number of reverse micellar aggregates were favourable for the formation of mesoporous and macropores, as seen from the broad pore size in the range 0-500 nm, as shown in Figure 4.6 (a).

Table 4.4. Effect of surfactant type and its concentration on percentage yield, particle size, pore volume and surface area of SGDV terpolymers

Factor	Span 80	Brij 52
Amount (wt.%)	17, 34, 54, 68	17, 34, 54, 68
Yield (%)	87.02, 79.88, 66.58, 48.15	92.11, 88.22, 89.19, 90.44
Average particle size (μm)	101.2, 95.4, 115.2, 120.4	42.5, 66.8, 79.8, 88.9
Pore Volume (cm^3/g)	0.34, 0.67, 0.44, 0.89	0.47, 0.87, 1.03, 1.12
Surface area (m^2/g)	23.24, 54.67, 89.39, 103.36	20.45, 34.44, 56.53, 80.20

The same SGDV system at 100% CLD was also synthesised with differing but identical concentration of Brij 52. Brij 52 has one -OH group as against three -OH groups in Span 80. The polymer yields after polymerisation at the same temperature and reaction time are consistently higher with Brij 52 as compared to Span 80. This clearly indicates that polymerisation is retarded with Span 80 due to chain transfer to -OH groups. As seen in Table 4.4, the average particle size increased with the concentration of Brij 52, from 42.5 to 88.9 μm. This is due to the formation of large agglomerates of micelles at higher concentration of Brij 52. Pore volume and surface area also show an increasing trend unlike that with Span 80. Large number of macropores are formed, as shown in Figure 4.6.(b). This leads to low surface area but high pore volumes (Table 4.4). Terpolymer has 20.45 m^2/g surface area at the 17 wt.% Brij 52 while at 68 wt.% this increases to 80.20 m^2/g, which is less than that observed for terpolymer prepared using same concentration of Span 80. When Brij is used terpolymer formed showed bimodal pore size distribution, indicating that there are two types of pore formation mechanisms in operation. Large number of macropores are formed in the range 100-500 nm at higher concentration of Brij surfactant especially at 54 and 68 wt.%, as shown in Figure 4.6(b). Thus, surface area, pore volume and pore size distribution are altered by surfactant type and its concentration in terpolymers of identical compositions.

4.4.4 Effect of Internal water

The amount of internal water used as discontinuous phase in the primary HIPE emulsion participates in the network structure formation as the porous matrix is built-up. Using the same styrene-GMA-DVB terpolymer composition of 100% CLD, as mentioned in Table 4.5, effect of differing amounts of internal water on the pore volume, surface

area, pore size distribution and morphology were investigated using Span 80. All parameters were found to be influenced by variance in oil:water ratio. The data presented in Table 4.5 shows that porous polymers of differing characteristics can be obtained by a simple alteration of internal water volume. Presence of higher amount of water increases the chain transfer reaction, resulting in lower terpolymer yields. Since water molecules do not take part in chain transfer reaction, more -OH molecules are exposed to the free-radicals and are available for chain transfer. This points to a change in hydrogen bonding mechanism, probably from one between surfactant molecules, which is not accessible to the free-radicals, to that with water which are accessible to the free-radicals. The type of initiator would also play a significant role in overall reaction rates.

Table 4.5. Effect of internal water on pore features in SGDV terpolymers synthesised by multiple emulsion

Factor	SGDV polymer
Oil to internal water ratio (v/v)	1:1, 1:3, 1:5, 1:7
Yield (%)	83.45, 79.88, 53.21, 48.09
Average particle size (μm)	110.2, 95.4, 98.1, 250
Pore Volume (cm^3/g)	0.37, 0.67, 0.61, 0.98
Surface area (m^2/g)	76.11, 54.67, 34.21, 20.22

Maximum surface area (76.11 m^2/g) was obtained when ratio of monomer to water was 1:1. As micelle formation is dependent on the amount of water, it plays an important role in designing the pore radii. Figures 4.7 and 4.8 show that with 1:1 and 1:3 oil:water ratio pores having radii up to 300 nm are formed. At 1:3 oil:water ratio pore radii in the range of 350-550 nm are also formed.

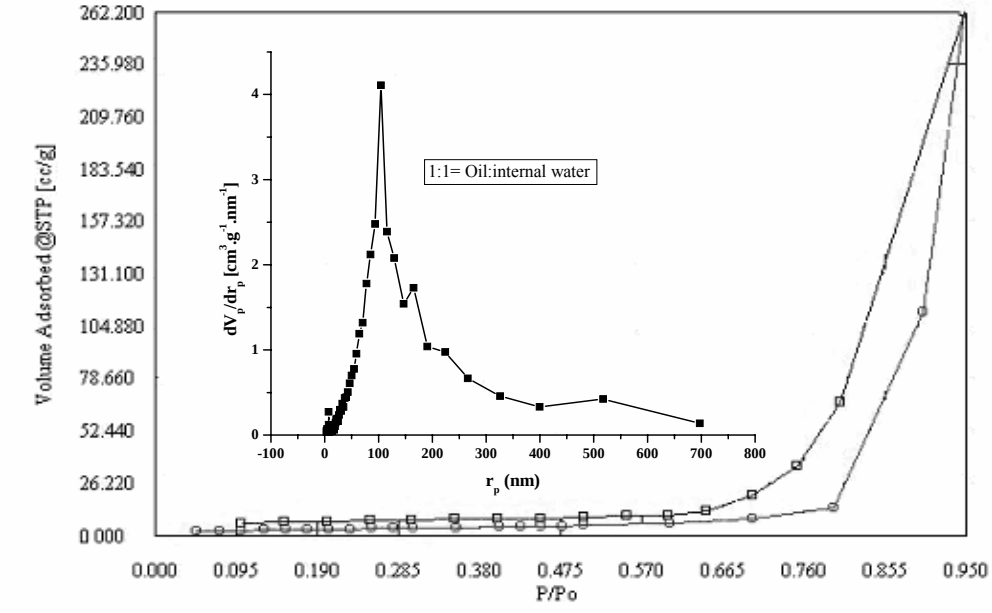

Figure 4.7. Nitrogen adsorption-desorption isotherm and pore size distribution of poly(styrene-GMA-DVB) terpolymers synthesised by HIPE emulsions using 1:1 oil to internal water ratio

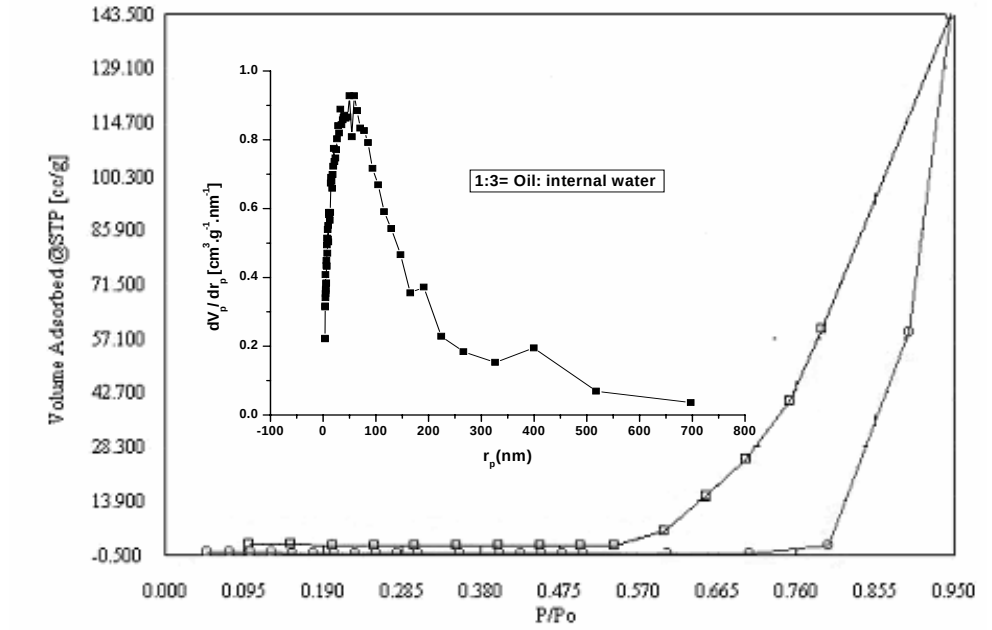

Figure 4.8. Nitrogen adsorption-desorption isotherm and pore size distribution of poly(styrene-GMA-DVB) terpolymers synthesised by HIPE emulsions using 1:3 oil to internal water ratio

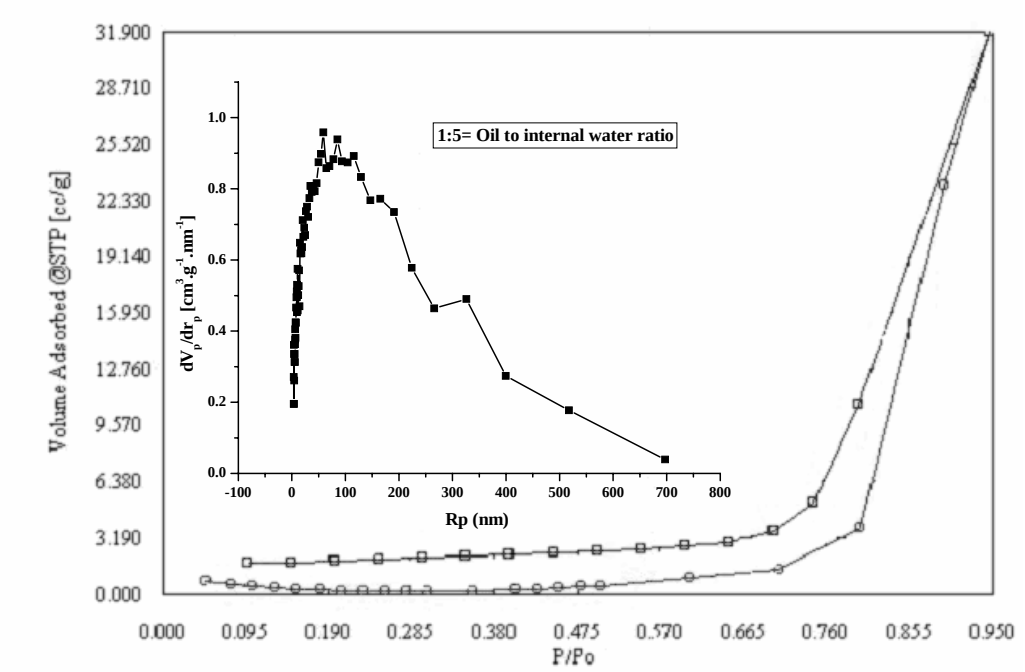

Figure 4.9. Nitrogen adsorption-desorption isotherm and pore size distribution of poly(styrene-GMA-DVB) terpolymers synthesised by HIPE emulsions using 1:5 oil to internal water ratio

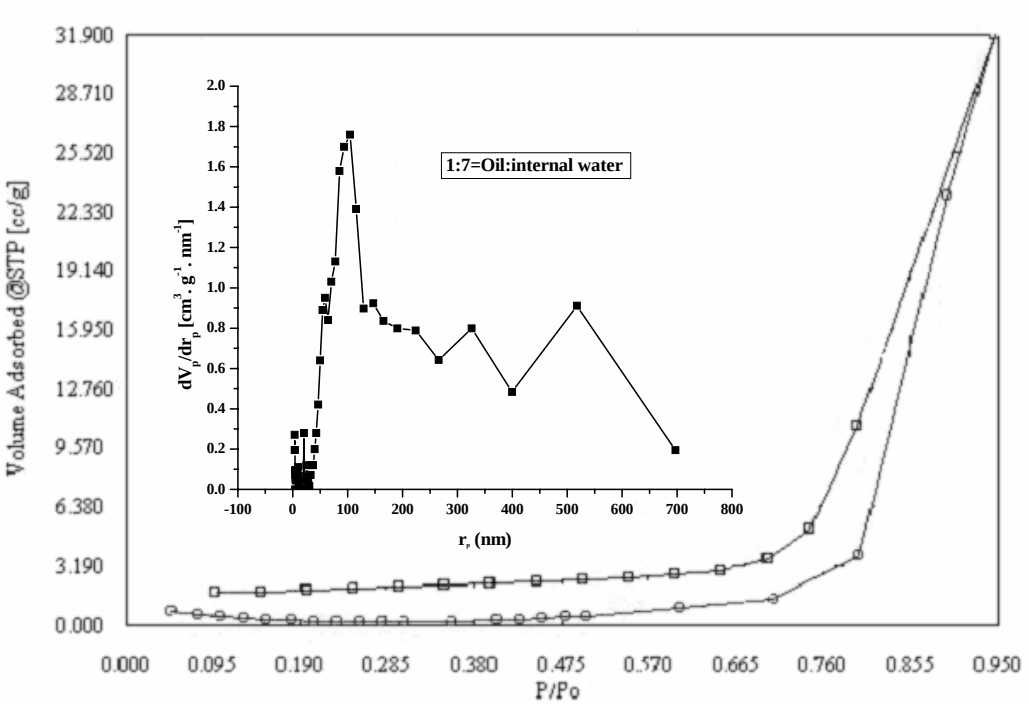

Figure 4.10. Nitrogen adsorption-desorption isotherm and pore size distribution of poly(styrene-GMA-DVB) terpolymers synthesised by HIPE emulsions using 1:7 oil to internal water ratio

As the internal water was increased from 1:1 to 1:7 there are formation of very big pores. In Figure 4.9 very broad pore size distribution are noted in the range 0-700 nm, with the median at 120 nm pore radii at the oil to internal water ratio of 1:5. At very high oil to internal water ratio (1:7) the instability of emulsion results in the random pore size distribution in the range 0-700 nm, as shown in Figure 4.10. When the amount of water increases more droplets are formed in the continuous oil phase and the droplet viscosity increased so much that there is formation of very thin film around the water droplets.

The thinness of film increased the possibility of rupturing resulting in the formation of bottleneck type openings. As shown in Table 4.5, the surface area decreases with increase in internal water from 76.11 to 20.22 m^2/g, as determined by nitrogen adsorption method. Even though the pore volume is high at high internal water amount i.e. 0.98 cm^3/g surface area is very low, around 20.22 m^2/g. This is due to the generation of predominantly macropores. At lower internal water micro and mesopores are generated which increases surface area (76.11 m^2/g at 1:1 oil to internal water ratio). Therefore, instead of conventional porogens (solvent, non-solvent or linear polymer) the surfactant together with internal water acts as pore forming component in the multiple emulsion methods.

The relative amount of internal water also plays an important role in designing the particle size of styrene-GMA-DVB terpolymers. The particle size data described in Table 4.5 shows the random distribution of average pore radii between 98.12-250 μm.

4.4.5 Effect on porous morphology

The morphologies and internal structures of the HIPE suspension terpolymers are distinctly different from the beads made by classical suspension polymerisation. The

morphology of the resulting material is determined by the structure of the emulsion prior to gelation. The morphologies and the internal structure of the polymers reflect the structure of the emulsion in case when the emulsion is stable and does not separate into individual components before gelation.

The properties of the emulsion like structure, stability and rheology depends on the composition, thickness and the viscoelasticity of the adsorbed stabilising layer at the oil-water interface. The stability of the emulsion with respect to creaming and coalescence depends mainly on the droplet-size distribution, the state of aggregation of droplets and the rheology of aqueous dispersion medium. The droplet size distribution is mainly dependent on the energy inputs during emulsification, as well as the hydrophobic-hydrophilic nature of emulsifying agent. The aggregation occurs as the adsorbing macromolecules get attached to more than one droplet at a time. Analysis of the beads by electron microscopy showed that some of the emulsion structure had been templated, but that there had also been significant emulsion collapse prior to gelation. This led to a relatively dense, partially porous structure.

It was found that the degree of porosity could be increased by raising the concentration of DVB. In addition to increasing porosity, these conditions also led to uniform, unagglomerated spherical beads. The beads are essentially monodisperse with an average diameter of 50 μm and a size distribution of just 2- 6%. Figures 4.11 (a) and (c) depict electron micrographs of individual spherical beads taken from SGDV terpolymers at 25 and 100% CLD, respectively. It can be seen that the internal structure is uniformly porous and consists of a “skeletal replica” of the original O/W HIPE. At 100% CLD the pore structure is highly interconnected and there are open pores on the

bead surface that are connected to the bead interior (Figure 4.11(d)), which is not the case at 25% CLD (Figure 4.11(b)). The size of the mesopores was found to be in the range 50-300 nm. The pore size distribution was somewhat narrow.

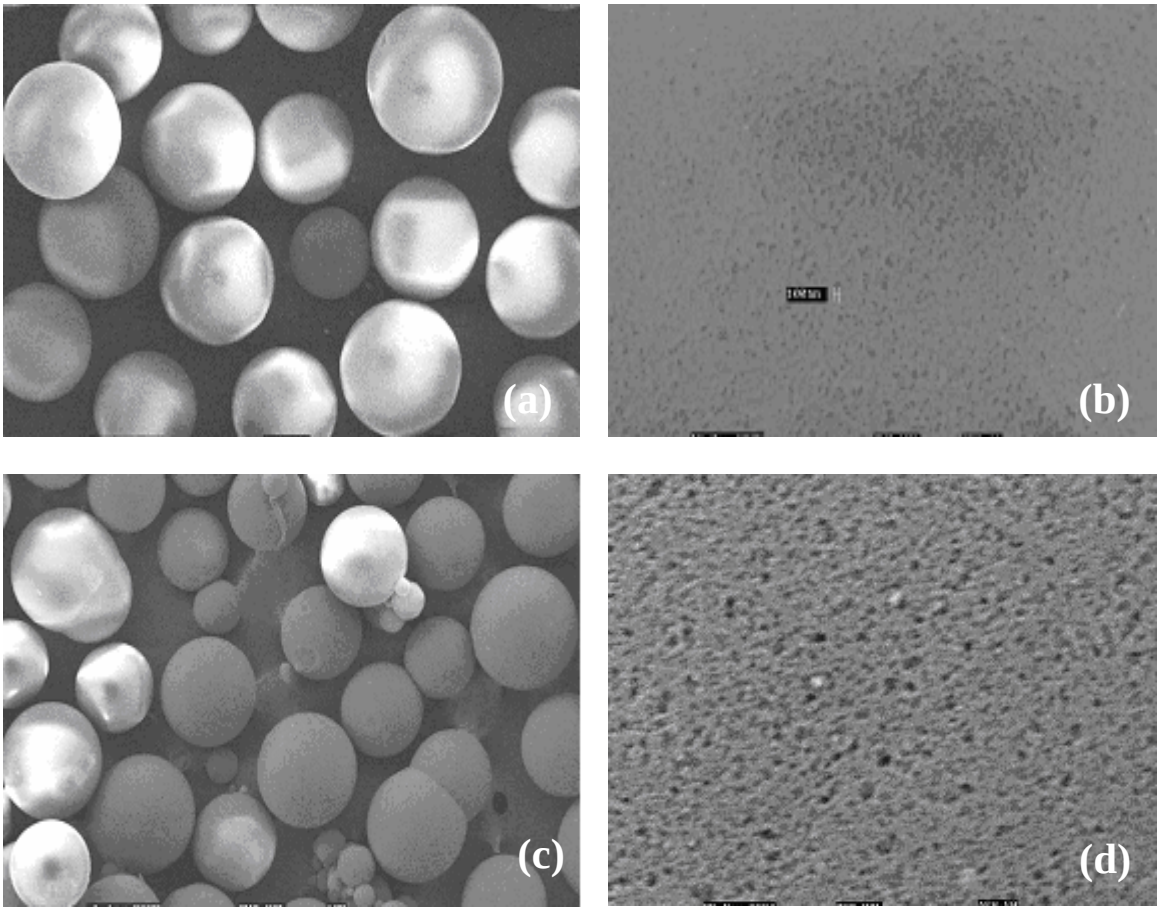

Figure 4.11. Scanning electron micrographs of styrene-GMA-DVB terpolymers of 25% CLD (a, b) and 100% CLD (c, d)

A similar observation was made in the case of emulsion-templated terpolymers synthesised using EGDM as cross-linker. Figure 4.12 shows the particulate nature and internal morphology of SGEG polyHIPE terpolymers. Figures 4.12 (a) and (c) show the spherical particle nature of beads prepared at 25 and 100% CLD, respectively. In this case pore size distribution was found to broaden with increasing EGDM concentration. Macrosporous polyHIPE structures were also observed at surface when lower cross-

linking levels were employed 25 [Figure 4.12 (b)], although some agglomeration between beads was observed at the highest cross-linking level (100%). The BET surface area is relatively low as compared to DVB system (Table 4.3).

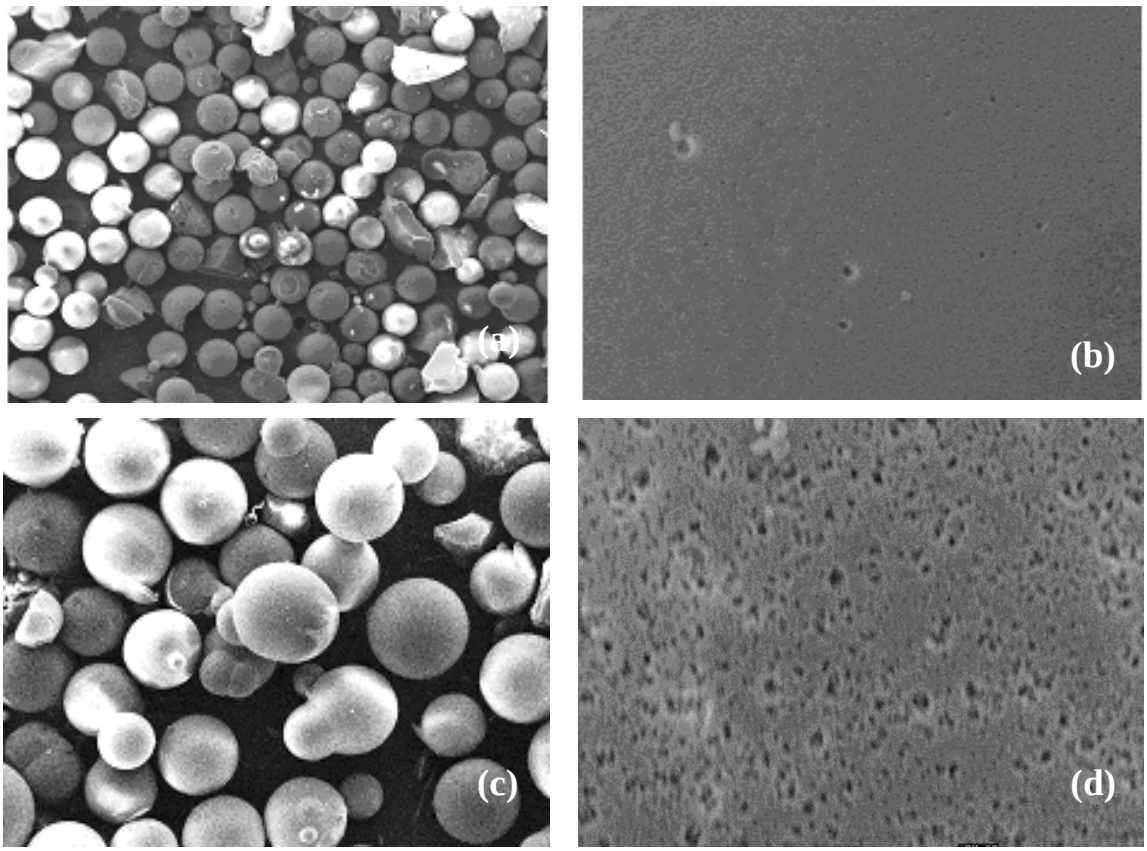

Figure 4.12. Scanning electron micrographs of styrene-GMA-EGDM terpolymers of 25% CLD (a, b) and 100% CLD (c, d)

This suggests that the removal of water during drying did not give rise to any permanent porosity that persisted in the dry state. At 100% CLD the pore seems to be irregular this is due the less stability of emulsion prior to gelation (Figure 4.12 d). It should be noted that the terpolymers synthesised by HIPE multiple emulsion technique differ from macroporous beads produced by suspension polymerisation in three important ways. First, intrusion volumes are much higher, reaching values of greater than 1.7 cm^3/g. Secondly, the pores in these materials are considerably smaller in the range of 2-

500 nm which is very difficult by conventional systems. Thirdly, the beads are produced give a quite narrow particle size distributions, as shown in Figures 4.11 (a) and (c).

The porous properties of the polymers synthesised by polymerising concentrated emulsion depend on the stability of the formed emulsions which in turn are dependent on the factors like type of surfactant, its concentration, the hydrophobicity /hydrophilicity of the monomers, etc. The emulsions, being thermodynamically unstable, require surfactant /emulsifying agents for stabilisation. The surfactants possess polar head groups (hydrophilic) and long fatty acid chains (lipophilic). It is because of these they can act at the interface between oil and water. They form a rigid film at the interface and prevent phase inversion. The choice of surfactant is dependent on the HLB (hydrophile-lypophile) number. The HLB number defines the polarity of nonionic surfactants in terms of an empirical quantity. The system HLB has an arbitrary scale of 1-20. If an emulsifier has a low HLB number, there are low numbers of hydrophilic groups on the molecule and it will have more of a lipophilic character.

It was observed that the amount of surfactant (Span 80) in oil phase had an important effect on the morphology of microspheres, as shown in Figure 4.13. Figures 4.13 (a) and (c) reveal the particle nature of styrene-GMA-DVB terpolymers synthesised with 17 and 68 wt.% Span 80. The porous structure was homogeneous on the particle surface and in the particle interior, which affect the mechanical strength of terpolymer. As shown in Figure 4.13 (b) at 17 wt.% Span 80 very small pores are formed in the 2-100 nm range, with a narrow distribution.

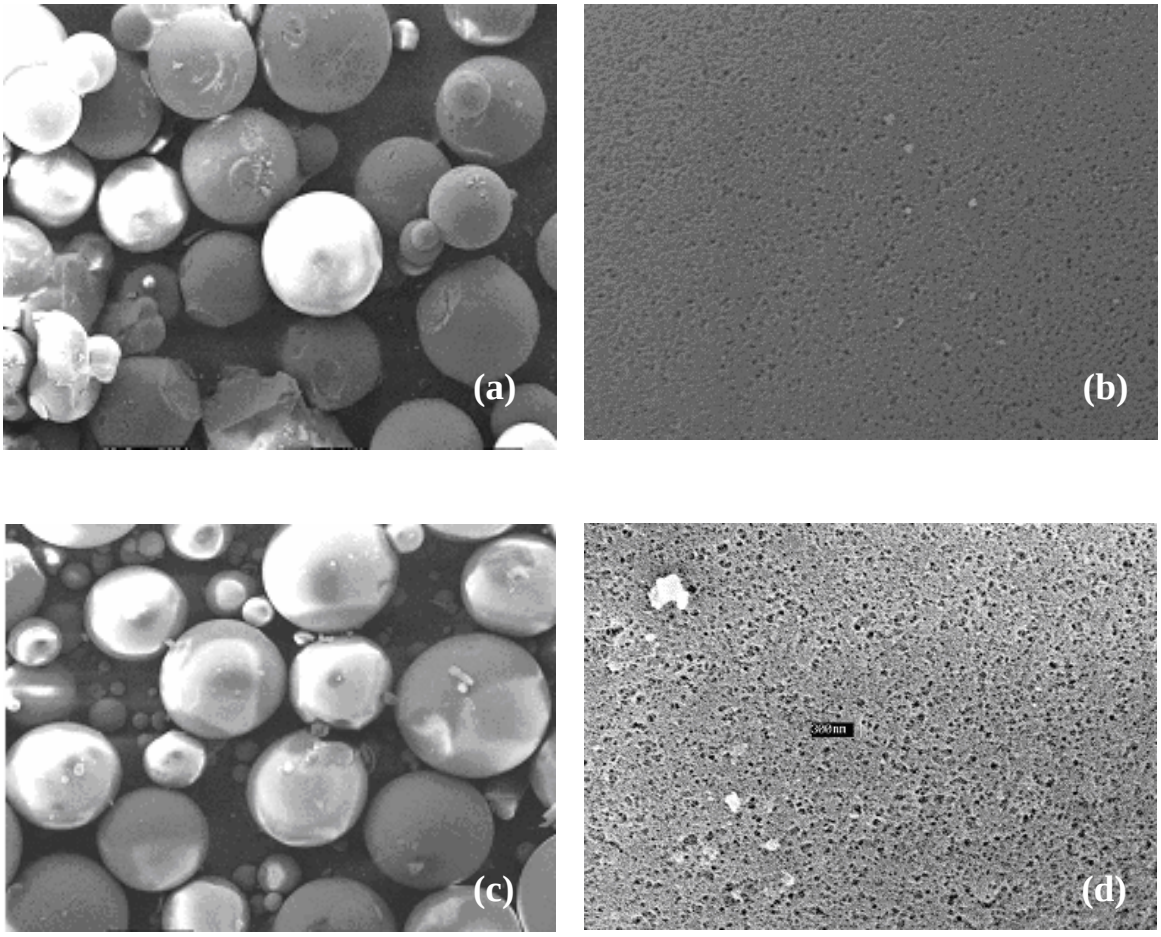

Figure 4.13. Scanning electron micrographs of styrene-GMA-DVB terpolymers synthesised using 17 wt.% Span 80 (a, b) and 68 wt.% Span 80 (c, d)

The solubility and consequently, chemical potential of the disperse phase in the bulk phase is dependent on the radius of curvature of that droplet, with the solubility increasing with decreasing radius. These result in smaller drops dissolving into the bulk phase and then diffusing to, and re-depositing on larger ones leading to an overall increase in average size of the emulsion, the process known as Ostwald ripening. The droplet size increased with the surfactant concentration due to Ostwald ripening, merging the small droplets into larger droplets. Here, two types of pore are obtained, as shown in Figure 4.13 (d) at 68 wt.% of Span 80. Higher concentration of Span 80 generated bimodal distribution mix of small and large pores, up to 500 nm.

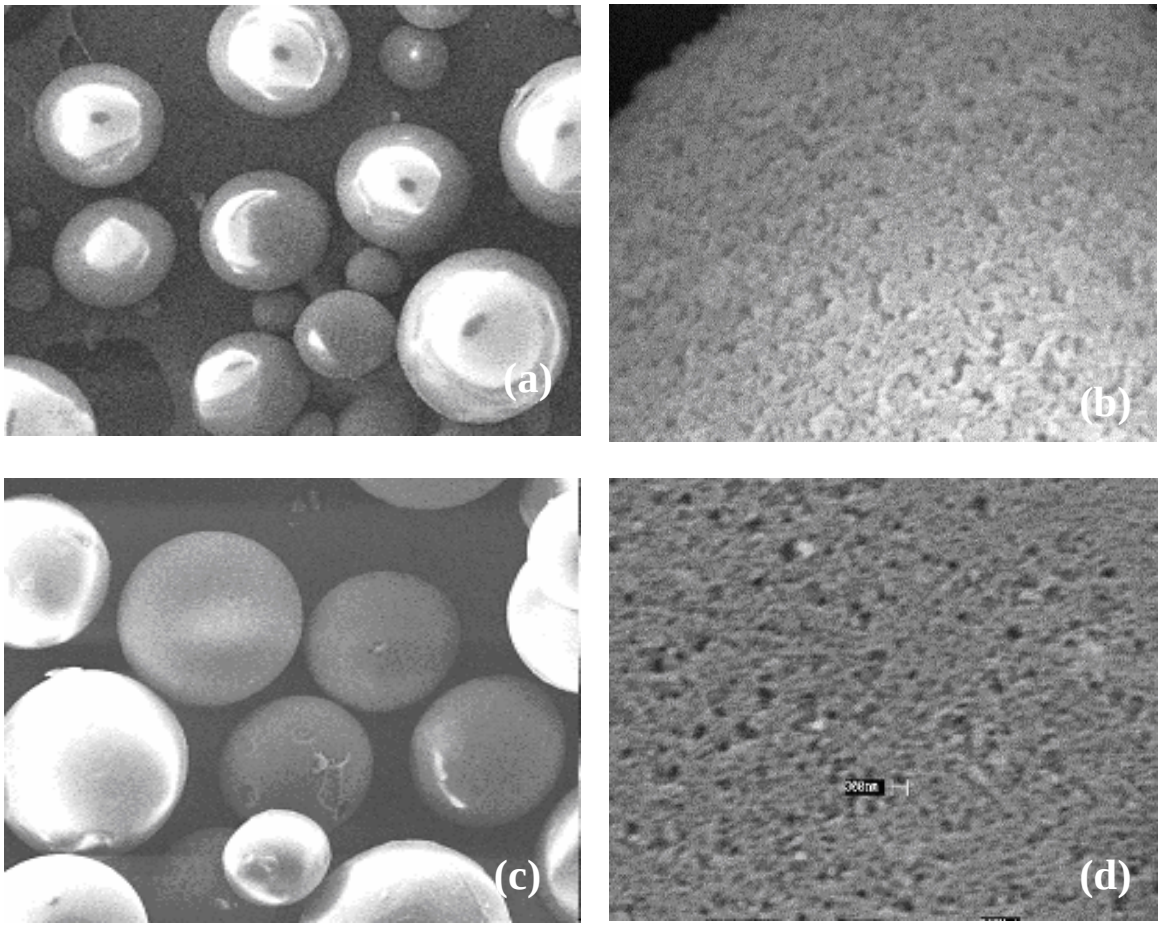

Figure 4.14. Scanning electron micrographs of styrene-GMA-DVB terpolymers synthesised using 17 wt.% Brij 52 (a,b) and 68 wt.% Brij 52 (c,d)

On the other hand very different morphology was observed with Brij 52, having a marginally higher HLB value (5.3) than Span 80, It gave a less stable W/O emulsion before gelation. Figures 4.14 (a) and (c) show the particle morphology synthesised using Brij 52 at 17 wt.% and 68 wt.%, respectively. Figure 4.14 (b) shows the surface morphology of SGDV terpolymer at 17 wt.% surfactant. Here large numbers of interconnected pores are formed as a result of early phase separation giving a pronounced bimodal distribution. Figure 4.14 (d) represents the surface micrograph of terpolymer synthesised using 68 wt.% of Brij 52. The pores are more regularly opened at the surface giving macropores that yield higher pore volume but low surface area.

4.4.6 Effect of internal discontinuous phase on morphology

In a theoretical treatment of the geometry of HIPEs, Lissant[34] showed that, for a monodisperse system, the dispersed phase droplets will assume a rhomboidal dodecahedral (RDH) packing [Figure 4.15 (a)] from 74 to 94% internal phase volume, with increasing deformation into polyhedra [Figure 4.15 (b)]. Above 94%, the packing changes to tetrakaidecahedral (TKDH) (truncated octahedral). It was assumed that monodisperse packing occurred throughout; theoretical calculations showed this system to be more favourable than a polydisperse arrangement.[35] The shape of the dispersed phase droplets was investigated experimentally by Lissant and coworker by scanning electron microscopy (SEM) on cured HIPEs of water in a styrene-based resin.[36] At high internal phase volumes, droplets were indeed polyhedral, and appeared to be relatively monodisperse.

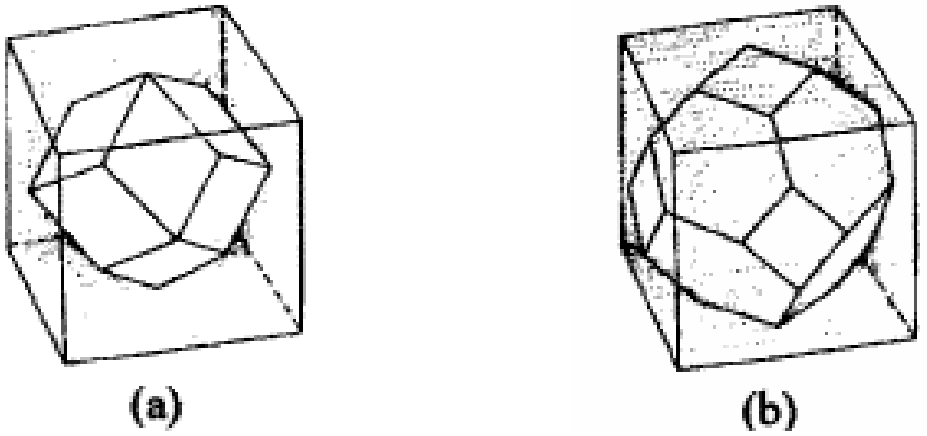

Figure 4.15. (a) Rhomboidal dodecahedron (RDH) (b) tetrakaidecahedron (TKDH)

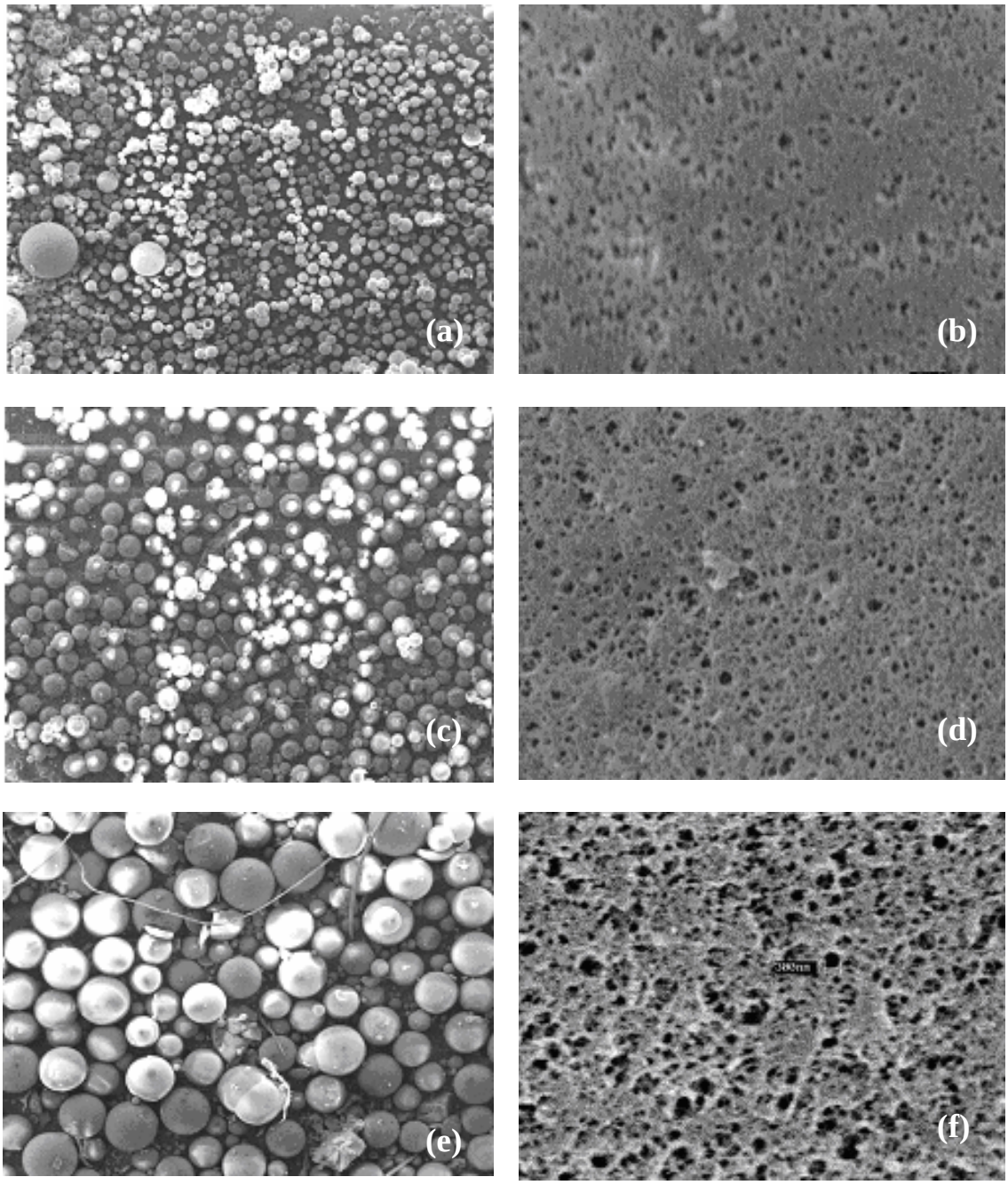

Figure 4.16 Scanning electron micrographs showing particle as well as surface morphology of terpolymer synthesised using (a, b) 50% internal water, (c, d) 75% internal water, and (e, f) 87% internal water.

The particle size reduced with an increase in the discontinuous water phase. There is maximum amount of dispersed phase that can be incorporated into a concentrated

emulsion. This is dependent on the interfacial free energy between the organic and water phases in the absence of surfactant. A large value of interfacial energy implies that the organic phase is very hydrophobic and hence its interaction with water is weak. As a result the interaction between hydrocarbon chain of surfactant and the organic molecules as well as those between the polar head groups of the surfactant and the water are strong, stabilising the interface between the two phases and consequently increasing the stability of emulsion.

The change in the internal structure with the change in volume of internal water is shown in Figures 4.16 (b), (d) and (f). Figures 4.16 (a) and (b) show the SEM of terpolymer synthesised using 50% internal phase (oil:water 1:1 v/v). As this is less than 75% it cannot be HIPE by definition. Here the particles obtained are spherical in shape (Figure 4.16 (a)) and diameter is in the range 2-100 μm. The internal morphology is somewhat non-uniform with very less opening on the surface (Figure 4.16(b)), because the organic and water phases are equal in volume and during HIPE formation aqueous droplets are packed loosely and in between two droplets there is considerable space. Figure 4.16 (c) shows the spherical nature of particles prepared using 75% internal water. As the amount of internal water was increased from 50 to 75% (i.e. oil to internal water ratio is 1:3 v/v) the droplets try to be dispersed in rhomboidal dodecahedral (RDH) with a number of bottle neck type pore opening at the surface, as shown in Figure 4.16 (d). Figure 4.16 (e) shows the bimodal particle nature of terpolymer synthesised using 87% internal water phase. At 87% internal water, the dispersed droplets try to occupy maximum space available in the organic phase. As a consequence, thin walls are formed between the organic and water interface, as shown in Figure 4.16 (f). The droplets now

occupy truncated octahedral shape. During this deformation the centre of cell walls get ruptured and create a circular hole and connect the neighbouring droplets. As result, large number of pore opening (interconnected) are seen Figure 4.16 (f).

4.5 Styrene-GMA-DVB terpolymers as catalysts for synthesis of bisphenol A

Step - 1

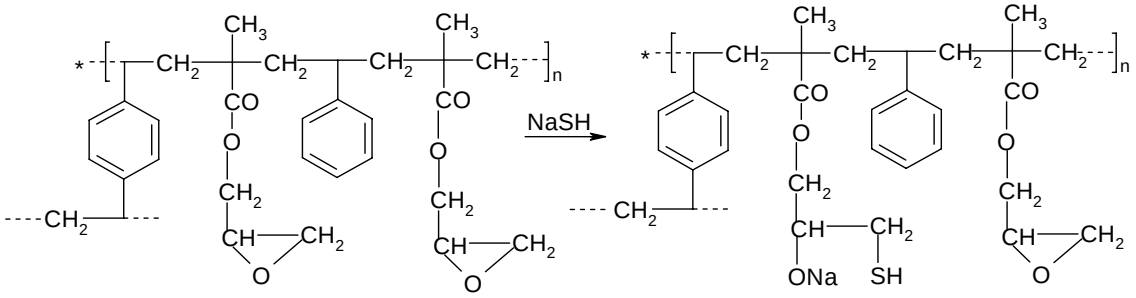

Step – 2

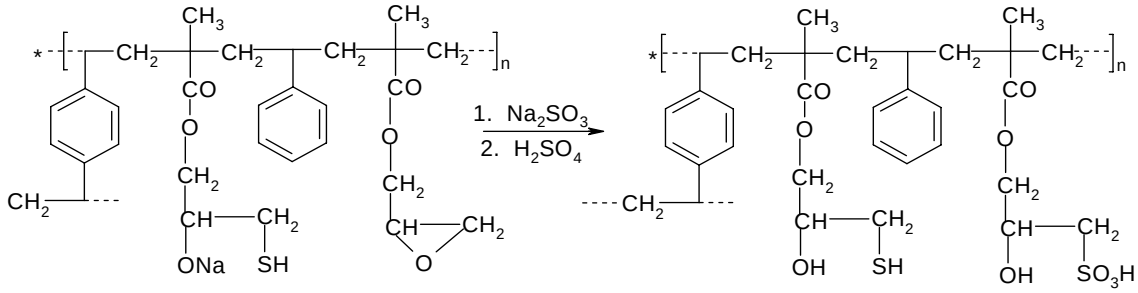

Step – 3

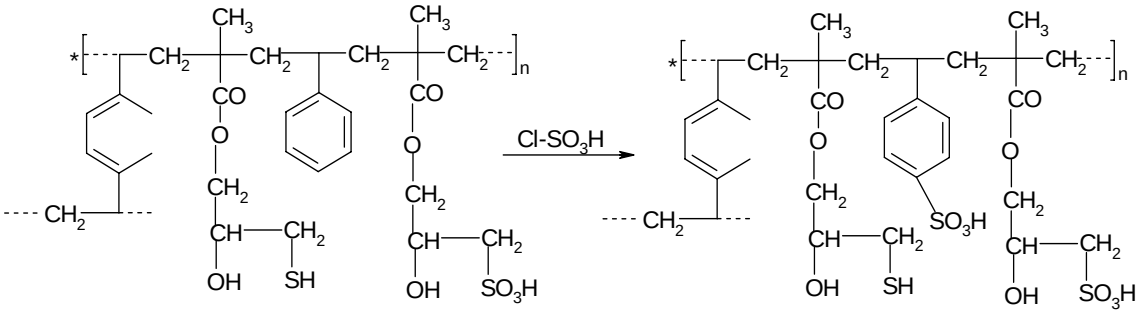

Figure 4.17. Three step reaction scheme showing functionalisation of terpolymer (SGDV-23) with sulphonic and mercaptosulphonic acid groups

One of the polyHIPE terpolymer from Styrene-GMA-DVB (SGDV-23) series was chosen and functionalised with sulphonic acid groups. In the two step method, the beads were treated with sodium sulphite under reflux using a mixture of isopropanol and deionised water as solvent to ring open the epoxy groups. In the second step, sulphonic acid group was introduced to the pendant position of the benzene ring using chlorosulphonic acid at ambient conditions using 1,2-dichloroethane as solvent. Analysis indicated modification to the extent of 5.7 milliequivalents of sulphonic acids per gram.

In the three-step method, the epoxy group was partially opened up using sodium thiol in methanol under reflux as shown in Figure 4.17. The unopened epoxy group was then converted into sodium salt of sulphonic acid by the process described above. Then by using chlorosulphonic acid, the pendent sulphonic acid group was introduced to the benzene ring. This styrene-GMA-DVB polyHIPE system showed about 4.8 milliequivalents of sulphonic acids per gram, as shown in Table 4.6.

4.5.1 Estimation of sulphonic acid groups

Since sulphonic acid groups attached to the phenyl ring will give higher acidity due to resonance, the acidity of these catalysts were found to be higher than that in beads where sulphonation is done by the ring opening of the epoxy groups. The commercial macroporous sulphonic acid catalyst Amberlyst-15 is prepared by suspension polymerisation, the porosity of Amberlyst is less and hence internal substitution will be limited. The synthesised HIPE beads have higher porosity and hence certain extent of internal substitution is possible, which accounts for the higher acidity of the HIPE beads over Amberlyst-15.

Table 4.6. Milliequivalents of sulphonic acid groups generated on styrene-GMA-DVB (SGDV-23) polyHIPE terpolymer beads

Sample No.	Sulphonation catalyst	Sulphonic acid Mequivalents/g
SGDV-23A	Sulphonated	0.38
SGDV-23B	Thiolated and sulphonated	0.34
SGDV-23C	Sulphonated and epoxide opened	5.70
SGDV-23D	Thiolated, sulphonated, epoxide opened	4.82
Commercial	Amberlyst-15	4.70

4.5.2 Estimation of 4,4'-bisphenol-A

The catalysts were used to estimate the percentage selectivity towards 4,4'-bisphenol-A synthesis, produced by the reaction of phenol with acetone. The results show that the percentage yield of the phenolic products is increased by the higher acidity of the catalyst. When mercapto groups are substituted there is a decrease in the yield of phenolic products, as shown in Table 4.7.

Table 4.7 Comparative reactivity of synthesised catalysts (SGDV-23) with Amberlyst-15

Sulphonation catalyst	Percentage yield of phenolic products	Selectivity of 4,4' – bisphenol A
SGDV-23C	15.24	61.20
SGDV-23D	10.99	66.78
Amberlyst-15	11.91	73.34

The presence of mercapto groups will decrease the acidity since some of the epoxy rings are opened to give thiols. This is seen to increase the selectivity for 4,4'-

bisphenol A, as shown in Table 4.7. It can be inferred that even though the styrene-GMA-DVB terpolymer HIPE beads give lower product yield, the high concentration of thiol groups in it enhances selectivity to the formation of 4,4'-bisphenol A. The percentage yield is found to be lower with the sulphonated styrene-GMA-DVB terpolymer HIPE beads. In this system also, the partial ring opening of oxirane to thiol group is found to increase the selectivity to 4,4'-bisphenol A with a reduction in yield of phenolic products.

Due to the substitution of sulphonic acid group as a pendant substituent to the benzene ring, the acidity is higher and hence the percentage yield of phenolic products are also higher. Presence of thiol groups in SGDV-23D increases the selectivity but decreases the overall reaction rate. In presence of commercial catalyst Amberlyst-15 the reaction rate lies in between SGDV-23C and SGDV-24D. The selectivity is better.

4.6 Conclusions

A systematic study of the effects of the synthesis parameters on specific surface area, pore volume, and pore size distribution of the monodisperse porous terpolymer particles was conducted. The physical characteristics of the monodisperse porous polymer particles depended on various synthesis parameters including: (1) cross-linker type; (2) overall cross-link density; (3) surfactant type; (4) concentration of surfactant; (5) Internal water. By the variation of these parameters, porous polymer particles with different physical features could be prepared. This multiple emulsion methodology allows the synthesis of emulsion-templated terpolymers in the form of monodisperse spherical beads and tailor made properties.

Polymers having cross-link density of 25, 50, 75 and 100% were synthesised by multiple emulsion high internal phase emulsified suspension (HIPE's) method. When the cross-linking degree was 25%, and the concentration of Span 80 was 17%, microspheres with pore size of about 20 nm were obtained.

The physicochemical character of the oil phase determined how the oil will be surrounded by the water droplet in the emulsion. The ratio of surfactant to oil is more important than the total amount of monomer or surfactant present.

The polymers formed had a high pore volume in the range of 0.34-1.12 cm^3/g and the surface area were 23-103 m^2/g. The low surface area is an anomaly, which arises from the evaluation technique due to collapse of the pores. The polymers synthesised by conventional suspension polymerisation had maximum pore radii in the 250-500 nm region while polymers synthesised using multiple emulsion HIPEs had maximum pore radii in the range 0.5-700 nm region. Polymers synthesised by HIPE using Span 80 as porogen had maximum pores in the 0.5-100 nm range. The pore size increased with an increase of Span 80 concentration in oil phase. Maximum surface area obtained using Span 80 was 103.36 m^2/g, which was due to the formation of micro and meso pores.

Macroporous terpolymer microspheres of SGDV and SGEG could be prepared at a higher concentration of surfactant in oil phase. The recipe was optimised, the effects of the amount and type of surfactant on the morphology of microspheres were investigated.

Similarly, the amount of internal water plays a very important role in the droplet packing during the HIPE emulsification, which in turn affects the porous structure formation. High amount of internal phase (higher than 80%) gives bimodal pore size distribution in the porous terpolymer matrix.

References:

[1] Iwakura, Y.; Kurosaki, T.; Ariga, N.; Ito, T. *Makromol. Chem*. **1966**. 97, 128.

[2] Mrkvickova, L.; Kalal, J.; Bednar, B.; Janca, J. *Makromol. Chem*. **1982**. 183, 203.

[3] Guyot, A.; Bartholin, M. *Prog. Polym. Sci*. **1982**, *8*, 277.

[4] Hodge, P.; Sherrington, *Syntheses and Separations Using Functional Polymers*, Wiley: New York, **1989.**

[5] Wijnhoven, J. E. G. J.; Vos, W. L. *Science* **1998**, *281*, 802.

[6] Tanev, P. T.; Chibwe, M.; Pinnavaia, T. J. *Nature* **1994**, *368*, 321.

[7] Maquet, V.; Jerome, R. *Mater. Sci. Forum* **1997**, *250*, 15.

[8] Peters, M. C.; Mooney, D. J. *Mater. Sci. Forum* **1997**, *250*, 43.

[9] Bancel, S.; Hu, W. S. *Biotechnol. Prog*. **1996**, *12*, 398.

[10] Camilla, V.; Frantisek, S.; Jean Frechet, M. J. Chem.mater. **1996**, *8*, 744.

[11] Glass, E. Hydrophilic Polymers, *Adv Chem. Series* **1996**, 248.

[12] Fishman, M.; Friedman, R.; Huang, S. *ACS Symp. Ser*. (Polymers from Agricultural Coproducts), Vol. 575, **1994.**

[13] Jhonson, P. Lloyd-Jones, G. *Drug Delivery Systems. Fundamentals and Techniques*, (Ellis Horwood Serires in Biomedicine), VCH Verlagsgesellschaft: Weinheim, Federal Republic of Germany, **1987.**

[14] Kenawy, E.; Sherrington, D. *Eur. Polym. J*. **1992**, *28*, 841.

[15] Galia, M.; Svec, F.; Frechet, J. *J. Polym. Sci. Polym. Chem. Ed*. **1994**, *32*, 2169.

[16] Sederal, W. I.; DeJong, G. J. *J. Appl. Polym. Sci*. **1973**, *17*, 2385.

[17] Horak, D.; Svec, F.; Ilavsky, Bleha, M.; Baldrian, M. J.; Kalal, J. *Angew. Makromol. Chem.* **1992**, *192*, 113.

[18] Rosenberg, J. E.; Flodin, P. *Macromolecules* **1987**, *20*, 1518.

[19] Okay, O.; Gurun, G. J. *J. Polym. Sci., Polym. Chem*. **1992**, *46*, 401.

[20] Rabelo, D.; Coutinho, F. M. B. *Eur. Polym. J*. **1994**, *30*, 675.

[21] Hamid, M. A.; Naheed, R.; Fuzail, M.; Rehman, E. *Eur. Polym. J*. **1999**, *35*, 1799.

[21] Lewandowski, K.; Svec, F.; Fréchet, J. M. J. *J. Appl. Polym. Sci*. **1998**, *67*, 597.

[22] Horak, D.; Svec, F.; Ilavsky, M.; Bleha, M.; Baldrian, J.; Kalal, J.; *Angew. Makromol. Chem*. **1981**, *95*, 109.

[23] Horak, D.; Svec, F.; Ilavsky, M.; Bleha, M.; Baldrian, J.; Kalal, J. *Angew. Makromol. Chem*. **1981**, *95*, 117.

[24] Liang, Y. C.; Svec, F.; Fréchet, J. M. J. *J. Polym. Sci., Part A: Polym. Chem*. **1997**, *35*, 2631.

[25] Chechilo, N. M.; Khviliviskii, R. J.; Enikolopyan, N. S. Dokl. Akad. Nauk. **1972**, USSR, *204*, 1180-1187.

[26] Li, N. H.; Benson, J. R.; Kitagawa, N. US Patent 5,653,922, **1997**

[27] Li, N. H.; Benson, J. R.; Kitagawa, N. US Patent 5,863,957, **1999**

[28] Li, N. H.; Benson, J. R.; Kitagawa, N. US Patent 6,100,306, **2000**

[29] Donfner. K. Ion-exchanger. Walter de Gruyter, Berlin, **1991**

[30] Kline, G. M. Analytical chemistry of polymers, Interscience, New York, p. 123, **1959**.

[31] Stefanec, D.; Krajnc, P. *Reactive and Functional Polymers* **2005,** 65, 37–45.

[32] Zhen, Zhou.; Midan, Li.; Heliang,Yan. *Colloids and Surfaces A*: *Physicochemical and Engineering Aspects* **2000**, 175, 263.

[33] Kulygin, O.; Silverstein, M. *Soft Matter* **2007**, 3, 1525.

[34] Lissant, K. J. *J. Coil. Interf. Sci*. **1966**, 22, 462.

[35] Lissant, K. J. *J. Soc. Cosmetic. Chem*. **1970,** 21, 141.

[36] Lissant, K. J.; Mayhan, K. G. *J. coil. Interf. Sci***, 1973**, 42, 201.

Chapter V

Functionalised polyHIPE materials for arsenic removal

5 Functionalised polyHIPE materials for arsenic removal

5.1 Introduction

Contamination of water by heavy metal ions is becoming more and more serious due to their associated ecological and health toxic effects even at very low concentrations.[1] Arsenic is a carcinogen and its ingestion may deleteriously affect the gastrointestinal tract, cardiac, vascular system and central nervous system.[2] Due to its high toxic effect on human health, recently the United States Environmental Protection Agency (USEPA) has lowered the maximum contaminant level for arsenic in drinking water from 50 to10 $\mu g/L^{-1}$. A vast majority of these systems use ground waters. World away, over 70 million people in Bangladesh and in other regions of Indian subcontinent are routinely exposed to arsenic poisoning through drinking ground water.[3-5]

Arsenic contamination of the ground water occurs by both natural processes such as weathering of arsenic containing minerals and anthropogenic activities such as uncontrolled industrial discharge from mining and metallurgical industries, and application of organo-arsenical pesticides.[6] Inorganic arsenic is predominantly present in natural waters. Arsenate [As (V)] and arsenite [As (III)] are primary forms of arsenic in soils and natural water. Under low pH and mildly reducing conditions As (III) is thermodynamically stable and exists as arsenious acid (H_3AsO_3, $H_2AsO_3^-$, $HAsO_3^{2-}$ and AsO_3^{3-}). Under oxidizing conditions, the predominant species is As (V), which exists as arsenic acid (H_3AsO_4, $H_2AsO_4^-$, $HAsO_4^{2-}$ and AsO_4^{3-}).[7] As (III) is more mobile in ground water and is 25-60 times more toxic than As (V). The concentration of arsenic species is mainly dependent on redox potentials and pH.[8, 9]

Research is intensive on improving the established or developing novel technologies for arsenic removal, in order to achieve the new concentration limits. The primary aim is to find the best available technology for arsenic removal from drinking water. A number of arsenic removal technologies are currently practiced, namely, activated alumina sorption, polymeric anion-exchange and sorption by iron oxide coated sand (IOCS) particles. Enhanced coagulation followed by micro-filtration, pressurised granulated iron particles, iron oxide doped alginate, manganese dioxide coated sand, polymeric legand exchange and zero valent iron have been tested in the laboratory and / field scale testing for removal of trace arsenic.[10-24] Among these techniques, adsorption is generally preferred for the removal of metal ion because of its high efficiency, easy handling, and availability of different adsorbents.[25]

Removal of toxic heavy metal by using chelating polymers is thus of great importance in environmental applications.[26-37] Several criteria are important in the design of chelating polymers with substantial stability for the selective removal of metal ions. These include specific and fast complexation of the metal ion as well as the reusability of the chelating polymeric ligands.[31] A large number of polymers incorporating a variety of chelating ligands, such as textile dyes, poly(ethyleneimine) (PEI), iminodiacetate, amidoxime, phosphoric acid, dithiocarbamate, and thiazolidine, have been prepared and their adsorption and analytical properties have been investigated.[32-37] Amino acids incorporated polymers and their different applications have been reported in series of recent publications.[38-42] The idea of using different amino acids as metal chelating ligands stems from that these are very reactive with different chemical substances including metal ions. Poly(ethyleneimine) (PEI) is a cationic polymer used for a wide

variety of applications. PEI acts as a chelating agent for the removal of many materials and also been used for the removal of cadmium. PEI was used for the metal binding, and this was followed by an ultra-filtration operation to retain the PEI polymer.[43] The immobilisation of PEI in suitable matrix can provide an attractive alternative to membrane processes. Chanda and Rempel[31] applied PEI-containing granular sorbents for the selective removal of Cr (III) from a mixture of Cr (III), Cu (II), Ni (II) and Fe (III). This sorbent was found to be superior to commercial resin Chelex-100. Navarro et al synthesised and tested cellulose based sorbents were used for the selective removal of mercury from aqueous solution.[36]

The immobilised chelation process for the removal of soluble metals has become an important option in the integrated approach to aqueous waste treatment.[44] This process incorporates the principle of metal coordination into traditional ion-exchange technology, thus affecting major changes in the application of adsorbents. In the past, many types of metal chelating adsorbents have been synthesised.[45] Processes have been developed with either polymerisation or simple functionalisation principles. The former involves the polymerisation of monomers containing the desired ligands. Although techniques for enhancing metal selectivity are easily developed with this method, difficulties in achieving regularly shaped polymers with sufficient porosity still remain the major drawback. In the other approach, the modification of preshaped polymers via the principle of polystep functionalisation is considered. Ease in performing functionalisation reactions and confidence that the properties of the product will be closely related to the starting materials make this a favorite process for much research.

In the present investigation, as support media epoxide based on GMA-EGDM and AGE-EGDM copolymer beads prepared by HIPE (Chapter 3 section 3.2.2.2) were selected and modified with PEI. The GMA-EGDM and AGE-EGDM co-polymer beads synthesised by HIPE are characterised by the presence of large cells (cavities). Furthermore these large cavities are interconnected by a series of smaller pores (windows), thereby enabling each to interact with those adjacent to them. The size of cells and windows can be controlled by changing the mixing speed, the type of surfactant (emulsion stabilser), the monomer composition and the water/monomer ratio.[46,47]

Poly(HIPE) containing styrene, divinylbenzene and varying amounts of either 2-ethylhexyl acrylate or the corresponding methacrylate monomer have been successfully employed as supports in solid phase peptide synthesis and for the immobilisation for flavin.[46] Additionally, styrene-DVB copolymers synthesised by HIPE have been coated with iron oxide and tested for the removal of arsenic from contaminated water.[48]

The present study is the first systematic, comparative research for arsenic removal; covering both trivalent As (III) and pentavalent As (V) inorganic arsenic anions using PEI modified poly(HIPE) GMA-EGDM and AGE-EGDM beads. The variables examined were the monomer type, cross-link densities, PEI concentration, contact time and pH of the treated water.

5.2 Experimental

5.2.1 Materials and methods

Glycidyl methacrylate (GMA), allyl glycidyl ether (AGE) and ethylene dimethacrylate (EGDM) were purchased from Sigma-Aldrich, USA, Sorbitan monooleate (Span 80) was from LOBA CHEMIE, Mumbai, India. Potassium peroxydisulphate was

from Merck, India. Azobisisobutyronitrile (AIBN) obtained from SISCO, India was crystallised from methanol before use. Poly(vinyl pyrrolidone) (PVP) from Fluka (Germany) was used as protective colloid. Polyethyleneimine (PEI) (relative molecular mass =1300) was supplied by Sigma Chemical Co. Stock solution of arsenite [As (III)] was prepared by dissolving appropriate quantity of arsenic trioxide (As_2O_3) [Loba Chemie Pvt, Ltd, Mumbai, INDIA] in distilled water containing 1% (wt./wt.) sodium hydroxide and the solution was then diluted up to 1L with distilled water before use. The arsenate (V) stock solution was prepared from the sodium arsenate, $Na_2HAsO_4.7H_2O$ [Loba Chemie Pvt, Ltd, Mumbai, INDIA]. The intermediate and secondary standards of arsenic solutions were prepared fresh for each experiment. The working solutions containing arsenic were prepared by dissolving appropriate amount of arsenic from stock solutions in demineralised (D.M.) water.

5.2.2 Preparation of microporous HIPE beads

The synthesis was conducted in double walled cylindrical reactor Figure 5.1.

Table 5.1. Composition of GMA-EGDM polyHIPE

Polymer Code	GMA mol	EGDM mol	CLD %	Mass g	Epoxy mmole/g
GEH-05	0.0592	0.0027	05	9.000	6.5850
GEH-10	0.0556	0.0055	10	9.005	6.1790
GEH-25	0.0494	0.0122	25	9.3988	5.2177
GEH-50	0.0389	0.0191	50	9.4111	4.1434
GEH-75	0.0324	0.0242	75	9.4192	3.4395
GEH-100	0.02771	0.0276	100	9.4250	2.9397

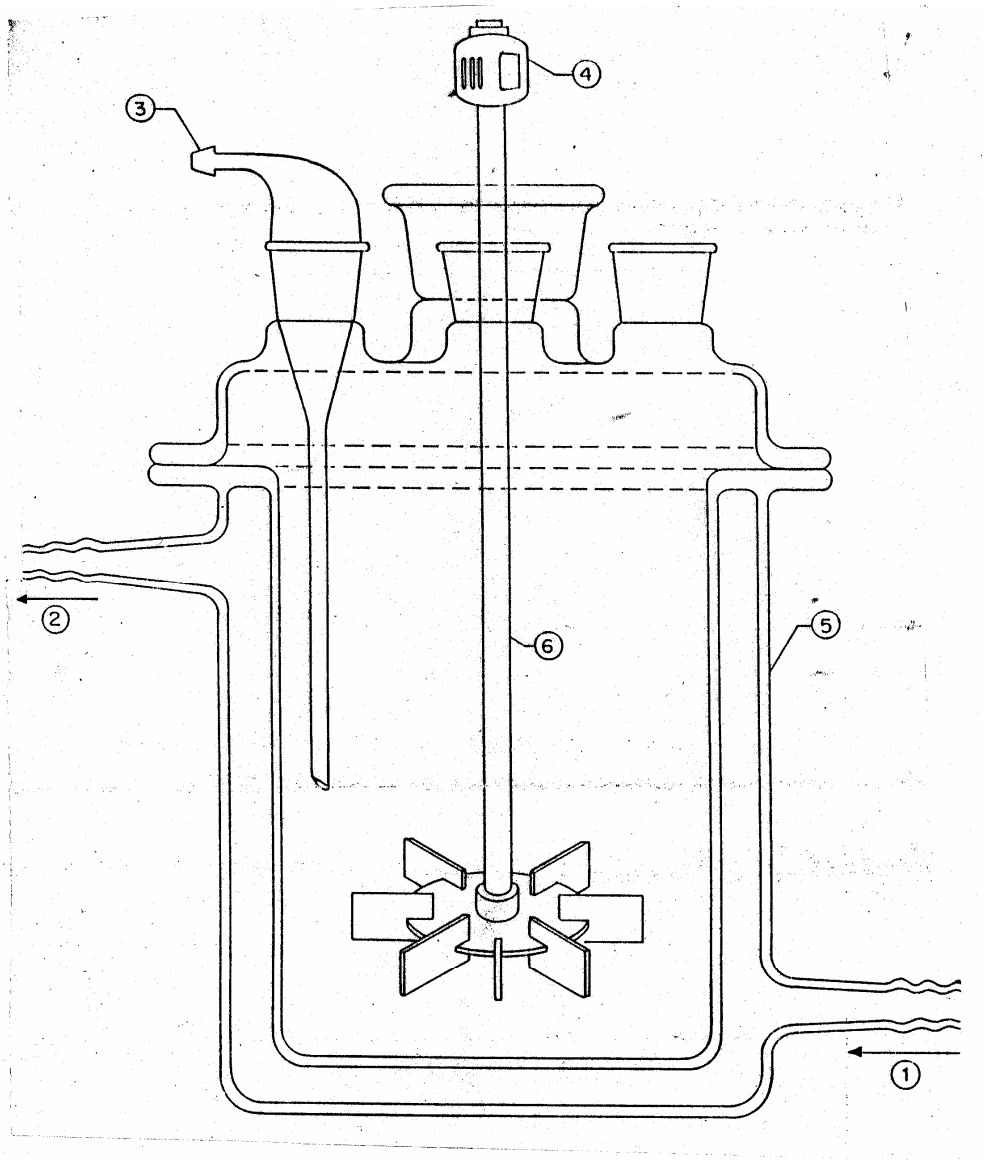

1) Hot water inlet, 2) Hot water outlet, 3) Nitrogen Bubbler, 4) Stirrer motor, 5) Glass reactor, 6) Stirrer, d = diameter of Ruston turbine stirrer and D = inner diameter of glass reactor

Figure 5.1. Schematic diagram of HIPE polymerisation reactor

The synthesis procedure presented in Section 3.2.2.2 was used to prepare the basic GMA-EGDM and AGE-EGDM polyHIPEs beads. The compositions are shown in the Tables 5.1 and 5.2 for various cross-link densities.

Table 5.2. Composition of AGE-EGDM polyHIPE

Polymer Code	AGE mol	EGDM mol	CLD %	Mass g	Epoxy mmole/g
AEH-05	0.0729	0.0033	05	8.990	8.1096
AEH-10	0.0679	0.0062	10	9.000	7.5617
AEH-25	0.0549	0.0131	25	8.878	6.1890
AEH-50	0.0422	0.0211	50	9.013	4.6843
AEH-75	0.0346	0.0259	75	9.093	3.8094
AEH-100	0.0293	0.0292	100	9.149	3.2057

5.2.3 Polyethyleneimine (PEI) immobilisation

GMA-EGDM and AGE-EGDM copolymers were modified by covalent attachment of PEI. Dry polyHIPE (GMA-EGDM) and polyHIPE (AGE-EGDM) beads (0.1g of each) of differing cross-link densities were added into aqueous solution (25 mL) containing polyethylenimine [(5 % wt./wt.), pH~10.5] and kept in test tubes. The mixture was degassed by applying a partial vacuum to remove air from pores of the beads. After degassing, water was added to maintain the level of beads, so that beads remained in solution. This mixture was stirred on the vibromill for 15 min., heated at 70^{o}C for 16 hours, with stirring at regular interval. PEI-attached polyHIPE (GMA-EGDM) and polyHIPE (AGE-EGDM) beads were washed several times with distilled water to remove any physically adsorbed PEI from the beads. The modified polymer was dried at room temperature under reduced pressure. The PEI binding capacities were calculated based on the amount of PEI covalently attached per gram of polyHIPE (GMA-EGDM) and polyHIPE (AGE-EGDM) beads. The amount of polyethylenimine attached to the

polyHIPE (GMA-EGDM) and polyHIPE (AGE-EGDM) beads was also determined by elemental analysis. Modification of polyHIPE (GMA-EGDM) and polyHIPE (AGE-EGDM) by PEI are given in Tables 5.3 and 5.4.

5.2.4 As (III) and As (V) binding on PEI derived poly(GMA-EGDM) and poly(AGE-EGDM) beads

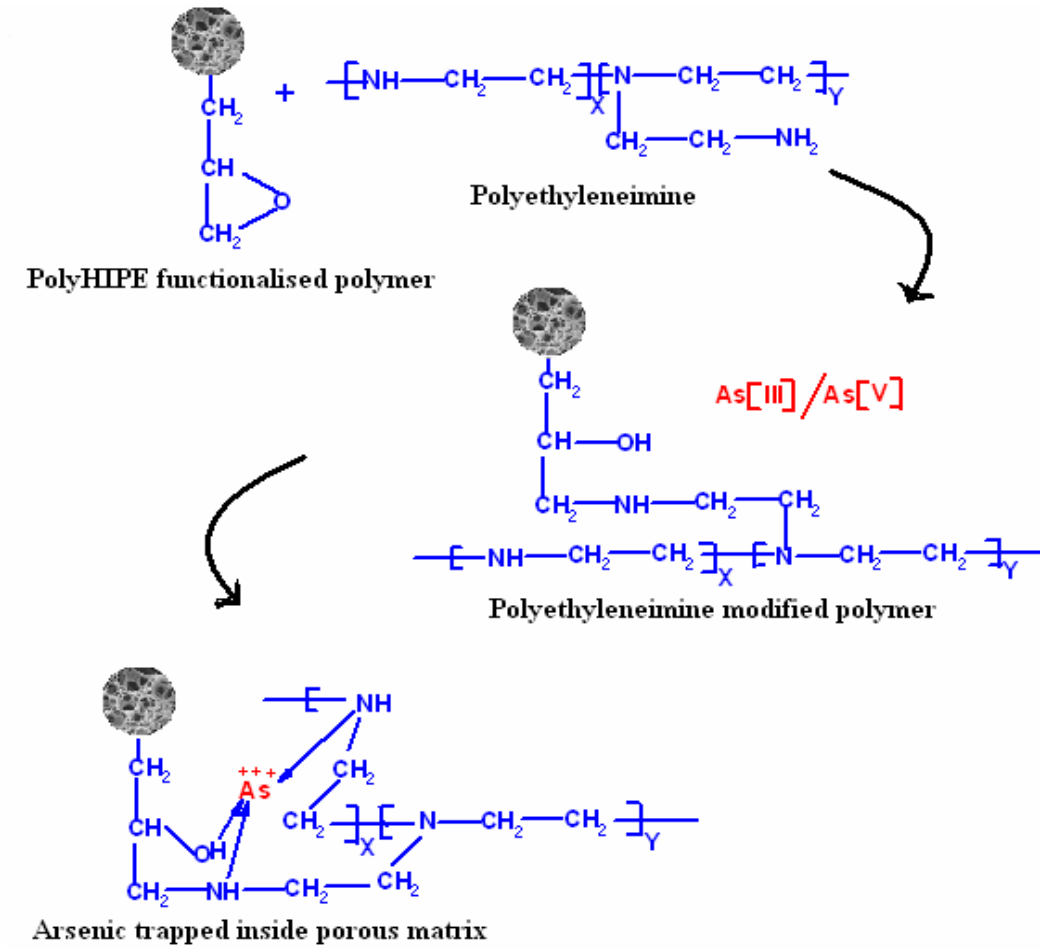

Figure 5.2. Probable mechanism of arsenic adsorption on PEI functionalised polyHIPEs

In sorption experiments, measured amount of the PEI derivatised poly(GMA-EGDM) and poly(AGE-EGDM) were vigorously shaken with definite volumes of arsenate and arsenite solution of known concentration (1 ppm) in tightly stoppered plastic bottles for 24 hours at room temperature. The equilibrium sorption was calculated from

residual concentration of sorbate in the equilibrated solution. A range of concentrations was employed for both arsenate and arsenite. The sorption was also measured as a function of time and pH under vigorous agitation. Probable mechanism of arsenic binding using polyHIPE materials is shown in Figure 5.2.

5.2.5 Analytical method

The residual arsenic in water sample was determined using molybdenum blue method.[49] The method was used to estimate As (III) and As (V) concentrations in treated water samples to assess the efficiency of the oxidation step and the subsequent removal of arsenic.

5.2.5.1 Molybdenum blue methodology

Mixed reagent*:* 125 mL of 5N sulphuric acid and 37.5 mL of 0.032 M ammonium molybdate [$(NH_4)_6$ $Mo_7O_{24}.H_2O$] solution were mixed thoroughly. Then, 75 mL of 0.1M ascorbic acid [$C_6H_8O_6$] (freshly prepared) and 12.5 mL potassium antimony tartarate [$K(SbO)C_4H_4O_6.4H_2O$] solution were added successively with thorough mixing after each addition. This reagent was prepared fresh when required.

The method allows for the routine analysis of As (III), As (V) and phosphate by spectroscopic measurement of arsenic and phosphate-molybdenum complexes.[49] Since water used in the experiment contained no, or negligible amount of phosphate, the method was modified for determination of As (III) and As (V). The mixed reagent added to an untreated aliquot of the sample produces a blue colour due to the formation of arsenomolybdate complex from any As (V) present. As (III) does not form the complex. Therefore, the intensity of the colour formed and hence the absorbance of untreated

aliquot is proportional to the As (V) concentration. Potasssium iodate is used as the oxidising agent to convert As (III) to As (V), and hence the absorbance of an oxidised aliquot of the sample is proportional to the total arsenic concentration. As (III) is then calculated as the difference between the total arsenic concentrations and As (V).

In the procedure, two sets of concentrations starting from 5 - 2000 μg/L of arsenite or arsenate were prepared from the standard solutions. One set was for oxidised aliquot and other was for untreated one. One mL of 1N HCl and two drops of a 50% saturated solution of potassium iodate were added successively to each of the oxidised aliquots with thorough mixing after each addition. Fifteen minutes were allowed for oxidation of As (III) to As (V). Thereafter, 4 mL of mixed reagent were added to each of the oxidised and untreated aliquots with thorough mixing. Then, flasks were placed for 2 hours for development of the blue colour, following which the absorbance was read in a 10 mm cell at 865 nm. Suitable blanks were run, by the above procedure, along with the samples. All samples were analysed in duplicate.

The standard curve for As III concentration Vs absorbance is shown in Figure 5.3. While, Figure 5.4 shows the standard curve for concentration of As (V) Vs absorbance.These standard calibration curve were plotted by taking each reading three times using UV-visible spectrophotometer at 865 nm . The As(III) and As(V) synthetic standard solutions were prepared freshly each times before the analysis.

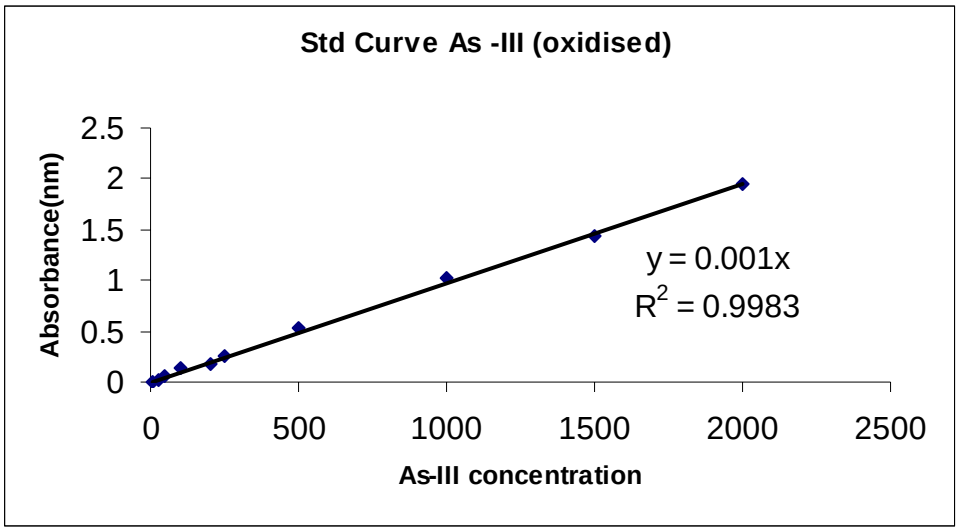

Figure 5.3. Standard curve for arsenic (III)

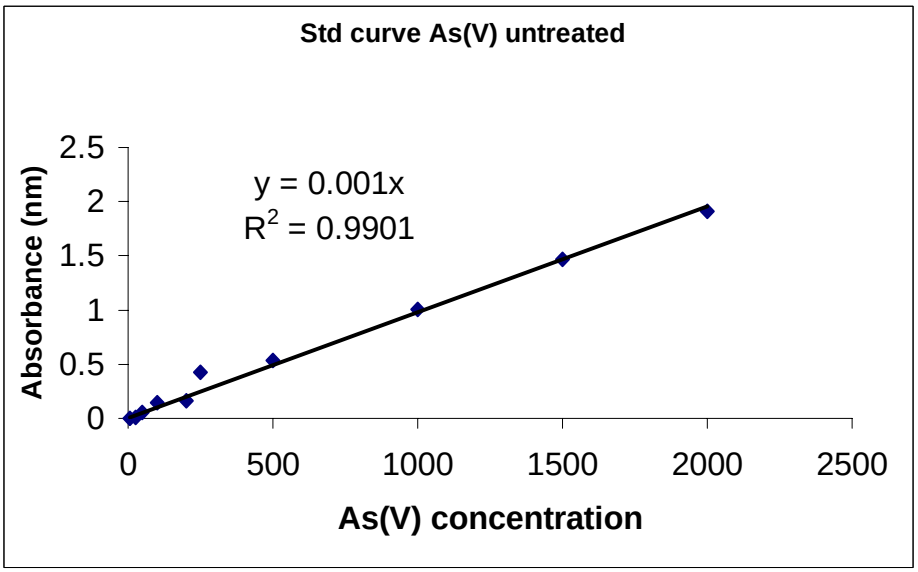

Figure 5.4. Standard curve for arsenic (V)

5.3 Evaluation and characterisation of poly(HIPE) beads

5.3.1 Elemental analysis

For the determination of extent of PEI covalently attached to poly(GMA-EGDM) and poly(AGE-EGDM) beads, carbon, hydrogen and nitrogen content of derivatised

beads were determined by an elemental analyser (CHNS-O, EA 1108-elemental analyser, Carlo Erba Instruments). The amount of PEI attached to the beads was determined from the percentage of nitrogen content. A JEOL model JSM-5200 SEM, UK equipped with X-ray (EDX) detector was used to image the PEI modified HIPE material and qualitatively determine the potential localisation of arsenic (Figure 5.22).

5.3.2 Fourier transform infra-red analysis

FTIR of copolymers and PEI modified polymers were obtained (JASCO FTIR 4000, Japan). Samples were prepared by mixing 1 mg with 100 mg potassium bromide pelletised and placed in the sample holder. The spectra were scanned over the range 4000-450 cm^{-1} at ambient temperature.

5.3.3 Surface topography

Specimens were prepared as presented in section 3.3.2. Micrographs of the beads were observed using scanning electron microscope, JEOL JSM-5200, UK, operated at an acceleration voltage of 10 kV.

5.3.4 Porosity measurement

The surface area of the polymers were measured using the single point Brauner-Emmett-Teller method by measuring the adsorption of nitrogen at liquid nitrogen temperature, using a monosorb surface area analyser (Quantachrome Corp., U.S.A.), based on dynamic adsorption/desorption technique. Before carrying out the surface area measurements, the instrument (analyser) was calibrated by injecting a known amount of air. The polymer (0.2-1.5 g) was pretreated *in situ* in the sample cell at 100^{o}C for 3 hour in the flow (30 cm^3 min^{-1}) of moisture free nitrogen in order to remove traces of moisture.

The pore volume was determined by mercury intrusion porosimeter in the pressure range 0-4000 kg/cm^2 with an Autoscan 33 mercury porosimeter from Quantachrome, USA.

5.3.5 Particle size analysis

Single particle optical sensing (SPOS) AccuSizer 780 was used to determine the particle size of copolymer beads. Details were presented in Section 3.3.1.

5.3.6 Surface epoxy content

The surface epoxy groups were analysed titrimetrically using hydrochloric acid – dioxane reagent.[50] The method is based on addition of hydrogen chloride to the epoxide, which results in formation of chlorohydrin. The difference between the amount of acid added and the amount unconsumed, as determined by titration with the standard base, is a measure of epoxide content at the pore surface. The typical procedure for the titration is as follows:

To the appropriate weight (0.5 g) of the porous polymer sample, 25 mL of purified dioxane and 25 mL of 0.2 N hydrochloric acid-dioxane solutions were added. It was kept in dark for 15 minutes. To this 25 mL of neutral cresol red indicator was added and excess of acid was titrated against 0.1N methanolic potassium hydroxide (KOH). The end point was appearance of first violet colouration.

$$\text{Epoxy content} = (B-S)\ N/\ 10\ W \qquad \textbf{5.1}$$

Where, B = Blank reading, S = main sample reading, W= weight of sample, N= normality of methanolic KOH solution.

5.4 Results and discussion

5.4.1 Pore volume, particle size distribution and surface area

Typical pore volume and surface area data of spherical, beaded poly(GMA-EGDM) and poly(AGE-EGDM) synthesised by high internal phase emulsified (W/O/W) suspension method is presented in Tables 5.3 and 5.4, respectively. In both sets, beads were in the range 0.5-200 μm. Poly(GMA-EGDM) beads were synthesised by HIPE polymerisation to generate spherical beads in the size range 2-100 micron where as poly(AGE-EGDM) beads obtained were in the range 0.5-150 micron, as shown in Figure 5.5. Particle size distribution of poly(GMA-EGDM), as well as poly(AGE-EGDM) beads with differing cross-linked densities, as determined by particle size analyser, are presented in Figures 5.6, 5.7, 5.8 and 5.9.

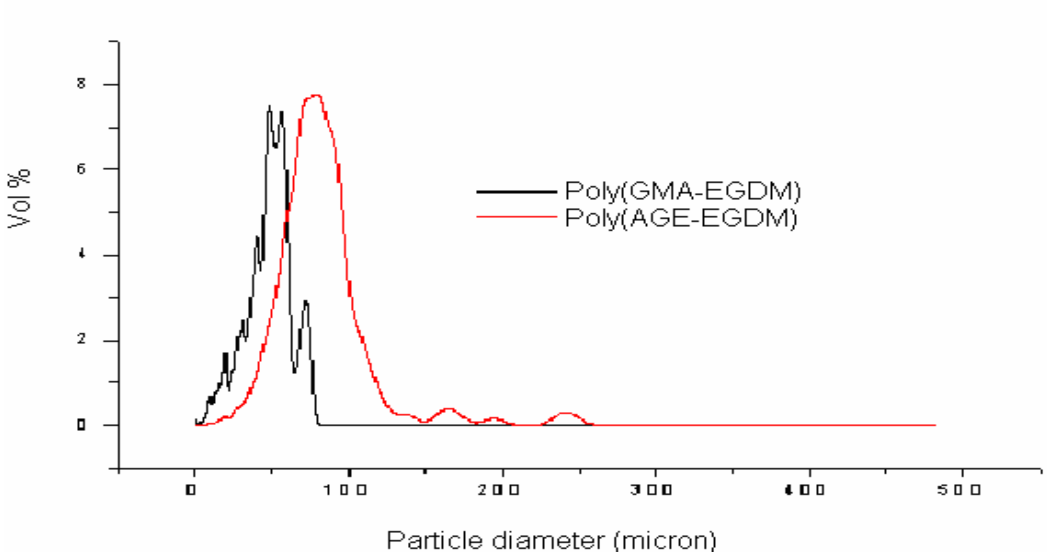

Figure 5.5. Comparative plot of poly(GMA-EGDM) and poly(AGE-EGDM) polyHIPE showing particle size distribution

From the figures it is clear that the majority of the beads lie in the range 0.5 to 100 microns. This is a narrower particle size distribution as compared to suspension polymerisation where one generally ends up with large beads having a wider particle size distribution (10-2000 micron) at the same stirring rate. The reason for this lies in HIPE

methodology. Unlike suspension polymerisation, the particle size in HIPE is determined by the initial rate of stirring. In our method we have used *quasi-dynamic* emulsion polymerisation. Here, the polymerisation proceeds in confined droplets, which are already formed at the beginning. Stirring speeds determine the particle size.

It is established that an increase in agitation speed causes a reduction of droplet size formed. The droplet size formed is primarily governed by its growth time prior to detachment, which is effectively reduced at higher shear stress as a result of higher agitation speeds. This indicates that smaller droplets are produced at higher stirring rates. Here, the beads were synthesised at fairly high shear rates so the particle size is low and distribution is narrow. Particle size distribution of poly(GMA-EGDM) at 5% CLD is shown in Figure 5.6 and the inset SEM photograph shows the spherical nature of polymers synthesised. The particle dimensions were in the range 5-400 microns. Particle size distribution observed was quite broad at low cross-link density (5% CLD) as compared to the high cross-link density (25% CLD). Figure 5.7 shows the narrow particle size distribution, in the range of 5-150 microns, of poly(GMA-EGDM) at 25 %.

Poly(AGE-EGDM) shows quite narrow particle size distribution (PSD) between 5-100 microns. Figure 5.8 shows the PSD of poly(AGE-EGDM) at 5% CLD as well as Figure 5.9 shows the PSD of poly(AGE-EGDM) at 25% CLD.

PolyHIPE materials have relatively high surface area as shown in Tables 5.3 and 5.4 of the order of 10-100 m^2/g. HIPE polymerisation completes in aqueous phase forming cross-linked polymer in which the water droplets are trapped. The average diameter of these water droplets is about 2-50 μm and therefore the surface area of polyHIPE beads is relatively lower than theoretically possible (1100 m^2/g). It also varies

with the cross-link density. The resulting beads have 'dual porosity'-large voids characteristic of polyHIPE materials, and much smaller pore, which can be in the micro and mesopore size range, resulting from phase separation of the polymer network from solution during polymerisation. In poly(GMA-EGDM) system the surface areas at all compositions were comparable and varied only within 70±15 m^2/g. After PEI binding the surface area was observed to decrease, because of surface coverage of PEI. The methodology generated moderate pore volumes suitable for arsenic binding. On the basis of surface area and mmoles/g of PEI, four copolymers GEH 5, GEH 25, AEH 5 and AEH 25 were evaluated further for arsenic binding.

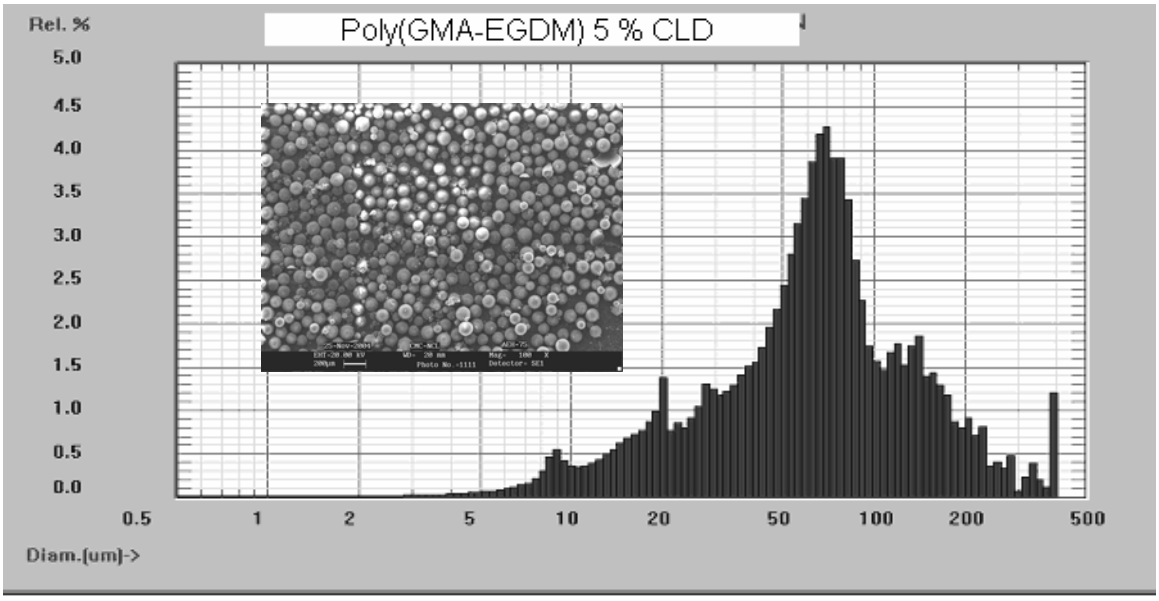

Figure 5.6. SEM photograph at 100X and particle size distribution (PSD) of poly(GMA-EGDM) beads with 5% cross-linked density synthesised by HIPE method.

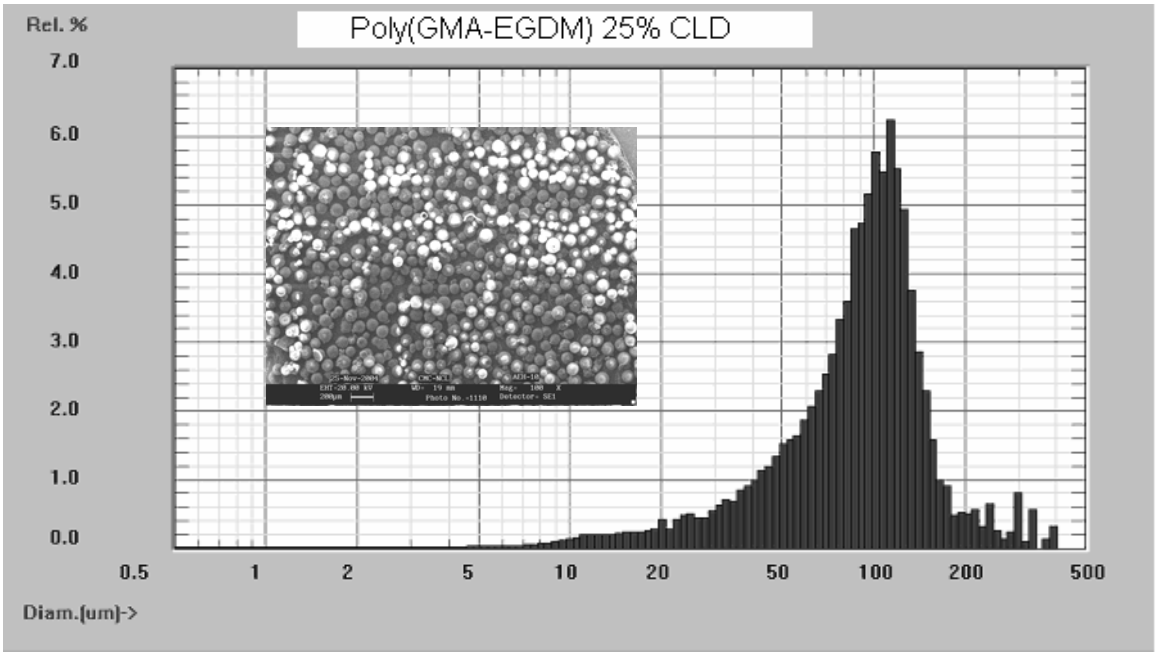

Figure 5.7. Particle size distribution (PSD) of poly(GMA-EGDM) beads with 25% cross-linked density synthesised by HIPE method

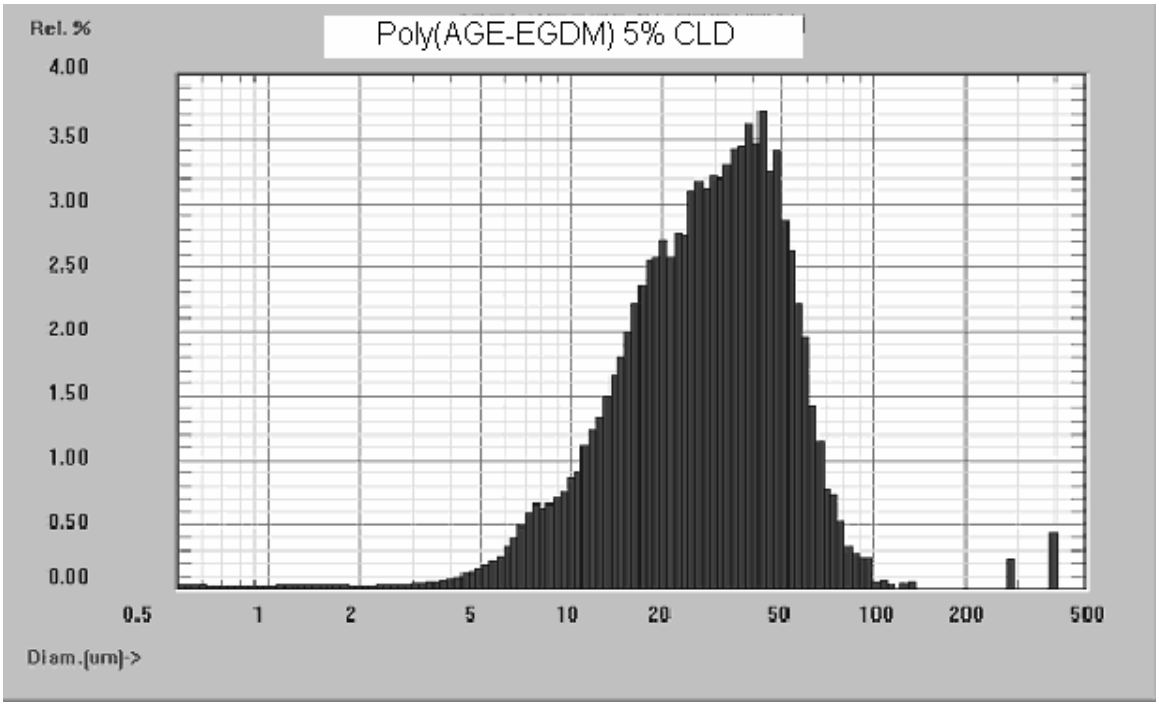

Figure 5.8. Particle size distribution (PSD) of poly(AGE-EGDM) beads with 5% cross-linked density synthesised by HIPE method

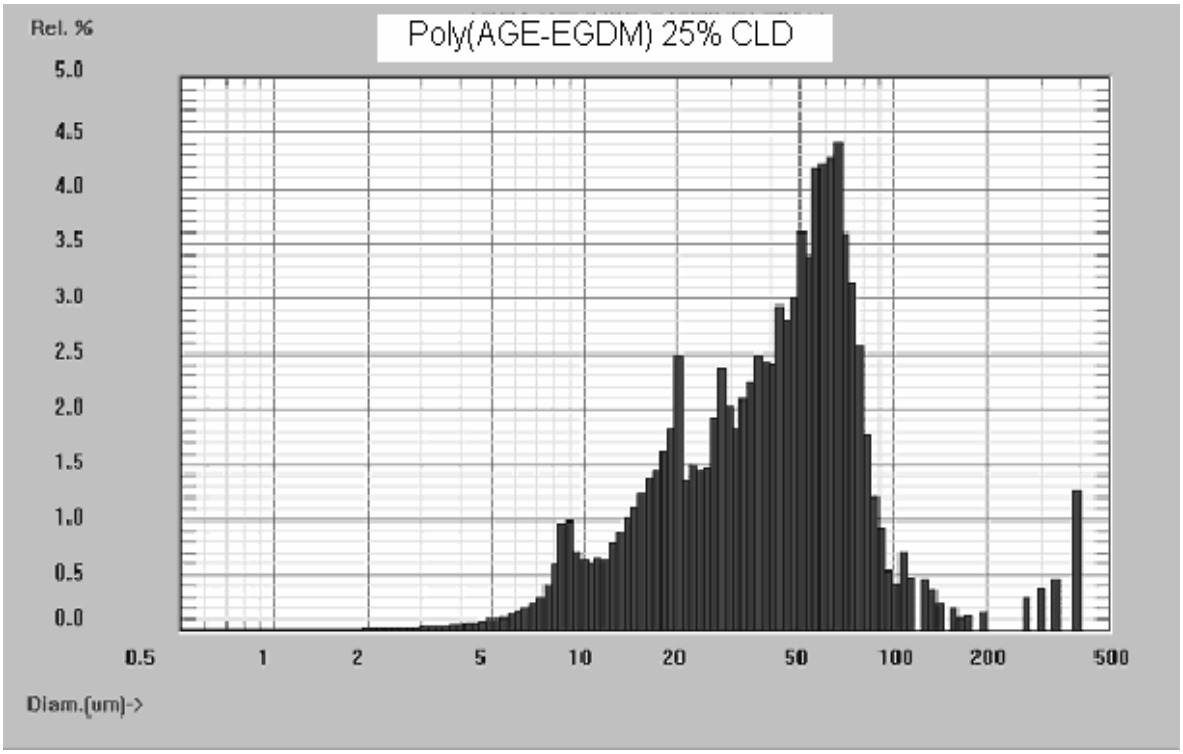

Figure 5.9. Particle size distribution (PSD) of poly(AGE-EGDM) beads with 25% cross-linked density synthesised by HIPE method

5.4.2 Control of morphology and properties

5.4.2.1 Cellular structure

PolyHIPE material can be either close or open celled. In the former, thin monomer films surrounding adjacent emulsion droplets form intact polymer membranes, trapping the contents of the droplets within the matrix. The inner aqueous phase therefore cannot be removed easily from the beads, which is consequently of a high density. The latter materials, however, have an open and interconnected structure in which each void is connected to some or all of its neighbours. As a result, these are highly permeable and exhibit relatively low density, which is largely determined by the internal phase volume fraction of the HIPE precursor.

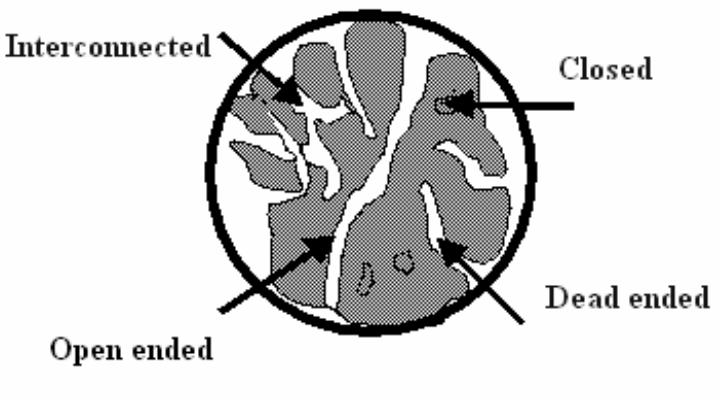

Figure 5.10. Schematic diagram of porous bead showing that types of pores formed depend on the surfactant concentration

Cellular structure was largely insensitive to the ratio of aqueous to oil phases but was affected to a very large degree by the amount of surfactant in the organic phase, as shown in Figure 5.10. Closed cell materials were formed at low (< 5 Wt% relative to oil phase) surfactant concentration. Interconnecting holes ([Surfactant] =5 wt% relative to oil phase) are produced by shrinkage occurring during cure. The influence of surfactant concentration on this process is likely to relate to its effect on the films separating emulsion droplets. At higher surfactant concentration, the films become thinner, thus shrinkage during curing results in the production of interconnects between voids.

5.4.2.2 Microscopic study

The polyHIPE methodology provided cross-linked poly(GMA-EGDM) and poly(AGE-EGDM) beads in the spherical form (2-20 μm in diameter). It is seen in Figure 5.11(a) that in primary emulsion, only two phases are present in which water droplets are in discontinuous phase and monomers are in continuous. This W/O primary emulsion gets converted into W/O/W phase when added into bulk water phase provided with protective colloid. This decreases the interfacial surface tension between the two

droplets. Figure 5.11(b) shows W/O/W emulsion in which tiny water droplets are trapped in the monomer droplets due to non-ionic surfactant, which are responsible for the formation of interconnected pores in HIPE matrices.

The microporous poly(GMA-EGDM) and poly(AGE-EGDM) beads may be visualised as cross-linked hydrogel. They do not dissolve in aqueous medium, but do swell, and the degree of swelling decreases with increase in cross-link density (i.e., percent EGDM). The dry beads are opaque (white), which is due to scattering and is an indication of the porosity in the matrix, as a result of the pore generating solvent (i.e., water) used in the polymerisation. However, the opacity of the beads is significantly decreased when the beads are swollen in water. Figure 5.12 depicts the spherical nature of the HIPE copolymers. Unlike suspension polymerisation, particle size distribution in HIPE method is narrower as seen in Figures 5.12 (a) and (b) for poly(GMA-EGDM) and Figures 5.12 (b) and (d) for poly(AGE-EGDM) at different magnifications.

Figures 5.13 and 5.14 show SEM micrographs of poly(AGE-EGDM) and poly(GMA-EGDM), respectively. Figures 5.13 (a) and 5.14 (a) show spherical and uniform nature of poly(HIPE). SEM of poly(HIPE) in Figures 5.13 (d) and 5.14 (d) clearly show a significant number of pore openings at the external surface reflecting their porous nature. The spherical form and porous nature of the poly(HIPE) microsphere favour better PEI binding because a number of epoxy group are available to react with PEI.

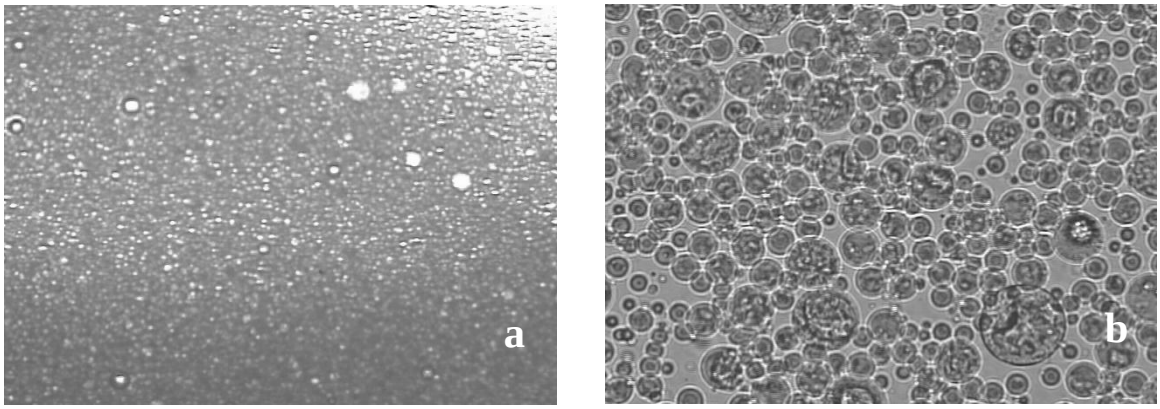

Figure 5.11. Optical micrographs of poly(HIPE) emulsions (a) W/O primary emulsion of HIPE system at 100X (b) W/O/W emulsion of HIPE system at 500X

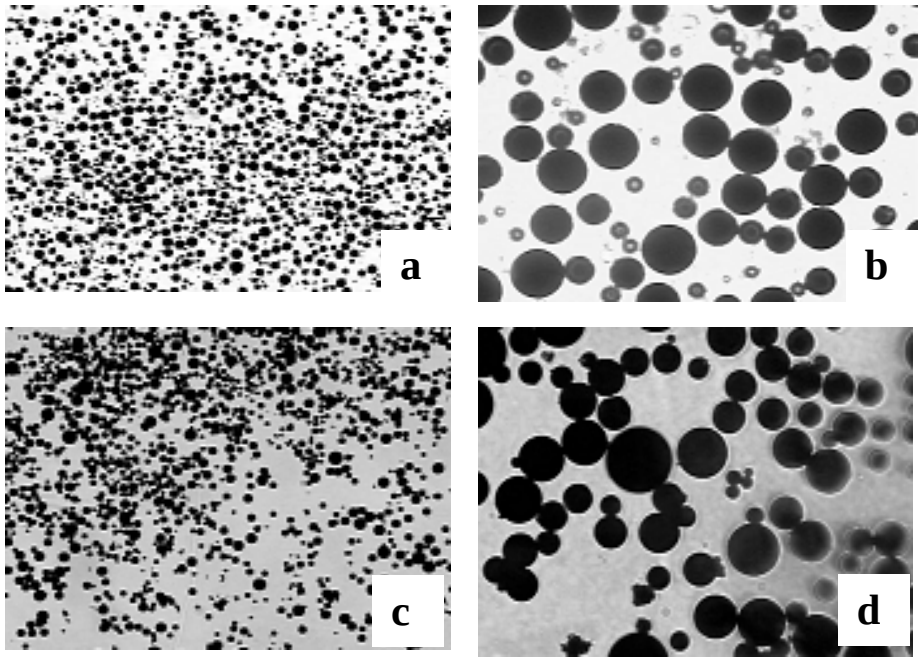

Figure 5.12. Optical Micrographs of (a and b) poly(GMA-EGDM) and (c and d) poly(AGE-EGDM) beads synthesised by HIPE methodology at 100X and 500X, respectively

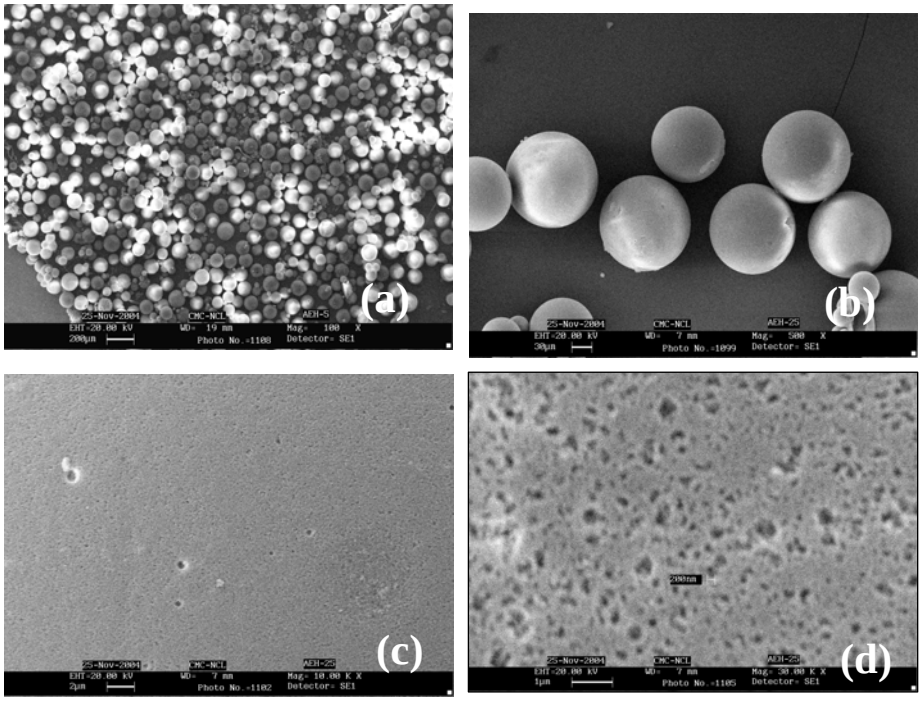

Figure 5.13. SEM micrograph of poly(AGE-EGDM) beads synthesised by HIPE at: a) 100X, b) 500X, c) 10000X and d) 30000X

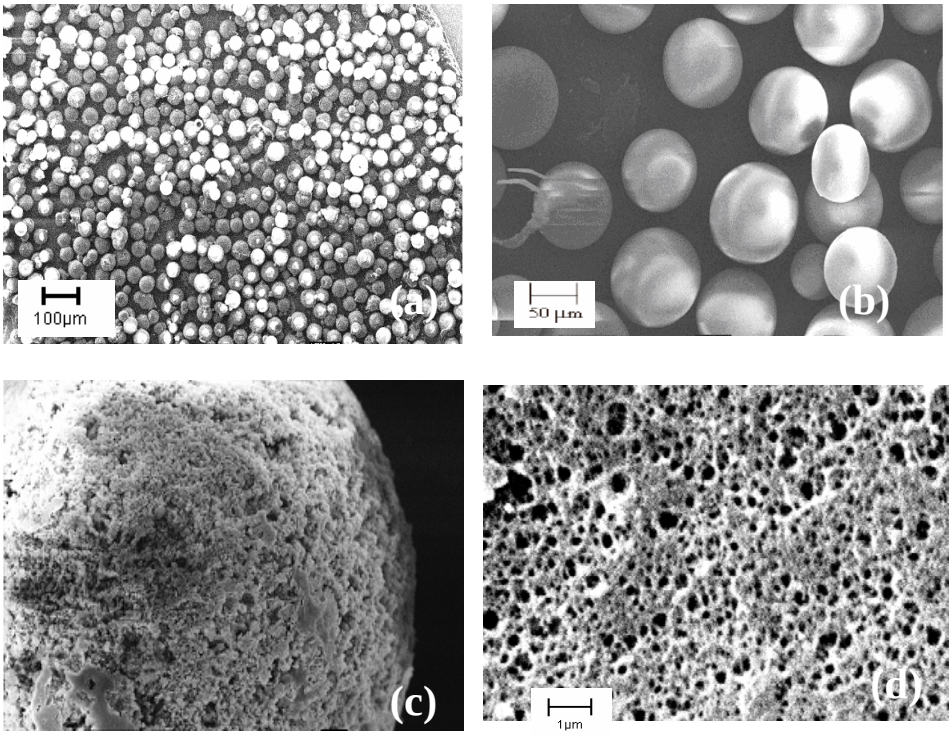

Figure 5.14. SEM micrographs of poly(GMA-EGDM) beads synthesised by HIPE at : a) 100X, b) 500X, c) 10000X and d) 30000X.

5.4.3 Surface epoxy content

The wet reactive epoxy titration gives an estimate of the available surface epoxy groups. The surface state of the prepared copolymer beads is controlled by the surface tension between the dispersed phase and the continuous phase. The surface tension of GMA and EGDM in contact with the water is approximately 6.9 and 33.1 dynes/cm. Therefore, GMA molecules will tend to migrate towards the surface of droplets.

However, in actually, the observed epoxy content is much lesser than the theoretical value because the concentration of epoxy groups present at or near the surface, which react with the hydrochloric acid, is rather low. The polymerisation condition (pH=7) did not open up epoxy groups. In case there were opened up, FTIR would have revealed their presence at 993 cm^{-1}. It is clear that majority of epoxy groups are buried in the matrix and are unable to react with hydrochloric acid under analytical conditions. Figure 5.15 represents the theoretical and analysed surface epoxy groups in poly(GMA-EGDM) relative to cross-link density at a monomer to water ratio of 1:3. This shows that surface tension issues are negated by other forces, which direct most epoxy groups away from the surface and available for reaction with amine functionality of PEI. More the surface epoxy groups available after the polymerization more is the binding of PEI on the poly(GMA-EGDM) and poly(AGE-EGDM) copolymer matrix.

Figure 5.15 shows theoretical and observed epoxy values of poly(GMA-EGDM) copolymers at different crosslink densities. There is drastic decrease observed epoxy values as compared to the theoretical epoxy values.

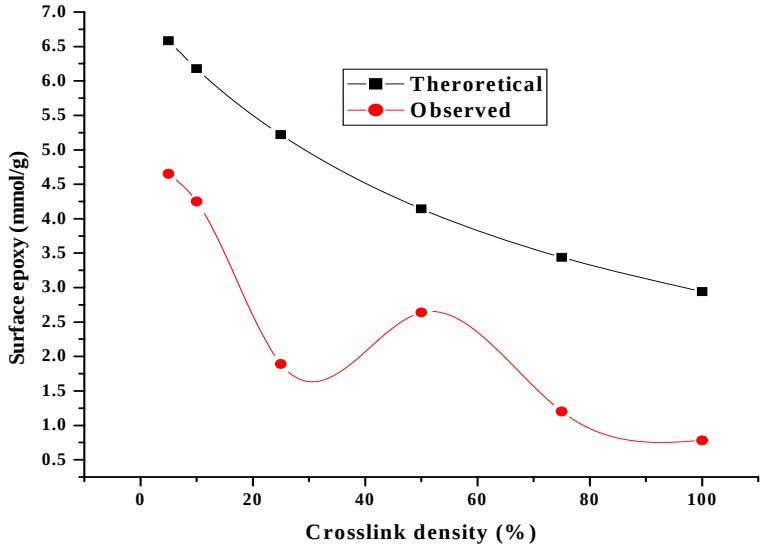

Figure 5.15. Surface epoxy group content of poly(GMA-EGDM) synthesised by high internal phase emulsion (HIPE)

The theoretical epoxy content decreases with GMA content in the copolymer, from 8.10 mmol/g at 5 % cross-link density to 3.20 mmol/g at 100 % cross-link density. The titratable epoxy groups (Figure 5.15) decreases from 6.23 mmol/g at 5 % cross-link density to 3.43 mmol/g at 100% cross-link density. Thus 20 times decrease in copolymer composition reduces the surface epoxy group concentration by only 2.5 times. This is due to greater porosity and larger surface area with increasing CLD, which exposes relatively higher concentration of epoxy functionality at the surface.

The theoretical epoxy content in poly(AGE-EGDM) studied here varies from 6.58 to 2.93 mmol/g (from 05 to 100% cross-link density) (Figure 5.16). The experimentally observed epoxy content by titration was in the range 4.65 to 0.78 mmol/g (05 to 100% cross-link density). Thus, only a fraction the epoxy groups in poly(AGE-EGDM) beads react with hydrochloric acid, just as observed with poly(GMA-EGDM) series at higher

cross-link density. A major fraction of the epoxy group in the beads is buried and is unable to react under analytical condition.

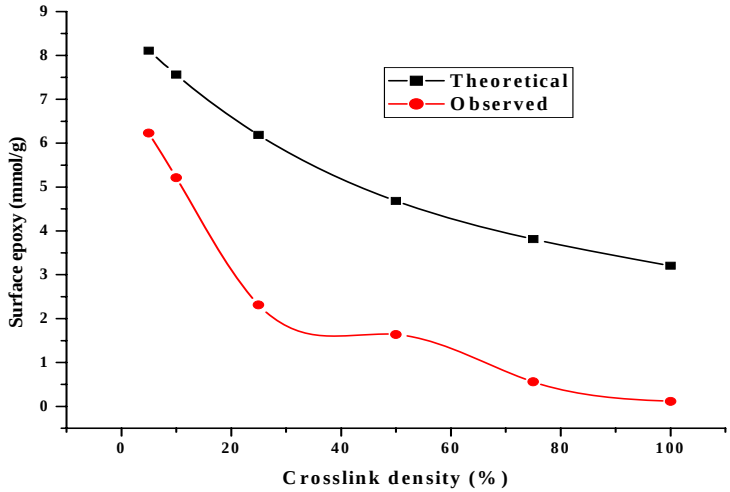

Figure 5.16. Surface epoxy groups of poly(AGE-EGDM) synthesised by high internal phase emulsion (HIPE)

In HIPE there is large amount of water is dispersed in the continuous monomer phase. Therefore, while stabilising the water droplets in the monomer phase large amount of epoxy groups avoid coming to the interface of oil and water, rather they remain in the oil (monomer) phase and are buried in the matrix of polymers.

5.4. 4 PEI-attachment onto poly(HIPE) beads

After the polyethylenimine (PEI) derivatisation, the colour of the beads change, a clear indication of the attachment of the polyethylenimine into the copolymer structure. It should be noted that these beads are quite rigid and strong, due to very high cross-link density.Polyethylenimine is a highly branched polymer with 50 %, 25 % and 25 % of secondary, primary and tertiary amino groups, respectively.

Polyethylenimine was covalently attached to the microbeads via nucleophilic addition between epoxy groups of poly(GMA-EGDM), poly(AGE-EGDM) and primary

amino group of polyethylenimine, under basic condition (pH=10.6). The PEI attachment to the poly(GMA-EGDM) beads, confirmed by elemental analysis of the PEI derivatised poly(GMA-EGDM) and poly(AGE-EGDM), are presented in Tables 5.3 and 5.4.

The covalent attachment of PEI on to the poly(GMA-EGDM) bead was also determined by the potentiometric titration of a sample withdrawn from the medium after the adsorption, with 0.1 M standard hydrochloric acid solution, as shown in Figure 5.17 and by nitrogen content by SEM-EDAX method shown in Figure 5.18. The amounts of polyethylenimine attached to the micro beads were in the range 47-79 %.

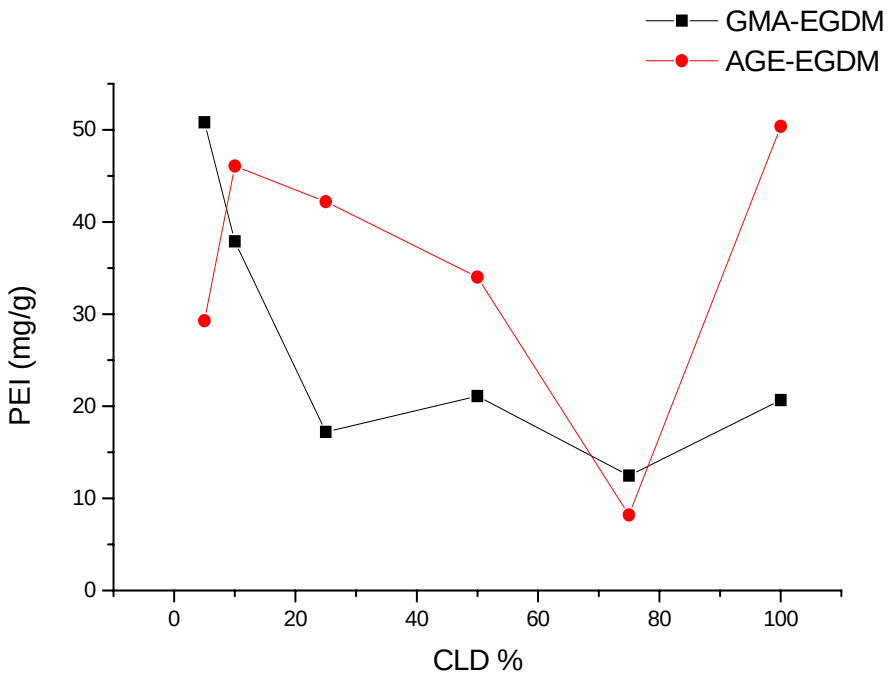

Figure 5.17. PEI binding on Poly(GMA-EGDM) and Poly(AGE-EGDM) co-polymeric beads synthesised by HIPE technique (Wet analysis)

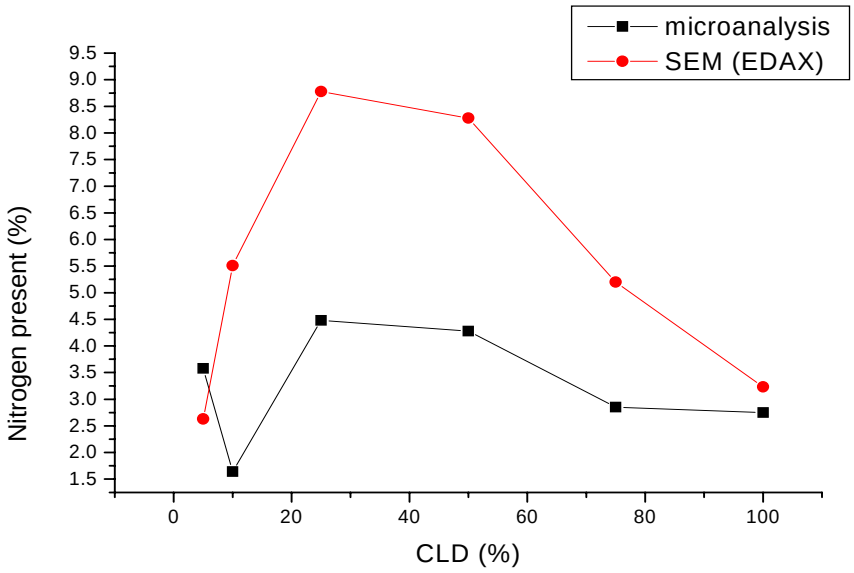

Figure 5.18. Nitrogen content of poly(AGE-EGDM) copolymer matrix by microanalysis and SEM (EDAX) analysis

It is seen in Tables 5.3 and 5.4 that as the cross-link density increases, the percentage of PEI attached to poly(GMA-EGDM) and poly(AGE-EGDM) beads decreases, due to decrease in epoxy content. Leaching of polyethyleneimine during metal ion adsorption experiment was also evaluated. For this purpose, metal ion solution was kept in a plastic vial containing PEI derivatised poly(GMA-EGDM) beads. The metal ion solution was filtered and filtrate was collected for elemental analysis. No leaching however, was observed. This was confirmed by absence of nitrogen content in filtrate after adsorption of metal ion solution onto to the PEI derivatised poly(GMA-EGDM) beads. This shows that washing procedure was sufficient to remove physically adsorbed PEI molecules from the polymer matrix.

Table 5.3. Pore volume, surface area, elemental and wet analysis data of poly(GMA-EGDM)

Sr. No	Polymer Code	CLD %	Intruded Volume (cm^3/g)	Surface area (BET) (m^2/g)	N_2 present (%) (Elemental analysis)	PEI binding mmole/g (Wet analysis)	PEI binding (mg/g of Polymer)
1	GEH-01	05	0.71	68.45	0.54	1.18	50.81
2	GEH-02	10	0.29	51.23	1.79	0.88	37.89
3	GEH-03	25	0.69	80.37	2.59	0.40	17.22
4	GEH-04	50	0.68	54.68	1.25	0.49	21.10
5	GEH-05	75	0.72	72.54	0.98	0.29	12.48
6	GEH-06	100	0.60	64.12	0.32	0.48	20.67

Table 5. 4. Pore volume, surface area, elemental and wet analysis data of poly(AGE-EGDM)

Sr. No	Polymer Code	CLD %	Intruded Volume (mL/g) Volume	Surface Area (BET) (m^2/g)	N_2 present (%) (Elemental analysis)	PEI binding mmole/g (Wet analysis)	PEI binding (mg/g of Polymer)
1	AEH-01	05	0.81	65.13	3.58	0.68	29.28
2	AEH-02	10	0.56	57.34	1.64	1.07	46.09
3	AEH-03	25	0.99	66.71	4.48	0.98	42.20
4	AEH-04	50	0.60	55.32	4.28	0.79	34.03
5	AEH-05	75	0.63	59.31	2.85	0.19	08.19
6	AEH-06	100	0.52	70.64	2.75	1.17	50.38

Figure 5.19 shows the FTIR of GMA-EGDM mixed monomer mixture composition corresponding to 25 % cross-link density. Vinyl double bond peak is observed at 1600 cm^{-1}, which disappears after polymerisation (Figure 5.20). The interaction between polyethylenimine and poly(GMA-EGDM) was investigated by FTIR. Spectra of underivatised poly(GMA-EGDM) (Figure 5.20) and PEI derivatised poly(GMA-EGDM) (Figure 5.21) are presented. FTIR spectra of poly(GMA-EGDM) shows peaks at 1730 and 993 cm^{-1} due to stretching vibrations of C=O of ester group and C-O-C of epoxy group, respectively.

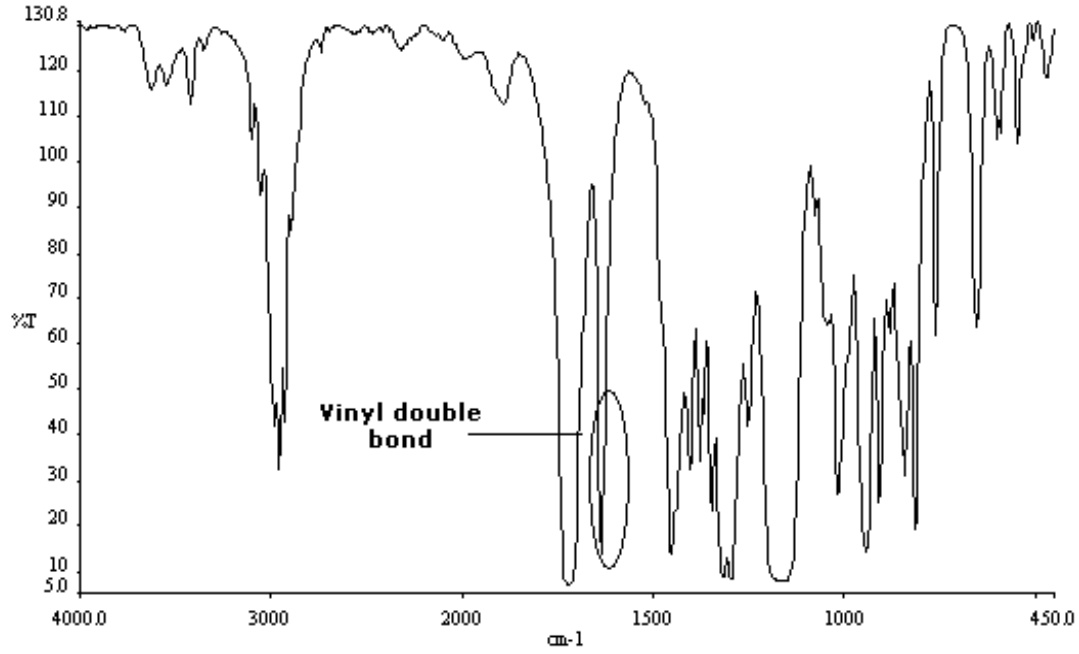

Figure 5.19. FTIR of GMA-EGDM monomer mixture corresponding to 25% cross-link density

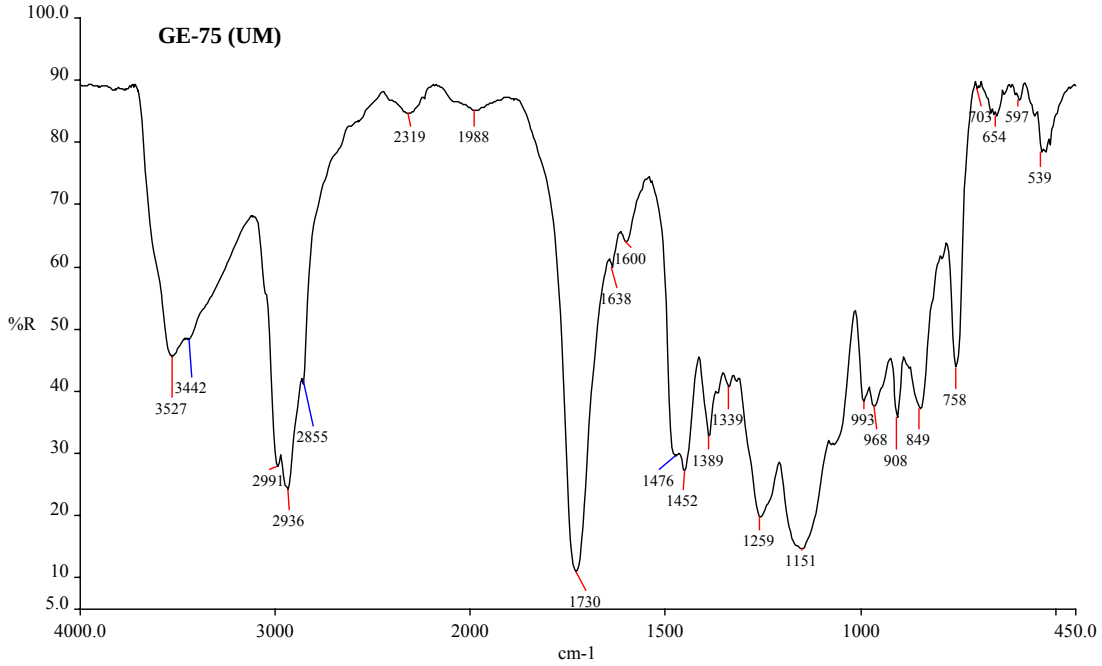

Figure 5.20. FTIR of unmodified poly(GMA-EGDM) of 25% cross-link density

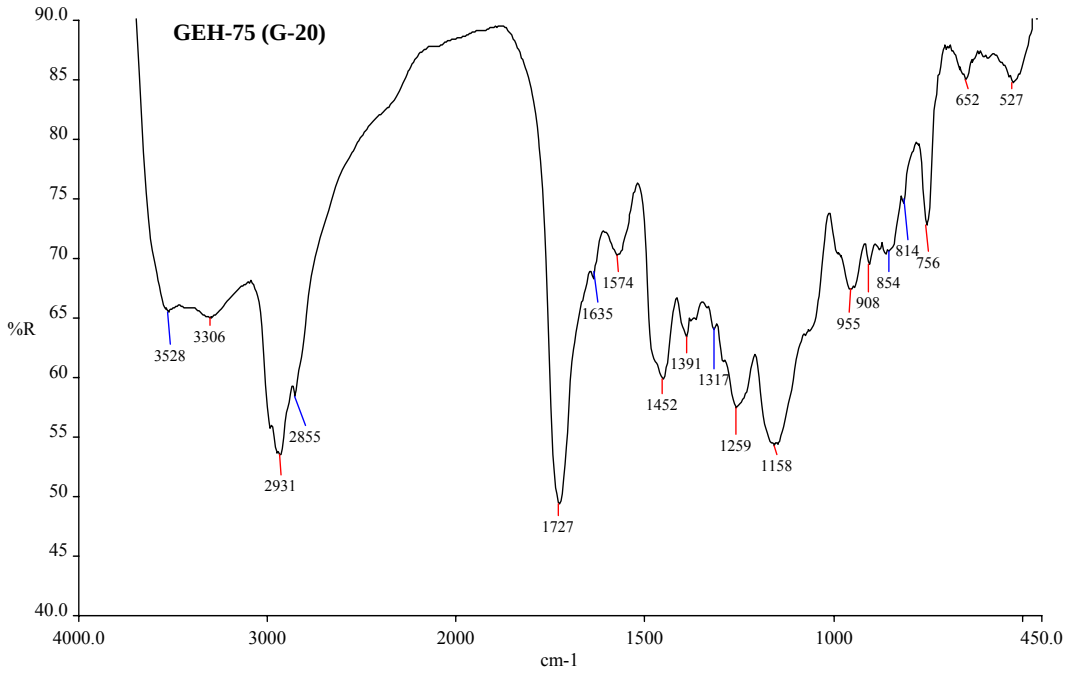

Figure 5.21. FTIR of modified poly(GMA-EGDM) of 25% cross-link density copolymer modified with polyethyleneimine

The band at 993 cm^{-1}, due to stretching vibration of C-O-C of epoxy group, disappears in PEI modified poly(GMA-EGDM), due to reaction of epoxy group of poly(GMA-EGDM) with primary amino group of polyethylenimine (PEI) and peak at around 3450 cm^{-1}, due to stretching vibration of NH, OH, were observed in PEI derivatised poly(GMA-EGDM). The presence of peak at 3527 cm^{-1} indicates the formation of -OH group after the reaction of polyethylenimine with poly(GMA-EGDM). The peak at 3306 cm^{-1} indicates the stretching vibration of -NH group.

5.4.5 Adsorption kinetics

The adsorption kinetic properties of the As (III) and As (V) ions by the PEI-chelating poly(HIPE) beads are important for assessment of the suitability of this polymeric material to serve as adsorbent in a through-flow column. Figure 5.22 clearly shows the bound arsenic on the PEI modified poly(HIPE) beads.

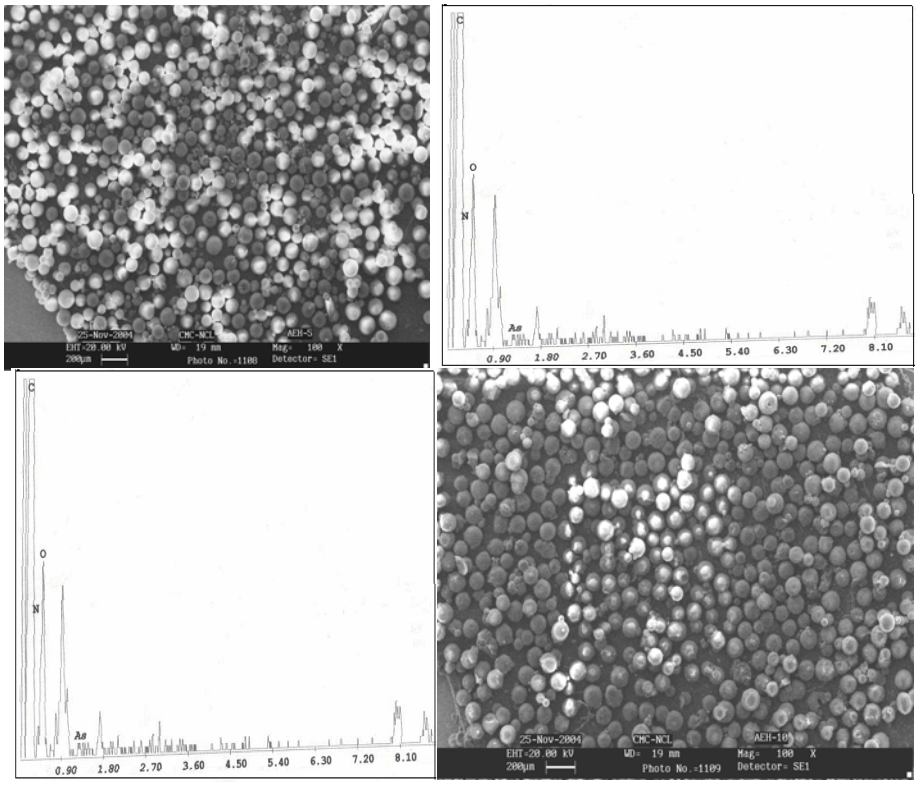

Figure 5.22. SEM-EDX spot analysis of PEI modified poly(AGE-EGDM) beads confirming presence of arsenic

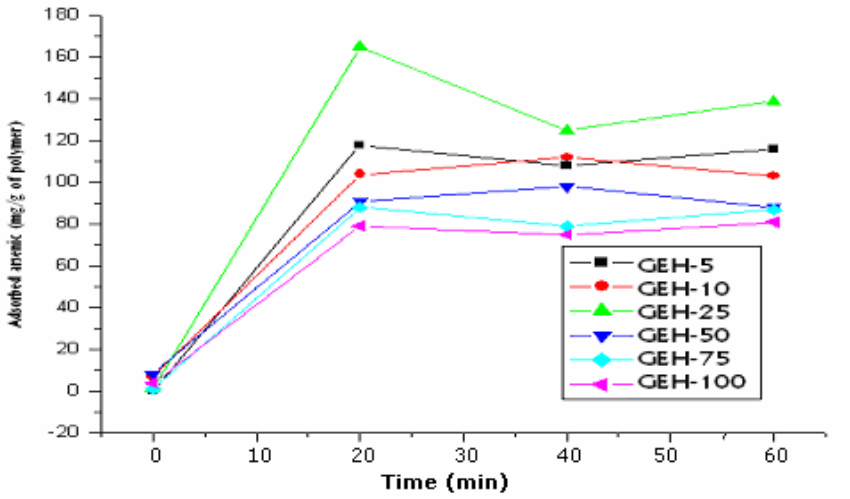

Figure 5.23. As (V) binding at different time interval on PEI modified poly(GMA-EGDM)

Figure 5.23 shows the adsorption rates of arsenic with time on the different PEI modified poly(HIPE) GMA-EGDM beads having different cross-link densities from the

aqueous solution containing different amounts of As (III) and (V) (in the range of 5-2000 μg/L) at constant pH of 6.0. As shown in Figure 5.23, arsenic adsorption capacity increases with time during the first 20 minutes and then levels off toward the equilibrium adsorption of arsenic.

5.4.5.1 Effect of pH on arsenic adsorption capacity

The adsorption of heavy metal ions by resins is strongly dependent on pH. Because of the protonation and deprotonation of the acidic and basic groups of the metal complexation ligand, its adsorption behaviour for metal ions is influenced by the pH, which affects the surface structure of sorbents and the interaction between sorbents and metal ions.

The dissociation reaction and the corresponding dissociation constants of H_3AsO_4 at 24°C, in mol/L, are [51]:

$$H_3AsO_{4\,(aq.)} \Leftrightarrow H^+ + H_2AsO_4^- : K_1 = 5.98 \times 10^{-3} \quad \textbf{5.2}$$

$$H_2AsO_4^- \Leftrightarrow H^+ + HAsO_4^{2-} : K_2 = 5.98 \times 10^{-7} \quad \textbf{5.3}$$

$$HAsO_4^{2-} \Leftrightarrow H^+ + AsO_4^{3-} : K_3 = 3.98 \times 10^{-12} \quad \textbf{5.4}$$

The equilibrium concentration of the different As (V) species at different pHs, as given in Figure 5.24, are calculated from the above K_i values at 24°C. At pH 1.0, for example, the arsenate molecule is virtually all in the undissociated form. Between pH 2 and 4 the arsenate molecule changes from being only one third dissociated to the mono-anionic form to being almost completely dissociated to this form. By pH 7.0 significant quantities of the molecule have dissociated to the di-anionic form. It is thus apparent that most of the sorption occurred when the arsenate was partly in the undissociated and

partly in the mono-anionic forms. Sorption dropped off as quantities of the undissociated or further dissociated form became prevalent. The arsenite sorption data presented in Tables 5.5 and 5.6 show that the arsenite sorbs onto the PEI modified HIPE polymers at an alkaline pH with practically no sorption taking place at pH 5, while the sorption increases considerably between pH 6 and 7, no further increase takes place, however, at still higher pH. This result may be attributed to the pH dependent dissociation behaviour of arsenite and amine species.

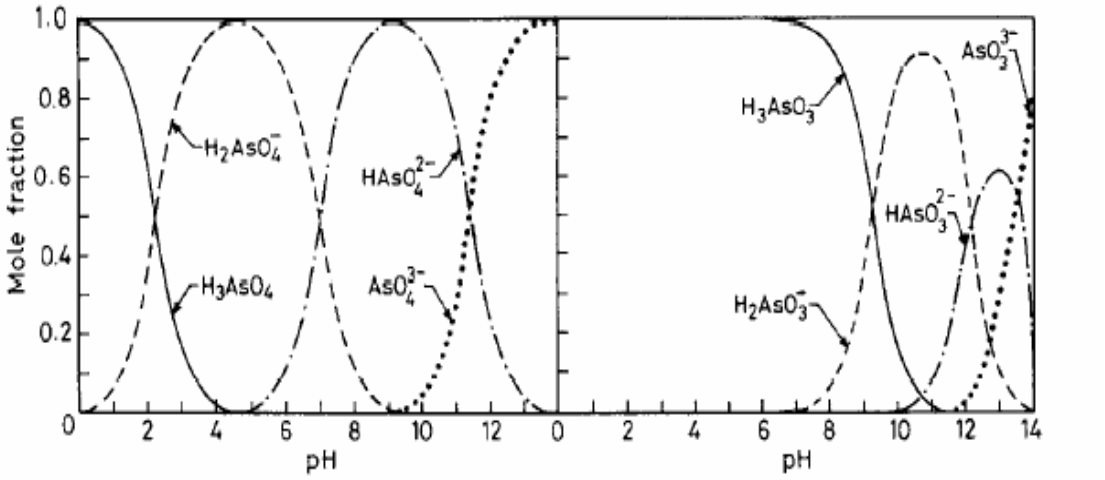

Figure 5.24. Speciation arsenate and arsenite species in aqueous solution at different pH values

The dissociation reaction and the corresponding dissociation constants of H_3AsO_3 at 24°C, in mol/L, are [51]:

$$H_3AsO_{3\,(aq.)} \Leftrightarrow H^+ + H_2AsO_3^- : K_1 = 6.0 \times 10^{-10} \quad \textbf{5.5}$$

$$H_2AsO_3^- \Leftrightarrow H^+ + HAsO_3^{2-} : K_2 = 7.4 \times 10^{-13} \quad \textbf{5.6}$$

$$HAsO_3^{2-} \Leftrightarrow H^+ + AsO_3^{3-} : K_3 = 5.0 \times 10^{-14} \quad \textbf{5.7}$$

The speciation of arsenite species calculated from these dissociation constants is shown in Figure 5.24. It is evident that significant concentrations of anionic species of As

(III) are obtained only at alkaline pH. Below pH 7, the arsenite is almost completely undissociated. This explains the observed fact that practically no sorption of As (III) takes place below pH 5 (Figure 5.25). The increase in sorption in the pH range between 6 and 7 indicates that arsenite undergoes redox sorption when it is in the monoanionic form.

Figure 5.26 shows that the maximum sorption of arsenate As (V) takes place at pH~ 2 to 5 where, according to Figure 5.24 as much as two third of the As (V) species occur as undissociated H_3AsO_4 and one-third in the monoanionic ($H_2AsO_4^-$) form**.** Maximum As (III) adsorption capacity of PEI-attached poly(GMA-EGDM) in alkaline region was 262 mg/g and that of poly(AGE-EGDM) was 266 mg/g (Table 5.5). Maximum As (V) adsorption capacity of PEI-modified poly(GMA-EGDM) in acidic region was 225 mg/g and that of poly(AGE-EGDM) was 234 mg/g (Table 5.6).

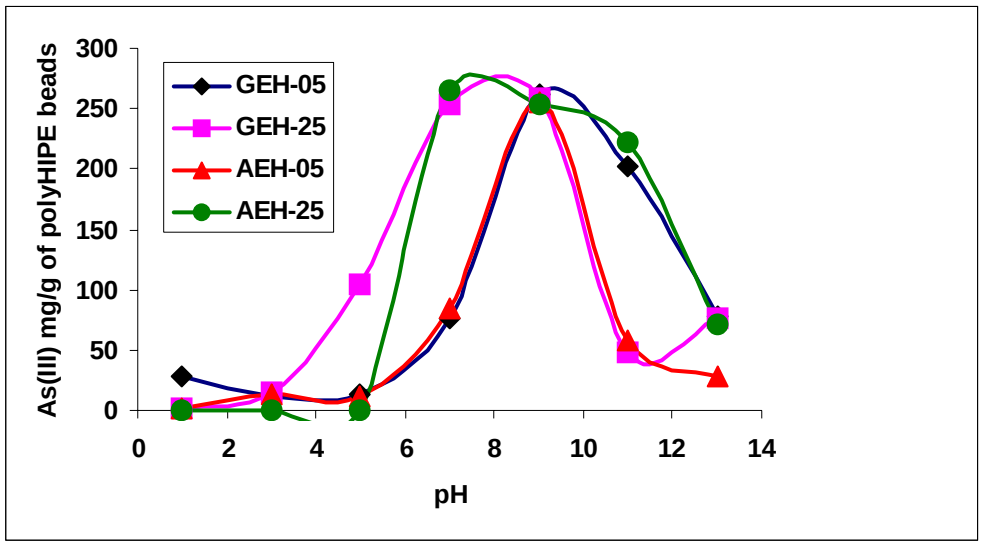

Figure 5.25. As (III) binding at different pH on PEI modified HIPE porous copolymers

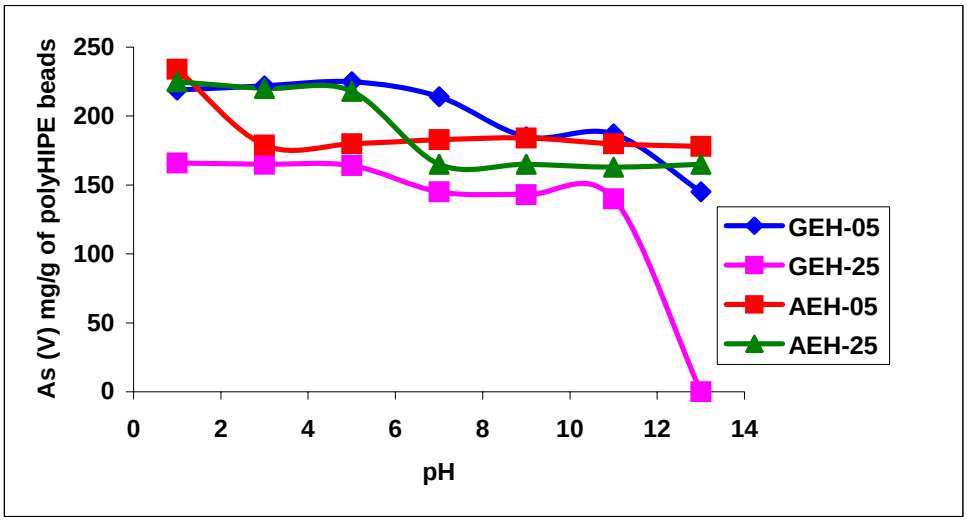

Figure 5.26. As (V) at different pH on PEI modified HIPE porous copolymers

Table 5.5. As (III) binding on PEI modified poly(HIPE) polymers at different pH

pH	Poly(GMA-EGDM)		Poly(AGE-EGDM)	
	5% CLD mg/g of polymer	25% CLD mg/g of polymer	5% CLD mg/g polymer	25% CLD mg/g of polymer
1	28	2	2	0
3	12	15	13	0
5	14	104	11	0
7	76	253	85	266
9	262	259	255	254
11	202	48	58	222
13	78	76	29	72

Table 5.6. As (V) binding on PEI modified poly(HIPE) polymers at different pH

pH	Poly(GMA-EGDM)		Poly(AGE-EGDM)	
	5% CLD mg/g of polymer	25% CLD mg/g of polymer	5% CLD mg/g polymer	25% CLD mg/g of polymer
1	219	166	234	225
3	222	165	179	220
5	225	164	180	218
7	214	145	183	165
9	185	143	184	165
11	187	140	180	163
13	145	0	178	165

5.4.6 Regeneration

The regenerability of the polymer beads is very important to reduce the process cost. Regeneration of the adsorbed arsenic ions from the PEI attached poly(GMA-EGDM) and poly(AGE-EGDM) beads was also studied**.** Desorption was performed by using 1.0 M HNO_3 and very high desorption ratios were achieved. These desorbed poly(HIPE) beads can be used for a number of cycles for arsenic removal. During desorption, the coordination spheres of chelated heavy metal ion is disrupted and subsequently arsenic ions are released from the solid surface into the desorption medium.

5.5 Conclusion

In this study novel metal chelating poly(HIPE) beads were prepared and were evaluated to remove arsenic ions from aqueous solutions. Microporous, cross-linked highly porous poly(GMA-EGDM) and poly(AGE-EGDM) epoxy beads completely insoluble in the water were prepared by W/O/W high internal phase emulsified suspension method. PEI was incorporated into the structure as metal-chelating ligand and these poly(HIPE) beads were used for adsorption-desorption of As(III) and As(V) ions from synthetic solutions.

Arsenic adsorption depends on the copolymer composition (cross-link density), porosity and surface area. Since adsorption is a surface phenomenon, the greater the surface of the medium, greater is the adsorption capacity. The sorption of both As (V) and As (III) is seen to be sharply influenced by pH, with the sorption of As(V) falling drastically both at low and high pH and that of As (III) at low pH. The sorption maximum for As (V) occurs under acidic conditions (pH 2-4) and that of As (III) under alkaline conditions (pH 7-10). High adsorption rates are observed at the beginning of adsorption

process, and then plateau values (i.e. adsorption equilibrium) are gradually reached in about 20 minutes. Maximum As (III) adsorption capacity of PEI-attached poly(GMA-EGDM) in alkaline region was found 262 mg/g and that of poly(AGE-EGDM) was 266 mg/g. Maximum As(V) adsorption capacity of PEI-attached poly(GMA-EGDM) in acidic region was found 225 mg/g and that of poly(AGE-EGDM) was 234 mg/g. Desorption was possible using strong acid and these desorbed poly(HIPE) beads can be used for number of cycles for arsenic removal.

References

[1] Rapsomanikis, S.; Craig, P. J. *Anal. Chim. Acta*. **1991**, 248, 563.

[2] Farrel, W. J.; Peggy, O. D.; Colklin. M. *Environ. Sci. Technol*. **2007**, 35, 2062-2032.

[3] Bagla, P.; Kaiser. J. *Science* **1996**, 274, 174-175.

[4] Nickson, R. et al. *Nature* **1998**, 395, 338.

[5] Bearer, D.; *New Bangladesh disaster: wells that pump poison*. The New York Times, November 10, **1998**.

[6] Krishna, B.; Chadrasekaran, K.; Karunasagar, D.; Arunachlam, J. *J. Hazard. Mater. B* **2001**, 84, 229-240.

[7] Ferguson, J. F.; Gavis, J. *Water Res*. **1972**, 6, 1259-1274.

[8] Masscheleyn, P. H.; Delaune, R. D.; Patrick, W. H. *Environ. Sci. Technol*. **1991**, 25, 1441-1419.

[9] Hering, J. G.; Chen, P. Y.; Wilkie, J. A. Elimelech, M. *J. Am. Water Works. Assoc*. **1996**, 88, 155-167.

[10] Ghosh, M. M.; Yuan, J. R. *Environ. Prog*. **1987**, 3(3), 150-157.

[11] Driehaus, W.; Jekel, M.; Hildebrandt, U. *J. Water SRT Aqua*. **1998**, 47(1), 30-35.

[12] McNeil, L. S.; Edward, M. *J. Am. Water Works. Assoc*. **1995**, 87(4), 105-114.

[13] Min, J. M.; Hering. J. *Water Res*. **1998**, 32(5), 1544-1552.

[14] Ramana, A.; SenGupta, A. K. *J. Environ. Eng. Div ASCS* **1992**, 118(5), 755-775.

[15] Sorg, T. J.; Logsdon, G. S. *J. Am. Water. Works. Assoc*. **1978**, 70(7), 379.

[16] Lackovic, J. A.; Nikolaidis, N. P.; Dobbs, G. M. *Environ. Eng. Sci*. **2000**, 17(1) 29-39.

[17] Chwirka, J. D.; Thomson, B. M.; Stomp, J. M. *J. Am. Water Works. Assoc*. **2000**, 92 (3), 79-88.

[18] Clifford, D.; Subramonian, S.; Sorg, T. *Environ. Sci. Technol.* **1986**, 20, 1072-1080.

[19] Driehaus, W.; Seith, R.; Jekel, M. *Water Res*. **1995**, 29(1), 297-305.

[20] Kartinen, E. O.; Martin, C. J. *Desalination* **1995**, 103, 79-88.

[21] Meng, X.; Bang, S.; Korfiatis, G. P. *Water Res*. **2000**, 34(4), 1255-1261.

[22] Shen, Y. S.; *J. Am Water Works Assoc*.**1973**, 65 (8), 543.

[23] Torrens, K. D. *Pollution Eng*. **1999**, 25-28.

[24] Vagliasandi, F. G. A.; Benjamin, M. M. *Water. Sci. Technol*. **1998**, 38(6), 337-343.

[25] Li, Y. H.; Wang, S.; Wei, J.; Zhang, X.; Xu, C.; Luan, Z.; Wu, D.; Wei, B. *Chem. Phys. Lett*. **2002**, 357, 263.

[26] Beuvais, R. A.; Alexandratos, S. D. *React. Funct. Polym*. **1998**, 36, 113.

[27] Rivas, B. L.; Pooley, S. A.; Maturana, H. A.; Villeges, S. *Macromol. Chem. Phys.* **2001**, 202, 443.

[28] Saito, T. *Sep. Sci. Technol*. **1991**, 26, 1495.

[29] George, B.; Rajasekharan Pillai, V. N.; Mathew, B. *J. Appl. Polym. Sci*. **1999**, 74, 3432.

[30] Beatty, S. T.; Fischer, R. J.; Hagers, D. L.; Rosenberg, E. *Ind. Eng. Chem. Res*. **1999**, 38, 4402.

[31] Chanda, M.; Rempel, G. L. *React. Functl. Polym*. **1997**, 35, 197.

[32] Li, W.; Zhao, H.; Teasdale, P. R.; Jhon, R.; Zhang, S. *Rect. Functl. Polym*. **2002**, 52 31.

[33] Denizli, A.; Kesenci, K.; Senel, S. *J. Appl. Polym. Sci*. **1999**, 71, 1397.

[34] Denizli, A.; Kesenci, K.; Arica, Y. *React. Functl. Polym*. **2000**, 44, 235.

[35] Wang, C. C.; Chang, C. Y.; Chen, C. Y. *Macromol. Chem. Phys*. **2001**, 202, 882.

[36] Navarro, R. R.; Sumi, K.; Fuji, N.; Matsumura, M. *Water. Res*. **1996**, 30, 2488.

[37] Saglam, A.; Bektas, S.; Genc, O.; Denizli, A. *React. Functl. Polym*. **2001**, 47, 185.

[38] Deng, Y.; Fan, X. D.; Waterhouse, J. *J. Appl. Polym. Sci*. **1999**, 73, 1081.

[39] Arvanitoyannis, I.; Nikolaou, E.; Yamamoto, N. *Macromol. Chem. Phys*. **1995**, 196, 1129

[40] Disbudak, A.; Bektas, S.; Patir, S.; Genc, O.; Denizli, A. *Sep. Purif. Technol*. **2002**, 19, 26.

[41] Arvanitoyannis, I.; Nikolaou, E.; Yamamoto, N. *Polymer* **1995**, 34, 4678.

[42] Berrera, D.; Zylastra, E.; Lansbury, P.; Langer, R. *Macromolecules* **1995**, 28, 425.

[43] Muslehiddinoglu, J.; Uludag, Y.; Ozbelge, H. O.; Yilmaz, L. *Talanta.* **1998**, 46, 557.

[44] Tomida, T.; Katoh, M.; Inoue, T.; Minamino, T.; Masuda, S. *Sep. Sci. Technol*. **1998**, 33, 2281.

[45] Meyers, P. *Plut. Surf. Finish* **1998**, 33, 2281.

[46] Cameron, N. R.; Sherrington, D. C. *J. Mater. Sci*. **1997**, 7 (11), 2209-2212.

[47] Sotiropoulos, S.; Brown, J. I.; Akay, G.; Lester, E. *Mater. Lett*. **1998**, 35 (5-6), 383-389.

[48] Katsoyiannis, I. A.; Zouboulis, A. I. *Water Research* **2002**, 36, 5141-5155.

[49] Johnson, D. J.; Pilson, M. E. Q. *Anal. Chim. Acta*. **1972**, 85, 219-230.

[50] Kline, G. M. *Analytical chemistry of polymers*, Interscience, New York, **1959**, p-123.

[51] Bard, A.; Parsons, R.; Jordan, J. *Standard Potentials in Aqueous Solution*. Marcel Dekker, New York, NY, **1985**.

Chapter VI

Hydroxy terminated porous polymers

6 Hydroxy terminated porous polymers

6.1 Introduction

The hydroxyl group in poly(2-hydroxyethyl methacrylate) (PHEMA) can be derivatised to produce a wide range of polymeric reagents suited to pharmaceutical, chromatographic applications as well as to immobilise biopolymers (enzymes, antibodies, cells), encapsulat mammalian cells and other sensitive compounds.[1-8] Open porous poly(HIPEs) have attracted attention as biological tissue scaffold, catalysis support and ion-exchange resins.

The first thoughts related to what we today call monoliths can be traced down to the work of Nobel Laurate Richard Synge, who in 1952 envisioned "a continuous block of porous gel structure".[9] First attempts to make "single piece" stationary phase from highly swollen polymer gel and open–pore polyurethane foams during the late 1960s and the early 1970s were less successful. Interest in the monolithic formats was revived in the late 1980s. Since then novel approaches towards true monoliths such as compressed hydrophilic gels, macroporous polymer discs, columns, tubes, rods, have been developed.[10]

6.1.1 Polymeric beads

Emulsion templating is the versatile method for the preparation of well-defined open and interconnected porous monolith as well as beads. In general, the techniques involve forming a high internal phase emulsion (HIPE) in which internal volume goes beyond 75% v/v.[11-20] The liquid but highly viscous nature of HIPEs allows the continuous phase to be given any shape that conform to the shape of the reaction vessels.[20]

Conventional polymer based chromatographic beads, which provide large surface to volume ratios are widely available, are well characterised, and easily functionalised. This makes them attractive medium for microencapsulation, as well as other microfluidic unit operations that benefit from high surface areas.[21-23] Beads have found wide, dispersed use in conventional packed bed chromatographic separation columns for several decades. However, their use in microfluidic channels has been much more limited. The primary reason for their limited implementation is due to the difficulty of packing and retaining beads within micro-channels.[21,24]

Monolithic media were originally developed as alternative to beads for chromatographic stationary phases, but additional applications have since been developed, especially with organic polymer monoliths.

6.1.2 Polymeric monoliths

Porous polymer monoliths are a new category of materials developed in the last decade. These materials are prepared using a simple molding process carried out within the confines of a closed mold. Polymeric monoliths are easily and rapidly prepared via thermal-or photo-initiated free radical polymerisation.[25-27] A typical polymerisation mixture consists of homogeneous solution of monomer, cross-linker, initiator and surfactant. The continuous porous structure of the polymer monolith results from phase separation between the growing polymer and the porogen during the polymerisation.[28] Organic polymer monoliths have been prepared from acrylamide, acrylate, methacrylate and styrene monomers.[29] The surface chemistry and porous properties of monoliths can be controlled through an appropriate formulation of the polymerisation mixture and selection of the polymerisation conditions.[28,30] In particular, a wide range of surface

chemistries are possible by selecting precursor monomers with the desired chemical functionalities. Further, the porosity, surface area, and pore size can be tuned by adjusting the composition of the porogenic solvent, the polymerisation condition, and/or the ratio of monomers, cross-linkers and surfactants. Advantages of polymer monoliths include their easy *in situ* preparation and the wide range of possible morphologies and chemistries. Grafting of the pore walls with selected polymers leads to materials with completely changed surface chemistries. The applications of monolithic materials are demonstrated in the chromatographic separation of biological compounds and synthetic polymers, electro-chromatography, gas chromatography, enzyme immobilisation, molecular recognition, and in advanced detection systems.[31]

Until now, the preparation of poly(HIPE) has been achieved predominantly by thermal curing. In order to introduce biological species, redox polymerisation would be beneficial. Our main emphasis was not only on the preparation of tuned porous architecture of the polymer matrix but also in the exploration of poly(HIPE) as useful biomaterials. The primary goal of this investigation was to synthesise, design and characterise a porous hydroxyl terminated polymer at room temperature with tuned morphology that would provide increased surface area within a beaded as well as in monolithic form for use in different applications. Here in this study, the inverse HIPE emulsion polymerisation was used to synthesise the hydroxyl terminated polymers.

6.2 Experimental

6.2.1 Materials

Analytical grade 2-hydroxyethyl methacrylate (HEMA) and N,N'-methylene bisacrylamide obtained from Sartomer, USA were used as received in the synthesis of

HEMA-MBA copolymers. Sodium peroxydisulphate (NaPS) was used as initiator and L-ascorbic acid was used as reducing agent in redox system. Brij 92 and Brij 700 were purchased from Aldrich and used as nonionic surfactants for making stable O/W emulsion. Poly(vinyl pyrrolidone) [PVP] (Polysciences, USA) was used as protective colloid.

6.2.2 HEMA-MBA PolyHIPEs

6.2.2.1 HEMA-co-MBA polyHIPE beads with single surfactant

Water (2 g) was accurately weighed in a beaker. Calculated amount of HEMA and MBA were added to this beaker as shown in Table 6.1, followed by NAPS (0.12 g; 0.0005 mol). The above mixture was homogenised for 5 minutes. Tween 80 surfactant (HLB = 15.0) (0.8 g) was then added and homogenised further for 5 minutes.

Table 6.1. Composition and porous properties of HEMA-MBA polyHIPE beads synthesised relative to cross-link density

Expt. code	CLD %	HEMA g	MBA g	Pore Volume cm^3/g	Surface area m^2/g	Av. pore size(BET) (nm)
HEM 1	25	2.35	0.65	0.70	89.21	225
HEM 2	50	1.89	1.11	1.02	100.54	350
HEM 3	75	1.56	1.44	1.21	90.46	452
HEM 4	100	1.36	1.64	0.81	113.17	34
HEM 5	150	1.08	1.92	0.78	128.62	27
HEM 6	200	0.89	2.11	0.69	189.78	50

Cyclohexane = 30 g, water = 3 g, Brij 92 = 0.6 g, NaPS = 0.12 g, Ascorbic acid = 0.088 g

This was the water phase. Cyclohexane (30 g) was accurately weighed and added slowly under continuous stirring (400 rpm) to the water phase. The emulsion formed was transferred to a polymerisation reactor, having 100 mL of cyclohexane as the suspending medium and 1 g Span 80 as the protective colloid. A stirring speed of 450 rpm was

maintained throughout the polymerisation. Once emulsion was stabilised, 1 mL of ascorbic acid solution was added to initiate the polymerisation at room temperature. HIPE suspension polymerisation was conducted for 3 h.

6.2.2.2 HEMA-co-MBA polyHIPE beads by mixed surfactants

Here, a mixture of low and high HLB surfactants was incorporated to stabilise the HIPE. The surfactants chosen were Brij 92 (HLB = 4.9) and Brij 700 (HLB = 18.8). In addition, the surfactant concentration was increased to 20% of the monomer to achieve higher surface areas.[32] Series of HEMA-MBA polymers were synthesised, by varying the Brij 92 to Brij 700 ratio keeping MBA constant at 25% CLD as shown in Table 6.2.

Table 6.2. Composition and pore chacteristics of HEMA-MBA polyHIPE beads synthesised using different Brij 92 to Brij 700 ratios

Expt. code	Brij 92 g (%)	Brij 700 g (%)	Pore Volume cm^3/g	Surface area m^2/g	Av. pore size (BET) (nm)
HEM 7	1.2 (100.00)	0.0	0.56	63.45	234
HEM 8	1.0 (83.33)	0.2 (16.66)	0.84	56.13	143
HEM 9	0.8 (66.66)	0.4 (33.33)	0.99	87.34	174
HEM 10	0.4 (33.33)	0.8 (66.66)	1.23	142.67	84
HEM 11	0.2 (16.66)	1.0 (83.33)	1.56	179.64	49
HEM 12	0.0	1.2 (100)	1.59	126.45	24

HEMA = 2.35 g, MBA = 0.65 g, water = 3 g, NaPS = 0.12 g, Ascorbic acid = 0.088 g

Here, instead of Tween 80 surfactant, we added mixture of Brij 92 and Brij 700 in the ratio as shown in Table 6.1 and polymerisation procedure described in Section 6.2.2.1was followed.

6.2.2.3 Synthesis of monolithic HEMA-MBA polymers

Calculated amount of HEMA and MBA were taken in a beaker containing 2 g water as shown in Table 6.3. NaPS (0.12 g, 0.0005 mol) was mixed to it.

Table 6.3. Composition and porous properties of HEMA-MBA monolithic polymers synthesised relative to cross-link densities.

Expt / Polymer code	CLD %	HEMA g	MBA g	Pore Volume cm^3/g	Surface area m^2/g	Av. pore size(BET) (nm)
HEM13	05	2.84	0.16	0.45	23.9	162
HEM14	10	2.69	0.31	0.89	30.7	184
HEM15	15	2.54	0.45	1.64	36.1	173
HEM16	25	2.35	0.65	0.68	101.3	2
HEM17	50	1.89	1.11	0.56	123.7	5
HEM18	75	1.56	1.44	0.75	82.4	15
HEM19	100	1.36	1.64	1.24	62.8	65
HEM20	150	1.08	1.92	0.98	72.4	261
HEM21	200	0.89	2.11	1.01	79.2	364

Cyclohexane = 30 g, water = 3 g, Brij 92 = 0.6 g, Brij 700 = 0.6 g, NaPS = 0.12 g, Ascorbic acid = 0.088 g

The surfactants Brij 92 (HLB = 4.9) (0.6 g) and Brij 700 (HLB = 18.8) (0.6 g) were added to form aqueous phase. Under continuous stirring at 400 rpm 30 g cyclohexane was added drop-wise to the aqueous phase. Once emulsion was formed 1 mL of ascorbic acid (0.088 g; 0.0005 mol in 1 mL water) solution was added to the emulsion, stirred for approximately 10 seconds to ensure uniform distribution. The emulsion was kept aside for 18 h without stirring at room temperature for polymerisation. The monolith was washed sequentially with water and methanol to remove residual monomers and surfactants, and dried at 60 ºC for 6 h under vacuum.

6.3 Evaluation and characterisation of HEMA-MBA monoliths

6.3.1 Surface topography

Internal as well as surface morphology of HEMA-MBA copolymers were observed using scanning electron microscope, JEOL JSM-5200, UK, operated at an acceleration voltage of 10 kV. The monoliths were cut into 1 mm x 1 mm. section, mounted on the standard specimen mounting stubs, coated with a thin layer (20 nm) of gold in sputter coater unit.

6.3.2 Porosity measurement

The surface area and pore volume of the copolymers were measured using mercury intrusion porosimetry and single point Brauner-Emmett-Teller method as described in chapter III (Sections 3.3.3 and 3.3.5).

6.3.3 Surface hydroxyl groups

The surface hydroxyl groups were analysed titrimetrically using acetic anhydride -pyridine. The method is based on acetylation of copolymer and then titration of acetic acid generated against standard potassium hydroxide solution. The mole of potassium hydroxide consumed equals mole of acetic acid generated in the reaction plus twice the unreacted acetic anhydride or number of surface hydroxyl groups present in the polymer.

To a appropriate mass of the polymer sample, 0.1 g of acetic anhydride, 0.1 g pyridine were added, followed by 25 mL of toluene and titrated against 0.1 M potassium hydroxide solution. The end point was colourless changing to pink.

Polymer-OH + excess $(CH_3CO)_2O$ Polymer $–OCOCH_3$ $+CH_3COOH$

Moles of KOH consumed = (Y-X) X molarity of KOH x 10^{-3}

= Z moles.

Moles of CH_3COOH consumed = Z mole = Z_1 mmole.

Therefore, X= 1x Z_1/ 0.1 = Z_2

Where, 0.1 g is mass of polymer and Z_2 is mmole of hydroxyl groups present.

6.4 Results and discussion

6.4.1 HEMA-MBA beads by inverse HIPE polymerisation

In multiphase emulsion system droplets of an emulsion are dispersed in a third medium, giving three-phase system with either a water-in-oil-in-water (W/O/W: droplets of water-in-oil emulsion are dispersed in aqueous medium) or an oil-in-water-in-oil (O/W/O: droplets of oil-in-water emulsion dispersed in oil).[33,34] To prepare a porous copolymer particle with an open cellular internal structure, a primary emulsion with high volume fraction of the internal phase is first made. This high internal phase emulsion is dispersed in a secondary medium and multiple HIPE emulsion is formed (droplet of HIPE dispersed in a secondary oil or water phase).[35] We term this system as high internal phase emulsified suspension (HIPE's).

This chapter describes an inverse O/W/O high internal phase emulsified suspension (HIPE's) polymerisation process for the synthesis of HEMA-MBA copolymers, which yield truly porous beads at room temperature. HIPE polymerisation is essentially a compartmentalised O/W/O polymerisation reaction-taking place in a large number of loci dispersed in a continuous oil external phase. The polymerisation of water soluble monomer after formation of O/W/O type multiphase emulsion, having a phase containing the monomer as an intermediate phase, generated porous polymer having sufficiently large surface area.

The reaction between peroxydisulphate and ascorbic acid involves a chain mechanism due to the formation of sulphate ion radicals, which are well-known ion chain carriers. The mechanism presented in Scheme 6.1.

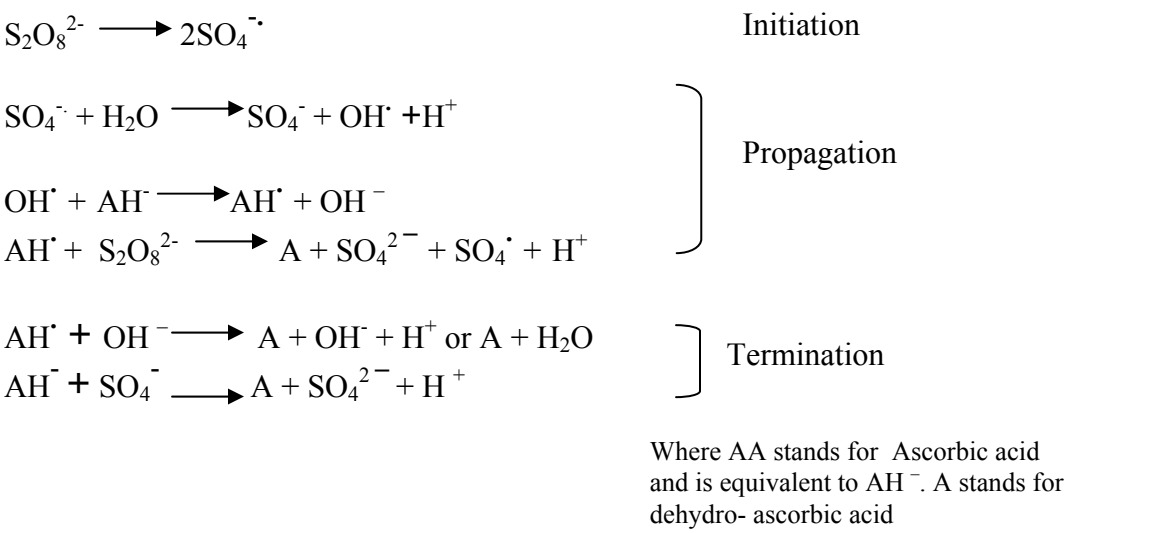

Scheme 6.1. Primary free radicals generation by $K_2S_2O_8$/ascorbic acid redox initiator

In this O/W/O method, oil is dispersed in a continuous water phase so as to generate an internal phase volume up to 90%, due to oil, the majority phase, which is not continuous. They form readily on adding oil slowly to a stirred solution of a high hydrophile - lipophile balance (HLB) surfactant dissolved in the oil phase, as shown in Figure 6.1. Surfactant is capable of forming well-defined micellar structures in solutions. The characteristics of the micelles are dependent on the type of solvent, type and amount of the surfactants. The internal discontinuous phase constitutes approximately 90% in each case and consists of small droplets, approximately 2-10 μm in diameter. By adjusting the amount of solvating porogen, cyclohexane, in the discontinuous inner oil phase, pore structure can be generated within the droplet of HIPE polymer. Large surface areas can thus be achieved.

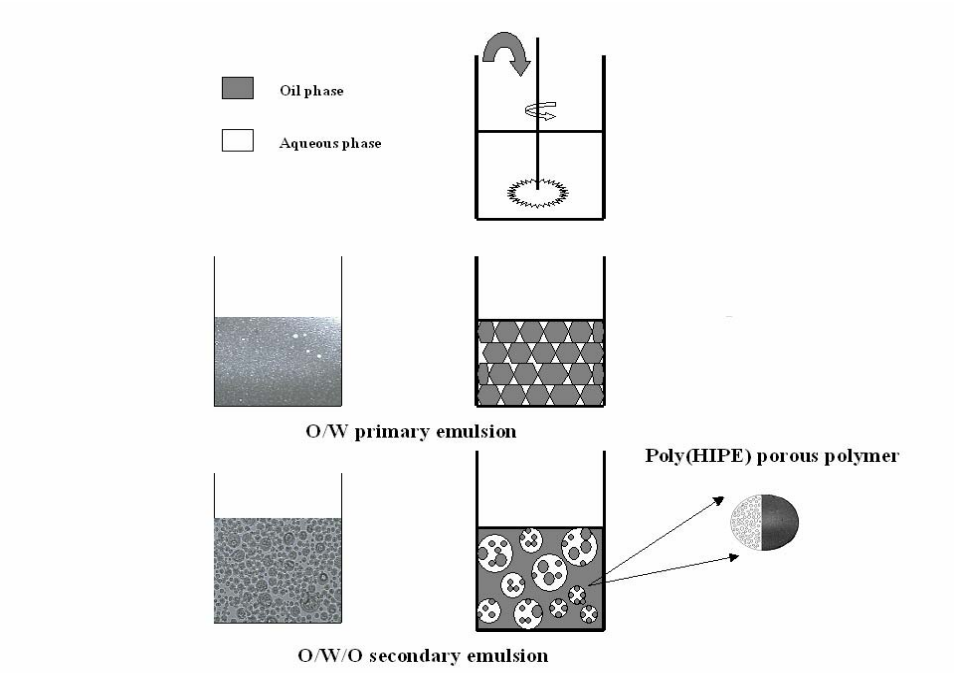

Figure 6.1. Schematic diagram for synthesis of porous poly(HEMA-MBA) spheres by O/W/O method

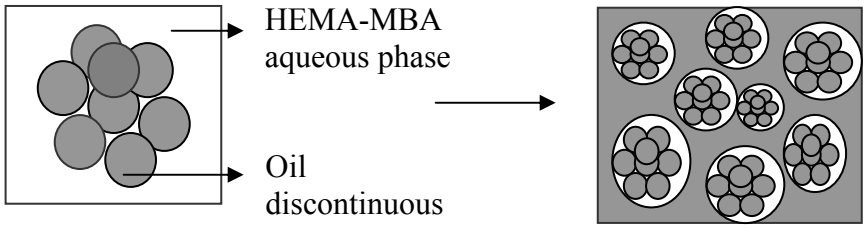

O/ W primary emulsion O/W/O secondary emulsified suspension

Figure 6.2. Schematic diagram showing droplet packing arrangement in primary and secondary emulsion during HIPE formation

In the formation of porous structures surfactant type and its concentration are very important, because only with the proper HLB it is possible to stabilise more than 74% of inner discontinuous oil phase to be dispersed into the continuous aqueous HEMA-MBA phase. The droplet size of the discontinuous oil phase is very important because this

dictates the pore volume (macropores) and surface area (micro and mesopores) after the polymerisation.

In inverse HIPE, nonionic surfactant (Span 80) stabilises the O/W emulsion, in which the inner oil phase occupies the maximum available place around the droplet in the primary emulsion phase. When primary emulsion is poured into the third oil phase, the O/W emulsion is dispersed in it. Tween 80 acts as a stabiliser to avoid coalescence between two droplets. Tween 80 forms a thin film around the droplets, and does not allow the complete diffusion of the inner oil phase into the outer oil phase. So inner oil droplets remain entrapped in the primary emulsion droplets, which are dispersed in the outer oil phase under constant stirring (Figure 6.2). A porous structure was obtained on removal of inner oil phase, which originally occupied more than 74% of emulsion volume.

6.4.2 Surface hydroxyl groups

The surface hydroxyl content of HEMA-MBA polymer beads synthesised using O/W/O HIPE inverse emulsion is shown in Table 6.4.

Table 6.4. Theoretical and experimental surface hydroxyl groups of HEMA-MBA particles

Polymer code	Theoretical hydroxyl group (mmole/g)	Observed hydroxyl group (mmole/g)
HEM 1, HEM 7	6.01, 6.01	2.46, 3.43
HEM 2, HEM 8	4.83, 6.01	2.02, 2.87
HEM 3, HEM 9	3.99, 6.01	1.57, 1.65
HEM 4, HEM 10	3.48, 6.01	1.00, 1.89
HEM 5, HEM 11	2.77, 6.01	0.23, 0.51
HEM 6, HEM 12	2.28, 6.01	0.01, 0.34

The theoretical hydroxyl content decreases as HEMA content in the copolymer decreases, from 6.01 mmole/g at 25% CLD (HEM 1) to 2.28 mmole/g at 200% CLD (HEM 6). The titratable hydroxyl groups [Figure 6.3 (a)], found at or near the surface of the pores, decreases from 2.46 mmole/g at 25% CLD to 0.01 mmole/g at 200% CLD. Thus, while 40 % hydroxyl groups are at the surface at 25% CLD, this drops to 0.1% at 200% CLD. As the cross-link density increases the amount of HEMA decreases, as a result very small fraction of hydroxyl groups are present at or near the surface. However, with increase in cross-link density, the swellability of the beads decreases. Simultaneously, the hydrophilicity of the beads also decreases. A large majority of the hydroxyl groups are buried in.

As the polymerisation proceeds, more hydroxyl groups get buried in the copolymer matrix and are not available for reaction with acetic anhydride-pyridine complex. It was also observed that at constant HEMA to MBA mole ratio, a change in surfactant ratio affects the concentration of surface hydroxyl groups. Table 6.4 shows the hydroxyl content of HEMA-MBA system at 25% CLD (HEM 7 to HEM 12). When Brij 92 concentration was 100% the surface hydroxyl groups (HEM 7) was 3.43 mmole/g, which exceeds that in HEM 1, synthesised using both surfactants at 0.5-0.5 ratio. That means lower HLB surfactant Brij 92 pushes out relatively a large fraction of hydroxyl groups towards the oil-water interface during the HIPE formation. As the relative concentration of Brij 92 decreases (or concentration of high HLB Brij 700 increases) the hydroxyl groups are pushed inward and surface concentration decreased from 3.43 mmole/g (HEM 7) to 0.34 mmole/g (HEM 12), as shown in Figure 6.3 (b). Therefore, proper surfactant system and the ratios are of critical importance to generating beads with

the hydroxyl groups at the pore surface in inverse HIPE methodology. As the Brij 700 concentration increases the emulsion becomes viscous probably due to the formation of a lyotropic phase where in the hydroxyl groups are hydrogen bonded with each other making hydrophobic matrix.

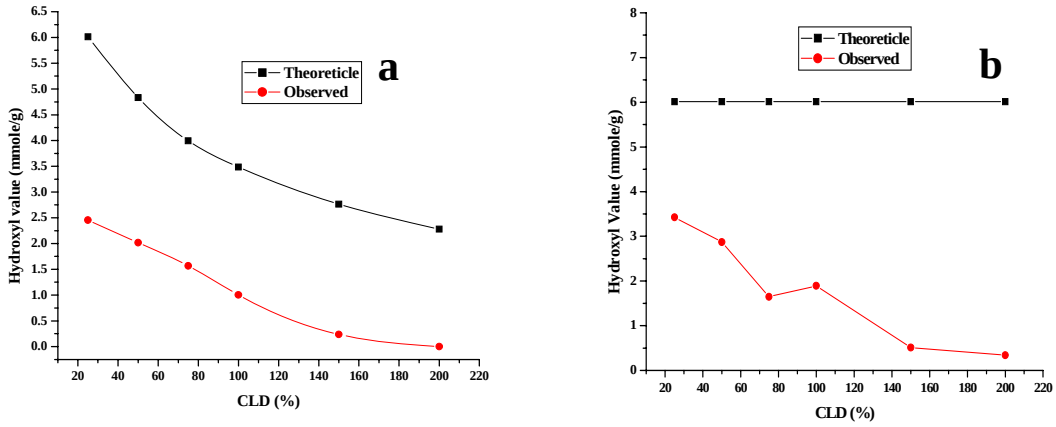

Figure 6.3. Theoretical and experimental surface hydroxyl groups of HEMA-MBA particles synthesised with (a) differing CLD, and (b) differing HLB surfactants

6.4.3 Particle size distribution

The size growth model of a bead suspension polymerisation proposed by Winslow and Matreyek indicates that the particle size is mainly determined by the droplet size in the lower conversion stage and the stability of monomer/polymer droplets in the high conversion stage.[34] In this inverse oil-in-water-in-oil (O/W/O) HIPE method initial droplet formation plays an important role in the particle size distribution in the final polymer. If the coalescence of monomer/polymer droplets is negligible during polymerisation, e.g., due to protection by a surfactant, the particle size distribution (PSD) of the polymerised HEMA-MBA is approximately the size distribution of the droplets of the monomer during the HIPE emulsion polymerisation. Therefore, the PSD of the

HEMA-MBA beads can be predicted by dynamic balance between breakage and coalescence of dispersed droplets during O/W primary emulsion formation.

Emulsions are understood as dispersed systems with liquid droplets (dispersed phase) in a liquid (continuous phase). Stabilisation can be obtained electrostatically or sterically. Either molecular diffusion degradation (Ostwald ripening) or coalescence may lead to the destabilisation and breaking down of emulsions.

In this study, when an oil-in-water (O/W) emulsion is created by the application of shear force to a heterogeneous fluid containing surfactants, a distribution of droplet size results. Inter droplet mass transfer (Ostwald ripening) determines the fate of this distribution because of their higher Laplace pressure. If the small droplets are not stabilised against diffusional degradation, they will disappear, increasing the average droplet size.

It was shown that this disappearance could be very rapid for small droplets. It was proposed in 1962 that unstable emulsions might be stabilised with respect to the Ostwald ripening process by the addition of small amounts of a third component, which must distribute preferentially in the dispersed phase.[35] The Figure 6.4 shows the particle size distribution when the MBA concentration is very low (25% CLD). The particles formed are quite mono-disperse, in the range 5-50 μm. The PSD broadens with increasing cross-link density. At 50% CLD the particle diameter was in the range 0.5 to 50 μm, as shown in Figure 6.5. This is probably due the Ostwald ripening in O/W primary emulsion step.

The rate of Ostwald ripening depends on the size, polydispersity and solubility of the dispersed phase in the continuous one. The already ultra-hydrophobic oil dispersed in small droplets of low polydispersity shows low diffusion. But, by the addition of a

hydrophobe, the stability can be further increased by additionally building up an osmotic pressure, merging of small droplets to form larger droplets. At 75% CLD, the particles formed at identical shear rate were in the range 0.5-200 µm (Figure 6.6).

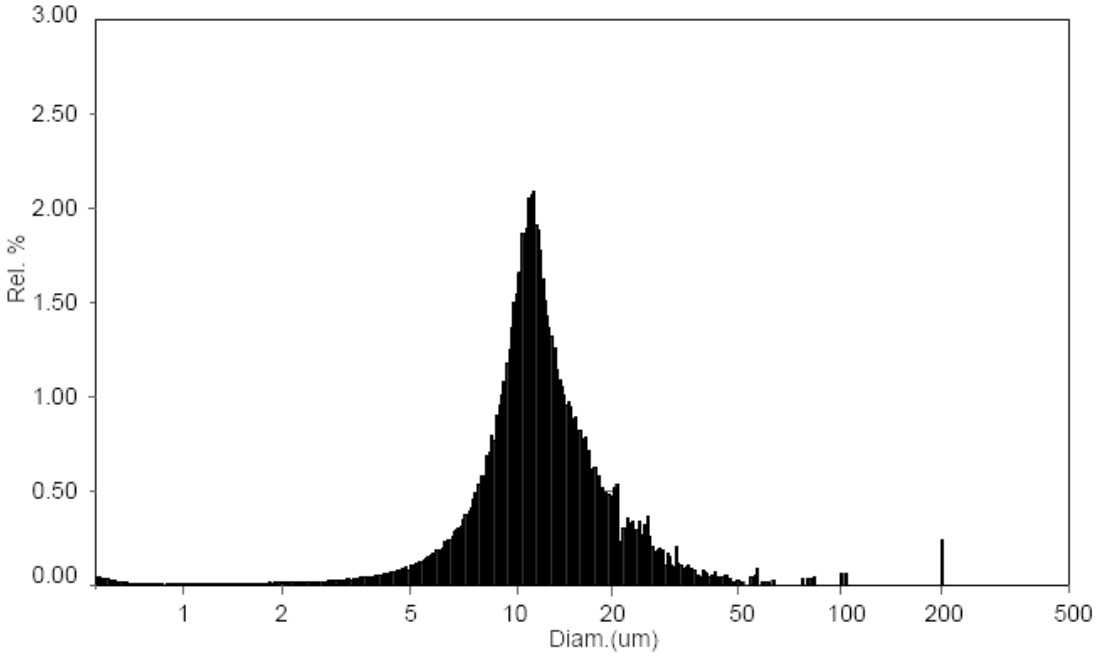

Figure 6.4. Particle size distribution of HEMA-MBA synthesized at 25%CLD

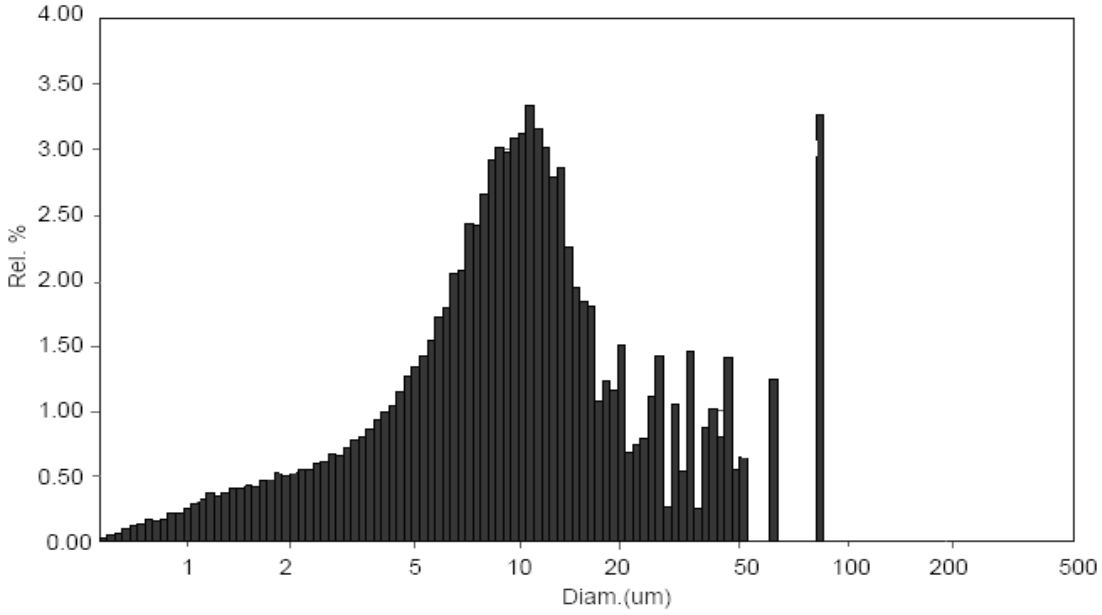

Figure 6. 5. Particle size distribution of HEMA-MBA synthesized at 50%CLD

Brij 92 and Brij 700 form highly viscous inverse emulsion of HEMA-MBA (at 1400 rpm) resulting in a thin film of surfactant at oil and water (monomer) interface. So it is very difficult for inner oil phase to diffuse out and form small droplets. Besides the molecular diffusion of the dispersed phase, destabilisation of emulsion can also occur by collision and coalescence processes. In rapid Brownian coagulation of dilute primary oil-in-water emulsions, the influence of deformation on droplet interaction and drainage is negligible at the final O/W/O suspension stage.[36] Observing the weak influence of droplet deformation on rapid coagulation, and taking into account the Borwankar-Ivanov theory[36] that the transition to charged droplets and lower electrolyte concentration decreases droplet deformation, it was concluded that both slow and reversible coagulation cannot be influenced by droplet deformation in mini-emulsions. A droplet surface is homogeneous in contrast to solid particle surfaces.

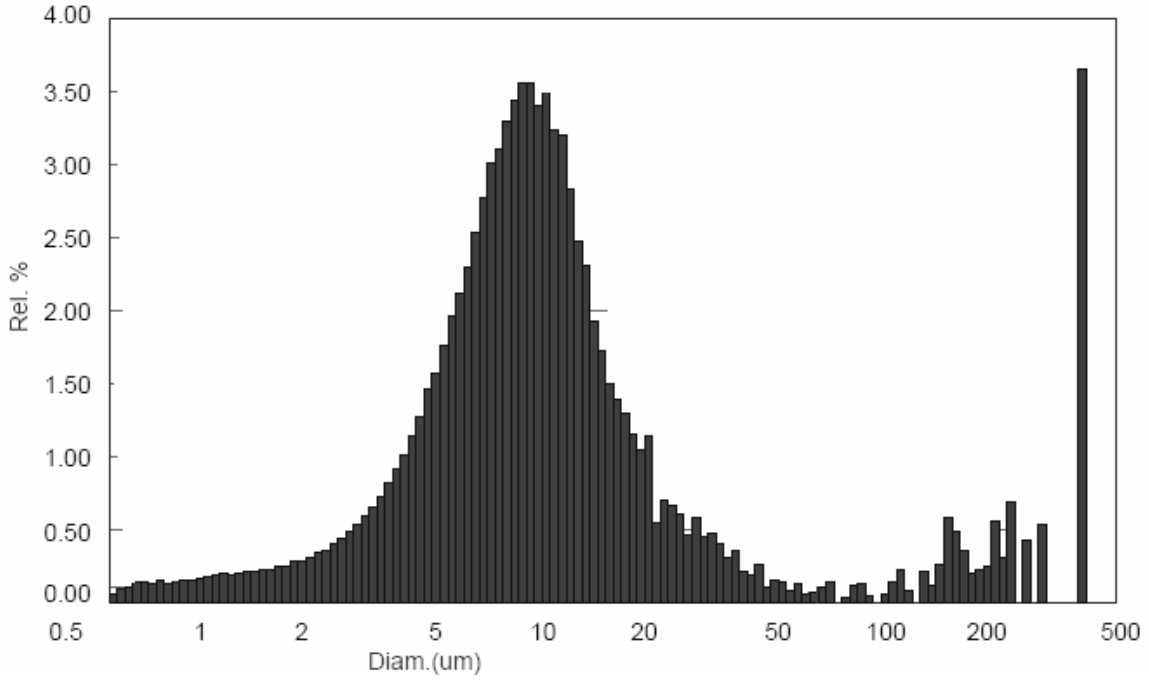

Figure 6.6. Particle size distribution of HEMA-MBA synthesized at 75%CLD

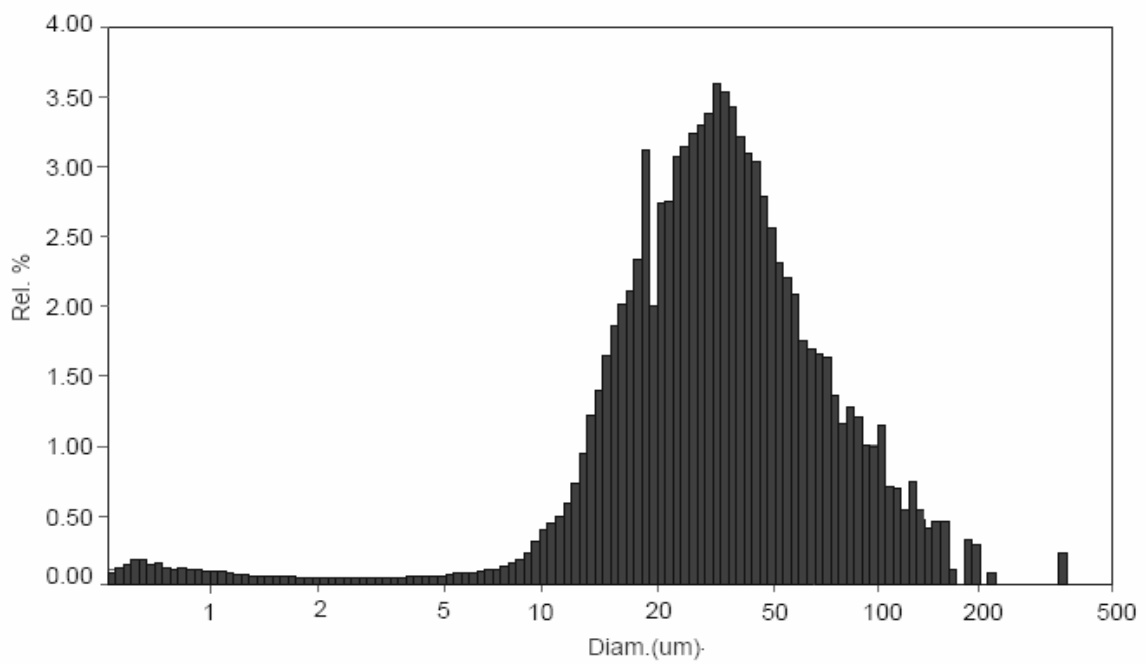

Figure 6.7. Particle size distribution of HEMA-MBA synthesized at 100%CLD

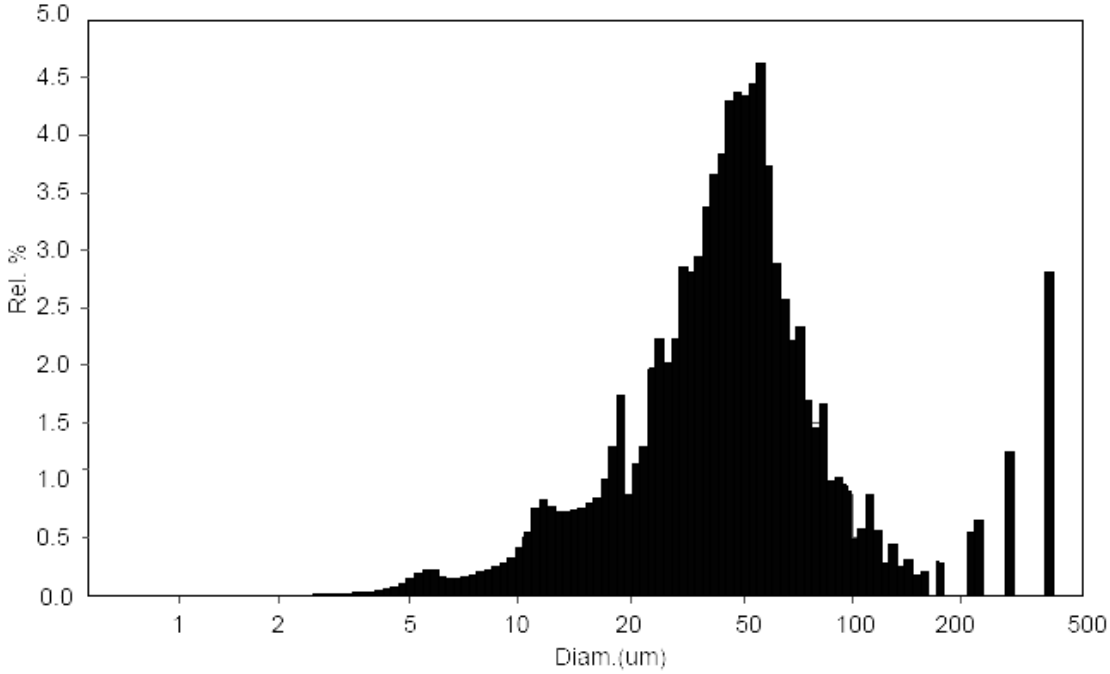

Figure 6.8. Particle size distribution of HEMA-MBA synthesized at 150%CLD

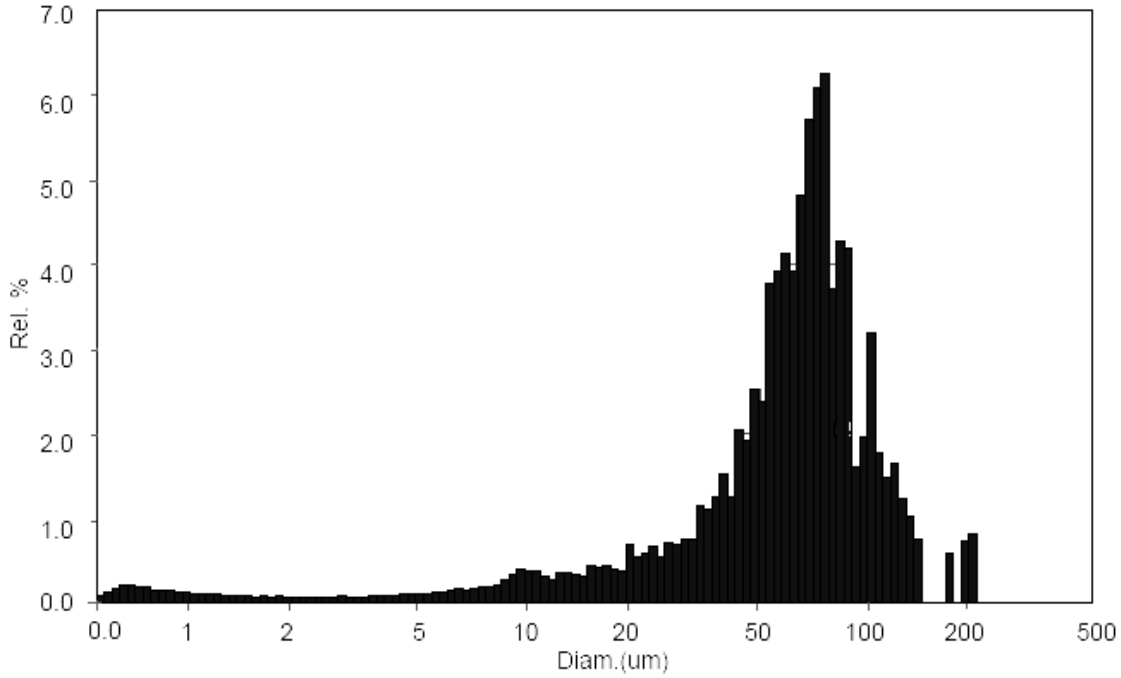

Figure 6.9. Particle size distribution of HEMA-MBA synthesized at 200%CLD

At high concentration of cross-linker (MBA) broad particle size distribution, between 5-200 μm was observed, as shown in Figures 6.7, 6.8 and 6.9. In this concentration range of MBA (100-150% CLD) the surfactants formed a strong film and it was very difficult to break the droplets into smaller size.

6.4.4 Variation in the surfactant concentration

The surfactant type and its concentration play a major role in determining the particle size and its distribution at constant stirring speed. Varying surfactant concentrations and its ratios with each other, different types of particle size distribution (PSD) can be achieved, as seen in Figures 6.10, 6.11, and 6.13. The poly(HEMA-MBA) beads synthesised using single surfactant Brij 92 (HEM 7) show bimodal particle size distribution in the range 0.2-50 μm. While, addition of very small amount of Brij 700 in the ratio 0.83:0.16 to the same composition shows drastic change in PSD as shown in

Figure 6.11 (HEM 8). HEM 8 shows bimodal PSD in the range 0.5-50 μm. HEM 9 also shows bimodal distribution with bigger particles in the range 20-200 μm and smaller particles in the range 1-20 μm (Figure 6.12), which was synthesised at 0.66:0.33 surfactant ratio.

The smaller the droplets are and the more collisions they undergo, the denser the coverage of the particles with surfactant must be to keep the HIPE O/W inverse emulsion stable. Interfacial surface tension can be used as a measure for the coverage of particles. As can be derived from the surface tension values, the particle surfaces of the droplets are incompletely covered with surfactant molecules because the surface tensions of the droplets lie well above the values of the saturated surfactant solution. The smaller the particles are, the lower the surface tension is and, therefore, the coverage of the particles with surfactant increases with decreasing particle size. However, as we go on increasing the concentration of Brij 700, the bimodal distribution of droplet size goes on increasing up to 200μm (Figure 6.12) indicating that there are different types of droplet breakage. Normally, small droplets merge into series of large droplets due to viscous shear force and Ostwald ripening, fluctuations of pressure, or relative speed, which results in disappearance of bimodal distribution, as shown in Figures 6.13, 6.14 and 6.15.

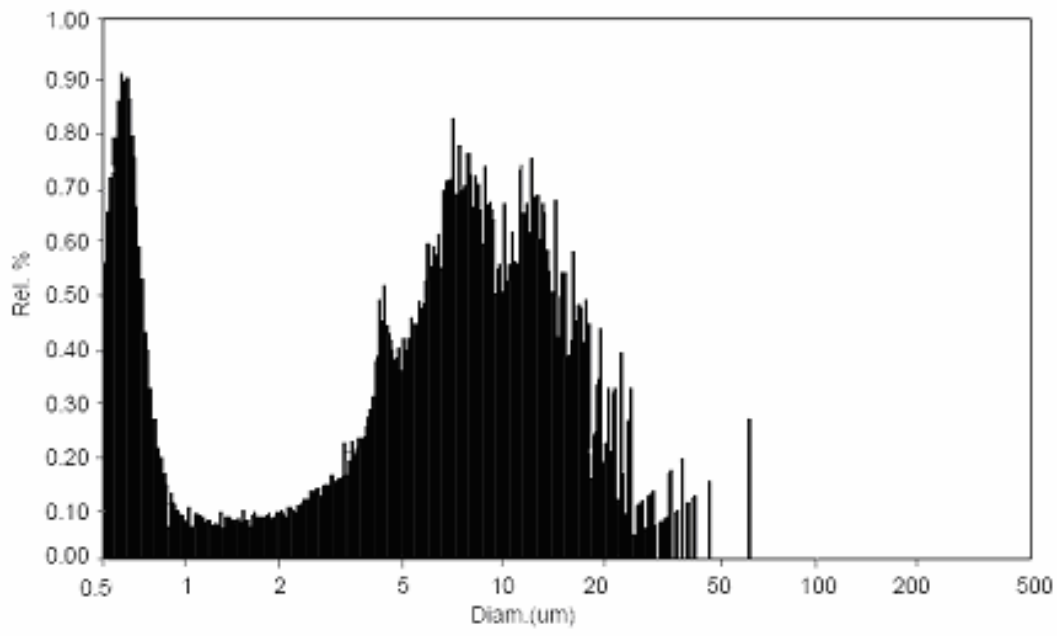

Figure 6.10. Particle size distribution of poly(HEMA-MBA) beads with 100% Brij 92.

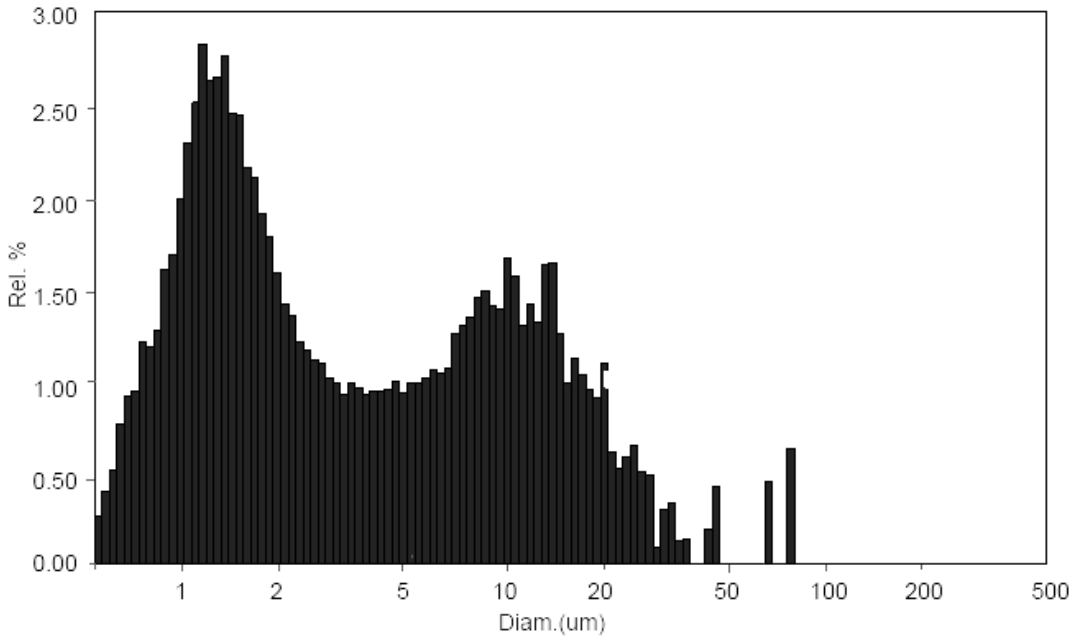

Figure 6.11. Particle size distribution of poly(HEMA-MBA) with 0.83: 0.16 Brij 92 to Brij 700 surfactants ratio

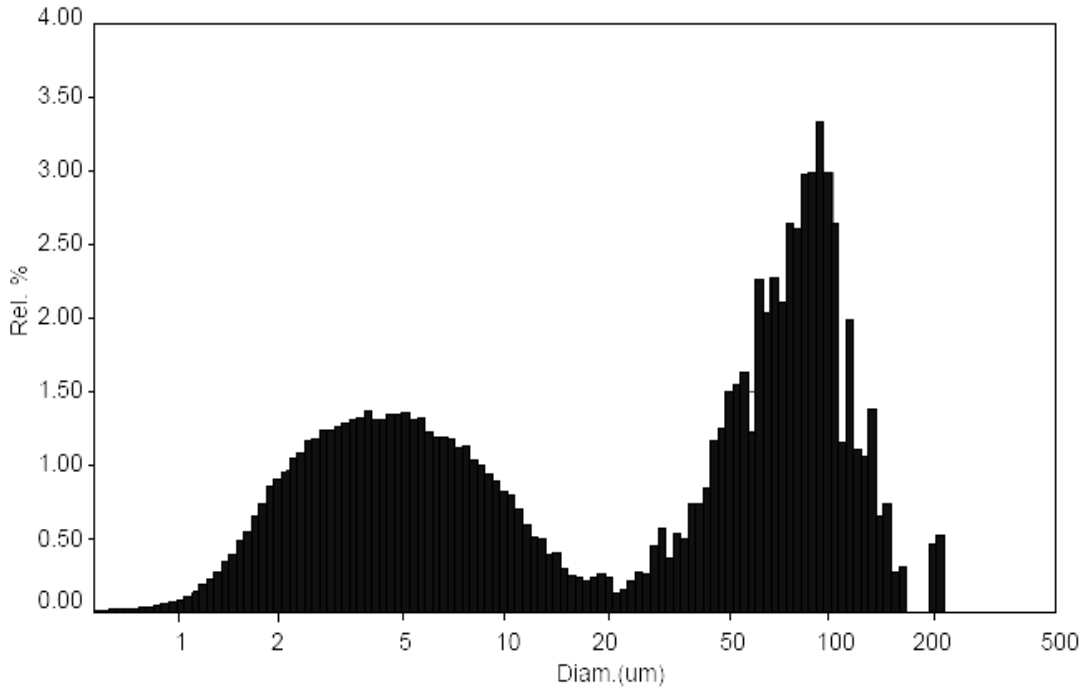

Figure 6.12. Particle size distribution of poly(HEMA-MBA) beads with 0.66: 0.33 Brij 92 to Brij 700 surfactants ratio

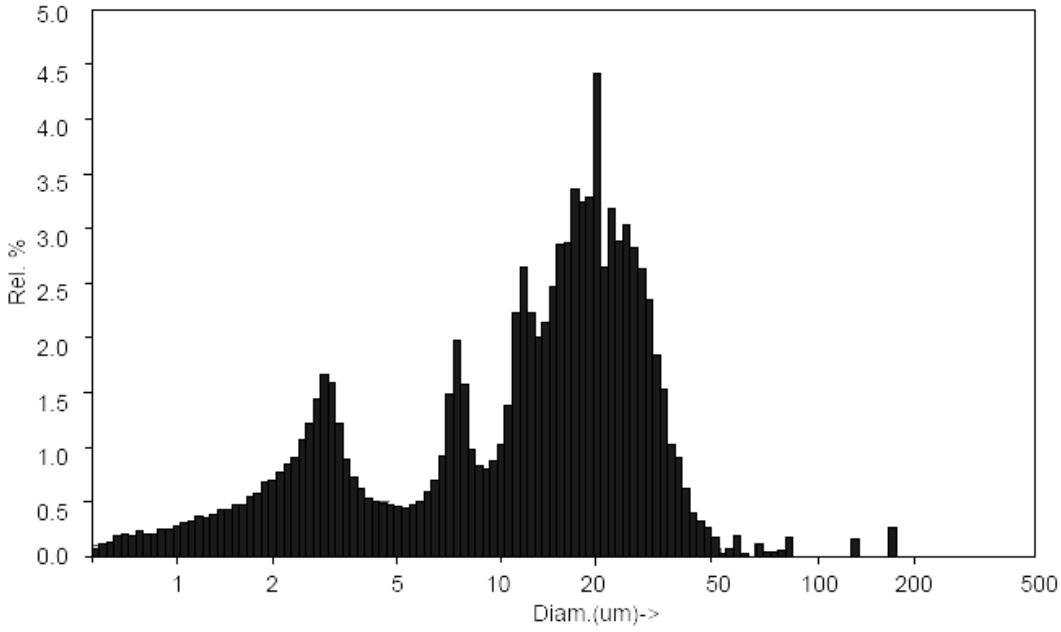

Figure 6.13. Particle size distribution of poly(HEMA-MBA) beads with 0.33: 0.66 Brij 92 to Brij 700 surfactants ratio

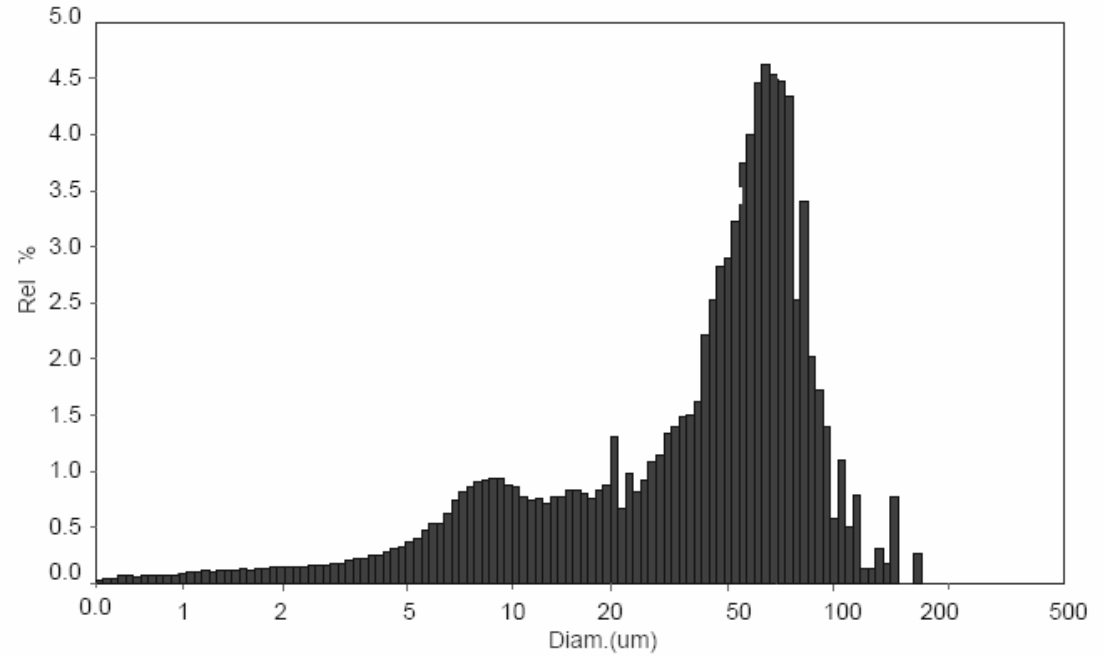

Figure 6.14. Particle size distribution of poly(HEMA-MBA) beads with 0.16: 0.83 synthesized using Brij 92 to Brij 700 surfactants ratio

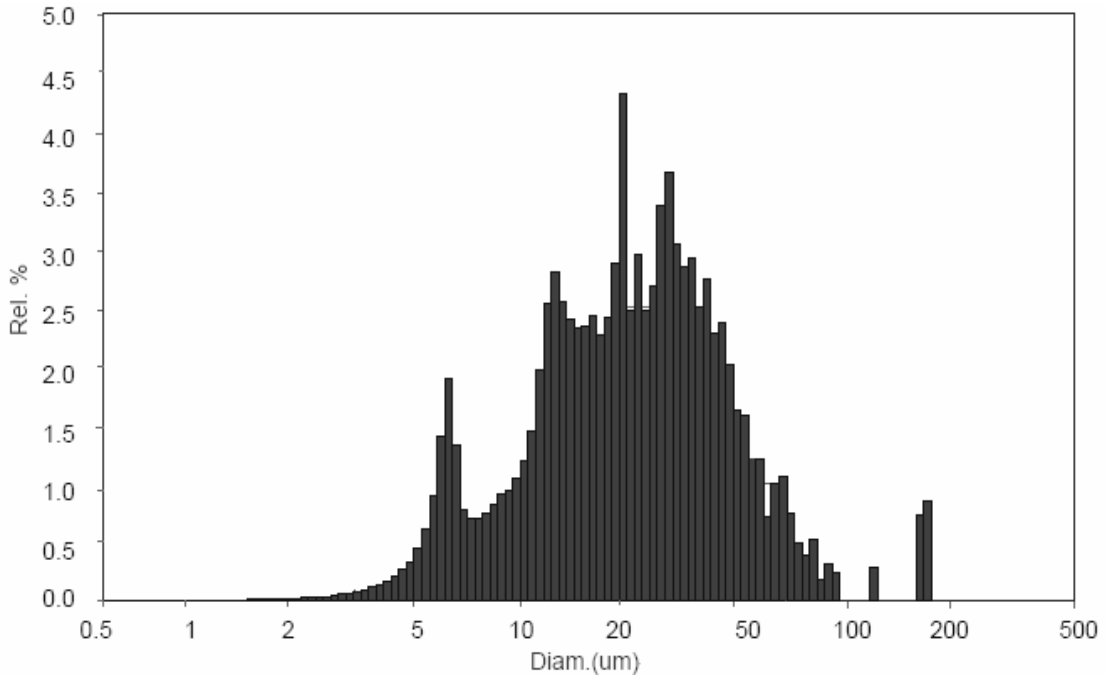

Figure 6.15. Particle size distribution of poly(HEMA-MBA) beads with 100% Brij 700

At 100% Brij 700 concentration, bimodality in PSD almost disappeared, as seen in Figure 6.15. It shows broad distribution in the range 2-100 μm. The concept of droplet breakage explains the bimodal distribution of droplet sizes well in multiple inverse emulsions. Therefore in the inverse O/W/O HIPE emulsion the ratio of surfactant to co-surfactant plays a very important role in the final particle distribution, which may be due the effect of stability of O/W emulsion, interfacial surface tension, Ostwald ripening, etc.

6.4.5 Pore size distribution, pore volume, surface area and morphology

Mercury penetration is a well-established method for the determination of pore-size distribution for pores in the size range 200–10,000 Å. Nitrogen adsorption is suitable for the measurement of micropores (20Å) and mesopores (20–500 Å), with a practical upper limit of 250 Å radius, based upon the classification adopted by IUPAC.[37]

According to Cheng et al.[37] these two methods are best regarded as complementary, for each becomes uncertain as the pore size range approaches a limit: nitrogen adsorption at the upper end of the mesopore range, and mercury at the lower end. The very high pressure involved in the detection of small pores in mercury porosimetry may raise the potential problem of collapse of the polymer matrices. Therefore, when samples are exposed to increasing pressure of mercury during the pore size distribution measurements, the polymer matrices are likely to be compressed and thin walls broken down. In the present study, the pore-size distribution has been measured by nitrogen desorption (10–2000 Å) and mercury intrusion method (50–5000 Å). The cumulative pore-size distribution of the dried samples has been measured at different times during the polymerisation process by the nitrogen desorption isotherm and

the mercury intrusion method for all systems. The differential pore-size distribution is based on a combination of nitrogen desorption and mercury intrusion.

The HEMA-MBA copolymer particles synthesised by inverse HIPE are highly meso and macroporous, having large surface area and particle size ranging within 2 to 100 micrometer. Nitrogen adsorption / desorption method were used to characterise the porous structures of HEMA-MBA spheres at different cross-link densities and also at different surfactant ratios. The BET equation was used to analyse the nitrogen adsorption isotherms and to calculate the surface areas of the particles. The complete nitrogen - desorption isotherm was measured and analysed for pore structure. The type of isotherm observed is indicative of the presence of both macropores, which fill with nitrogen at low pressure, and mesopores, which fill with nitrogen as the pressure increases. The characterisation data of HEMA-MBA particles are summarised in Table 6.1.

As stated above, the pore size distribution obtained indicates the presence meso- as well as macroporous structures in HEMA-MBA copolymer series. HEM 1 (25% CLD), HEM 2 (50% CLD) and HEM 3 (75% CLD) copolymers show the formation of macropores with average pore radius 225 nm, 350 nm and 452 nm, respectively [Figure 6.16]. This is due the formation of large channels. It generates very high pore volumes as shown in Table 6.1.

The relatively low hydrophilic monomer phase diffuses into the discontinuous oil phase. At higher cross-link density, [HEM 4 (100% CLD), HEM 5 (150% CLD) and HEM 6 (200% CLD)], the pores are meso- and macroporous, while the distribution is relatively narrow, in the 0.5-100 nm diameter range.

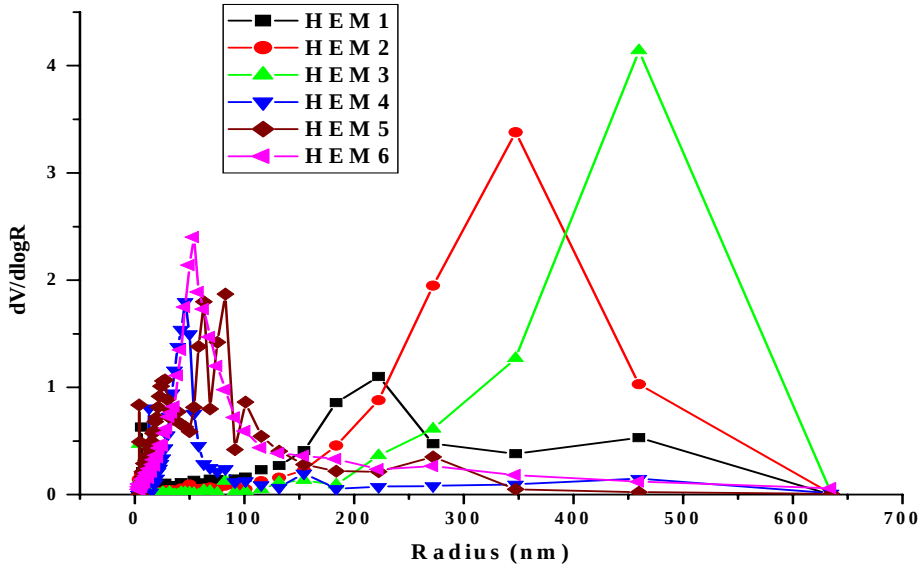

Figure 6.16. The pore size distribution curves of porous poly(HEMA-MBA) beads prepared from differing cross-link densities

At high MBA concentration the monomer phase is slightly more hydrophilic and surfactant concentration are enough to make it highly stable by forming a strong thin film at the oil and water interface. During this the film around the droplets gets ruptured and forms a small hole, which interconnects the pores. This interconnected pores form the micro-channels within the matrix and give narrow pore size distribution with very high surface areas, as shown in Table 6.1. At very high 100, 150 and 200 % CLD, HEMA-MBA copolymers have very high surface areas such as 113.17, 128.62 and 189.78 m^2/g respectively compared to HEMA-MBA copolymers with 25, 50 and 75 % CLD, which have relatively lower (89.21, 100.54 and 90.46 m^2/g) surface areas.

At a fixed CLD and surfactant concentration, the average pore diameter goes on decreasing from 234 nm to 24 nm as the relative concentration of Brij700 with respect to

Brij 92 is increased (Table 6.2, Figure 6.17). The pore size distribution shifts towards the micro region.

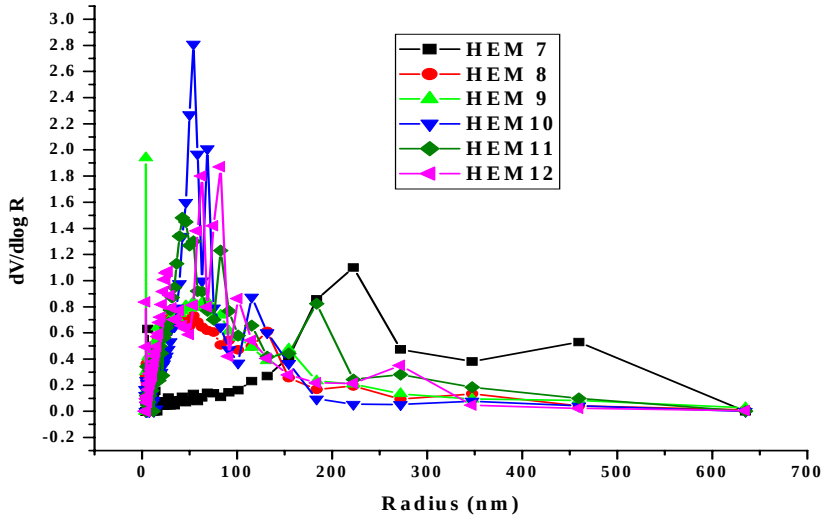

Figure 6.17. The pore size distribution curves of porous poly(HEMA-MBA) beads prepared with differing surfactant ratios

All copolymers within this series had narrow pore size distribution and the porous structure was uniform. This narrow pore size distribution arises during polymerisation due to the close packing of droplets with the proper choice of nonionic surfactant used i.e. Brij 92 and Brij 700, which is not possible in conventional emulsion methods.

Figures 6.18 (a), (c) and (e) show narrow pore size distribution at 25, 75 and 200% CLD. Figures 6.18 (b), (d) and (f) show the surface morphology of HEMA-MBA copolymer particles at 25, 75 and 200% CLD. Large number of pore openings are formed with a mixture of low and high HLB surfactants which gives highly porous surface to the copolymers. Thus, cross-link density and surfactant concentration play very important role in the formation of porous structure in inverse O/W/O HIPE polymerisation with a redox initiator system.

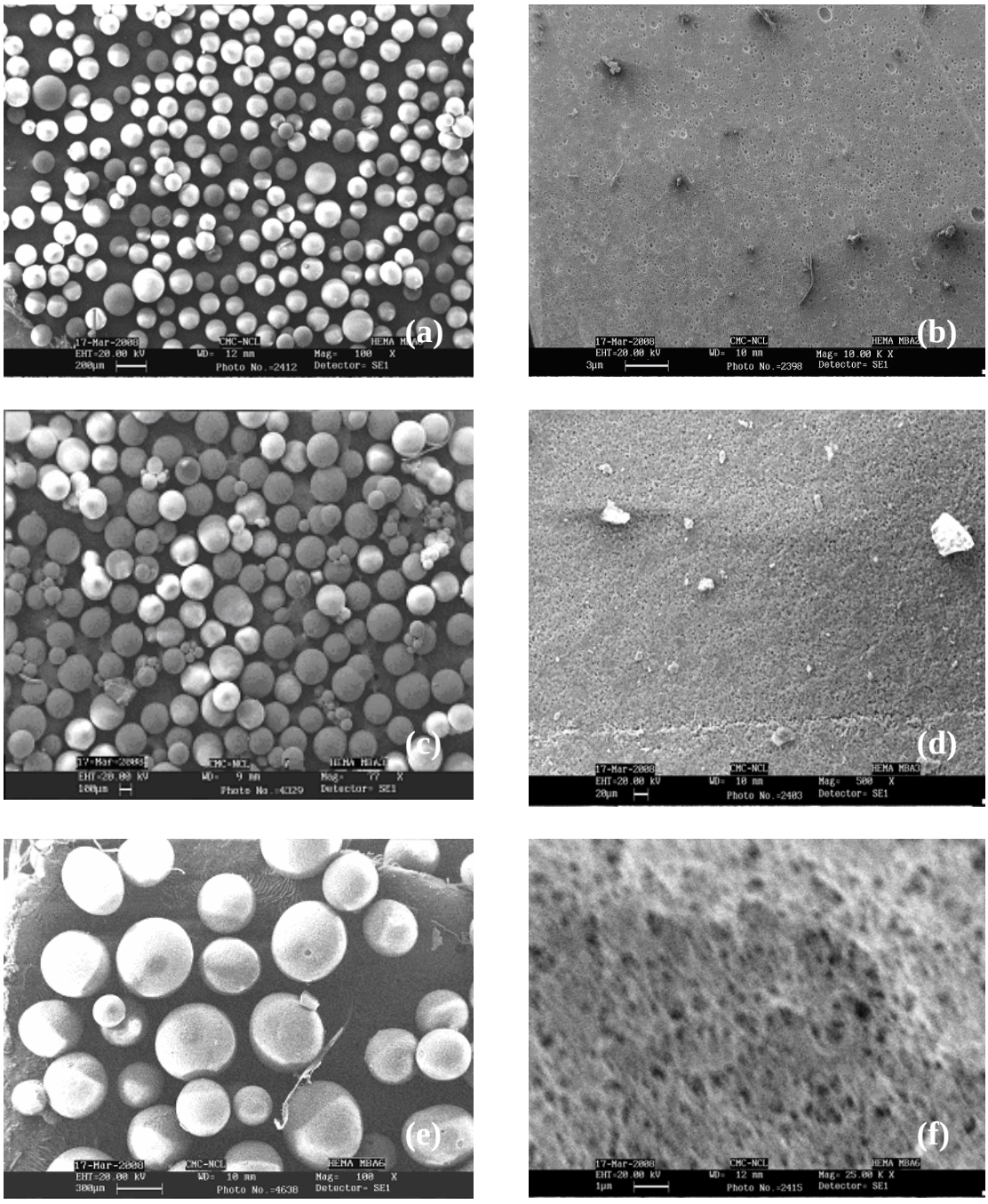

Figure 6.18. SEM micrographs (a, b) showing spherical nature as well as surface morphology of HEMA-MBA copolymer of 25% CLD, (c, d) at 75% CLD, and (e, f) at 200% CLD

A proper choice of HLB is critically important to stabilise more than 74% of inner discontinuous phase into the minor continuous monomer (HEMA) phase as small

droplets. This droplet gets converted into the pores in the final polymer. In Inverse HIPE, after a number of failed efforts, we were able to stabilise the O/W emulsion using a combination of low and high HLB nonionic surfactant of Brij 92 and Brij 700.

When the primary emulsion was poured into the third oil phase O/W emulsion was dispersed and Tween 80 acted as a stabiliser to prevent coalescence between to droplets. Tween 80 forms a small thin film around the droplets, which does not let inner oil phase to come into the outer oil phase. So inner oil droplets remain entrapped into the primary emulsion droplets, which are dispersed in the outer oil phase under constant stirring. Figures 6.19 (a), (c) and (e) show the bimodal nature of HEMA-MBA copolymer particles synthesised using a combination of Brij 92 and Brij 700 surfactants in wt.%/wt.% ratios of 0.83:0.16, 0.66:0.33 and 0.16:0.83 at constant HEMA to MBA ratio. These entrapped cyclohexane droplets were removed after the polymerisation by evaporation or by soxlet extraction leaving behind porous channels. Figures 6.19 (b), (d) and (f) show the surface morphology of HEMA-MBA copolymers synthesised using different surfactant ratios such as 0.83:0.16, 0.66:0.33 and 0.16:0.83, respectively. Nitrogen adsorption analysis shows that all HEMA-MBA copolymers are microporous and mesoporous and exhibit large intrusion volume and surface area due to presence of micro-channels in the particles.

In the absence of Brij 700, HEMA-MBA copolymer HEM 7 synthesised shows a broad pore size distribution in the range 50 to 600 nm at 25% cross-link density and fixed water to oil ratio. HEM 8 also shows quite broad pore size distribution in the 0.5 to 300 nm range. There is absence of interconnected pores or presence of dead ended pores

because the values of surface area and pore volume are low. HEM 7 and HEM 8 copolymers have 56.13 and 87.34 m^2/g surface area, respectively.

When Brij 700 was added in small amount the pore size distribution shifted towards micro and mesoporous region, as seen in Figure 6.17. A small amount of high HLB Brij 700 enhances the stability of emulsion by increasing the viscosity of emulsion in the primary O/W stage. A large amount of oil phase is able to occupy maximum space available in the continuous monomer phase without merging into other droplets. At this time, there is deformation of discontinuous oil droplets and formation of bottleneck type pores. As seen in Figure 6.17 increasing the relative concentration of Brij 700 results in the formation of micro and mesoporous porosity in the region 0.5 to 50 nm. Due to narrow pore size distribution, HEM 10, HEM 11, and HEM 12 give very high surface areas such as 142.67, 179.64 and 126.45 m^2/g (Table 6.2). In the absence of Brij 92 HEMA-MBA copolymers have very high pore volume (1.59 cm^3/g) and surface area mainly because of formation of both meso and micro channels.

SEM morphology of HEMA-MBA copolymers prepared by HIPE show the presence of a large number of open pores on the surface of the particles (Figure 6.19) which are absent in the HEMA-MBA copolymer particles prepared by the classical suspension technique. This methodology allows for greater control of morphology, which is useful in the efforts to generate functional polymeric materials for variety of applications.

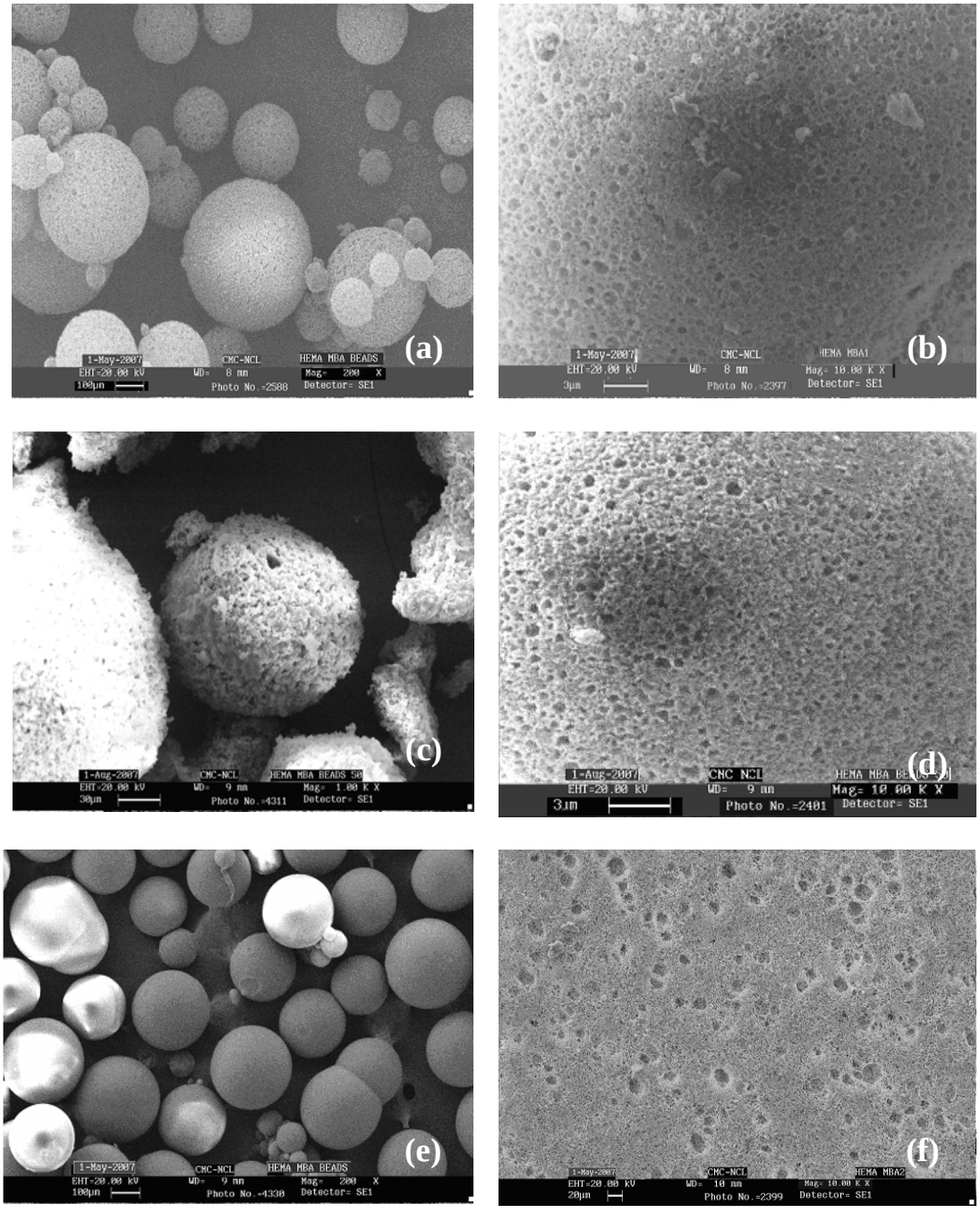

Figure 6.19. SEM micrographs (a, b) showing spherical nature as well as surface morphology of HEMA-MBA copolymers using wt./wt. ratios of Brij 92 to Brij 700 surfactants as (a, b) 0.83:0.16, (c, d) 0.66:0.33, and (e, f) 0.16: 0.83

6.5 Synthesis of HEMA-MBA monoliths

An alternative method to the preparation of highly porous monolithic polymethacrylates is polymerisation of high internal phase emulsion (HIPE) of monomers. HIPE is emulsion polymerisation where the internal aqueous phase represents more than 74 % of total emulsion volume. The materials prepared using this approach are highly porous and, usually, extremely permeable. The polyHIPE monoliths have an open cellular structure with interconnections, resulting from the internal phase being trapped inside the continuous phase during polymerisation. After extraction of the internal phase, a permanent porous structure persists. Although the preparation of these macroporous monoliths via bulk polymerisation required the use of porogenic solvents for pore formation, the mechanism of formation of poly(HIPE) monoliths is different compared to processes described above. An emulsion is a thermodynamically labile system that needs addition of surfactant to achieve stabilisation. Synthesising a HEMA-MBA polyHIPE meant preparation of the ‘‘reversed’’, oil-in-water-type emulsion instead of what has so far been used for polyHIPE preparations, namely water-in-oil emulsions. Switching the phases in the emulsion required switching the surfactants from the ones used for water-in-oil-type emulsions (typically sorbitan oleates) to the surfactants with higher HLB (hydrophilicity-lipophilicity balance) value.

The inverse polyHIPE was produced by the gradual addition of the oil phase, cyclohexane, drop-wise to the water phase (comprising HEMA, MBA, NaPS, ascorbic acid, Brij 92 and Brij 700) with vigorous stirring. The composition is shown in Table 6.3. The surfactant with the highest HLB value, combination of Brij 92 and Brij 700, gave an emulsion stable enough to withstand curing (29ºC, 18 h). After curing, purification, and drying, a white solid monolithic material was obtained as seen in Figures 6.20 (a) and (b).

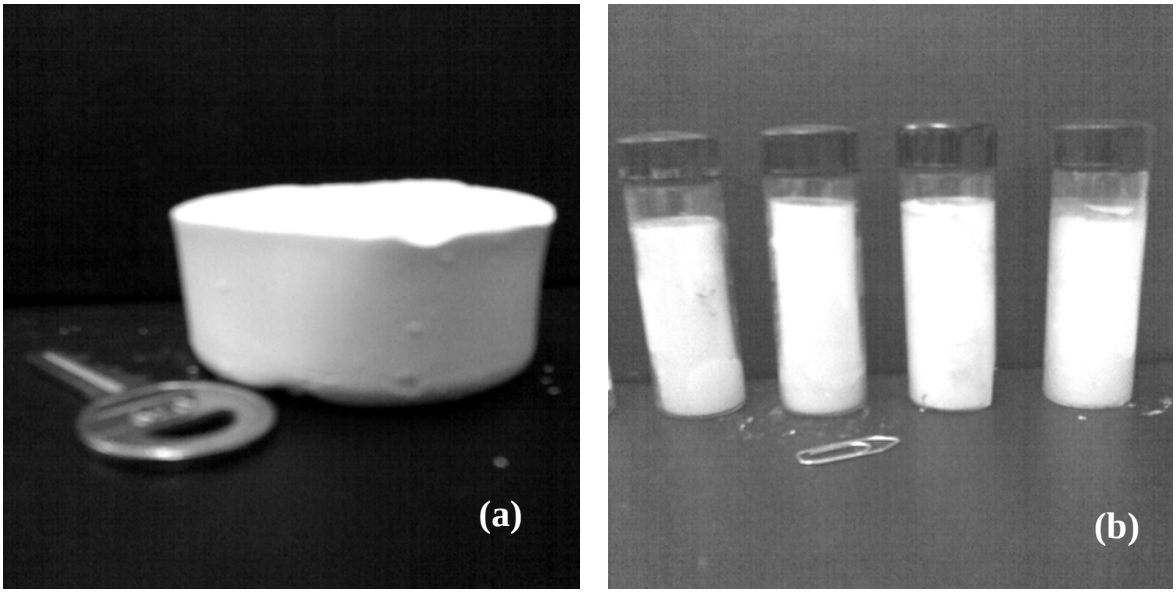

Figure 6.20. (a) HEMA-MBA copolymer monolith synthesised in plastic bottle, and (b) HEMA-MBA copolymer monoliths of differing CLD synthesised in glass vials

6.5.1 Pore structure

One of the criteria for an ideal monolith is that the porosity should be at least 90% so as to provide high surface area. HEMA-MBA copolymers were prepared by radical co-polymerisation of HEMA with N,N'-methylenebisacrylamide (MBA) as cross-linker using inverse O/W HIPE technique. The interior morphology of HEMA-MBA copolymer was observed using scanning electron microscopy (SEM). Scanning electron microscopy reveals a highly porous structure of HEMA-MBA copolymeric monoliths with smooth and thick but non-interconnected walls and large pores (pore size in the range 2-300 μm) at low CLD, when MBA content is very low (HEM 13, HEM 14 and HEM 15).

The porous structure of HEMA-MBA monoliths consists of distorted non-interconnected irregular shaped voids (50 to 250 μm) separated by porous walls (Figures. 6.21 a, b, c). This structure is quite different from the typical polyHIPE structure and this difference is reflected in the relatively low surface areas of 23.93, 30.71 and 36.05 m^2/g

(Table 6.3). The distorted structure and the relatively low surface area at this relatively low MBA content (low CLD) indicate a partial collapse during the polymerisation of the porous structure present at the HIPE emulsion making. Here, small pores in range of 0.5 to 3 μm are present in the walls of voids, as seen in Figure 6.21(c). These kinds of pores are ideally suited to water absorption applications because pores in the walls act as capillaries to suck in water during absorption of water.

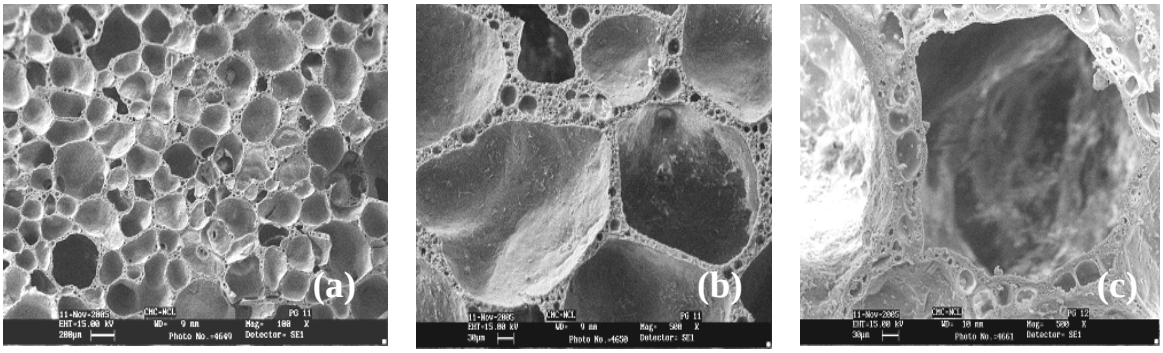

Figure 6.21. Internal morphology of HEMA-MBA monoliths synthesised at (a) 5% CLD, (b) 10 % CLD, and (c) 15% CLD

HEM 16 has a higher degree of cross-linking (25% CLD) and a completely different porous structure (Figures 6.22 a,b). The structure of HEM 17 (50% CLD) is reminiscent of a typical polyHIPE (Figures 6.22 c,d). There are voids, 2 to 50 μm in diameter, from the evacuated droplets of the organic phase. The pore volumes of copolymers HEM 16 and HEM 17 arise from micro- as well as macropores because surface areas, 101.32 m^2/g and 123.67 m^2/g, are relatively high, indicating bimodal nature of pores, as shown in Table 6.3. On the other hand, the hydrogel type walls in themselves have an unusual nanoscale porous structure (Figure 6.21 c).

The porosity of the polyHIPE walls reflects the relatively low monomer content in the continuous phase. The increase in cross-linking (MBA content) increases the tendency towards phase separation during polymerisation. Individual, localised gel

structures are formed in free radical polymerisation. These gel particles phase separate yielding water-swollen micro-gel particles that contain reactive groups on their surfaces. The micro-gel particles agglomerate, react, and form a nanoscale porous, heterogeneous polyHIPE wall.

At higher cross-link density, as in HEM 18 with 75% CLD, the pore structure (Figures 6.22 e, f) is similar. The surface area (82.41 m^2/ g) arises from a large number of interconnected windows. The copolymer has bimodal pore size distribution. Increasing the relative concentration of the cross-linking comonomer further (HEM 19)(100% CLD), however, destabilises the HIPE and leads to Ostwald ripening, merging the small droplets into larger ones (Figures 6.23 a, b).

These macroscopic voids were so prevalent that they caused a significant reduction in surface area from 82.41 m^2/g to 62.78 m^2/g and increase in the pore volumes from 0.75 cm^3/g to 1.24 cm^3/g due the formation of macroporous channels. Further increases in MBA content (HEM 20 and HEM 21) produced highly inhomogeneous, brittle polyHIPEs (Figures 6.23 c, d and Figures 6.23 e, f) giving surface areas 72.36 m^2/g to 79.21 m^2/g, respectively. Thus, there is only a narrow composition window, near 25-75% CLD, that can be used to synthesise homogeneous, highly porous, high surface area HEMA-MBA copolymer monoliths.

O/W inverse HIPE method gives the new way to synthesise the open porous HEMA-MBA monoliths at room temperature using redox inititor system. This room temperature synthesis of porous polymer will be very helpful for bio chemist because all the bioprocesses carried out at room temperature.especially for enzyme immobilization, enzyme denaturation using these porous polymers.

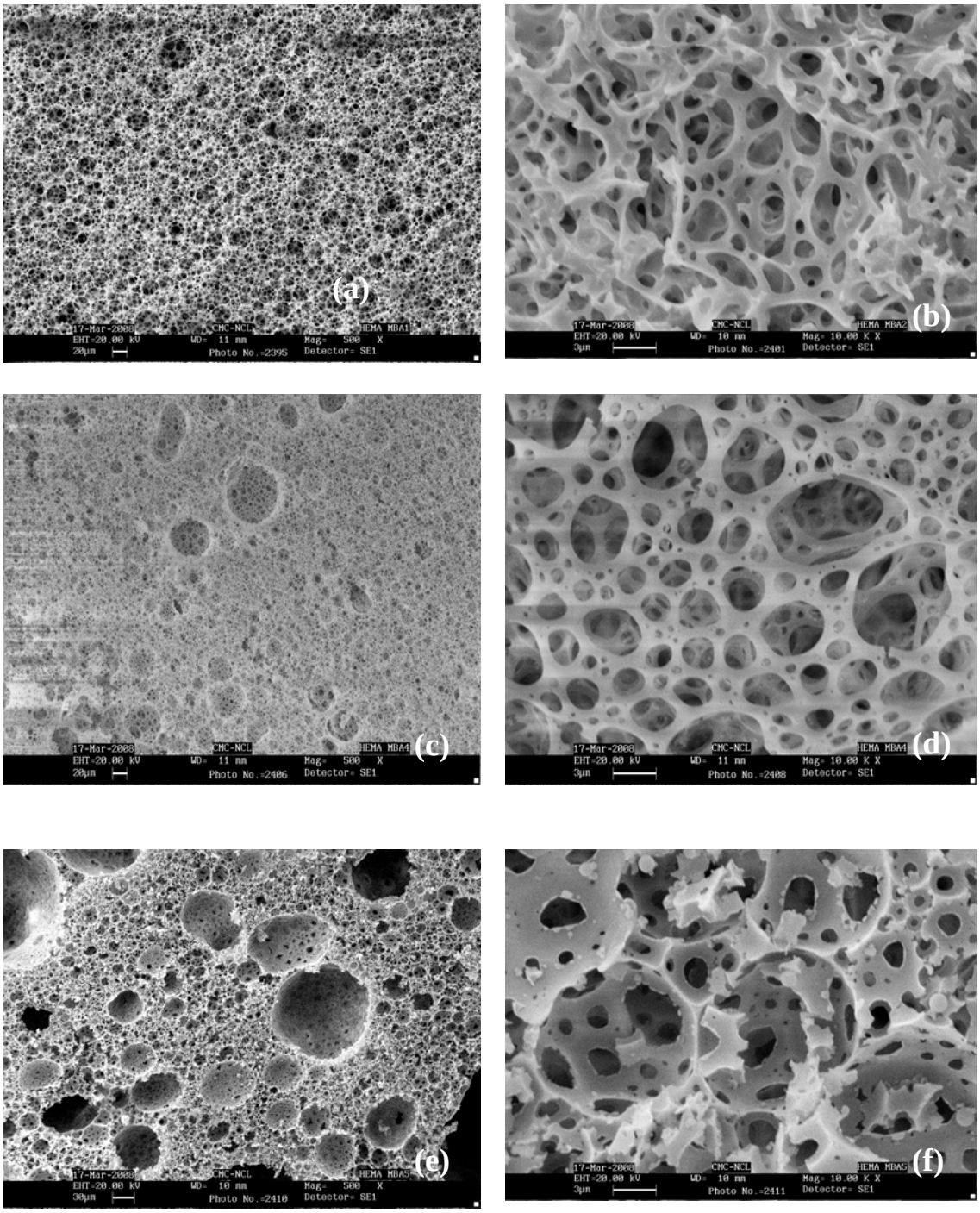

Figure 6.22. SEM micrographs (a, b) showing surface as well as internal morphology of HEMA-MBA at 25% CLD, (c, d) at 50% CLD, and (e, f) at 75% CLD

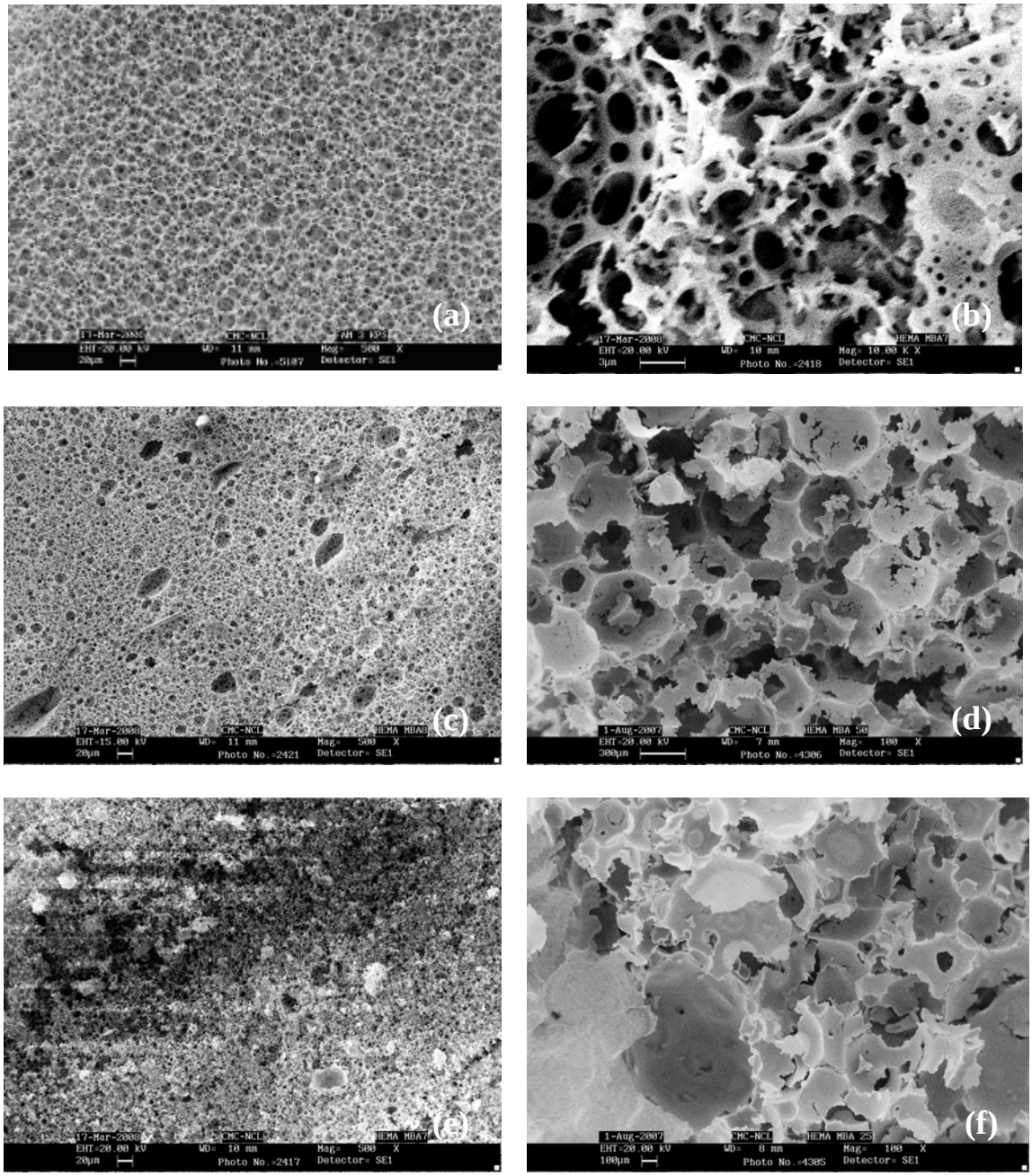

Figure 6.23. SEM micrographs (a, b) showing surface as well as internal morphology of HEMA-MBA at 100% CLD, (c, d) at 150% CLD, and (e, f) at 200% CLD

6.6 Conclusion

In this work, a new methodology has been established to produce well-defined open porous poly(HEMA-MBA) materials in beaded as well as monolithic forms by

inverse O/W/O and O/W HIPE emulsions with nonionic surfactants (Brij 92 and Brij 700). The free-radical copolymerisation was carried out at room temperature using sodium peroxydisulphate and ascorbic acid redox pair. The process of preparation of highly concentrated emulsions by mixing all components consists of three steps: (a) dispersion of the oil in the water phase, (b) coalescence of the oil droplets and formation of a multiple W/O/W emulsion, and (c) uptake of the external water phase of step (b) as internal phase until a W/O emulsion is formed. This process requires the initial O/W emulsion to be very stable against coalescence. With proper choice of initiator system and surfactant concentration, we were able to design materials, which have controllable porosity required for various biomedical applications. Ultimately, it is the influence of the MBA content on the copolymer hydrophilicity and on the porous structure that determines its effects on the properties.

References

[1] Guyot, A.; Bartholin, M. *Prog. Polym. Sci*. **1982**, *8*, 277.

[2] Kahovec, J.; Jelinkova, M.; Coupek, *J. Polym. Bull*. **1987**, *18*, 495.

[3] Hodge, P.; Sherrington, D. C. "*Syntheses and Separations Using Functional Polymers",* Wiley: New York **1989**.

[4] Piskin, E. *Int. J. Artif. Organs* **1986**, *9*, 289.

[5] Horak, D.; Sevec, L.; Kalal, J.; Adamyan, A.; Volynskii, O.; Voronkova, L. K.; Gumargalieva, K. *Biomaterials* **1986**, *7*, 467.

[6] Robert, C.; Buri, P. A.; Peppas, N. A. *J. Controlled Release* **1987**, *5*, 151.

[7] Kamei, S.; Okubu, M.; Matsumoto, T. *J. Appl. Polym. Sci*. **1987**, *34*, 1439.

[8] Stevenson, W. K. T.; Sefton, N. O. *Biomaterials* **1987**, *8*, 449.

[9] Mould, D. L.; Synge, R. L. M. *Analyst*. **1952**, 77, 964.

[10] Svec, F.; Tennikova, T. B.; Deyl, Z. *Monolithic materials: Preparation, Properties and Applications*, Elsevier, Amsterdam, **2003**.

[11] Lissant, K. J. editor. *Emulsion and Emulsion Technology*, part 1. New York: Marcel Dekker Inc.: **1974.**

[12] Barby, D.; Haq, Z. *Eur. Pat. Appl*. 60138, **1982.**

[13] Cameron, N. R.; Sherrington, D. C. *Adv. Poly. Sci*. **1996**, 126, 163-214.

[14] Mork, S. W.; Green, D. P.; Rose G. D. *US Pat. No*. 6,147,131, **2000.**

[15] Zhang, H.; Cooper, A. I. *Soft. Matter*. **2005**, 1, 107-13.

[16] Cameron, N. R. *Polymer* **2005**, 46, 1439-49.

[17] Menner, A.; Powell, R.; Bismarck, A. *Soft Mater* **2006**, 2, 337-42.

[18] Haibach, K.; Menner, A.; Powell, R.;Bismarck, A.; *Polymer* **2006**, 47,4513-9.

[19] Menner, A.; Powell, R.; Bismarck, A. *Polymer* **2006**, 47, 7628-35.

[20] Menner, A.; Powell, R.; Bismarck, A. *Macromolecules* **2006**, 39, 2034-35.

[21] Delamarche, E.; Juncker, D.; Schmid, H. *Adv. Mater*. **2005**, 17, 2911-2933.

[22] Wang, J., Electrophoresis **2002**, 23, 713-728.

[23] Miyazaki, M., Maeda, H., Trends Biotechnol. **2006**, 24, 463-470.

[24] Blanch, H. W.; Clark, D. S. *Biochemical Engineering; Marcel Dekker*: **1996.**

[25] Zhan, W.; Seong, G.H.; Crooks, R. M. *Anal. Chem*. **2002**, 74, 4647-4652.

[26] Heo, J.; Crooks, R. M. *Anal. Chem*. **2005**, 77, 6843-6851.

[27] Koh, W. G.; Pishko, M. *Sens. Actuators*, *B* **2005**, 106, 335-342.

[28] Zimmerman, S.; Fienbork, D.; Flounders, A. W.; Liepmann, D. *Sens. Actuators-B* **2004**, 99, 163-173.

[29] Svec, F.; Tennikova, T. B.; Deyl, Z. Eds. *Monolithic materials: preparation, properties, and application*; Elsevier; **2003.**

[30] Petro, M.; Svec, F.; Frechet, J. M. J. *Bitechnol. Bioeng*. **1996**, 49, 355-363.

[31] Tsai, E. C.; Dalton, P. D.; Shoichet, M. S.; Tator, C. H. Synthetic hydrogelguidance channels facilitate regeneration of adult rat brainstem motor axons after complete spinal cord transection. J Neurotrauma, submitted for publication.

[32] Cameron, N. R. *Journal of Materials Chemistry*, **2000**, 10(11), 2466-2471.

[33] Dalton, P. D.; Tsai, E.; Van Bendegem, R. L.; Tator, C. H.; Shoichet, M. S. *Hydrogel nerve guides promote regeneration in the central nervous system*. Tampa Bay, FL: Society for Biomaterials; **2002**.

[34] Winslow, F. H.; Matreyek, W. *Particle size in suspension polymerisation*. *Ind. Eng. Chem.* **1951**, *43*, 108-112.

[35] Higuchi, W. I.; Misra, J. *J. Pharmaceutical Sci*. **1962**, 459- 466.

[36] Danov, K. D.; Denkov, N. D.; Petsev, D. N.; Ivanov, I. B.; Borwankar, R. *Langmuir* **1993**, 9, 1731-1740.

[37] Cheng, C. E.; Micale, F. J.; Vanderhoff, J. W.; El-Aasser, M. S. *J. Colloid Interface Sci*. **1992**, 150, 549.

Chapter VII

Morphological study of Porous polymeric monoliths

7 Morphological study of porous polymeric monoliths

7.1 Introduction

Porosity represents an important structural feature of many inorganic and organic materials. Organic/polymeric, porous monolithic materials are of particular interest because of their intriguing properties in many areas of materials research.[1] The term monolith refers to unibody structures composed of interconnected repeating cells or channels.[2] Richard Synge in 1952 envisioned a continuous block of porous gel structure.[3] In the late 1980s, many researcher developed novel approaches to synthesise monoliths in various forms such as compressed hydrophilic gels, macroporous polymer discs, columns, tubes, as well as silica rods.[4]

Porous polymer monoliths became the research interest for Svec and Fre´chet in early 1990s.[5] The porous polymer rods prepared were shown to be an alternative to columns packed with polymeric beads or particles.[6] The monolith columns could be connected to chromatographic systems immediately after the synthesis, circumventing most problems associated with tedious column packing protocols.[7] Monoliths are typically characterised by interconnected pores with a bimodal distribution: the small pores provide the desired surface area required for the specific interactions, while the larger channels allow a high flow rate at moderate pressures. Therefore, additional advantages of using such monoliths in chromatography would be increased speed, capacity and resolution. Different monoliths available are depicted in Figure 7.1.

Emulsion templating is a versatile method for the preparation of well-defined open porous monoliths. In general, the technique involves forming a high internal phase emulsion (HIPE) (= 75% v/v internal phase).[8-17] The liquid but highly viscous nature of

HIPEs allows the continuous phase to be given any shape that conforms to the shape of the reaction vessels.[17]

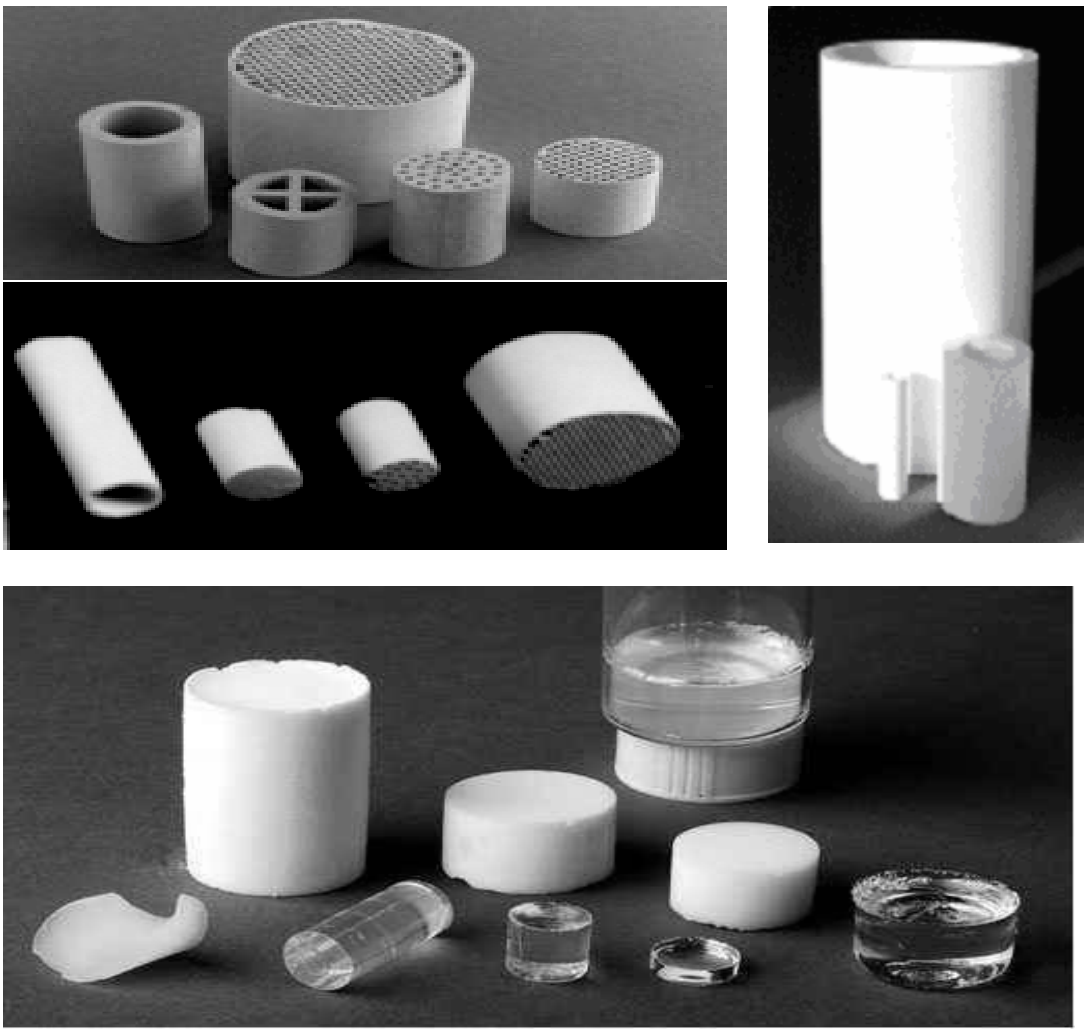

Figure 7.1. Porous monoliths in different forms

The polymerisation of HIPEs (W/O) provides a direct synthetic route to a variety of novel, porous monoliths (polyHIPEs) for applications as biological tissue scaffolds,[18-22] sensor materials,[23] catalysis supports,[24-26] and ion-exchange resin.[27] Over the past two decades, significant advances have been recorded on polyHIPEs due to several research groups. Surfactants used were either non-ionics or the mixture of non-ionic with ionics.[8-28] Hitherto, it has been considered impossible to prepare W/O HIPE with only ionic

surfactant,[29] because ionic surfactants (e.g., cetyltrimethyl ammonium bromide (CTAB)) contradict the Bancroft rule and are water-soluble. The rule states that the liquid phase in which the surfactant has greater solubility would form the external or continuous phase.[30]

Only nonionic surfactants are suitable for W/O HIPE because ionic surfactants are water-soluble. Bancroft rule states is that contrary to common sense, what makes an emulsion oil-in-water or water-in-oil is not the relative percentages of oil or water, but in which phase the emulsifier is more soluble in.[31,32] So, even though there may be a formula that's 60% oil and 40% water, if the emulsifier chosen is more soluble in water, it will create an oil-in-water system and if the emulsifier chosen is more soluble in oil, it will create a water-in-oil system. Thus, rule of thumb is: for oil-in-water emulsions – use emulsifiers that are more soluble in water than in oil (High HLB surfactants). In water-in-oil emulsions – use emulsifiers that are more soluble in oil than in water (Low HLB surfactants).

All surfactant molecules comprise of oil loving part and a water-loving part. HLB scale was invented 60 years back by William C. Griffin of the Atlas Powder Company. The hydrophilic group of the surfactant is usually a polyhydric alcohol or ethylene oxide, and the lipophilic or hydrophobic group is usually a fatty acid or a fatty alcohol. HLB is calculated by dividing the molecular weight of water-loving portion of the surfactant by 5, which will give the HLB value of the surfactant. HLB value is an indication of the solubility of the surfactant, the lower the HLB value the more lipophilic or oil soluble the surfactant is and higher the HLB value the more water-soluble or hydrophilic the surfactant is. It is better to use a blend of two surfactant mixtures of a low HLB and a

high HLB because it will give better coverage at the interface. HLB required for each application needs is presented in Table 7.1.

Table 7.1. Required HLB values for emulsion

Purpose	Required HLB
Making water in oil emulsions	4-6
Wetting powder into oil	7-9
Making oil in water emulsions	8-16
Making detergent solution	13-15
For solubilizing oil into water	13-18

The heterogeneous structure can be used as a template for the production of a variety of materials with different morphologies. For example, curing of the droplet phase leads to agglomerates of particles, which have been studied extensively by Ruckenstein.[33] Conversely, solidification of the continuous, or nondroplet phase produces porous materials since polymerisation occurs around and between the emulsion droplets.[34-37] Depending on the condition, the droplets either remain trapped within the solid matrix or can be removed, resulting in closed and open cell solid foams, respectively.

The latter type of material is arguably the most interesting from an application point of view; such materials have been termed polyHIPE and have been the subject of considerable study. An extremely low dry bulk density, typically less than 0.2 g/cm^3, characterises the open-cell polymers, which is due to complete interconnection between all neighbouring cells. The morphology of these solid foams is determined by the structure of the emulsion prior to gel point and so is dependent on emulsion stability, as

defined by such factors as surfactant type and content, temperature, type of initiator, composition of the emulsion phases, preparation conditions such as shear rate, and so on.

One application of HIPEs is as templates to create highly porous structures. Such materials, formed by curing the continuous, or non-droplet phase of the emulsion, are known polyHIPEs. Following solidification of the continuous phase, the emulsion droplets are embedded in the resulting material. Under the correct conditions (vide infra), small interconnecting windows are formed between adjacent emulsion droplets allowing the droplet phase to be removed by drying. This produces a highly porous and permeable material. The spherical cavities in the material are referred to as 'cell'. Secondly, the interconnecting pores between each cell and its neighbours are referred to as 'windows'. Finally, the much smaller holes present within the walls of certain PolyHIPE materials are known as 'pores'.

Porous materials are characterised by their size distribution, shape, pore size, extent of interconnectivity and amount of porosity (open or closed). In this chapter, investigation into influence of synthesis parameter on the porous characteristics, morphology of the resultant polyHIPE polyacrylates are all presented.

7.2 Experimental

7.2.1 Materials

Monomers such as 2-ethyl hexyl acrylate (EHA), 2-ethyl hexyl methacrylate (EHMA), and ethylene dimethacrylate (EGDM) and surfactants such as poly(alkylglycerol succinate) and ditallow dimethyl ammonium methyl sulphate (DTDMAMS) were used as received. Sodium peroxydisulphate (NaPS), potassium peroxydisulphate (KPS), ammonium peroxydisulphate (APS), benzoyl peroxide (BPO),

2,2'-Azobisisobutyronitrile (AIBN), and calcium chloride received form MERCK and were used as received. De-ionised water was prepared from distilled water with a Millipore unit and this ultra-pure deionised water had a resistivity of 18.31 MΩ·cm.

7.2.2 Synthesis of HIPE monoliths

In a typical experiment, the oil phase (1 g) comprised of monomer and surfactant, as shown in Table 7.2, was taken in a 250 mL cylindrical plastic bottle. It was then fixed on the overhead stirrer having 1400 rpm.

Table 7.2. Composition of acrylic polyHIPEs

Expt No	**Initiator**					**Inhibitor**
	Water soluble			Oil soluble		
	APS (mole x 10^{-5})	NaPS (mole x 10^{-5})	KPS (mole x 10^{-5})	BPO (mole x 10^{-5})	AIBN (mole x 10^{-5})	Phenothiazine (mole)
HIPE 1	5.69	-	-	-	-	-
HIPE 2	-	5.46	-	-	-	-
HIPE 3	-	-	4.80	-	-	-
HIPE 4	-	-	-	5.36	-	-
HIPE 5	-	-	-	-	7.91	-
HIPE 6	-	5.46	-	5.36	-	-
HIPE 7	-	5.46	-		7.91	-
HIPE 8	-	5.46	-	-	-	$5.42x10^{-7}$
HIPE 9	-	5.46	-	-	-	$1.08x10^{-6}$
HIPE 10	-	5.46	-	-	-	$1.62x10^{-6}$
HIPE 11	-	5.46	-	-	-	$2.16x10^{-6}$

2-Ethylhexyl acrylate (EHA) =0.0020 mol, 2 -ethyl hexyl methacrylate (EHMA) = 0.0019 mol; ethylene dimethacrylate (EGDM) = 0.0008 mol; water = 27 mL, $CaCl_2$ =1.08 g (4 wt.%), poly(alkylglycerol succinate) = 6.5%; DTDMAMS = 0.8%; Temp = 65ºC; Constant stirring speed =1400 rotation per minute.

APS = ammonium peroxydisulphate; NaPS = Sodium peroxydisulphate; KPS = Potassium peroxydisulphate; BPO = benzoyl peroxide; AIBN = 2,2'-Azobisisobutyronitrile; DTDMAMS = ditallow dimethyl ammonium methyl sulphate.

Table 7.3. Composition of acrylic polyHIPEs synthesised varying different surfactant concentrations

Expt No	Surfactant			Temperature (ºC)	Stirring speed (RPM)
	Concentration to monomer phase %	S1 g	S2 g		
HIPE 12	100	0.065	0.008	65	1400
HIPE 13	100	0.065	0.008	75	1400
HIPE 14	100	0.065	0.008	85	1400
HIPE 15	30	0.0195	0.0024	65	1400
HIPE 16	40	0.0260	0.0032	65	1400
HIPE 17	50	0.0325	0.0040	65	1400
HIPE 18	60	0.039	0.0048	65	1400
HIPE 19	70	0.0455	0.0056	65	1400
HIPE 20	80	0.0520	0.0064	65	1400
HIPE 21	90	0.0585	0.0072	65	1400
HIPE 22	100	0.065	0.008	65	1400
HIPE 23	100	0.065	0.008	65	250
HIPE 24	100	0.065	0.008	65	500
HIPE 25	100	0.065	0.008	65	700
HIPE 26	100	0.065	0.008	65	1000
HIPE 27	100	0.065	0.008	65	1400

2-Ethylhexyl acrylate (EHA) = 0.0020 mol; 2-ethyl hexyl methacrylate (EHMA) = 0.0019 mol; ethylene dimethacrylate (EGDM) = 0.0008 mol; water = 27 mL; $CaCl_2$ =1.08 g (4 wt.%); S1 = poly(alkylglycerol succinate); S2 = DTDMAMS = dialkyl dimethyl ammonium methyl sulphate; RPM = rotations per minute.

After complete homogenisation at a constant speed of 1400 rpm with a Ruston turbine agitator, the aqueous phase comprised of water, calcium chloride and initiator

maintained at 65ºC, was added drop-wise. After addition, the emulsion was stirred for 5 minutes. The resulting W/O emulsion is called HIPE of large internal phase volume. The plastic bottle with HIPE emulsion was kept in oven and polymerised at 65ºC for 12 h. The monoliths could be easily removed from the plastic bottles.

The monoliths were washed thrice with the distilled water to remove calcium chloride. Final traces of water present in the monoliths were squeezed out under vacuum. The monoliths were then sliced into 4-6 mm thick cylindrical sections.The dried foam slices were stamped using 1 inche circular die to produce 25 mm discs. Each slice was then placed in an oven set at 70-75ºC. To see the effect of different synthesis parameters on morphology of porous monoliths, experiments were carried out varying the composition as given in Tables 7.2 and 7.3.

7.3 Characterisation

7.3.1 Optical microscopy

Optical microscopic photographs of HIPE emulsion were taken using Olympus BX 50 microscope by dispersing by micropipette a drop of emulsion prior to gelation. The average droplet size was estimated with an image analysis software (Image pro).

7.3.2 Internal morphology and cell sizes by SEM

SEM is a useful tool to analyse morphology of low-density micro cellular foams. A close examination of the micrographs allows the estimation of average cell size at high magnification, where as at lower magnification, the medium range homogeneity of the structure can be appreciated with some accuracy. SEM micrographs of the synthesised foams were recorded at two different magnifications, 2000 and 5000x to facilitate textural comparison, using a JEOL model JSM-5200 SEM operating at between 20–25

kV. The dried foams were carefully sliced into 1x 5x 5mm thickness pieces, mounted on double sided conducting carbon pads, attached to aluminium stubs and gold coated using sputter coater. The average cell size was estimated using image analysis software. The diameter of fifty voids chosen at random from an SEM image of the material were determined and entered into an Excel spreadsheet, from which a distribution plot of frequency versus diameter range was constructed.

7.3.3 Surface area measurement

Polymer surface areas and pore volumes were measured using the BET method using a monosorb surface area analyser (Quantachrome Corp., U.S.A.), based on dynamic adsorption/desorption technique. Samples were out gassed for 3 h at 60ºC under N_2 flow before analysis. In mercury intrusion porosimetry, low density HIPE samples usually collapsed under high pressure. Therefore, BET alone gives an accurate estimate of surface area.

7.4 Results and discussion

PolyHIPE materials have complex morphologies. They possess spherical cavities, known as cells, and windows that interconnect these cells. Furthermore, a much finer porous texture within the walls of the base material can be created.

Types of cells formed are very much dependent on composition of emulsion as well as the synthesis parameter (stirring speed, temperature). As shown in Figure 7.2 (a) the cells formed are spherical with thick walls between the oil/water interfaces. Large numbers of small pores are formed at the walls. Similarly, very thin walls with spherical cells (with no pores on the wall) are formed on changing the surfactant concentration (Figure 7.2 (b)).

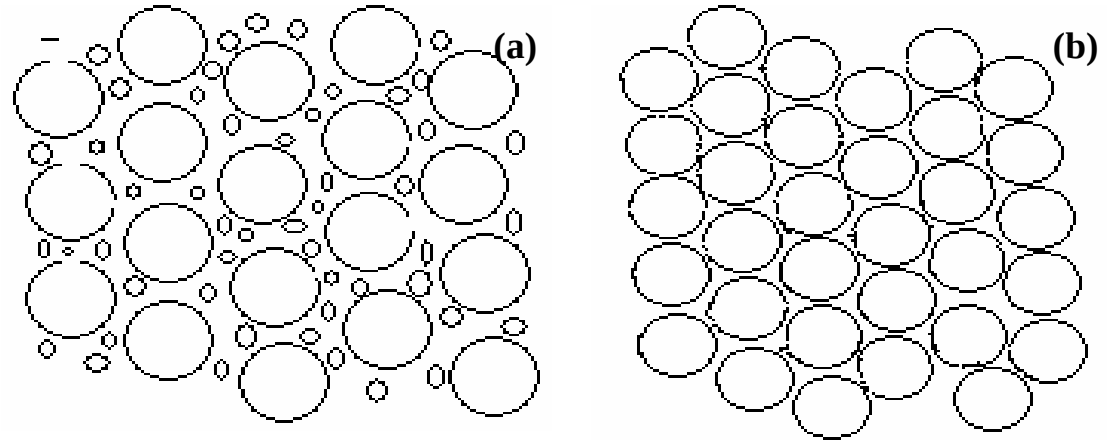

Figure 7.2. Different shapes of water droplets formed during the HIPE formation

In the HIPE system the major aqueous phase occupies the dispersed state and the minor, the continuous oil phase. During this, the aqueous phase is deformed in various shapes as shown in Figure 7.3(a) to occupy maximum available space in the emulsion. In Figure 7.3 (a) mixture of elliptical as well as circular shaped droplets formed with thick wall, are ultimately converted into the porous cavities in polymer structure, while in Figure 7.3 (b) mixture of small as well as large spherical droplets are formed giving the polydispersed morphology.

The shapes of interconnected windows also vary from circular to trapezoidal, or ellipsoidal or partially having angular cups instead of rounded corners depending on deformation of droplets during HIPE formation. More the water phase more the deformation of water droplet takes place in order to close pack arrangement in the available oil continuous phase

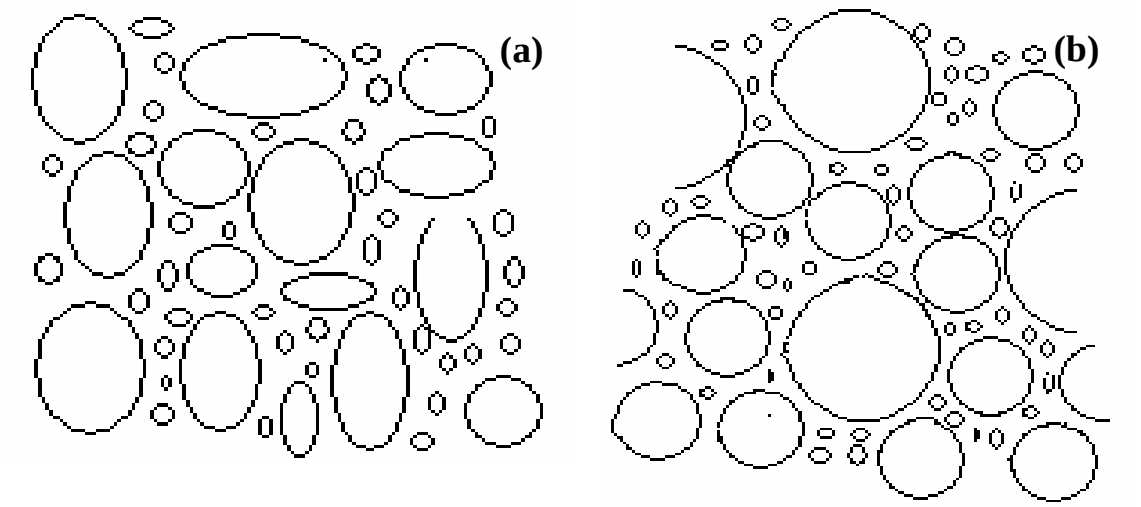

Figure 7.3. Different shapes of water droplets formed during the HIPE formation

The dimensions of the cell wall can be varied from nano- to micrometer. Much is now known about the methods by which each of these parameters can be varied; this is important, as any advanced materials application in which PolyHIPEs may be used will require careful control of morphology and properties. The cellular nature of polyHIPEs can be varied between open- and closed-cell.

It was found that, while internal phase volume ratio played a role, initiator type and their placement, surfactant concentration were in fact more important to design the porous architecture within the polymer matrix. Formation of porous structure depends on the initial droplets formation and droplets formation depends on the HLB of nonionic surfactant.

7.4.1 Effect of initiators

The initiator can be either oil- or water-soluble or a combination of both. In the case of an oil-soluble initiator, the initiator is dissolved in the monomeric phase prior to emulsification. Then the reaction starts within the droplets. In case of water soluble

initiator, it is dissolved in water and, therefore, the formation of free primary radicals takes place in the aqueous phase.

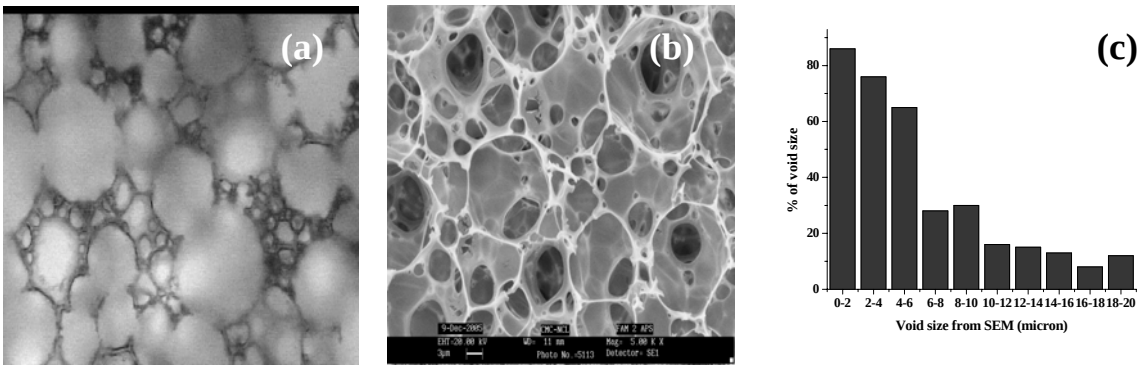

Figure 7.4. (a) Optical micrograph, (b) internal morphology, and (c) pore size distribution of HIPE monolith synthesised using ammonium peroxydisulphate

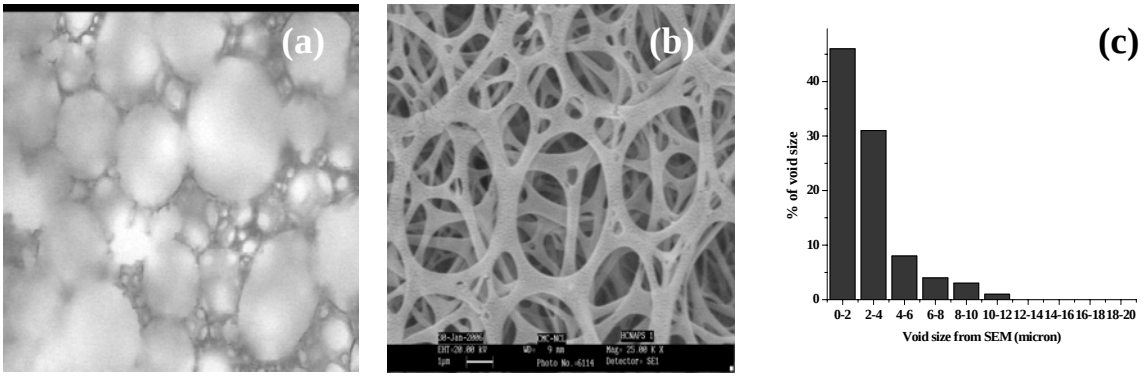

Figure 7.5. (a) Optical micrograph, (b) internal morphology, and (c) pore size distribution of HIPE monolith synthesised using sodium peroxydisulphate

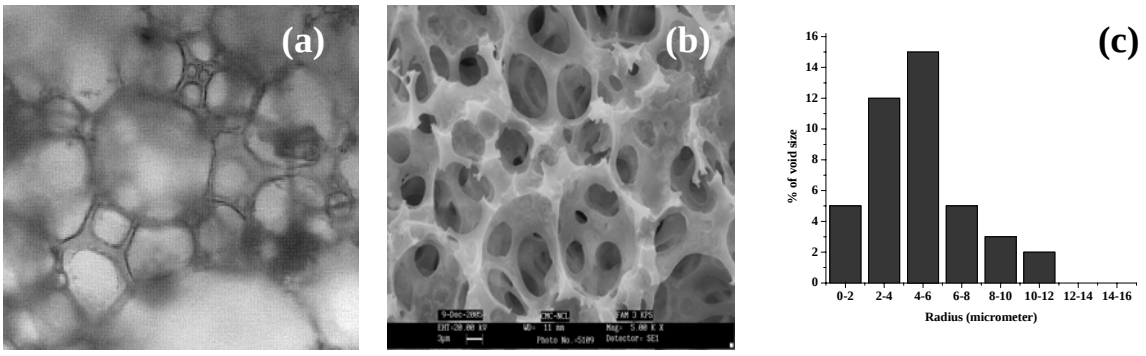

Figure 7.6 (a) Optical micrograph, (b) internal morphology, and (c) pore size distribution of HIPE monolith synthesised using potassium peroxydisulphate

In this study three water soluble initiators were used namely ammonium peroxydisulphate (APS), sodium peroxydisulphate (NaPS) and potassium peroxydisulphate (KPS) in the experiments HIPE 01, HIPE 02 and HIPE 03, respectively, as shown in Table 7.1. Figures 7.4, 7.5 and 7.6 show the optical as well as scanning electron micrographs of the HIPE monoliths synthesised using APS (HIPE 01), NaPS (HIPE 02) and KPS (HIPE 03), respectively. There is distinguishable difference in the porous architecture. The final porous morphology depends on the type of initiator used because the rates of formation of free radicals are different for different initiator.

For polymerisation to proceed the free radicals formed has to travel across the water phase and diffuse into the oil phase where monomer is situated. Initial droplets formed using APS are shown in Figure 7.4 (a). The porous morphology formed using ammonium peroxydisulphate (APS) showed closed cells having very small number of interconnected opening or windows, as shown in Figure 7.4 (b).Though the cell walls are very thin, the near absence of interconnected pores is probably due to insufficient amount of the surfactants used. Table 7.4 shows the pore volume (0.45 cm^3/g) and surface area (23.64 m^2/g) of HIPE 01 monolith. Closed cell morphology without pores on the wall yields low surface area. The Figure 7.4 (c) shows the pore size distribution to be in the range 2-20 microns. Most cells are in the range 10-12 microns.

The monolith synthesised using sodium peroxydisulphate gave uniform porous morphology of open and interconnected cells. As seen in Figure 7.5 (a) large numbers of oval shaped droplets are formed which finally convert into similar shaped porous cells having large number of windows. The intercellular pores are ellipsoidal, bordering on trapezoidal, with angular cusps instead of rounded corners. The three dimensional nature

of the (HIPE 02) structure can be seen in Figure 7.5(b), where porous cell walls are clearly visible behind the intercellular pores. The cell walls appear smooth and uniform at high magnifications. The uniform cell wall having a thickness of 0.2-0.5 μm and large number of nanometer scale pores are present in the cell wall, as shown in Figure 7.5(b).

Table 7.4. Pore volumes and surface areas of acrylic polyHIPEs estimated by BET.

Polymer code	Pore volume (cm^3/g)	Total surface area (m^2/g)
HIPE 01	0.45	23.64
HIPE 02	0.64	84.27
HIPE 03	0.69	74.23
HIPE 04	0.73	88.42
HIPE 05	0.59	61.03
HIPE 06	0.71	93.21
HIPE 07	0.84	64.64
HIPE 08	0.81	89.43
HIPE 09	0.79	86.32
HIPE 10	0.34	56.66
HIPE 11	0.43	68.74
HIPE 12	0.68	77.31
HIPE 13	0.72	87.44
HIPE 14	0.89	51.98
HIPE 15	0.51	83.01
HIPE 16	0.54	90.23
HIPE 17	0.73	80.43
HIPE 18	0.79	51.50
HIPE 19	0.66	33.89
HIPE 20	0.79	27.76
HIPE 21	0.43	94.54
HIPE 22	0.45	98.11
HIPE 23	0.89	43.54
HIPE 24	0.63	58.19
HIPE 25	0.68	71.09
HIPE 26	0.40	86.46
HIPE 27	0.56	98.23

This morphology generated using NaPS has pores in the range 0.2- 20 μm, as shown in Figure 7.5 (c). More pores are in the range 2-3 μm. The polymer synthesised

using NaPS (HIPE 02) gave low pore volume (0.64 cm^3/g) but very high surface area (84.27 m^2/g) because of microporous nature of pores created by pores in the cell walls. Optical microscopy Figure 7.6 (a) shows the formation of non-uniform droplets in emulsion in presence of potassium peroxydisulphate. The monolith synthesised using the potassium peroxydisulphate (KPS) yielded very thick cell wall (6-9 μm), shown in Figure 7.6 (b). An average of 2-3 windows, of diameter 2-3 μm, were formed in each cell. Pore size distribution was in the range 0.2 –12 μm, as shown in Figure 7.6 (c). The pore volume and surface area were 0.69 cm^3/g and 74.23 m^2/g respectively, as given in Table 7.4.

Figures 7.7 and 7.8 show the optical as well as SEM morphology of acrylate monoliths synthesised using organic phase initiators benzoyl peroxide (BPO) and azobisisobutyronitrile (AIBN), which generate free-radicals exclusively in the oil phase. Up on heating, the initiator molecules decompose, generating free radicals that start the polymerisation in some of the monomer droplets. The droplet formation and their packing in the continuous monomer phase using BPO and AIBN are shown in Figures 7.7 (a) (HIPE 04) and 7.8 (a) (HIPE 05), respectively. Figure 7.7 (b) and (c) shows the circular porous cells having diameter 0.2 to 40 μm. With BPO large number of interconnected windows with diameter in the range 0.2 to 10μm are observed.

The morphology shown in Figures 7.8 (b) and (c) using AIBN is quite irregular. There is mixture of small as well as large cells, having diameter in the range 2-50 μm, with interconnected windows, having diameter in the range 1-5 μm. This kind of morphology gives bimodal pore size distribution, as shown in Figure 7.9 (b). The pore size distribution of monoliths prepared using BPO is shown in Figure 7.9 (a). Large

numbers of pores are in the range 15-20 μm. Pore volume and surface area were 0.73 cm^3/g and 88.42 m^2/g, as presented in Table 7.4.

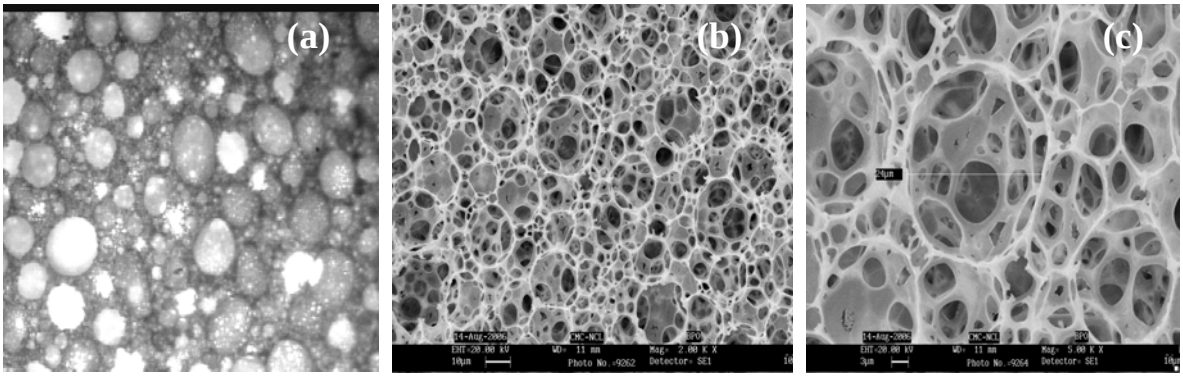

Figure 7.7. (a) Optical micrograph, (b) internal morphology at 2000X and (c) at 5000X magnification of HIPE monolith synthesised using benzoyl peroxide (BPO) initiator

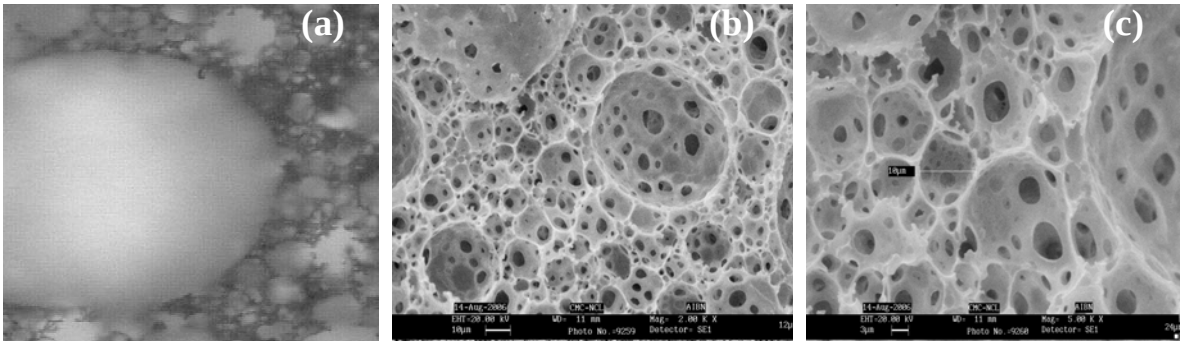

Figure 7.8. (a) Optical micrograph, (b) internal morphology at 2000X and (c) at 5000X magnification of HIPE monolith synthesised using 2, 2'-Azobisisobutyronitrile (AIBN) initiator

Compared to BPO the pore volume and surface area with AIBN were low only because of irregular distribution of cells within the matrix. The surface area and pore volume were 61.06 m^2/g and 0.59 cm^3/g, respectively, as given in Table 7.4. SEM pictures showed that the morphology of polymer matrices changes drastically by varying the types of oil soluble initiator .This is because of difference in the rate of formation of free radical and their placement in the oil and water phase during the stabilization of HIPE emulsion.

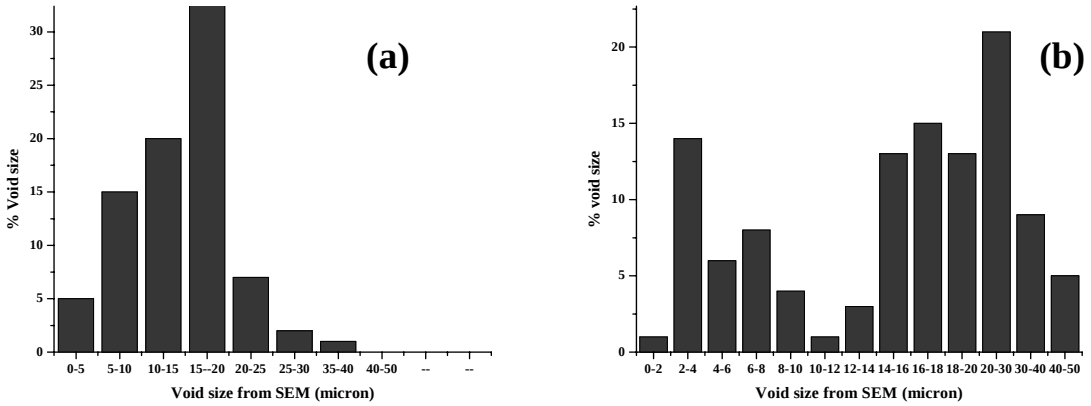

Figure 7.9. Pore size distribution of polyHIPE materials synthesised using (a) BPO and (b) AIBN

Completely different morphology was observed when monolith of identical composition was synthesised under identical reaction conditions using a combination of oil and water-soluble initiators. In this case, the probability of nucleating increases sharply with droplet size and is closely related to the probability of the formation of a long enough polymer chain in the monomer droplet. A polymer chain will be formed whenever a single radical enters the monomer droplet. Single radical refers to radicals that enter monomer droplets one at a time as opposed to pair generation in which, due to initiator decomposition, two radicals appear in the monomer droplet at the same time. Single radicals can be formed by desorption of one of the radicals originating from initiator decomposition and the entry of a radical from the aqueous phase. In the aqueous phase, radicals appear after the decomposition of the oil-soluble initiator fraction dissolved in water and desorption of radicals from the oil phase. Monomer will also be nucleated if the pair of radicals formed in the monomer droplet does not suffer instantaneous bimolecular termination. Comparing oil-soluble initiators, the probability of nucleation is much higher for AIBN than for BPO. AIBN also shows a significant

aqueous-phase distribution. The oil-soluble initiator fraction is responsible for single radical generation.

Figures 7.10 (a) and (b) (HIPE 06) show the porous morphology generated when a mixture of BPO and NaPS is used. In this case pentagonal or hexagonal shaped cells are formed with a thin wall between them, shown in Figure 7.10 (a), having diameter in the range 5-30 μm, as shown in Figure 7.10 (c). Number of circular windows, approximately five-to six per cell, are formed on cell walls, as shown in Figure 7.10 (b). Very high surface area (93.21 m^2/g) and pore volume (0.71 cm^3/g) are noted.

When a combination of AIBN-NaPS was used, irregularly shaped morphology was observed, as shown in Figures 7.11(a) and (b) (HIPE 07) having pore size range in the range 2-35 μm (Figure 7.11(c)). The emulsion was not stable for long period and stable aqueous phase droplets were not observed. Even though pore volume was quite high (0.84 cm^3/g) the surface area (64.64 m^2/g) was lower than that with the combination BPO-NaPS.

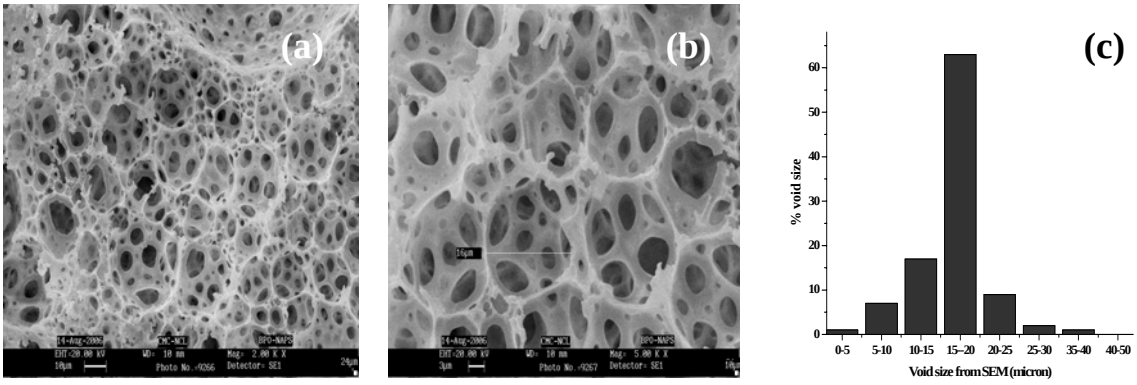

Figure 7.10. (a) Internal morphology at 2000X, (b) at 5000X magnification, and (c) pore size distribution of HIPE monolith synthesised using a mixture of BPO and NaPS

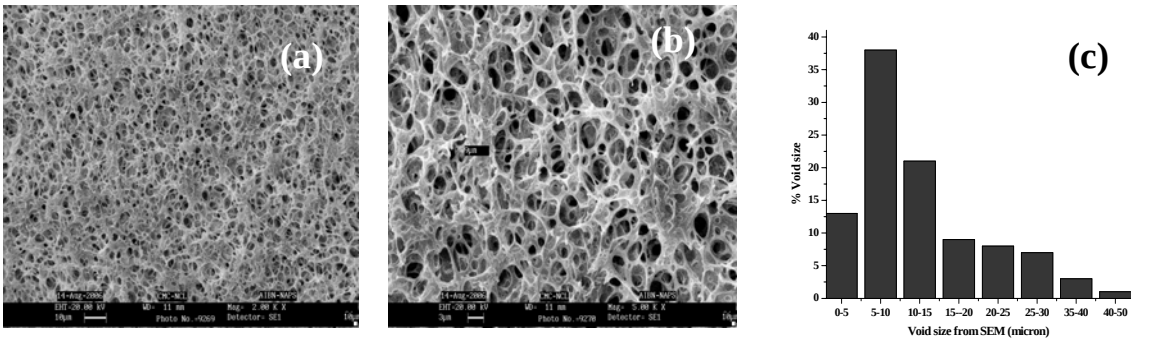

Figure 7.11 (a) Internal morphology at 2000X, (b) at 5000X magnification, and (c) pore size distribution of HIPE monolith synthesised using a mixture of AIBN and NaPS

7.4.2 Inhibitor effects

Extremely low concentrations of phenothiazine relative to the low concentration of initiator not only affects the rate of polymerisation but also affects the morphology of polymer, as shown in Figures 7.12, 7.13, 7.14, and 7.15. Phenothiazine kills the radicals generated by decomposition of initiator and stops the polymerisation. Simultaneously it also alters the functioning of surfactant. Thus, the droplets change their dimensions in various ways from circular to ellipsoidal, as shown in Figures 7.12 (a), 7.13 (a), 7.14 (a), and 7.15 (a) at 1 (HIPE 08), 2 (HIPE 09), 3 (HIPE 10), and 4 mol% (HIPE 11), phenothiazine concentration relative to initiator, respectively. The cell size increases with the amount of phenothiazine, as shown in Figures 7.12 (b), 7.13 (b), 7.14 (b), and 7.15 (b) respectively for 1, 2, 3 and 4 mol% of phenothiazine relative to the initiator.

The monoliths prepared in presence of 1 and 2 mol% phenothiazine show circular cells with large number of windows at the walls. Pore size distribution in Figures 7.12 (c) and 7.13 (c) show bimodal distribution in the range 5-50 μm. Both monoliths have relatively high surface areas and pore volumes. HIPE 08 has 0.81 cm^3/g pore volume and 89.43 m^2/g surface area, while monolith (HIPE 09) prepared with 2 mol%

phenothiazine has 0.79 cm^3/g pore volume and 86.32 m^2/g surface area. As shown in Figure 7.12 (c) the pore size distribution is bimodal in the range 2-40 μm in HIPE 08 and 2-50 μm in HIPE 09 [Figure 7.13 (c)]. At 3 and 4 mol% phenothiazine the droplets are distorted (HIPE 10, 11) and become elliptical [Figure 7.14 (a) and 7.15 (a)]. The HIPE 10 has an open-cell morphology and intercellular pores within the cell walls, as seen in Figure 7.14 (b), while HIPE 11 has circular shaped pore openings on the wall as shown in the Figure 7.15 (b). The cells are 25-35 μm in diameter and the intercellular pores are 0.4-8 μm in diameter. As shown in Figures 7.14 (c) and 7.15 (c) both HIPE 10 and HIPE 11 show bimodal pore size distribution.

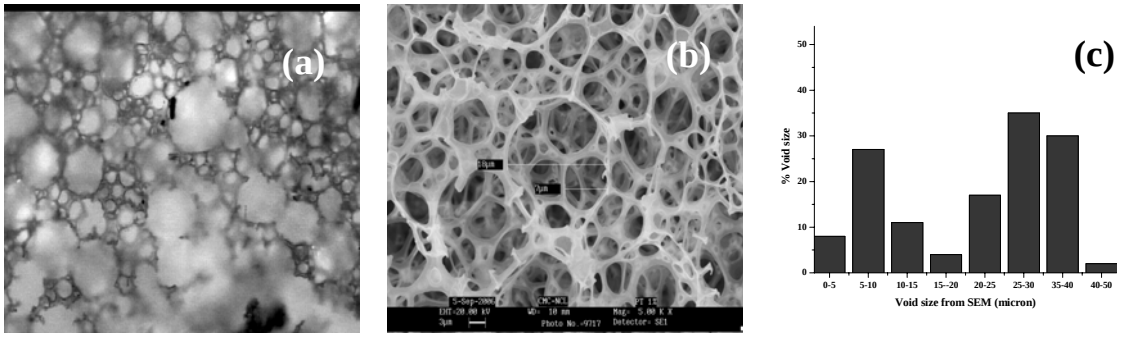

Figure 7.12. (a) Optical micrograph, (b) internal morphology and (c) pore size distribution in HIPE monolith synthesised using 1 mol% phenothiazine relative to peroxydisulphate

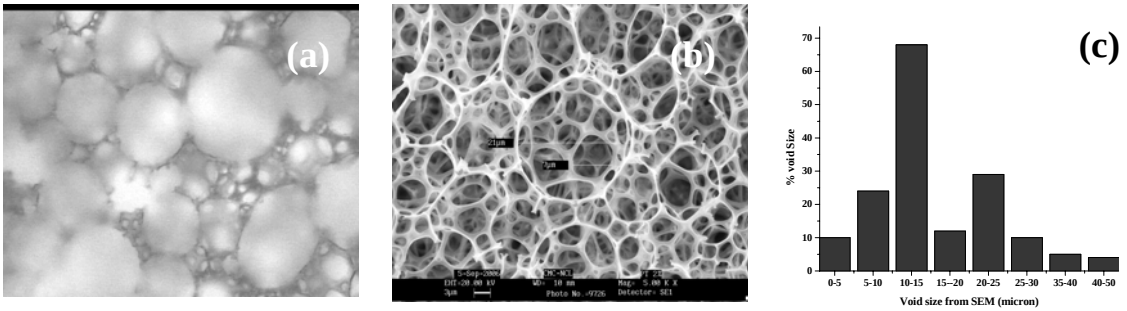

Figure 7.13. (a) Optical micrograph, (b) internal morphology and (c) pore size distribution in HIPE monolith synthesised using 2 mol% phenothiazine relative to peroxydisulphate

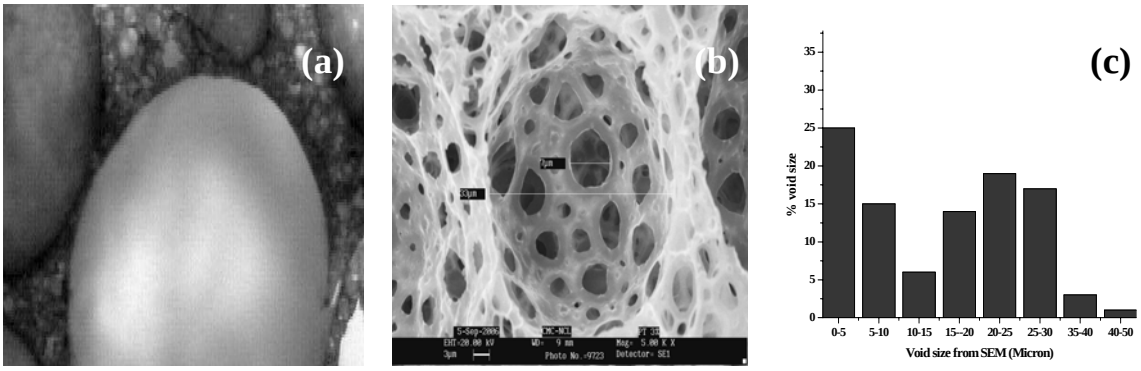

Figure 7.14. (a) Optical micrograph, (b) internal morphology and (c) pore size distribution in HIPE monolith synthesised using 3 mol% phenothiazine relative to peroxydisulphate

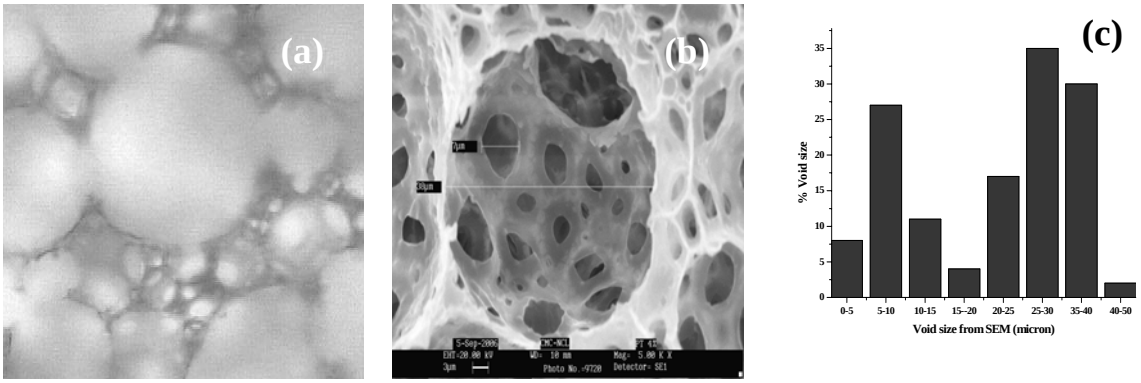

Figure 7.15. (a) Optical micrograph, (b) internal morphology and (c) pore size distribution in HIPE monolith synthesised using 4 mol% phenothiazine relative to peroxydisulphate

As shown in Figure 7.14 (b) the walls have small pores surrounding each large pore. Large pores are therefore connected only via small pores. Compared to HIPE 08 and HIPE 09 these polymers have low surface areas. HIPE 10 has surface area of 56.66 m^2/g and HIPE 11 has 68.74 m^2/g, as shown in Table 7.4. Pore volumes are 0.34 cm^3/g and 0.43 cm^3/g, respectively. Brown colouration was observed during the emulsion making with increasing phenothiazine concentration due to oxidation.

7.4.3 Effect of temperature

Temperature plays a very important role in the formation of stable droplets and their shape, which in turn influence the final morphology of porous materials. Increase in temperature increases both the cell size as well as interconnected pores diameters as shown in Figures 7.16 (b), 7.17 (b), and 7.18 (b). At higher temperature the emulsion is subjected to greater turbulence and the surfactant at the interfacial wall separating the droplets becomes more soluble in the bulk liquid phase and therefore migrates from the interface. This raises interfacial tension and promotes droplet coalescence. At 65ºC more uniform droplets are formed as shown in Figure 7.16 (a). The morphology of HIPE 12 shown in Figure 7.16 (b) is quite uniform.

Pentagonal as well as octagonal shaped cells of diameter 2-30 μm are formed and the interconnected pores have diameter in the range 0.2-7 μm, as shown in Figure 7.16 (c). The pore volume was 0.68 cm^3/g and surface area was 77.31 m^2/g. At 75ºC (HIPE 13) larger cell are formed due to coalescence. Therefore smaller droplets, as shown in Figure 7.17 (a), merge into the larger ones giving a broad pore size distribution in the range 5-50 μm with interconnected windows from 0.2 to 9 μm. At 75ºC in addition to the circular shaped windows, some star shaped opening are also observed on the walls of cells as shown in Figure 7.17(b). This might be due to the tearing of thin walls during the gellation by the contraction brought forth by polymerisation.

The pore volume and surface area, 0.72 cm^3/g and 87.44 m^2/g, are slightly higher than the monilith (HIPE 12) synthesised at 65ºC, respectively. Rate of polymerisation is so high that it gives very short time to stabilise the droplets in its equilibrium state. Before equilibrium takes place the droplets adopt the shape, as shown in Figure 7.17 (a),

in sticky period. Therefore, the larger droplets are not able to split into the smaller uniform droplets. Rather, they distribute heterogeneously and give a broad distribution.

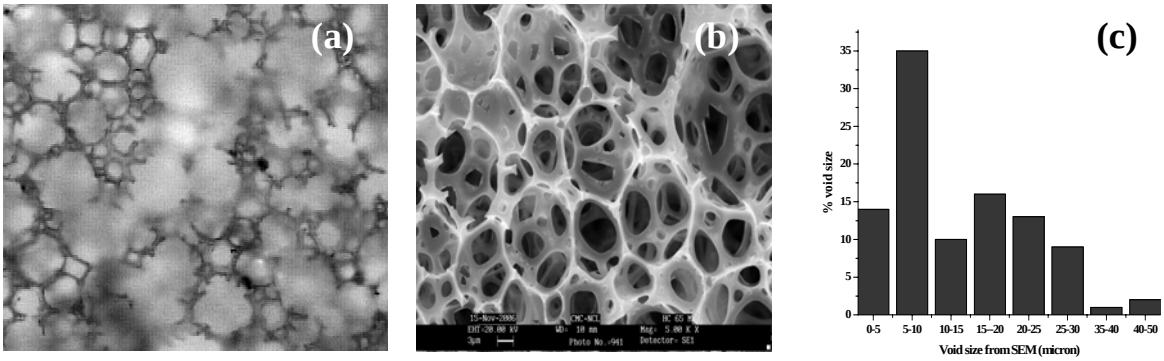

Figure 7.16. (a) Optical micrograph, (b) internal morphology and (c) pore size distribution of HIPE monolith synthesised at 65ºC

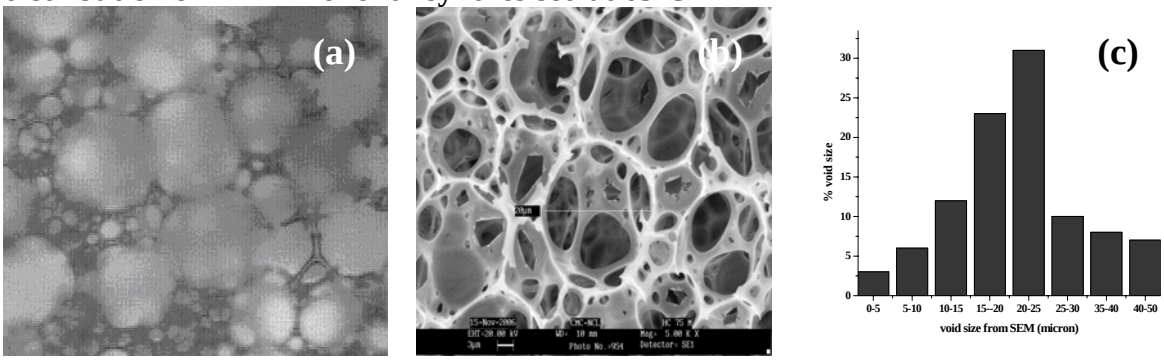

Figure 7.17. (a) Optical micrograph, (b) internal morphology and (c) pore size distribution of HIPE monolith synthesised at 75ºC

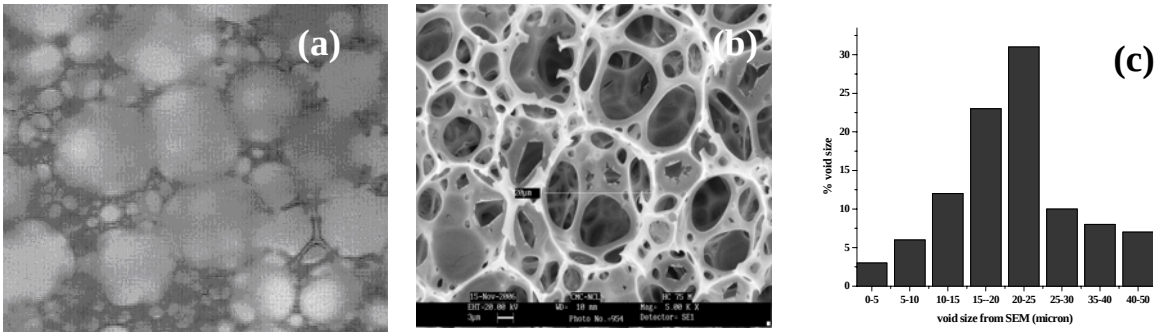

Figure 7.18 (a) Optical micrograph, (b) internal morphology and (c) pore size distribution of HIPE monolith synthesised at 85ºC

The optical micrograph of W/O droplets of monolith (HIPE 14) synthesised at 85ºC is shown in Figure 7.18 (a). In this, irregular shaped cells are formed in the range between 2 to 60 μm as shown in Figure 7.18 (b), with the interconnected pores in the range 0.5 to 5 μm. This broadness in pore size distribution (Figure 7.18(c)) results in higher pore volume and low surface area than that synthesised at 65ºC and 75ºC. The pore volume and surface area are 0.89 cm^3/g and 51.98 m^2/g, respectively. Here high pore volume is due to the formation of large number of macroporous channels.

7.4.4 Effect of surfactant concentration

The morphology of water droplets in W/O emulsion was controlled by an optimum concentration of a combination of water- and oil-soluble surfactants. Since water droplets serve as a support to the promotion of porous structure, their morphology influences the shape, size, and size distribution of cell and windows. The radius of curvature at the water/oil interface is determined in part by the head and tail components of the surfactant. Creating a concentrated HIPE emulsion involves mixing a small amount of an oil-based component with a much larger amount of water-based component in the presence of a suitable surfactant combination so that HIPE emulsion is obtained (one in which the oil phase is the continuous phase). To obtain such an emulsion, the choice of the surfactant is crucial.

HIPE monoliths synthesised using 30 % (HIPE 15) and 40 % (wt./wt.) (HIPE 16) surfactant were highly interconnected materials with large number openings on the cell walls, as shown in Figures 7.19 (b) and 7.20 (b), respectively. The pore structure was highly interconnected and there were open pores on the wall surface that were connected to the interior cells. The size of the macropores was found to be in the range 5-60 μm and

that of interconnected widows from 0.2 to 9 μm. The pore-size distribution was often bimodal in these materials, as shown in Figures 7.19 (c) and 7.20 (c). BET surface areas were relatively high (> 80 m^2/g) in both these samples (see Table 7.4), suggesting that there was micro- or mesoporosity in the walls of the templated polymer structures because of nanoscale pores. It can be seen that the internal structure is uniformly porous (Figures 7.19 (b) and 7.20 (b)) and consists of a "skeletal replica" of the original W/O HIPE emulsions, as shown in Figures 7.19 (a) and 7.20 (a).

Uniform cell size began to appear as the surfactant level reached between 40–60%. Figures 7.21 (a) and 7.22 (a) shows the W/O droplet formation of emulsion prepared using 50 and 60% surfactant concentrations, respectively. The interconnect size increased with increasing surfactant concentration. The windows shown in Figure 7.21(b) are more open than those shown in Figure 7.22 (b). Even though the pore volume are high, 0.73 cm^3/g for HIPE 17 and 0.79 cm^3/g for HIPE 18, the relative surface areas go on decreasing, from 80.43 m^2/g for HIPE 17 to 51.50 m^2/g for HIPE 18, as shown in Table 7.4 because of formation of macro-channels. The pore size distribution, shown in Figure 7.21 (c) at 50% and Figure 7.22 (c) at 60% surfactant concentration, reveals the broad distribution, in the range 2 to 50 μm. Large number of pores are present in the 20 to 25 μm diameter range.

At 70 and 80% surfactant, the polymer formed was no longer a connected monolithic material. Figures 7.23 (a) and 7.24 (a) show the W/O droplet formation of emulsion prepared using 70% (HIPE 19) and 80% (HIPE 20) surfactant concentrations, respectively. Closed cell with very little interconnected pores are formed, as shown in SEM Figures 7.23 (b) for 70% and 7.24 (b) for 80%, respectively. This is because of

retraction of the thin oil layer separating droplets as the surfactant concentration is increased. The appearance of holes between adjacent voids coincided with the polymerisation gel time. The surface areas in these concentrations are very low which is 33.89 m^2/g for HIPE 19 at 70% and 27.76 m^2/g for HIPE 20 at 80% surfactant concentration, as shown in Table 7.4. As shown in Figure 7.23 (c), broad pore size distribution between 5-50 μm indicates the formation of irregular shaped cells without the interconnecting windows, while Figure 7.24 (c), which was synthesised using 80% surfactant concentration, shows narrow pore diameter distribution in the range 2 to 30 μm.

A further increase in the surfactant concentration to 90% (HIPE 21) again shows up interconnected pores at the cell walls. As shown in Figure 7.25 (a), very uniform spherical water droplets are formed. The resulting HIPE has highly interconnected morphology, with open windows as shown in Figure 7.25 (b) and high surface area (94.54 m^2/g) (HIPE 21) as shown in Table 7.4. At higher surfactant concentrations the films become thinner, which on curing produce large number of interconnecting holes between voids. The pore size distribution was quite narrow as shown in Figure 7.25 (c), in the range 2 to 20 microns.

There fore, the surfactant concentration plays a very important role in determining the pore architecture of the final polymer matrix. Further detailed study is required to arrive at final conclusion because there are various parameters which determine the pore structures such as surfactant concentration at different temperatures, at different HLB values, etc.

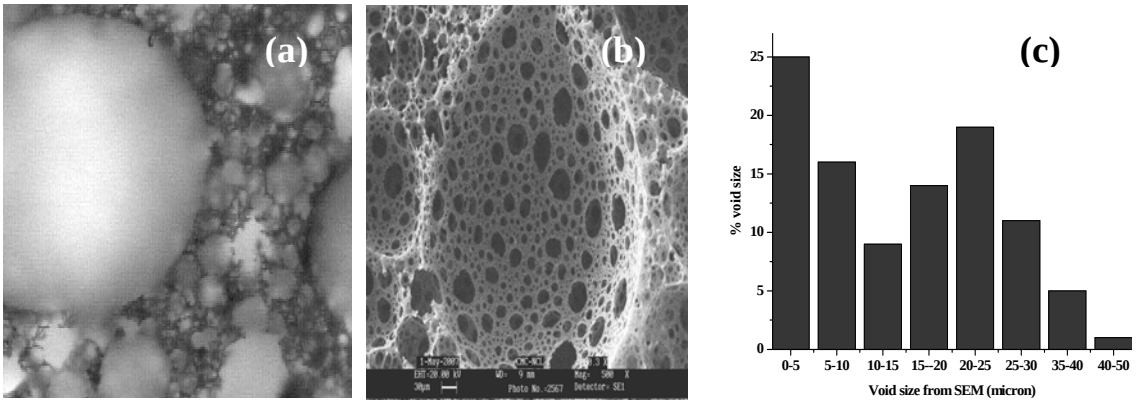

Figure 7.19. (a) W/O optical micrograph, (b) internal morphology and (c) pore size distribution of HIPE monolith synthesised using 30 % surfactant concentration

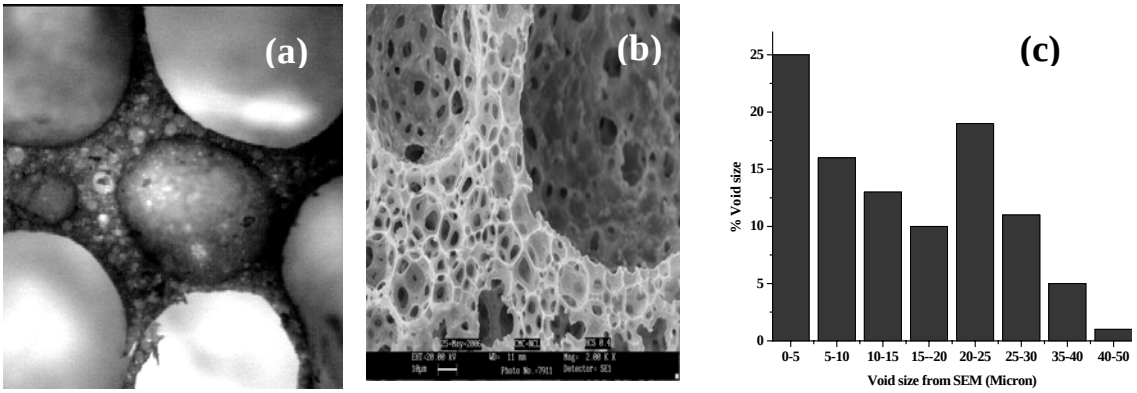

Figure 7.20. (a) W/O optical micrograph, (b) internal morphology and (c) pore size distribution of HIPE monolith synthesized using 40 % surfactant concentration

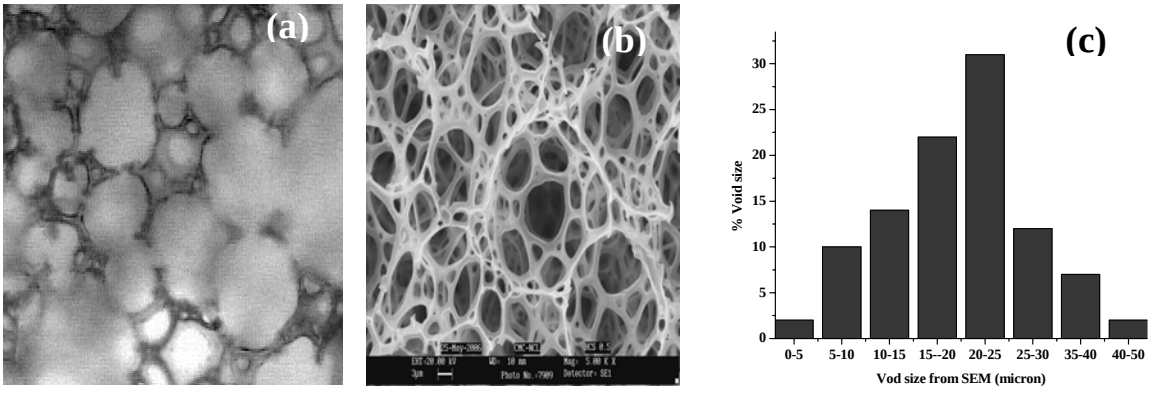

Figure 7.21. (a) W/O optical micrograph, (b) internal morphology and (c) pore size distribution of HIPE monolith synthesised using 50 % surfactant concentration

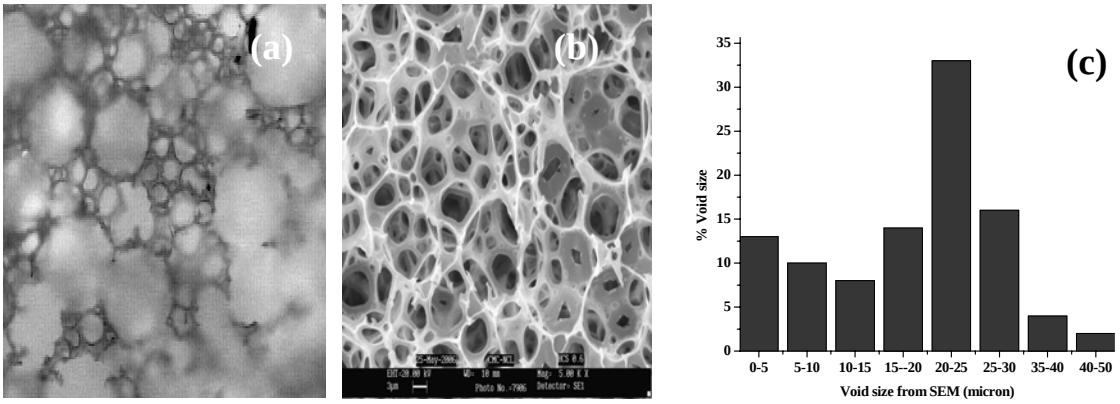

Figure 7.22. (a) W/O optical micrograph, (b) internal morphology and (c) pore size distribution of HIPE monolith synthesised using 60 % surfactant concentration

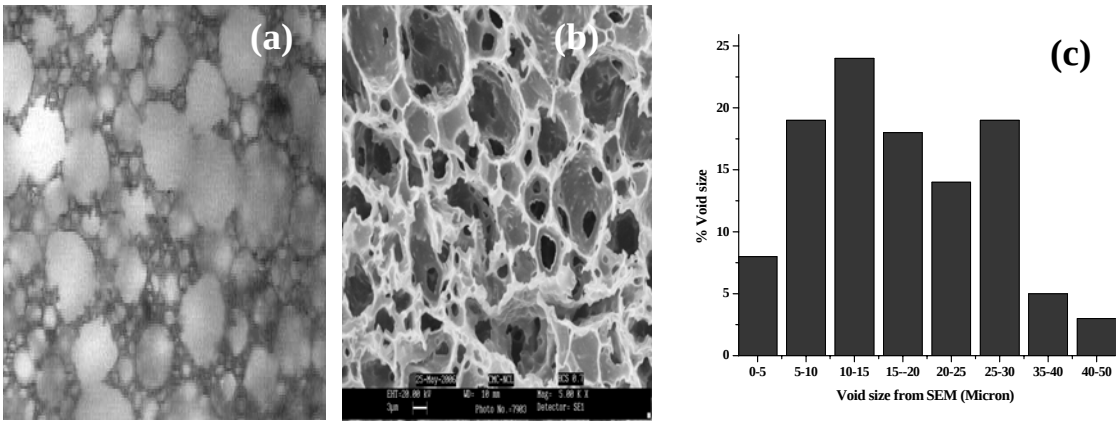

Figure 7.23. (a) W/O optical micrograph, (b) internal morphology and (c) pore size distribution of HIPE monolith synthesised using 70 % surfactant concentration to the monomer phase

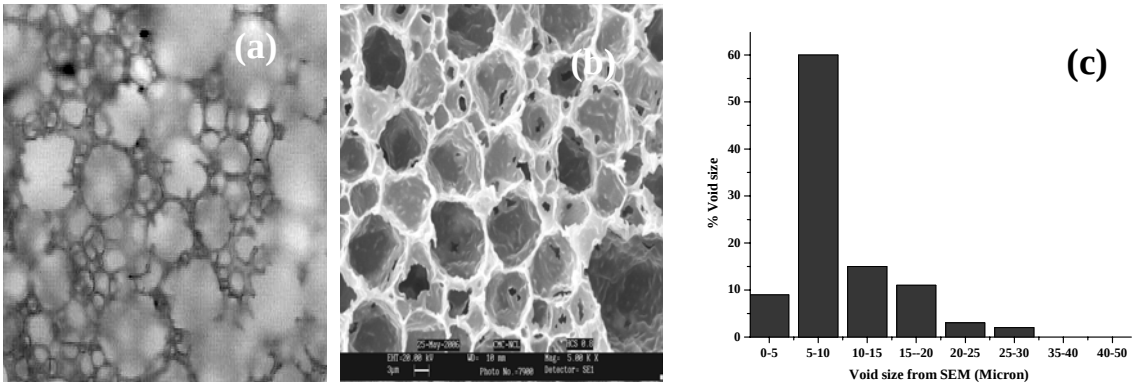

Figure 7.24. (a) W/O optical micrograph, (b) internal morphology and (c) pore size distribution of HIPE monolith synthesised using 80 % surfactant concentration to the monomer phase

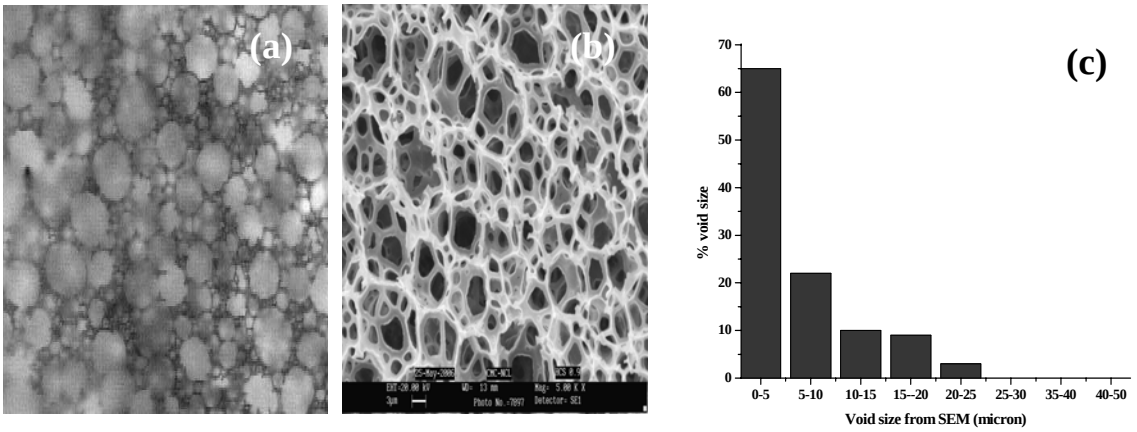

Figure 7.25. (a) W/O optical micrograph, (b) internal morphology and (c) pore size distribution of HIPE monolith synthesised using 90 % surfactant concentration to the monomer phase

7.4.5 Effect of stirring speed

Droplet formation very much depends on the stirring speed during the formation of emulsion. Droplet coalescence and breaking are two major causes of instability in emulsions and result in a coarsening of droplet size and a widening of droplet size distribution. Both phenomena occur due to the difference in shear rates during emulsion making. Droplet breaking results from the high shear rate, which leads to breaking of large droplets into smaller ones. Smaller droplets have a greater solubility in the continuous phase than larger droplets, due to the Kelvin effect. The chemical potential increases with decreasing droplet radius and, as a consequence, the solubility of the material comprising the droplet phase also increases. The smaller droplets tend to dissolve as material diffuses through the interfacial layer and re-deposits into larger droplets. Coalescence results from the thinning and rupture of the thin interfacial films between droplets. The shape of blades and speed of the stirrer are important parameters in controlling the rate of both coalescence and breaking of the droplets. These processes will therefore also have an effect on the final morphology of porous materials derived

from HIPEs. Average void diameters were calculated from a set of 50 voids, the diameters of which were determined by image analysis of the SEM micrographs.

Porous morphology of polyHIPE materials synthesised at low stirring speed (250 rpm) are shown in Figures 7.26 (a) and (b) (HIPE 23). At this speed, there is less possibility of droplets breaking. The original droplets size remains the same through out the emulsion making and polymerisation. The pore size distribution of polyHIPE materials synthesised at 250 rpm is given in Figure 7.26 (c). Large numbers of pores formed have size in the range 35-50 micron.The interconnect pore also give a broad pore size distribution in the range 5-30 microns. The pore volume and surface area of sample prepared at 250 rpm were 0.89 cm^3/g and 43.54 m^2/g, respectively.

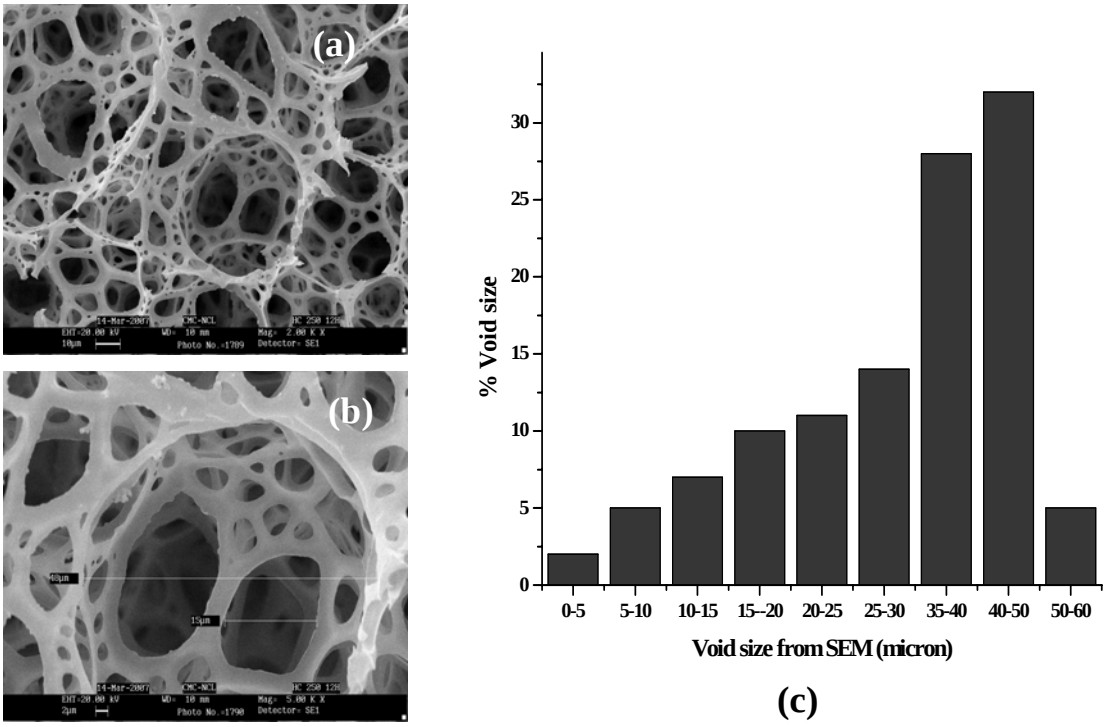

Figure 7.26. (a) Internal morphology at 2000X, (b) at 5000X magnification and (c) pore size distribution of HIPE monolith synthesised at a stirring speed of 250 rpm

At 500 rpm, the pore size starts to decrease, as shown in Figures 7.27 (a) and (b) (HIPE 24). Because of increasing stirring speed, the shear rate increases. This causes the break-down of large droplets into smaller ones. The porous morphology, shown in Figure 7.27 (b), indicates that there is formation of large cells with small windows. Cells from 35 to 45 microns are formed along with windows having dimensions from 5 to 15 micron, as shown in Figure 7.27(c). A slightly increased surface area of 58.19 m^2/g was obtained.

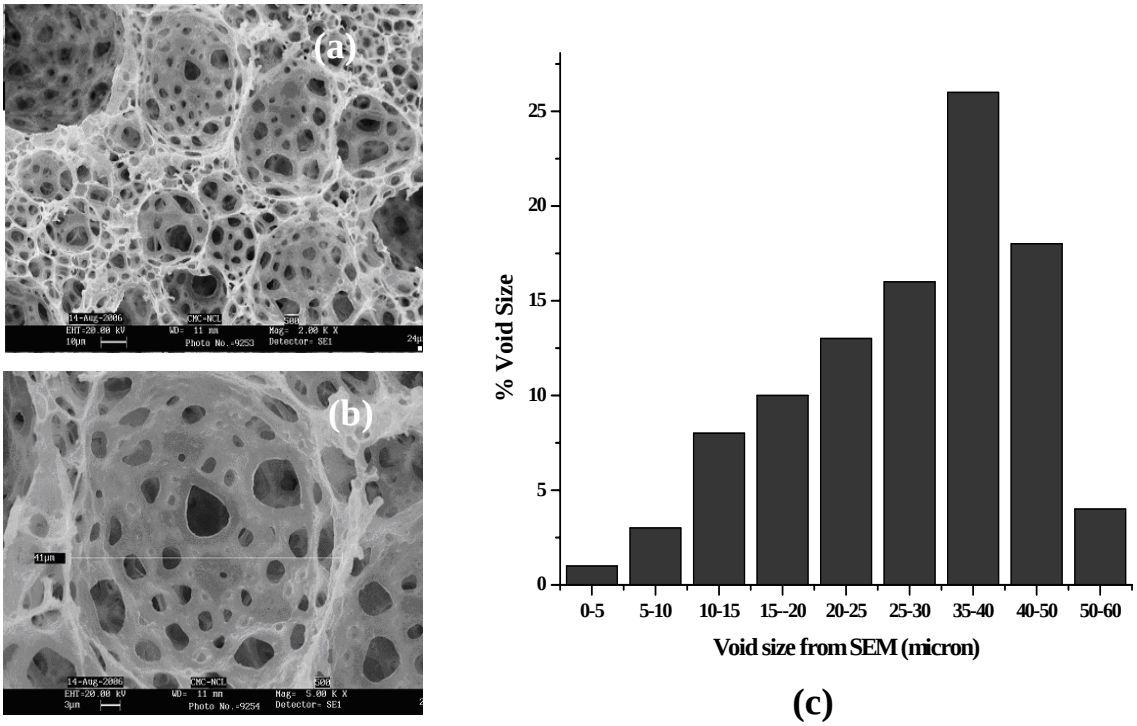

Figure 7.27. (a) Internal morphology at 2000X, (b) at 5000X magnification and (c) pore size distribution of HIPE monolith synthesised at a stirring speed of 500 rpm

When the emulsion is prepared at 700 rpm (HIPE 25), large number of cells are within the 25-30 micron range, as shown in Figures 7.28 (a) and (b). The pore size distribution is broad, from 5 to 50 micron (Figure 7.28 (c)). This is because the breaking droplets also coalesce into larger droplets. Agitation increases the frequency of contact

and results in a higher probability of droplet coalescence. As the emulsion is stirred, surfactant in the interfacial film separating the droplets become more soluble in the bulk liquid phase and therefore migrates from the interface. This will raise the interfacial tension and thus promote droplet coalescence. Figures 7.28 (a) and (b) show that cells formed are quite uniform through out the matrix as compared to the windows, which are quite irregularly formed on the walls. The poly(HIPE) has open-cell morphology with intercellular pores in the cell walls. Surface area and pore volume obtained were 71.09 m^2/g and pore volume 0.68 cm^3/g, respectively.

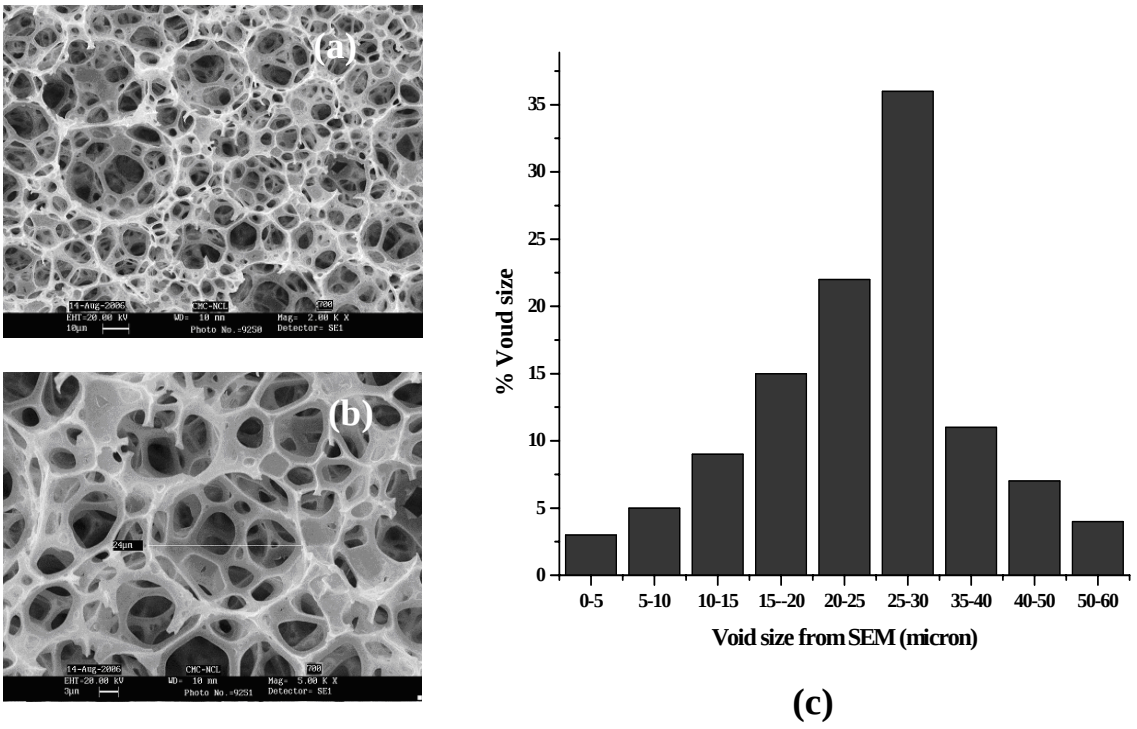

Figure 7.28. (a) Internal morphology at 2000X, (b) at 5000X magnification and (c) pore size distribution of HIPE monolith synthesised at a stirring speed of 700 rpm

Further increase in stirring speed during initial mixing was found to cause a striking decrease in both the average interconnect and void diameter of the PolyHIPE material. Figures 7.29 (a) and (b) show the internal morphologies of polyHIPE materials synthesised at 1000 rpm. The shear rate is high enough to ensure that rate of breaking of

droplet dominates over rate of coalescence. So large droplets get broken down into small ones, which is reflected in Figures 7.29 (a) and (b). The cells are more spherical and the intercellular pores are more circular. Small cells, having average pore size of 10 microns, are formed as shown in Figure 7.29 (c). As a consequence pore volume decreases (0.40 cm^3/g) while surface area obtained is quite high (86.46 m^2/g).

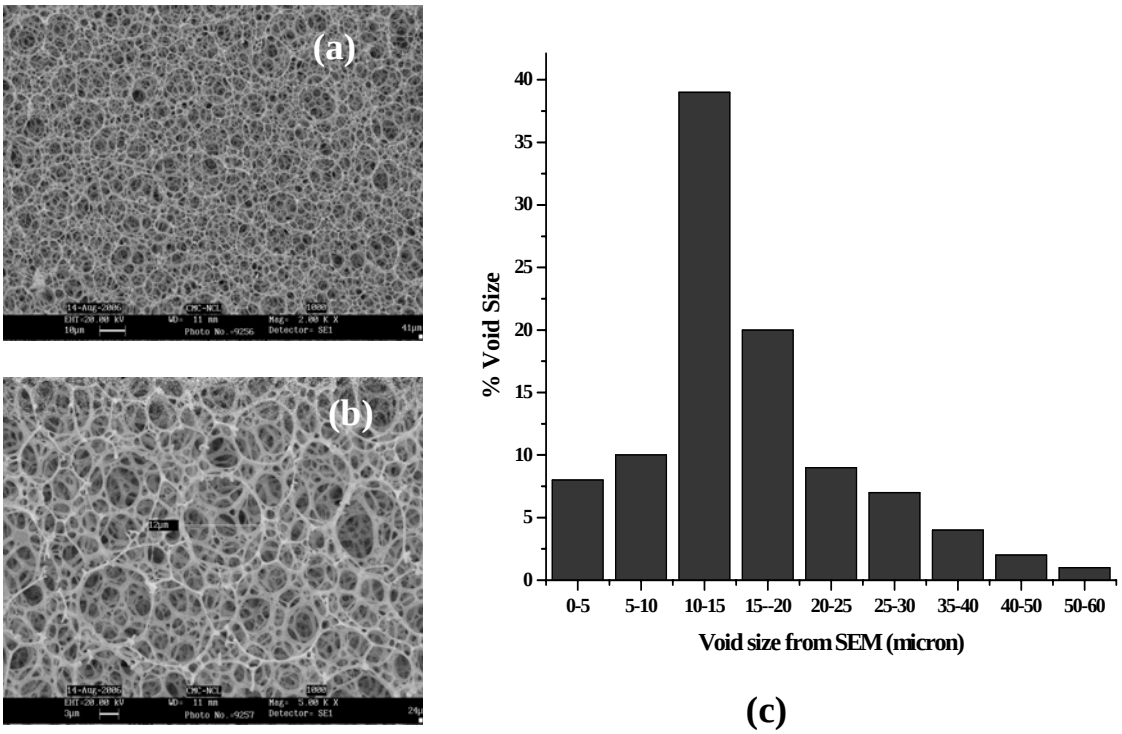

Figure 7.29. (a) Internal morphology at 2000X, (b) at 5000X magnification and (c) pore size distribution of HIPE monolith synthesised at a stirring speed of 1000 rpm

At 1400 rpm, the shear rate is so high that one cannot distinguish between the cells and windows. The morphology shown in Figures 7.30 (a) and (b) are quite different from polyHIPEs prepared at lower rpm. As shown in the pore size distribution graph presented in Figure 7.30 (c), very small pores in the range 5-10 micron are formed. Very high surface area (98.23 m^2/g) was obtained, which might be due to the formation of micropores on the interconnected cell walls.

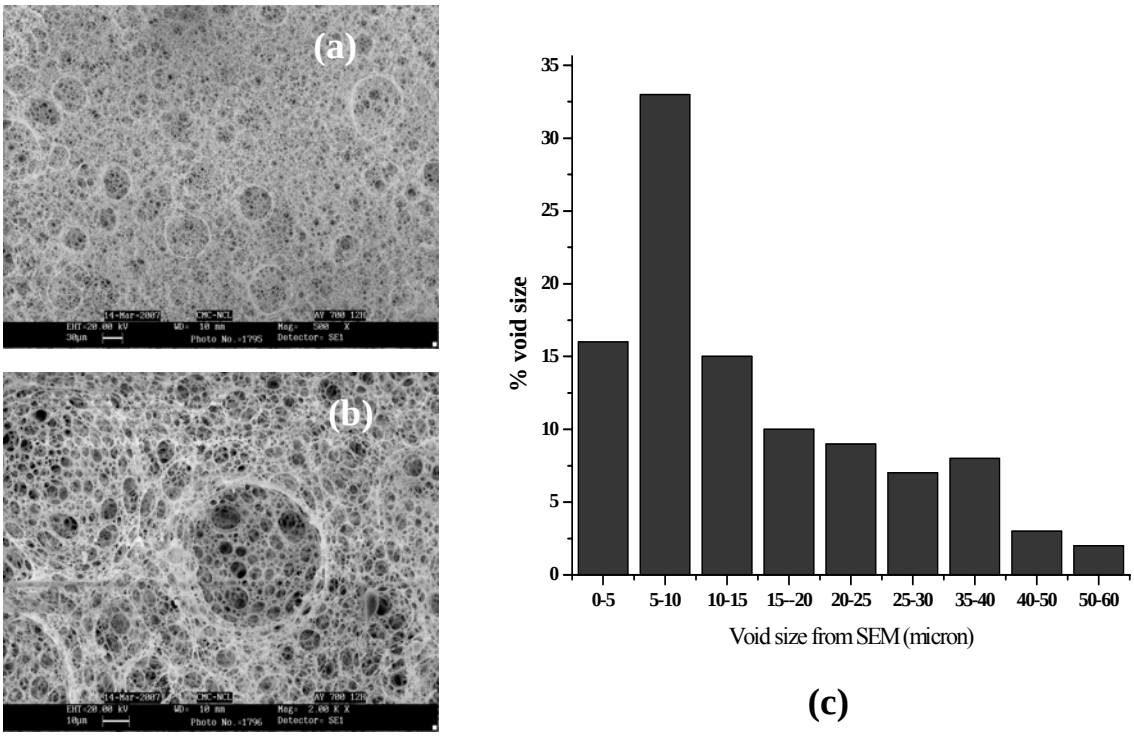

Figure 7.30. (a) Internal morphology at 2000X, (b) at 5000X magnification and (c) pore size distribution of HIPE monolith synthesised at a stirring speed of 1400 rpm

7.5 Conclusion

The effect of the different synthesis parameter on the morphology and microstructure of acrylate polyHIPE materials has been described. Highly porous polymer monoliths were prepared using different water-soluble and two oil soluble as well as a combination of both water and oil soluble initiators. Each type gives different porous morphology from thin thick cell walls with or without the formation of interconnecting windows. The combination of both oil soluble and water-soluble initiators generated very complex morphologies in the monoliths.

Addition of extremely low concentration (0.005 to 0.020 mol%) of phenothiazine in the oil phase changed the morphology quite extensively. The size of cells and windows increased from 10 to 40 micron with increasing phenothiazine concentration.

Polymerisation temperature also has considerable influence on the formation of porous architecture. The shape of droplet in emulsion changed from pentagonal to circular at different temperatures. At 65ºC pentagonal shaped droplets were formed, which changed into octagonals at 85ºC. Polymerisation at 65ºC generated lower number of windows compared to that at 85ºC.

The effects of the amount and type of surfactant on morphology of acrylate polyHIPE formed were investigated. Decreasing the surfactant concentration led to materials with a larger average cell and window size. The complex morphology observed in HIPE also depends on the stirring speed during emulsion making and the polymerisation temperature. Increase in stirring speed decreased average cell and window size due to increasing rate of breaking of droplets caused by increased droplet collision.

It has been shown that a number of parameters control porous morpholgy such as cell and window sizes, surface area and pore volume in PolyHIPE materials. Controlling these parameters will allow the production of different scaffold structures, each tailored and customised toward use in the different applications.

References

[1] Viklund, C.; Svec, F.; Frechet, J. M. J.; Irgum, K. *Chem. Mater*. **1996**, 8, 744-750.

[2] Heck, R. M.; Gulati, S.; Farrauto, R. J. *Chem. Eng. J*. **2001**, 82, 149-156.

[3] Mould, D. L.; Synge, R. L. M. *Analyst*. **1952**, 77, 964.

[4] Svec, F.; Tennikova, T. B.; Deyl, Z. *Monolithic Materials: Preparation, Properties, andApplications.* Elsevier, Amsterdam, **2003.**

[5] Svec, F.; Fre´chet, J. M. J. *Anal. Chem*. **1992**, 64, 820-22.

[6] Josic, D.; Buchacher, A.; Jungbauer, A. *J. Chromatogr. B*. **2001**, 752, 191-205.

[7] Svec, F.; Fre´chet, J. M. J. *Ind. Eng. Chem. Res*. **1999**, 38, 34-48.

[8] In: K.J. Lissant, Editor, *Emulsions and emulsion technology, part 1*, Marcel Dekker Inc., New York (**1974**).

[9] Barby, D.; Haq, Z. *Eur. Pat. Appl.* 60138; **1982.**

[10] Cameron, N. R.; Sherrington, D. C. Adv. *Polym. Sci.,* **1996**, 126, 163–214.

[11] Mork, S.W.; Green, D. P.; Rose, G. D. *US Pat. No*. 6,147,131, **2000**.

[12] Zhang, H.; Cooper, A. I. *Soft Matter.* **2005**, 1, 107–113.

[13] Cameron, N. R. *Polymer*. **2005**, 46, 1439–1449.

[14] Menner, A.; Powell, R.; Bismarck, A. *Soft Mater.* **2006**, 2, 337–342
.

[15] Haibach, K.; Menner, A.; Powell, R.; Bismarck, A. *Polymer.* **2006**, 47, 4513–4519.

[16] Menner, A.; Haibach, K.; Powell, R.;Bismarck, A. *Polymer.* **2006**, 47, 7628–7635.

[17] Menner, A.; Powell, R.; Bismarck, A. *Macromolecules.* **2006**, 39, 2034–2035.

[18] Busby, W.; Cameron, N. R.; Jahoda, C. A. B. *Biomacromolecules.* **2001**, 2**,** 154–164.

[19] Akay, G.; Birch, M. A.; Bokhari, M. A. *Biomaterials.* **2004**, 25, 3991–4000.

[20] Bokhari, M. A.; Akay, G.; Zhang, S. G.; Birch M. A. *Biomaterials.* **2005**, 265, 198–5208.

[21] Haymana, M. W.; Smith, K. H.; Cameron, N. R.; Przyborski, S. A. *J. Biochem Biophys. Methods.* **2005**, 62, 231–240.

[22] Barbetta, A.; Dentini, M.; De Vecchis, M. S.; Filippini, P.; Formisano, G.; Caiazza, S. *Adv. Funct. Mater.* **2005**, 15, 118–124.

[23] Silverstein, M.S.; Tai, H.; Sergienko, A.; Lumelsky, Y.; Pavlovsky, S. *Polymer.* **2005**, 46, 6682–6694.

[24] Ottens, M.; Leene, G.; Beenackers, A.; Cameron, N. R.; Sherrington, D. C. *Ind. Eng. Chem. Res.* **2000**, 39, 259–266.

[25] Brown, J. F.; Krajnc, P.; Cameron, N. R. *Ind. Eng. Chem. Res.* **2005**, 44, 8565–8572.

[26] Pierre, S. J.; Thies, J. C.; Dureault, A.; Cameron, N. R.; van Hest, J. C. M.; Carette, N. Adv. *Mater.* **2006**, 18, 1822–1826.

[27] Wakeman, R. J.; Bhumgara, Z.; Akay, G. *Chem. Eng. J.* **1998**, 70, 133–141.

[28] Barbetta, A.; Cameron, N. R. *Macromolecules.* **2004**, 37, 3202–3213.

[29] Cameron, N.R.; Barbetta, A. *J. Mater. Chem.* **2000**, 10, 2466–2471.

[30] Myers, D. *Surfactant science and technology (3rd ed.)*, John Wiley and Sons, New Jersey (**2006**), p. 291–92.

[31] Bancroft, W. D. *J. Phys. Chem*. **1913**, *17*, 501.

[32] Ruckenstein, E. *Langmuir,* **1996,** *12,* 6351.

[33] Ruckenstein, E. Adv. *Polym. Sci*. **1997**, 127, 1-58.

[34] Bartl, H.; von Bonin, W. *Makromol. Chem*. **1962**, 57, 74-95.

[35] Barby, D.; Haq, Z. *Eur. Pat. Appl*., 60138, **1982**.

[36] Cameron, N. R.; Sherrington, D. C. *Adv. Polym. Sci*. **1996**, 126, 163-214.

[37] Cameron, N. R., *J. Chromatogr. Libr*. **2003**, 67, 255-276.

Chapter VIII

SUMMARY & CONCLUSION

8 Summary and conclusion

We have demonstrated that it is possible to synthesise highly porous emulsion templated materials by polymerisation of W/O/W or O/W/O and W/O or O/W HIPEs. This work has focused on the preparation as well as application of various emulsion-templated materials including hydrophobic and hydrophilic systems. Most of these materials were produced by polymerisation of the continuous phase of a concentrated emulsion. An emulsion in which the internal phase occupies more than 74% of the volume has been termed a high internal phase emulsion (HIPE). 'PolyHIPE' are porous polymers that result from the polymerisation of monomers and cross-linking comonomers in a HIPE's continuous phase. The internal phase was removed, leaving a highly porous, open-pore, polymer particles as well as monolith. Many different monomers and cross-linking comonomers were investigated for polyHIPE synthesis and many different polyHIPE-based systems were developed. PolyHIPE typically had high porosities, high degrees of inter-connectivity, and unique micrometre- to nanometre-scale open-pore structures.

HIPE W/O/W multiple emulsion copolymerisation of glycidyl methacrylate (GMA) - ethylene dimethacrylate (EGDM), allyl glycidyl ether (AGE) - ethylene dimethacrylate (EGDM) and 2-hydroxyethyl methacrylate (HEMA) - ethylene dimethacrylate (EGDM) monomer systems was optimised using proper choice of nonionic surfactant. The amount of cross-linker and oil to water ratio altered both surface area as well as morphology of polyHIPE materials. Similarly, internal phase volume has a profound effect on the type and morphology of porous structures formed.

The HIPE polymers differed drastically from polymers of identical compositions synthesised using conventional suspension polymerisation with cyclohexanol as porogen. The polymers of different CLDs (25, 50, 75, 100, 150, 200 and 300) synthesised revealed that the reaction parameters profoundly influenced morphology, porous properties and surface functionalities. The study revealed that HIPE polymers have superior properties as compared to the polymers synthesised by conventional suspension polymerisation. The polymers synthesised using HIPE gave narrow particle size distribution (PSD) in the range 2-150 μm, while conventional suspension technique gave very broad PSD in the range 5-500 μm. It was observed that polyHIPE materials had very much higher pore volumes and surface areas due the formation of highly interconnected porous structures. The surface as well as internal morphology of poly(HIPE) materials were more open and interconnected throughout the surface, while the morphology in the suspension were more or less closed and irregular.

The experimental protocol was established for making porous beaded terpolymers having styrenic backbone using low HLB non- ionic surfactant such as Brij 52 and Span 80. A series of networked, cross-linked, microporous styrenated terpolymers with styrene-glycidyl methacrylates (GMA)-divinyl benzene (DVB) of varying cross-link densities were synthesised by water-in-oil-in-water ($W_1/O/W_2$) high internal phase emulsion (HIPE) polymerisation using azobisisobutyronitrile as initiator. The cross-link density, internal water and surfactant type all had significant influence on the pore characteristics.

The average surface area of terpolymer beads were found to be around 120 – 150 m^2/g and the average pore volume was around 1.5 cm^3/g. The polymers had pore volume

in the range 0.34-1.12 cm^3/g. The surface area of these materials were rather low; 23-103 m^2/g. In case of polymers synthesised by HIPE using Span 80 as porogen, maximum pores were in the 0.5-100 nm range. The pore size increased with the increase of Span 80 concentration in oil phase. The maximum surface area obtained using span 80 was 103.36 m^2/g, which was due to the formation of micro and mesopores.

A few chosen polymers were modified with thiol and SO_3H- functionality and evaluated as catalyst for the synthesis of bisphenol A. The system had around 5.7 milliequivalents of sulphonic acids per gram of catalyst. In the three-step method, the epoxy group was partially opened up using sodium thiol in methanol under reflux. The unopened epoxy group was then converted in to sodium salt of sulphonic acid. Then by using chlorosulphonic acid, the pendent sulphonic acid group was introduced to the benzene ring. This system showed about 4.8 milliequivalents of sulphonic acids per gram of catalyst. The modified terpolymer was found to be an efficient catalyst in synthesis of 4,4'-bisphenol A.

Microporous, cross-linked highly porous poly(GMA-EGDM) and poly(AGE-EGDM) epoxy beads, completely insoluble in the water, were prepared by W/O/W high internal phase emulsified suspension method. PEI was grafted into the structure. The sorption of both As (V) and As (III) by the above polymers were sharply influenced by pH, with the sorption of As (V) falling drastically both at low and high pH and that of As (III) at low pH. The sorption maximum for As (V) was under acidic conditions (pH 2-4) and that of As (III) was under alkaline conditions (pH 7-10). High adsorption rates were observed at the beginning of adsorption process, and then plateau values (i.e. adsorption equilibrium) were gradually reached in approximately 20 minutes. As (III) adsorption capacity of PEI-

attached poly(GMA-EGDM) in alkaline region was 262 mg/g and that of poly(AGE-EGDM) was 266 mg/g. As(V) adsorption capacity of PEI-attached poly(GMA-EGDM) in acidic region was found to be 166mg/g and that of poly(AGE-EGDM) was 234 mg/g. These poly(HIPE) beads were used for number of cycles for arsenic removal.

A new approach were developed to obtain networked, cross-linked poly(2-hydroxyethyl methacrylate-*co*-N,N'-methylenebisacrylamide) (HEMA-co-MBA) beads by oil-in-water-in-oil (O/W/O) inverse high internal phase emulsion (HIPE) suspension polymerisation using sodium peroxydisulphate-L-ascorbic acid as redox initiator pair. Mixed surfactant system such as Brij 92 having low HLB and Brij 700 having high HLB was used to make stable O/W/O HIPE emulsion. HEMA-MBA copolymers of similar compositions were also synthesised by using different concentrations of cross-linker, surfactant and monomer to porogen ratio, which influenced the architecture of pore. Similarly, a new protocol was established to synthesise HEMA-MBA monoliths using oil-in-water (O/W) inverse HIPE method at room temperature using redox initiator system. Both the pore diameter and average pore size of the HEMA–MBA monolith increased with increase in MBA and oil phase. Poly(HEMA-co-MBA) had a specific surface area up to 123.56 m^2/g. A tunable porous morphology of poly(HEMA-co-MBA) was obtained by this redox initiated emulsion polymerisation at ambient temperature, which is suitable for numerous applications especially in biomedical field.

Series of highly porous monoliths were synthesised with acrylate monomers using ethylene dimethacrylate (EGDM) as the cross-linker. It was shown that different synthesis parameters can be used to control porous architecture in polyHIPE materials with a wide range of cells and interconnected windows.

List of publications

1} **G. C. Ingavle**, T. S. Pathak, A. Kotha, S. Ponrathnam, Biocatalysis by Penicilin G Acylase Anchored on beaded Macroreticular Glycidyl methacryate-divnyl benzene polymers: Effect of Pore structure on Catalytic activity, ***Bulletin of Catalysis Society of India,*** 2, **2003**, 75-81.

2} **G. Ingavle,** R. Harikrishna, S. Ponrathnam, C. R. Rajan, M. S. Qureshi, High Internal Phase Polymeric Sulphonation Catalyst for Synthesis of Bisphenols, ***Communicated. Bulletin of Catalysis society of India, 2008***

3} Praveen Sher, **Ganesh Ingavle**, Surendra Ponrathnam, Atmaram Pawar,Low-density porous carrier: Drug adsorption and release study by response surface methodology using different solvents, ***International Journal of Pharmaceutics,*** *Volume 331, Issue 1*, ***22 February 2007***, *Pages 72****,***

4} Praveen Sher, **Ganesh Ingavle**, Surendra Ponrathnam, James R. Benson, Nai-Hong Li, and Atmaram P. Pawar, Novel/ Conceptual Floating Pulsatile System Using High Internal Phase Emulsion Based Porous Material Intended For Chronotherapy, ***Communicated to*** Journal of ***Molecular Pharmaceutics, December 2008***

5} I. Bhushan, R. Prashad, G. N. Qazi, **G. C. Ingavle**, T. Jamalpure, C. R. Rajan, S. Ponrathnam, Lipase enzyme immobilization on synthetic beaded macroporous copolymers for kinetic resolution of chiral drug intermediates, ***Process Biochemistry,*** *Volume 43, Issue 4*, ***April 2008,*** *Pages 321-330*

6] T. S. Pathak, S. Ponrathnam, C. R. Rajan, **G. C. Ingavle**, S. V. Deshpande, A. M. Kotha, Macroporous Poly (2-hydroxyethacrylate-co-ethylene dimethacrylate): effect of cross linking density and porogens on pore volume and specific surface area, **Membrane society of Korea,** 1, **2005**, 25.

7] I. Bhushan, R. Prashad, G. N. Qazi, **G. C. Ingavle**, T. Jamalpure, C. R. Rajan, S. Ponrathnam, Lipase Enzyme Immobilization on Beaded Macroporous Cross Linked Alkylated Glycidyl Copolymer, ***Journal of Bioactive and compatible***

Material, 2007*; vol. 22: pp. 174 - 194.*

8} N. S. Pujari, J. Trivedi, **G. C. Ingavle,** S. Ponrathnam, Novel beaded polymers from telechilic divinyl methacrylic ether esters, ***Reactive and Functional Polymers***, *Volume 66, Issue 10*, ***October 2006***, *Pages 1087-1096.*

9} Bhalchandra K. Vaidya, Abhijeet J. Karale, Hitesh K. Suthar, **Ganesh Ingavle**, Tara Sankar Pathak, S. Ponrathnam and Sanjay Nene, Immobilization of mushroom polyphenol oxidase on poly(allyl glycidyl ether-co-ethylene glycol dimethacrylate) macroporous beaded copolymers, ***Reactive and Functional Polymers***, *Volume 67, Issue 10*, ***October 2007***, *Pages 905-915*

10} Praveen Sher, **Ganesh Ingavle**, Surendra Ponrathnam and Atmaram P. Pawar, Low density porous carrier based conceptual drug delivery system ***Microporous and Mesoporous*** *Materials*, *Volume 102, Issues 1-3*, *4* ***May 2007***, *Pages 290-298*

11} Bhalchandra Vaidya, **Ganesh Ingavle**, B. D. Kulkarni, Surendra Ponrathnam, Sanjay Nene. Immobilistion of Candida rugosa lipase on poly (glycidyl methacrylate-co-ethylene dimethacrylate) and poly (allyl glycidyl ether-co-ethylene dimethacrylate) macroporous beaded copolymers, ***Bioresource Technology,*** *Volume 99, Issue 9*, ***June 2008***, *Pages 3623-3629*

12} **Ganesh Ingavle**, C. R. Rajan, Surendra Ponrathnam**.** High internal phase emulsified suspension: A novel route for synthesis of highly porous conducting polyaniline microspheres, ***Manuscript ready for submission***.

13} **Ganesh Ingavle,** Rajiv Tayal, Abdul Wasif Shaikh, Sanjeev Chaudhari, C. R. Rajan, Surendra Ponrathnam**.** Novel amine functionalized microporous W/O/W poly (HIPE) beads for arsenic removal, ***Manuscript ready for submission*****.**

14} **Ganesh Ingavle,** Surendra Ponrathnam. Novel beaded monodispersed styrenated epoxy ter-polymer by water-in-oil-in-water high internal phase emulsion polymerization and comparative study with water-in-oil suspension polymerization. ***Manuscript under preparation*****.**

15} **Ganesh Ingavle**, Timothi Ponrathnam and S. Ponrathnam. High Internal Phase Emulsion: A novel route to synthesis of highly porous monolithic poly (2-hydroxyethyl methacrylate) at ambient temperature. ***Manuscript under preparation***

16} **Ganesh Ingavle**, A. A. Shaikh, S. S. Bhongale, S. Scariah, N. N. Chavan, M. S. Qureshi,and S. Ponrathnam. Poly(High Internal Phase Emulsion) of EHA, EHMA and EGDMA with naturally occurring phenolic compounds. ***Manuscript ready for submission***